# Stiffness Modelling of Large Timber Connections in Stability Trusses

Master Thesis

Mike Mellaard

**T**U Delft

# STIFFNESS MODELLING OF LARGE TIMBER CONNECTIONS IN STABILITY TRUSSES

Author:

Mike Mellaard

In partial fulfilment of the requirements for the degree of

**Master of Science**
in Civil Engineering

with a specialisation in Structural Engineering
at the Delft University of Technology
to be publicly defended on October 25, 2023

*"It always seems impossible until it's done"*

- Nelson Mandela -

# Preface

Reading the book "Tomorrow's Timber" [35] sparked an interest in the discipline of timber engineering. The attraction towards timber seemed to come naturally to me, probably because nature has always intrigued me.

I decided to do my thesis in cooperation with the engineering firm Lüning. At Lüning, I was told about the plans for a tall timber building in the Netherlands. This building would consist of timber beams, columns and floors and a concrete core for stability. However, at Lüning, they expressed their interest in a design in which stability is provided by a timber structure.

I stumbled on two extraordinary timber buildings; Treet and Mjøstårnet, which are stabilized using glulam trusses. I came to learn that the engineering of these buildings is challenging because they are susceptible to excessive deformation and vibrations. The connections are acknowledged to play a significant role in making sure that the serviceability requirements are met. However, up to fairly recently, there has not been much research into the serviceability stiffness of large timber connections.

The objective of this thesis is to increase our knowledge regarding the influence of the stiffness of large timber connections in stability trusses on the serviceability behaviour of multi-storey timber buildings. Hopefully, this will contribute to improving serviceability design and will lead to a more widespread application of these exceptional stability structures.

*M. Mellaard*
*Delft, October 2023*

# Acknowledgements

# Abstract

The demand for timber buildings is rising because of the need to make the construction industry more sustainable. Eurocode 5 provides guidance in the design process of timber structures. Numerical modelling is generally used for complex structures like multi-storey timber buildings. Currently, there is limited understanding of the serviceability behaviour of multi-storey timber buildings that are stabilized by glulam trusses. This is partly because the load-slip behaviour of large timber connections is not well understood.

The aim of this thesis is to develop a better understanding of the influence of the connections on the serviceability behaviour of timber buildings with glulam stability trusses. In the first part of this thesis, the state-of-the-art of timber connection design is discussed. The second part is dedicated to the development of a finite element model. A modelling approach is developed that allows for the specification of the load-slip behaviour of the truss connections in the end nodes of the modelled members. A sensitivity study focused on the serviceability stiffness of the truss connections is performed using the FE model. Next, variants on the base design are modelled and studied for comparison, which provides insight into the effect that changing geometry has on serviceability behaviour.

This thesis shows that the load-slip behaviour of the truss connections has a significant influence on the serviceability behaviour of a timber building. It is also found that the current design rules are not suitable for predicting the serviceability stiffness of these connections. For timber connections with slotted-in steel plates and dowels, their load-slip behaviour can be idealized by an initial slip followed by its elastic stiffness. The initial slip is caused by the hole clearance in the steel plates in combination with various non-linear effects like densification of the timber. The hole clearance in the steel plates is also responsible for the sequential activation of the dowels, which is considered to be the primary cause for the reduction in elastic stiffness per dowel per shear plane as the number of dowels increases. This so-called 'group effect' results in a much lower stiffness of the truss connections than the current design formula suggests.

The results from the numerical modelling show that the load-slip behaviour of the connections between the diagonals and columns has a large influence on the serviceability behaviour of the truss. A distinction is made between diagonal connections and vertical components. The initial slip in the connections causes an increase in the maximum displacement of the structure. The elastic stiffness of the truss connections decreases the global stiffness of the structure. This resulted in an increase in maximum displacement, a decrease in the natural frequency, and an increase in peak accelerations.

The serviceability behaviour of large timber connections should be explored further. Current design codes are not suitable for predicting their serviceability behaviour, which can have consequences for the design of complex structures like multi-storey timber buildings with glulam stability trusses. To ensure the proper design of these buildings, our understanding of their serviceability behaviour is critical. This thesis is anticipated to be a valuable contribution to bridging the knowledge gap. It shows the shortcomings of the current design rules and provides practical information about how to predict the serviceability behaviour of a timber building that is stabilized using glulam trusses.

# Contents

# Nomenclature

## Abbreviations

| Abbreviation | Definition |
|---|---|
| glulam | glued laminated timber |
| SLS | Serviceability Limit State |
| ULS | Ultimate Limit State |
| LC | Load Combination |
| EC0 | Eurocode 0 |
| EC5 | Eurocode 5 [20] |
| prEC5 | Pre-norm Eurocode 5 [1] |
| YM | Yield Model |
| EYM | European Yield Model |
| FM | Failure Mode |
| hss | high strength steel |
| vhss | very high strength steel |
| BOF | Beam On Foundation |
| FEM | Finite Element Model |
| FEA | Finite Element Analysis |

## Symbols

| Symbol | Definition | Unit |
|---|---|---|
| A | Area | $[mm^2]$ |
| a | Fastener spacing | $[mm]$ |
| $f_h$ | Embedment stress | $[MPa]$ |
| $f_{h,0}$ | Embedment strength parallel-to-grain | $[MPa]$ |
| $k_f$ | Foundation modulus | $[N/mm^3]$ |
| F | Force | $[kN]$ |
| R; $F_{max}$ | Ultimate strength of connection | $[kN]$ |
| n | Number of fasteners | - |
| n0 | Nr. of fasteners parallel to the grain | - |
| n90 | Nr. of fasteners perpendicular to the grain | - |
| $n_{ef}$ | Effective number of fasteners | - |
| u | Slip / Displacement | $[mm]$ |
| d | Fastener diameter | $[mm]$ |
| $M_y$ | Yield moment of fastener | $[Nmm]$ |
| $f_y$ | Yield strength of steel | $[MPa]$ |
| $f_u$ | Ultimate strength of steel | $[MPa]$ |
| k | Stiffness | $[kN/mm]$ |
| $K_{ser}$ | Connection stiffness EC5 | $[kN/mm]$ |
| t | Member thickness | $[mm]$ |
| $F_{ax}$ | Rope effect | $[kN]$ |
| $\rho$ | Density | $[kg/m^3]$ |

| Lower Indices | |
|---|---|
| 0 | direction parallel to the grain |
| 90 | direction perpendicular to the grain |
| R | resistance |
| k | characteristic |
| m | mean |
| d | design |
| c | compression |
| t | tension |
| est | estimated |
| ser | under serviceability loading |
| u | ultimate |
| i | initial |
| inst | instantaneous |
| ef | effective |
| el | elastic |
| pl | plastic |
| bs | block shear |
| sp | shear plane |
| SP | steel plates |

<div style="text-align: right; font-size: 3em;">1</div>

# Research Framework

## 1.1. Context

Timber is currently returning as a widely applied construction material. This re-introduction is mainly due to the increasing pressure to construct more ustainable. The development of mass timber products enables the construction industry to use wood in a wider range of building applications. One application is multi-storey timber buildings. The stability of these buildings is commonly provided by a concrete core [51]. However, they can also be stabilized using glulam trusses, as the projects Treet [5] and Mjøstårnet [3] have successfully shown. Due to the lack of experience, the prediction of the serviceability behaviour of these buildings is difficult. Recent studies by, for example, Malo et al. [36] and Tulebekova et al. [52] have increased our knowledge regarding their serviceability behaviour, but more research is necessary to create familiarity among structural engineers.

## 1.2. Problem description

For multi-storey timber buildings, compliance with serviceability requirements can be cumbersome. Wind causes the horizontal displacement of a building. Furthermore, it has a fluctuating component, which can induce vibrations. A commonly used limit for the maximum lateral displacement of a building is 1/500 of its height [48]. This limit should ensure that non-structural components are not affected or visibly damaged. Vibrations can be perceived as uncomfortable by occupants of the building. Recommended design criteria for wind-induced vibrations are prescribed in ISO 10137 [2]. Whether the vibrations are perceived as uncomfortable is dependent on the accelerations and the natural frequency of the building. Peak accelerations can be calculated using Eurocode 1991-1-4 [19].
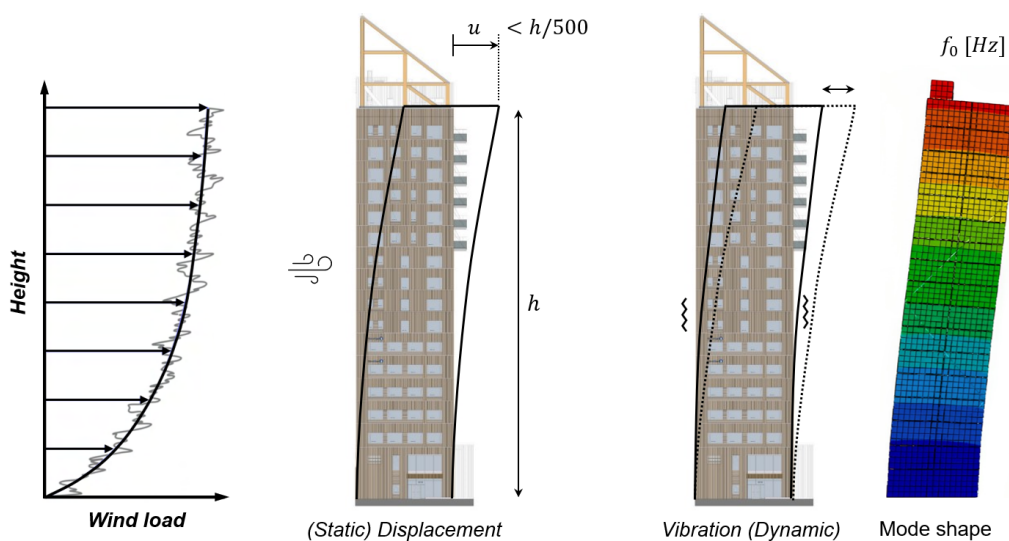


**Figure 1.1:** Serviceability design of multi-storey timber buildings. Adapted from [52, Fig. 1b & Fig. 15a].

In current practice, the members in glulam stability trusses are commonly modelled with pinned connections without any additional adjustments [36]. This is due to the lack of knowledge about the stiffness of large timber connections. In numerical studies by Utne [53], Reed & Wigg [39], and Tulebekova et al. [52] "connection zones" are used to research the sensitivity of the truss behaviour to the stiffness of the connections. In this approach, the cross-sectional area at the end of a timber member is reduced to account for lower stiffness. The reduction is expressed as a percentage of the area of the connected timber member. Thus, the incorporated connection stiffness is related to the dimensions of the connected member instead of being dependent on its actual design.

More knowledge about the stiffness of truss connections and their influence on the behaviour of the structure is considered to be important to improve serviceability design. In Europe, Eurocode 5 [20] prescribes the design rules for timber structures. EC5 provides a single formula to calculate the stiffness of timber connections with (predrilled) dowel-type fasteners. However, for example, Sandhaas & van de Kuilen [44] and Reynolds et al. [41] have reported that this equation does not capture the stiffness of steel-to-timber connections with sufficient accuracy. The difference between the predicted $K_{ser}$ and measurements is especially evident for connections with numerous dowels [37].

Therefore, the load-slip behaviour of large timber connections should be researched. In addition, we need to investigate how this behaviour can be incorporated into numerical models. This thesis aims to fill these knowledge gaps by first analysing the state-of-the-art regarding timber connection stiffness, followed by numerical modelling. The acquired knowledge will contribute to the improvement of the serviceability design of timber buildings that are stabilized with glulam trusses.

## 1.3. Research questions

Based on the problem description, the main research question is formulated as follows:

*"To what extent does the stiffness of timber connections with dowels and slotted-in steel plates influence the serviceability behaviour of multi-storey timber buildings with glulam stability trusses?"*

Sub-questions are formulated in order to answer the main research question:

1. What design rules are currently used for the design of timber connections with dowels and slotted-in steel plates?
2. How can the stiffness of large timber connections be predicted more accurately?
3. Can a representative numerical model of a stability frame be made that incorporates the stiffness of the connections?
4. What model parameters influence the predicted serviceability behaviour of a multi-storey timber building with stability trusses?

The first two sub-questions will be dealt with in the literature review. The second part of this thesis, modelling, will focus on the last two sub-questions.

## 1.4. Structure of the thesis

This thesis is subdivided into three parts: Literature review - Modelling - Research outcome. For each part, a description is provided below. The corresponding outline of the thesis is shown in figure 1.2.

*Part I - Literature Review*
A literature review is performed to obtain state-of-the-art knowledge about timber connection design and estimation of their stiffness. First, the design of timber connections according to Eurocode 5 is discussed. Second, connection stiffness is researched more in-depth by studying the load-slip behaviour of timber connections. How to idealize this behaviour for large timber connections is discussed.

*Part II - Modelling*
This part is dedicated to developing a finite element (FE) model which can be used to analyse the influence of the stiffness of the connections on the serviceability behaviour of a multi-storey timber building with glulam trusses. To research this influence within a realistic design, a case is used. The stability frame applied in the short facade of the Mjøstårnet building is chosen for this. A 2D FE model

of the stability structure is made prior to performing a sensitivity- and variant study. The model is drawn up and verified using the information provided by Sweco Norway. The design is in accordance with the Eurocodes.

A base model is constructed which is then used to perform a sensitivity study. The main focus of this study is to analyse the influence of the connections on the serviceability behaviour of the system. The knowledge about large timber connections, obtained in the literature review, is applied. How to account for the load-slip behaviour of the connections within the FE model is discussed. Thereafter, variations on the current truss design are analysed by performing a variant study. This is meant to provide structural engineers with more information about the consequences of preliminary design choices.

The results obtained from the modelling studies are summarized in a separate chapter. A comparison is made between the models in which the connection behaviour is incorporated and the models in which the timber members are simply modelled as pinned (with no further adjustments). Furthermore, the serviceability performance of the modelled structures, in which the connection behaviour is considered, is presented.

*Part III - Research Outcome*
The results are discussed in the final part of the thesis. The interpretation of the results, application and limitations are discussed. At last, conclusions are drawn and recommendations are given.
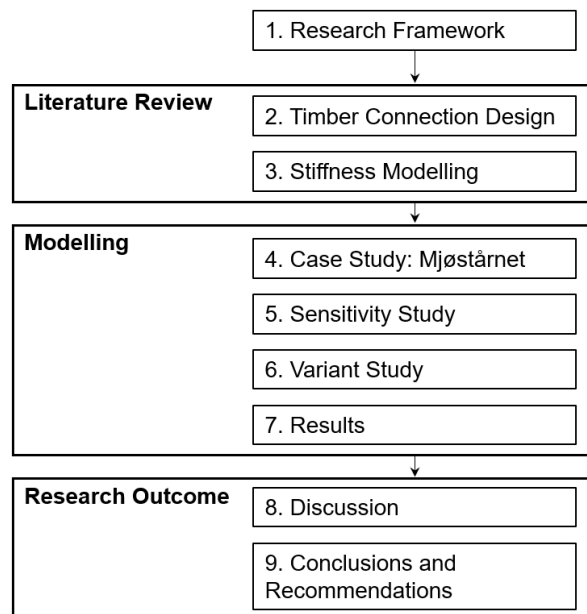


**Figure 1.2:** Thesis Outline

# Part I
## Literature Review

# 2

# Timber Connection Design

## 2.1. Introduction

Connections require special attention when it comes to the design of timber structures, especially when the structure is large because the connections will then also be of considerable size. Ensuring the structural integrity of these connections is critical to ensure safe design. In this chapter, literature on connection design, with a specific focus on connections with dowels and slotted-in steel plates loaded parallel to the grain, is discussed.

## 2.2. Load-bearing capacity

The design equations from the European yield model (EYM) are used for timber connections with dowel-type fasteners. This model is a modified version of the yield model (YM) by Johansen [29]. These models can be used to estimate the ultimate load-bearing capacity of timber connections. In this chapter, a distinction is made between the model developed by Johansen and the equations adopted in Eurocode 5 (2004). The yield models can be used for both timber-to-timber connections and for steel-to-timber connections. Several assumptions, primarily about the behaviour of the timber, are made in the derivation of the equations which consider equilibrium at ultimate load-bearing capacity. When the connection capacity is governed by the yielding of the fastener, we speak of ductile failure. Connection failure can also occur before this ductile capacity is reached. The load-carrying capacity is then governed by brittle failure.

### 2.2.1. Johansen's yield model

Johansen [29] researched the load-carrying capacity of timber-to-timber connections with dowel-type fasteners. Dowel-type fasteners include nails, screws, staples, dowels and bolts. Johansen found that the capacity is not only dependent on the resistance of the timber but also on the bending resistance of the fastener. He established equations, commonly referred to as the yield model, to calculate the load-carrying capacity of dowel-type timber connections. The equations are based on a mechanical model in which the connection dimensions and material properties of the timber and the steel fasteners are considered. The mechanical model can also be used to determine the load-bearing capacity of steel-to-timber connections. When the steel plate is sufficiently thick, it acts as a clamped restraint for the fastener. This explains the development of plastic hinges at the shear plane between the steel plate and timber for certain failure modes [7]. The embedment strength of the steel plate is not considered in the mechanical models, since it is assumed to be negligible in comparison to that of timber. The failure modes for steel-to-timber connections are shown in figure 2.1. Figure 2.2 shows the mechanical model used for the derivation of the equation for failure mode d. Equations 2.1 to 2.5 correspond to the failure modes shown in figure 2.1
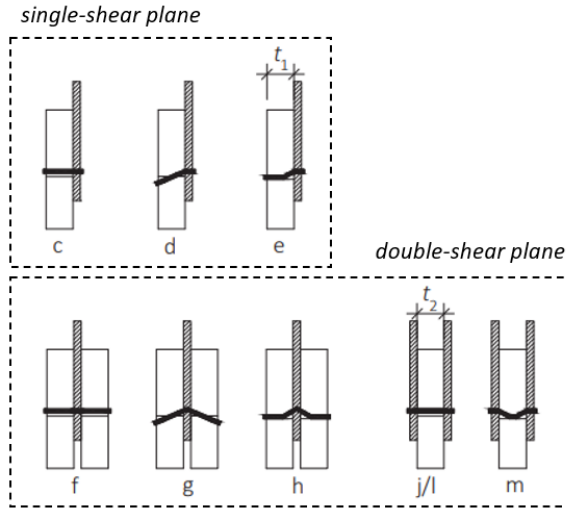
**Figure 2.1:** Failure modes (FM's) for steel-to-timber connections. Adapted from [7, Figure E2-9].
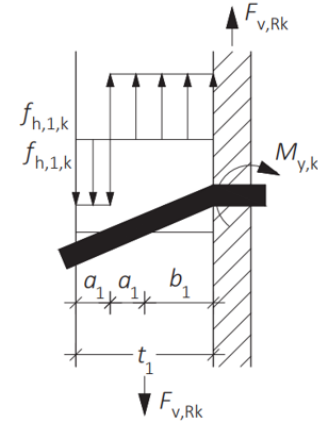
**Figure 2.2:** Mechanical model of failure mode d [7, Figure E2-10].

Johansen's equations for determining the characteristic load-bearing capacity $F_{v,Rk}$ [$N$]:

$$\textbf{(c/f)} \qquad f_h t_1 d \qquad (2.1)$$

$$\textbf{(l)} \qquad 0.5 f_h t_2 d \qquad (2.2)$$

$$\textbf{(d/g)} \qquad f_h t_1 d \cdot \left( \sqrt{2 + \frac{4 M_{y,Rk}}{f_h d t_1^2}} - 1 \right) \qquad (2.3)$$

$$\textbf{(m)} \qquad 2\sqrt{M_{y,Rk} f_h d} \qquad (2.4)$$

$$\textbf{(e/h)} \qquad 2\sqrt{M_{y,Rk} f_h d} \qquad (2.5)$$

where $f_h$ = embedment strength [$MPa$], $t_1$ = side member thickness [$mm$], $t_2$ = inner member thickness [$mm$], $d$ = fastener diameter [$mm$], and $M_{y,Rk}$ = characteristic yield moment of the fastener [$Nmm$].

## 2.2.2. European yield model

Modified versions of Johansen's equations are incorporated in EC5. This set of equations is referred to as the European yield model (EYM). A rope effect is incorporated, which can increase the characteristic connection capacity depending on the type of fastener. In addition, some of the formulas for steel-to-timber connections contain correction factors, also called pre-factors [7]. These are incorporated to include the partial safety factors related to the steel material. The derivation of the correction factor for failure mode e/h can be found in the Appendix (section A.2.2). In equations 2.6 and 2.7 the difference in comparison to the equations from Johansen's YM is highlighted in colours. Note that for failure mode d/g there is no correction factor even though a plastic hinge develops, and thus the material factor for steel should be considered [7]. For both equations, the rope effect is added. This withdrawal capacity is dependent on the type of fastener. For example, this effect is not present when dowels are applied. The loading angle with respect to the direction of the timber grain is considered by adjusting the value for the embedment strength.

$$\textbf{(d/g)} \qquad f_{h,k} t_1 d \cdot \left( \sqrt{2 + \frac{4 M_{y,Rk}}{f_{h,k} d t_1^2}} - 1 \right) + \frac{F_{ax,Rk}}{4} \qquad (2.6)$$

$$\textbf{(e/h)} \qquad 2.3 \sqrt{M_{y,Rk} f_{h,k} d} + \frac{F_{ax,Rk}}{4} \qquad (2.7)$$

where $F_{ax,Rk}$ = characteristic axial withdrawal capacity of the fastener [N], and $f_{h,k}$ = characteristic embedment strength [MPa].

### 2.2.3. Multiple shear plane connections

For large timber connections with slotted-in steel plates, the use of multiple plates is common. Consequently, the connection will contain more than two shear planes and decomposition is required. To illustrate this, a timber connection with two slotted-in steel plates, i.e. with four shear planes, is discussed in this section. The connection can be decomposed into a double-shear connection representing the outside members and a double-shear connection for the inner timber member. This is shown in figure 2.3. Next, kinematically possible failure modes are determined. These are shown in figure 2.4, for the presented example. Failure modes for the inner- and outer timber members are written in the figure.
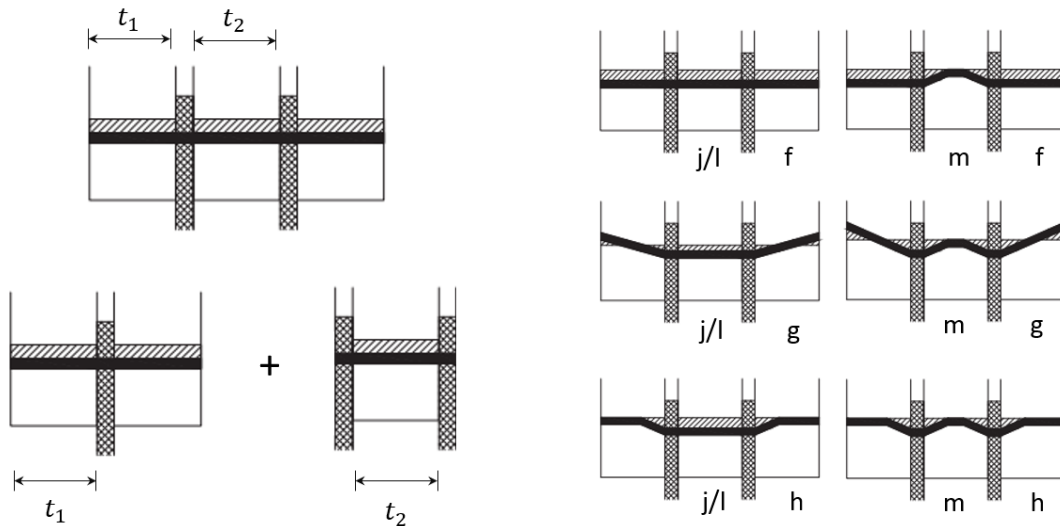


**Figure 2.3:** Decomposition of a steel-to-timber connection; example. Adapted from [7, Figure E15-2].

**Figure 2.4:** Kinematically compatible failure modes; example. Adapted from [7, Figure E15-2].

The load-bearing capacity of the multi-shear plane connection is calculated as the sum of the capacities of the decomposed parts. In the pre-norm of the new EC5 [1] it is prescribed that the governing failure modes for the individual members should either all be governed by embedment failure or by plastic hinges forming in each of the members. Combinations of these failure modes should be avoided. This should ensure the compatibility of failure modes for connections with four or more shear planes. The governing failure mode of an individual member is related to its thicknesses. An example of this dependency is shown in figure 2.5 for a connection with 12mm dowels with a yield strength of 755MPa (high-strength steel). The yield moment is calculated using equation 2.11 from theory. The mean density is 430 $kg/m^3$ and the embedment strength is determined using equation 2.10. The characteristic connection capacity per shear plane is determined using Johansen's yield model (discussed in section 2.2.1).

**(a)** for outer members (t1)



**(b)** for inner member (t2)
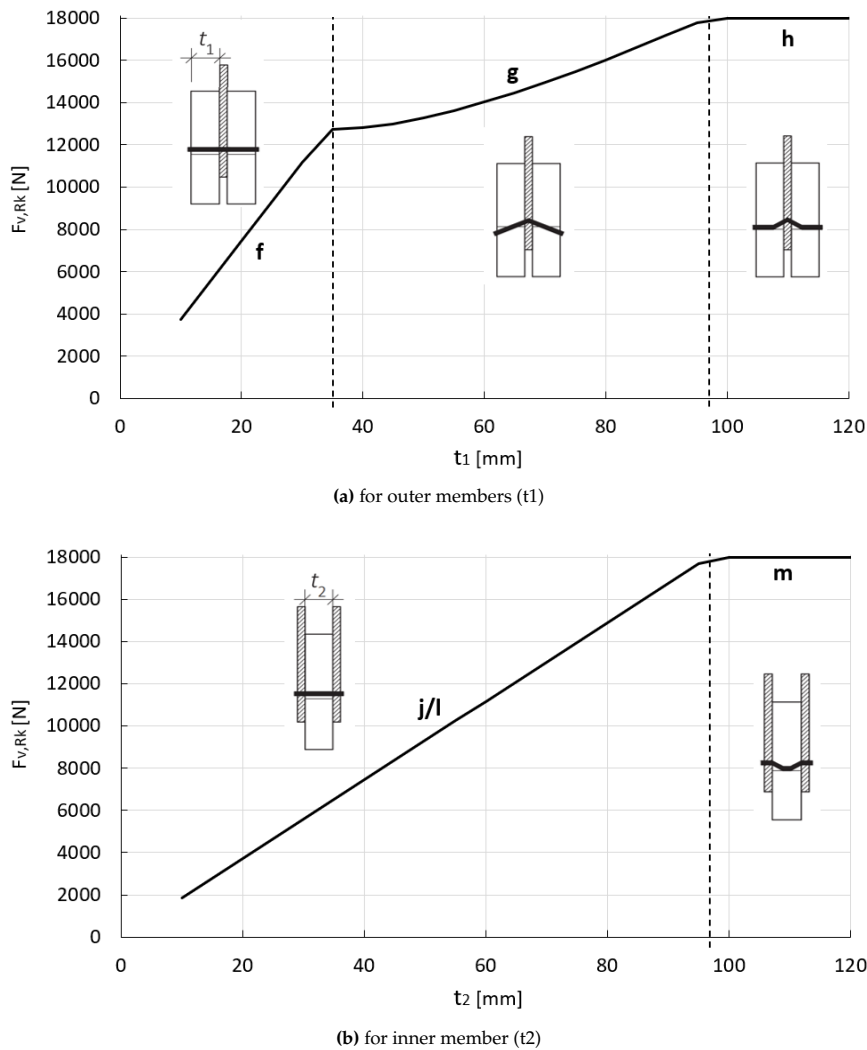
**Figure 2.5:** Characteristic load-bearing capacity (per shear plane) and governing failure mode, according to Johansen's yield model, as a function of member thickness; example. Failure modes: equations 2.1 to 2.4. Illustrations of failure modes are adapted from [7, Figure E2-9]. Equation 2.11 for yield moment and equation 2.10 for the embedment strength with
$$d = 12mm, f_y = 755MPa, \rho_{mean} = 430kg/m^3.$$

## 2.2.4. Embedment strength

The embedment strength is a system property rather than a material property. It is dependent on the interaction between the fastener and the timber [7]. Tests by Jorissen [30] and Ehlbeck & Werner [13] show that the embedding behaviour is strongly dependent on the grain direction. The embedment strength is an important parameter for connection behaviour. Johansen [29] conducted experiments to determine the embedment strength of different wood species. The results showed the plastic behaviour of timber, on the basis of which Johansen established his yield model. Many more tests [43] [47] [46], to determine the embedding behaviour of timber, have been performed afterwards. In this section, the embedment behaviour of fasteners loaded parallel to the grain is discussed.

The European method to determine the embedding strength is prescribed in EN383 [24]. The embedment strength $f_h$ of the timber is defined as the maximum stress measured in the embedment test at or before a displacement of 5mm. The stress is determined by measuring the applied load and dividing this by the projected area of the fastener. In the embedment test, it is important to prevent elastic deformation of the fastener to ensure uniform embedment behaviour of the timber [7]. A typical stress-displacement relationship for a dowel, with predrilled holes, loaded parallel to the grain is shown in figure 2.6. In Johansen's YM and the EYM (section 2.2.1 and 2.2.2) a simplified relationship for the embedment is used, as shown in figure 2.6. It shows that only the ultimate embedment stress, referred to as the embedment

strength, is used to determine the load-bearing capacity of a connection. The embedment strength is calculated with equation 2.8.

$$f_h = \frac{F_{max}}{d \cdot t} \tag{2.8}$$

where $f_h$ = embedment strength [$MPa$], $F_{max}$ = maximum load [$N$], $d$ = fastener diameter [$mm$], and $t$ = thickness of the timber specimen [$mm$].
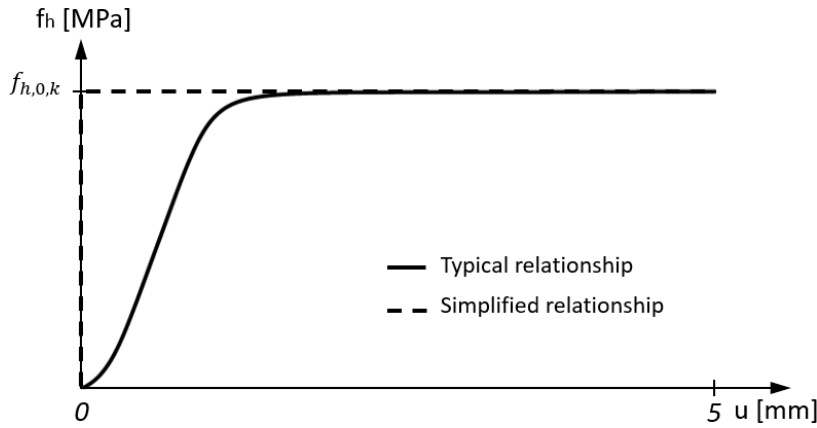


**Figure 2.6:** Typical- and simplified embedment behaviour parallel to the grain. **Figure 2.7:** Embedment test.
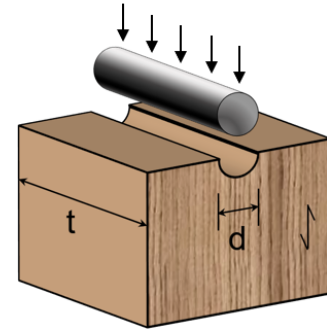
In EC5, equations to determine the embedding strength have been adopted based on empirical data from scientific research. For dowel-type fasteners in softwood, loaded parallel to the grain, and with predrilled holes, the characteristic embedment strength is calculated using equation 2.9. This equation is based on embedment tests performed on several wood species by Ehlbeck and Werner [13] who fitted equation 2.10 on their tests. The test data and the linear fit are shown in figure A.5 in Appendix A.4. The mean density of the specimens is present in this fitted formula. In the equation adopted in EC5 (equation 2.9), the mean density is simply replaced by the characteristic density.

$$f_{h,0,k} = 0.082(1 - 0.01d) \cdot \rho_k \tag{2.9}$$

$$f_{h,0} = 0.082(1 - 0.01d) \cdot \rho_{mean} \tag{2.10}$$

where $f_{h,0,k}$ = characteristic embedment strength parallel to the grain [$MPa$], $d$ = fastener diameter [$mm$], $\rho_k$ = characteristic density of the timber [$kg/m^3$], $f_{h,0}$ = embedment strength parallel to the grain [$MPa$], and $\rho_{mean}$ = mean density of timber [$kg/m^3$].

### 2.2.5. Yield moment

The yield moment of a dowel-type fastener can be determined using a four-point bending test as described in EN409 [25]. In figure 2.8 this test is illustrated on a nail. The rotation angle ($\alpha$) on the basis of which the yield moment should be determined is prescribed. For nails, this is at an angle of 45°. For dowels or bolts, the angle is $110/d$ degree. Thus, for dowels and bolts, the angle is dependent on the diameter of the fastener.
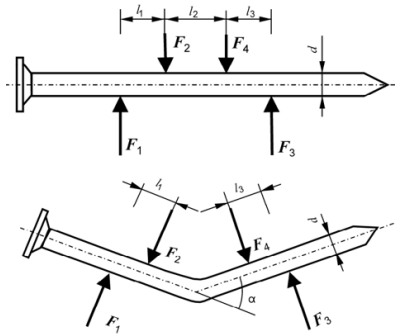
**Figure 2.8:** Four-point bending test EN409 [25].                **Figure 2.9:** Plastification of a fastener [44, Fig. 6-3].
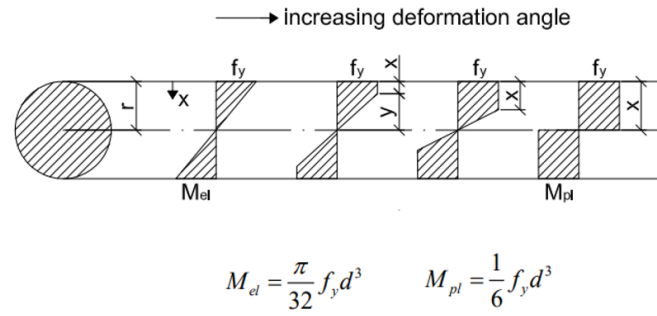
The characteristic yield moment can also be estimated using formulas. The first formula, equation 2.11, follows from mechanics. It is derived based on full plastification of a fastener, which is shown in figure 2.9. In the formula, the yield moment is dependent on the diameter of the fastener and its characteristic yield strength. Sandhaas [44] mentioned that equation 2.11 is most accurate for high-strength steel (hss) and very high-strength steel (vhss) fasteners.

$$M_{y,Rk} = f_{y,k}\frac{d^3}{6} \tag{2.11}$$

where $M_{y,Rk}$ = characteristic yield moment [$Nmm$], $f_{y,k}$ = characteristic yield strength of the fastener [$MPa$], and $d$ = fastener diameter [$mm$].

The second formula, equation 2.12, follows from research by Blaß et al. [6] and is adopted in the current EC5 (2004). Blaß et al. observed test specimens from Jorissen [30] and concluded that the bending angles of the bolts were significantly below 45°. This meant that the full plastic capacity of the fasteners has not been reached because it was assumed that fasteners reach their full plastic capacity at bending angles of 45° [43]. Therefore, Blaß et al. composed a simplified expression for the effective bending capacity of dowel-type fasteners for a connection deformation of $\delta = 15mm$ [6].

$$M_{y,Rk} = 0.3f_{u,k}d^{2.6} \tag{2.12}$$

where $f_{u,k}$ = characteristic ultimate strength of the fastener [$MPa$].

Before the adoption of equation 2.12 in EC5 (2004), equation 2.13 was specified for bolts and dowels, and equation 2.14 for nails. The latter was only to be used for circular nails with a minimum tensile strength of 600 $N/mm^2$ [6].

$$M_{y,Rk} = 0.8f_{u,k}\frac{d^3}{6} \tag{2.13}$$

$$M_{y,Rk} = 180d^{2.6} \tag{2.14}$$

Nowadays, there is a wide range of dowel-type fasteners and steel grades available to practitioners. It is, therefore, most accurate to use yield moments that are determined by tests executed by the suppliers. Especially for fasteners with a large diameter, the yield moment obtained using the different formulas discussed above can vary significantly. This is illustrated in figure 2.10 by using an example. It shows the increasing difference in yield moment as a function of dowel diameter for high-strength steel (hss, $f_y = 500 - 800MPa$) and very high-strength steel (vhss, $f_y = 800 - 1300MPa$) dowels.
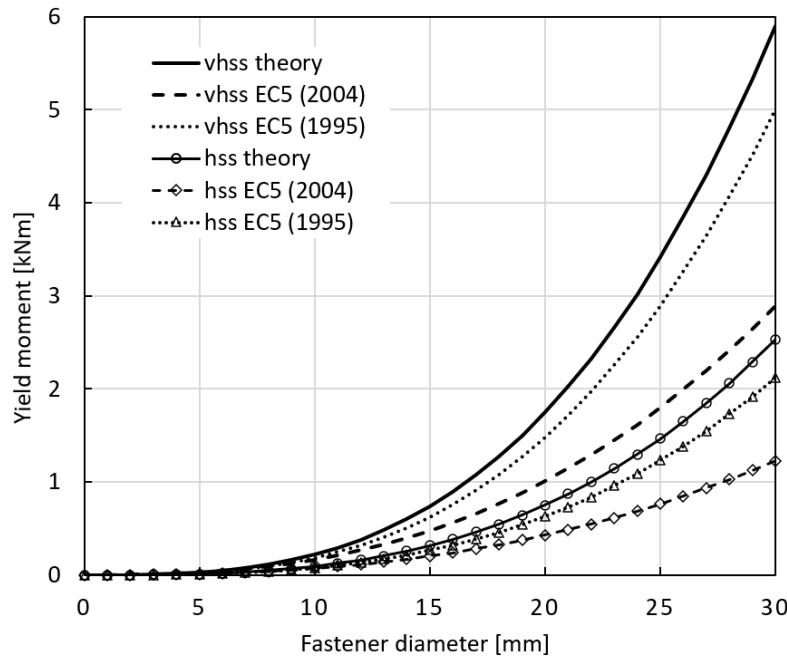
**Figure 2.10:** Example; yield moment of hss ($f_y = 563MPa$, $f_u = 590MPa$) and vhss ($f_y = 1311MPa$, $f_u = 1389MPa$) dowels determined using different equations (eq. 2.11, 2.12, and 2.13) as a function of dowel diameter. Based on [43, Fig. 6-1].

## 2.2.6. Brittle failure modes

In the previously discussed yield models, the term ductile failure is used for connections whose capacity is governed by the yielding of the fastener. The term brittle failure is used when the embedment strength is governing. In addition to this, there are additional brittle failure modes for connections with multiple fasteners, which will be discussed in this section.

In the current EC5 (2004), minimum fastener spacings are prescribed (see table A.1 in Appendix A.1 for minimum dowel spacing). These are meant to prevent the connection from failing prematurely, i.e. before reaching its capacity determined using the EYM. Brittle failure modes become more likely as the number of fasteners in the connection increases. Block shear is adopted in Annex A of EC5 [20] as an informative chapter for steel-to-timber connections with multiple dowel-type fasteners. This check became normative and in the pre-norm of the new EC5 [1] brittle failure modes are adopted as compulsory design checks. This section focuses on brittle failure modes that can occur for a connection with multiple dowel-type fasteners loaded parallel to the grain. The possible brittle failure modes are shown in figure 2.11. Connections with multiple fasteners in a row are particularly inclined to fail in a brittle manner [7].



**(a)** Splitting      **(b)** Row shear      **(c)** Block shear      **(d)** Net tensile failure      **(e)** Plug shear
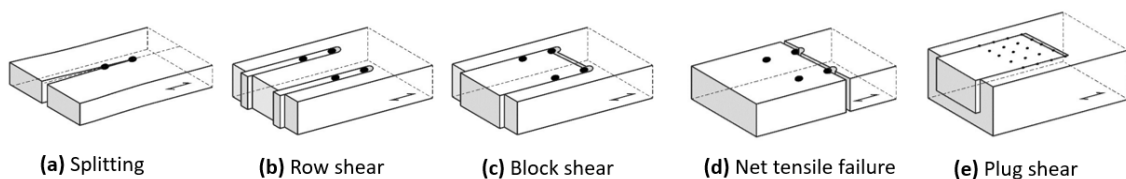
**Figure 2.11:** Possible brittle failure modes of timber connections [1, Fig. 11.22].

For steel-to-timber connections with multiple shear planes, it is important to acknowledge the possible difference in load-bearing capacity and stiffness between the inner and outer timber members. The load-bearing capacity of the connection should be based on the lowest capacity of the individual timber members. This is extensively discussed in a study by Bocquet et al. [8]. They used an example to show the consequences of a non-uniform load distribution within a connection and concluded that a uniform stress distribution amongst individual members is required to ensure that the connection is able to reach its anticipated load-bearing capacity. The stiffness of the individual shear planes is found to be essential for realizing such uniform stress among members.

The ratio between the inner- and outer member thickness plays a large role in the efficient design of a connection with multiple shear planes. Failure in one member should be considered to govern the capacity of a connection since it is unrealistic to anticipate stress redistribution after one member has broken [8]. Correspondingly, the capacity of each member should be limited by the lowest capacity of all individual members in combination with the ratio between the member thicknesses. To clarify, this approach considers equal stresses in each timber member within the connection. This is incorporated in the new EC5 [1] by providing the following formula for the brittle failure design capacity of a connection:

$$F_{br,Rd} = min \begin{cases} F_{b1,d}(n_1 + n_2 \frac{t_2}{t_1}), & \text{failure of outer timber members} \\ F_{b2,d}(n_1 \frac{t_1}{t_2} + n_2), & \text{failure of inner timber members} \end{cases} \quad (2.15)$$

$F_{br,Rd}$ = the design brittle failure resistance of a symmetrical multiple shear plane connection [$N$].
$F_{b1,d}$ = the design brittle failure resistance of the outer timber member [$N$].
$F_{b2,d}$ = the design brittle failure resistance of the inner timber member [$N$].
$n_1$ = the number of outer timber members. $\qquad$ $n_2$ = the number of inner timber members.
$t_1$ = the thickness of the outer timber members [$mm$]. $\qquad$ $t_2$ = the thickness of the inner timber members [$mm$].

### Splitting
Splitting is considered by using an effective number of fasteners in a row ($n_{ef}$). Equation 2.17 is used for screws, dowels, and bolts to take into consideration splitting along the grain for a row of fasteners. This formula is based on tests by Jorissen [30] on timber-to-timber connections. In the experiments he performed, spruce and 12mm bolts were used. Jorissen varied with the geometry, i.e. timber member thickness and fastener spacing, of the timber connections.

$$F_{v,Rd} = n_{ef} \cdot F_{v,d} \quad (2.16)$$

$F_{v,Rd}$ = the design force per fastener row [$N$].
$F_{v,d}$ = the design resistance per fastener [$N$].
$n_{ef}$ = the effective number of fasteners in a row.

$$n_{ef} = n^{0.9} \cdot \sqrt[4]{\frac{a_1}{13d}} \quad (2.17)$$

where $n$ = number of fasteners (screws, dowels, or bolts) in a row, $a_1$ = spacing (between the fasteners) parallel to the grain [$mm$], and $d$ = fastener diameter [$mm$].

In literature, it has been reported that equation 2.17 might be too conservative for various connections with specific dowel-type fasteners [44] [9]. Furthermore, the effective number of fasteners is only used to calculate the ultimate capacity and not for the stiffness of the connection. However, Sandhaas and van de Kuilen [44] reported that such a "group effect" also seems present for the stiffness of connections.

### Row shear
The row shear capacity is calculated as the sum of the shear capacity of an individual fastener row. The latter can be calculated by multiplying the design shear stress with the side shear plane area. Each individual fastener row will shear out on both sides of the fasteners, and thus the resistance should be multiplied by two.

$$F_{rs,d} = 2n_{90}F_{v,l,d} \quad (2.18)$$

$F_{rs,d}$ = design row shear failure of a timber member [$N$].
$n_{90}$ = number of fasteners perpendicular to the grain (number of rows).
$F_{v,l,d}$ = the design shear resistance per side shear plane [$N$].

### Block- and plug shear
When the fasteners penetrate over the full width of the timber member thickness, block shear can occur. The capacity of this brittle failure mode should be taken as the maximum capacity of either the tensile plane or the two side shear planes (equation 2.19). For fasteners that penetrate partially, which is only possible for side members, the plug shear must be checked in accordance with equation 2.20. Figure

2.12 shows both failure modes. The shear planes are marked in yellow and the tensile (end) plane is marked in blue.

$$F_{bs,d} = max(2F_{v,l,d}; F_{t,d}) \qquad (2.19) \qquad\qquad F_{ps,d} = max \begin{cases} 2F_{v,l,d} \\ F_{t,d} + F_{v,b,Rd} \end{cases} \qquad (2.20)$$

$F_{bs,d}$ = design block shear failure resistance of a timber member (for fully penetrating fasteners) [$N$].
$F_{ps,d}$ = design plug shear failure resistance of a timber member (for partially penetrating fasteners) [$N$].
$F_{t,d}$ = the design tensile failure resistance of the head plane [$N$].
$F_{v,l,d}$ = the design shear resistance per side shear plane [$N$].
$F_{v,b,Rd}$ = the design shear plane resistance of the bottom shear plane [$N$].



(a) Block shear                                            (b) Plug shear
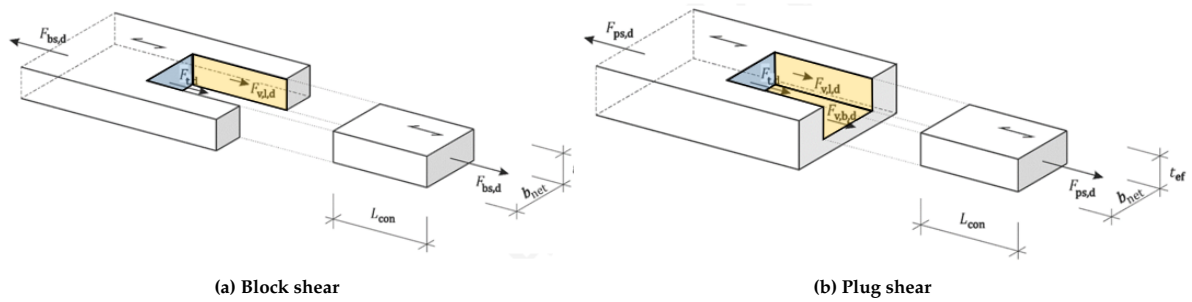
**Figure 2.12:** Block- and plug shear failure. Tension planes marked in blue and shear planes in yellow.
Adapted from [1, Fig. 11.25 & Fig. 11.26].

## 2.3. Stiffness
### 2.3.1. Load-slip behaviour
In Europe, connections with mechanical fasteners are most regularly tested using the test procedure from EN26891 [22]. The loading protocol from this standard is shown in figure 2.13. To determine the elastic stiffness ($k_e$) of a connection, i.e. stiffness without the impact of the connection settlement, a reloading cycle is used [28]. Figure 2.14 shows the corresponding idealized load-slip curve. The terminology and calculations related to the measurement points in figure 2.14 can be found in Appendix A (section A.3).
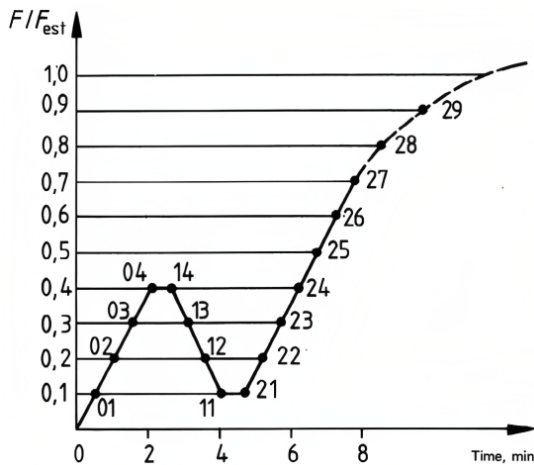


**Figure 2.13:** Loading protocol according to EN26891 [22].          **Figure 2.14:** Idealized load-slip curve [22].
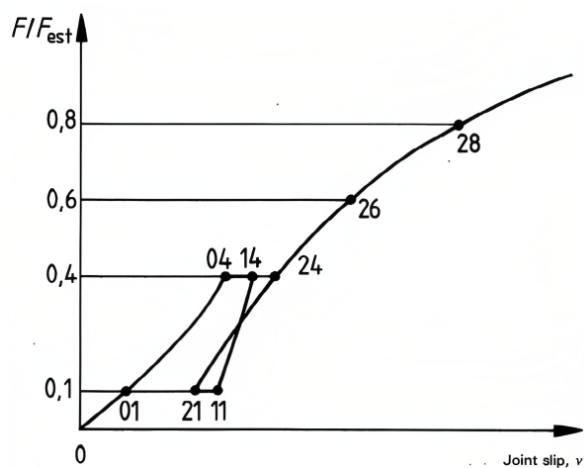
The loading procedure is related to the estimated maximum load ($F_{est}$) of the connection. This value can be determined based on experience, calculations or preliminary tests. If during testing, the mean maximum load deviates more than 20% from $F_{est}$, the estimated load should be adjusted for the subsequent tests. The testing may be stopped when the ultimate load is reached (failure occurs) or when the measured slip reaches a value of 15mm [22].

Researchers will sometimes deviate from the specified loading procedure. For example, Sandhaas [43], who evaluated the ultimate strength of connections, regularly used a force lower than 40% of $F_{est}$ for big specimens to avoid any damage in the first loop of the testing procedure. Whereas, Reynolds et al. [41] and Malo et al. [37] used divergent loading protocols to evaluate the elastic stiffness of their connections.

## 2.3.2.  Evaluation of stiffness

In structural design codes, different formulas to determine the stiffness of connections can be found [28]. Some of these formulas are shown in Appendix A.5 for comparison. Design according to EC5 [20] is considered throughout this thesis. The stiffness values and corresponding terminologies adopted in the testing procedure from EN26891 [22] are discussed in this section. In the test procedure, a distinction is made between three types of stiffness parameters:

1. The **initial slip modulus $k_i$** which is specified as the secant stiffness at 40% of the estimated maximum load $F_{est}$. This value is obtained using the initial deformation $v_i$.

$$k_i = \frac{0.4 \cdot F_{est}}{v_i} \quad \text{where} \quad v_i = v_{04} \tag{2.21}$$

2. The **slip modulus $k_s$**, determined using a modified initial slip $v_{i,mod}$ which is calculated using the difference in slip at 10% and 40% of $F_{est}$.

$$k_s = \frac{0.4 \cdot F_{est}}{v_{i,mod}} \quad \text{where} \quad v_{i,mod} = \frac{4}{3} \cdot (v_{04} - v_{01}) \tag{2.22}$$

3. The **elastic modulus $k_e$** which is obtained from the performed unloading-reloading cycle. Equation 2.23 shows how the elastic modulus is calculated.

$$k_e = \frac{0.4 \cdot F_{est}}{v_e} \quad \text{where} \quad v_e = \frac{2}{3} \cdot (v_{14} + v_{24} - v_{11} - v_{21}) \tag{2.23}$$

Figure 2.15 illustrates the idealized load-slip behaviour of a timber connection when the testing procedure is followed. The initial slip modulus ($k_i$), slip modulus ($k_s$), and elastic modulus ($k_e$) are graphically shown in this figure.
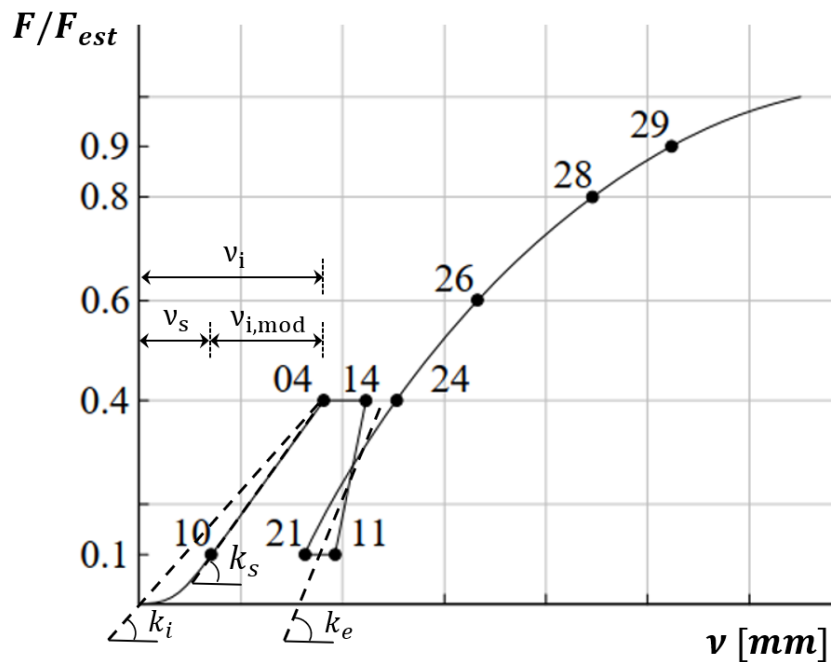


**Figure 2.15:** Stiffness parameters as specified in EN26891 [22]. Adapted from [28, Fig. 7]

### 2.3.3. Kser in Eurocode 5

EC5 provides two formulas to calculate the stiffness of a connection, depending on whether the timber holes are predrilled or not (see table A.2). In this chapter, the focus is on connections with **predrilled holes** because dowels with pre-bored holes are commonly used in combination with slotted-in steel plates for the connections in timber trusses. EC5 prescribed that dowels must be "tight-fitted" into the timber, therefore, the diameter of the predrilled holes should not be greater than the diameter of the dowel. Equation 2.24 shows the formula for the stiffness per shear plane per fastener within a timber-to-timber connection. For **steel-to-timber** connections, the equation may be multiplied by two. This multiplication is based on the assumption that the elastic deformation of the steel plates is negligible in comparison to that of the timber members.

$$K_{ser} = \frac{\rho_m^{1.5} \cdot d}{23} \quad \times 2 \tag{2.24}$$

where $K_{ser}$ = slip modulus [$N/mm$], $d$ = fastener diameter [$mm$], and $\rho_m$ = mean density of timber [$kg/m^3$].

The stiffness $K_{ser}$, is related to the parameter $k_s$ in EN26891 (equation 2.22). It can be questioned if this slip modulus is a representative parameter for the stiffness of timber connections. Reasons for this are that it is influenced by manufacturing processes and tolerances [44] and various non-linear effects like densification of the timber are not considered [41]. In addition, connections are generally exposed to fluctuating loads. In some cases, like in a stability truss, connection forces will even alternate between tension and compression. Therefore, the elastic stiffness (elastic modulus $k_e$ in EN26891, see also fig. 2.15) might be a more appropriate parameter to express the stiffness of timber connections.

For connections with multiple shear planes and fasteners, the value $K_{ser}$, calculated with equation 2.24, can simply be multiplied by the number of shear planes and fasteners. However, it has been widely reported [44] [28] [37] that this is not an accurate method to determine the stiffness of large connections since it assumes a linear increase in stiffness when scaling up the connection. The formula suggests that the stiffness per dowel per shear plane is equal for connections with a small and large number of fasteners. The so-called "group effect" expresses the idea that multiple connectors do not behave like the summation of the response of an individual fastener [41].

In EC5, it is stated that equation 2.24 can be used for fasteners with a diameter up to 30mm. However, the equation is based on tests with fasteners with a small diameter ($\leq 8mm$). The background of the equation will be discussed extensively in the next section. Ehlbeck and Werner [12] conducted tests on timber-to-timber connections using fasteners with larger diameters (8-30mm) and fitted equation 2.25 on the measured slip modulus.

$$K_{ser} = (1.2d - 1.6) \cdot \rho_m \tag{2.25}$$

where $K_{ser}$ = slip modulus [$N/mm$], $d$ = fastener diameter [$mm$], and $\rho_m$ = mean density of timber [$kg/m^3$].

Equation 2.24 and 2.25 are plotted in figure 2.16 for comparison. It can be seen that the difference between the extrapolated stiffness from EC5 and the fitted equation from Ehlbeck and Werner increases when the fastener diameter becomes larger. This suggests that the formula from EC5 is less accurate for fasteners with large diameters.
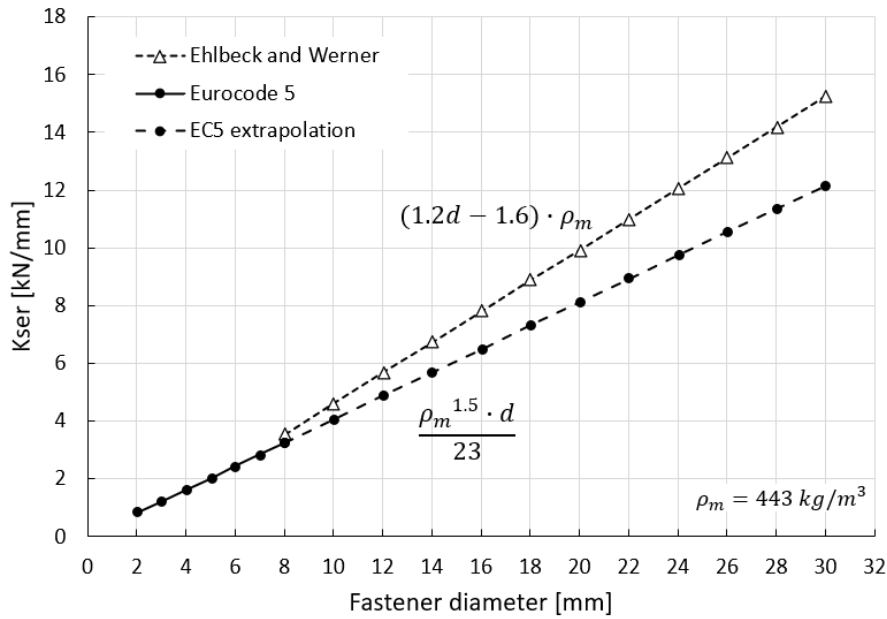
**Figure 2.16:** Slip modulus $K_{ser}$ (per fastener per shear plane) as a function of fastener diameter; example.

## 2.3.4. Background Kser

In Ehlbeck and Larsen [11], the derivation process of stiffness formulas, similar to the ones adopted in EC5, is briefly discussed. The assumptions and used test data are not explicitly mentioned, which makes the background somewhat vague, as has also been noted by Jockwer and Jorissen [27]. Nevertheless, the paper from Ehlbeck and Larsen does make it possible to trace back the origin of the formulas for $K_{ser}$ in EC5. In addition, it gives a lot of background information, which makes it possible to distinguish applications in which the formula is likely to be sufficiently accurate and in which it is not. The replication of the complete derivation process is shown in Appendix A.6. In his paragraph, the input parameters and the derivation process are briefly shown for connections with predrilled holes.

Stiffness describes deformation as a response to an applied force. In structural design, the applied force is dependent on whether the serviceability limit state (SLS) or ultimate limit state (ULS) is considered. Global displacement and the dynamic response of a building concern SLS design. The serviceability stiffness of connections should, therefore, be determined under SLS loading conditions. For the design of timber connections, 40% of the ultimate connection capacity is generally accepted as a measurement point for stiffness under SLS loads. This load level is also adopted in the test procedure of EN26891 (section 2.3.2). In Ehlbeck and Larsen [11], the same 40% of the ultimate connection capacity is used as a reasonable measurement point for stiffness under serviceability conditions. Hence, $F_{ser} = 0.4R$ in which R is the ultimate connection capacity. A linear load-deformation relationship between zero and 0.4R is assumed to be acceptable for design purposes. The instantaneous stiffness can then be determined using equation 2.26 in which the force $F_{ser}$ is divided by a corresponding displacement.

$$K_{ser,inst} = \frac{F_{ser}}{u_{inst}} = \frac{0.4R}{u_{inst}} \tag{2.26}$$

Note that the instantaneous stiffness $K_{ser,inst}$ is related to the parameter $k_i$ in EN26891 (equation 2.21) in which the settlement of the joint $v_s$ (see figure 2.15) is included. This settlement is assumed to be small for predrilled nails, and thus a typical load-deformation diagram is commonly drawn as shown in figure 2.17. However, Dubas [10] stated that joint settlement can be observed for all types of connections, even if the fasteners are predrilled. This statement corresponds with the initial non-linear embedment behaviour for fasteners loaded parallel to the grain, shown in figure 2.6. The figure shows that the embedment is initially non-linear, and thereafter the relationship is linear until it approaches the embedment strength. The initial non-linear joint settlement, also called "initial slip", is also reported in Ehlbeck and Werner [12] who performed tests on dowelled timber-to-timber connections. They proposed using an initial slip of 0.2mm for softwood connections.
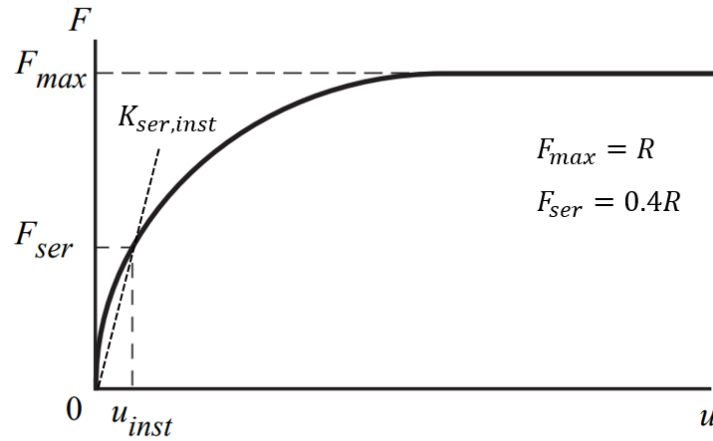
**Figure 2.17:** The instantaneous stiffness drawn in a typical load-deformation diagram of a nailed connection. Adapted from [7, Figure E3-2].

The secant stiffness $K_{ser,inst}$ between zero and $F_{ser}$ is drawn in figure 2.17. It shows that to determine this stiffness, the deformation/slip $u_{inst}$ at the serviceability load is required. Ehlbeck and Larsen [11] estimated this deformation using test results from various laboratories. Hence, equation 2.27 has been composed to estimate the deformation, for predrilled nails, corresponding to approximately 40% of the load-carrying capacity.

$$u_{inst} = 40 \cdot \frac{d^{0.8}}{\rho_k} \tag{2.27}$$

where $d$ = fastener diameter [$mm$], and $\rho_k$ = characteristic density of the timber [$kg/m^3$].

Next, it is assumed that **failure mode f/k** (for timber-to-timber), is governing the connection capacity. In this failure mode, two plastic hinges per shear plane develop. The characteristic ultimate capacity (R) is calculated using equation 2.28 from Johansen's yield model [29]. The capacity is dependent on the yield moment of the fastener, the embedment strength of the timber, and the diameter of the fastener.
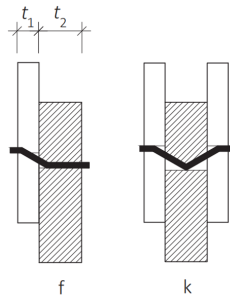


$$R = \sqrt{2M_{y,Rk}f_{h,0,k}d} \tag{2.28}$$

where $d$ = fastener diameter [$mm$], $M_{y,Rk}$ = characteristic yield moment of the fastener [$Nmm$], and $f_{h,0,k}$ = characteristic embedment strength parallel to the grain [$MPa$].

**Figure 2.18:** FM f and k [7, Fig. E2-5 & E2-8].

For the embedment strength and the yield moment, equation 2.9 and 2.14 are used. The latter is no longer part of the current EC5 (2004) and is replaced by equation 2.12 based on research by Blaß et al. [6]. The formulas used in the derivation by Elhbeck and Larsen are repeated for convenience:

$$f_{h,0,k} = 0.082(1 - 0.01d) \cdot \rho_k \tag{2.9 revisited}$$

$$M_{y,Rk} = 180d^{2.6} \tag{2.14 revisited}$$

where $d$ = fastener diameter [$mm$], and $\rho_k$ = characteristic density of the timber [$kg/m^3$].

To obtain the instantaneous stiffness, the ultimate connection capacity (equation 2.28) and the instantaneous deformation at 0.4R (equation 2.27) are filled in equation 2.26. This procedure is written out in

Appendix A.6. The result is a formula for predrilled nails (2-8mm) in timber-to-timber connections, which is shown in equation 2.29

$$K_{ser,inst} = \frac{0.4R}{u_{inst}} = \frac{\rho_k^{1.5} \cdot d}{20} \qquad (2.29)$$

Equation 2.29 contains the characteristic density of the timber. In the formula for $K_{ser}$ (eq. 2.24) from EC5, the stiffness is expressed as a function of the mean density. The stiffness equation from Elhbeck and Larsen translates into the equation adopted in EC5 when changing the density parameter from characteristic to mean. This is done by taking a factor of (approximately) 1.1, as shown in equation 2.30.

$$K_{ser,inst} = \frac{\rho_k^{1.5} \cdot d}{20} \quad \text{and} \quad \rho_k \approx \frac{\rho_m}{1.1} \quad \longrightarrow \quad K_{ser,inst} \approx \frac{\rho_m^{1.5} \cdot d}{23} = K_{ser,EC5} \qquad (2.30)$$

Thick nails in predrilled holes are assumed to behave similarly to thin dowels driven into tight-fitting holes [11]. Therefore, Elhbeck and Larsen also prescribed equation 2.29 for dowels and screws $\geq 8mm$, as can be read from table A.5. For bolted connections, the instantaneous slip under service load should be taken according to equation 2.31 to account for an initial slip due to hole clearance inside the timber members. This increased slip causes a shift of the load-deformation curve, as shown in figure 2.19.

$$u_{inst} = \frac{F_{ser}}{K_{ser,inst}} + 1mm \qquad (2.31)$$
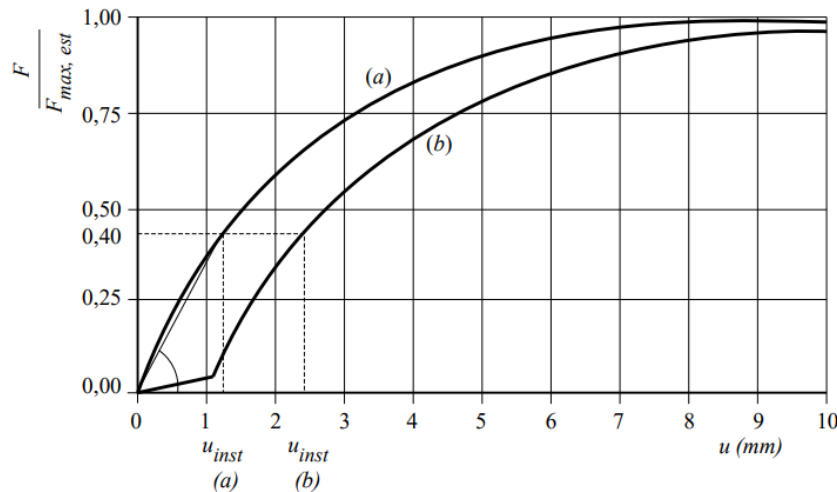


**Figure 2.19:** Idealized load-deformation curves of a (a) dowelled and a (b) bolted connection [7, Figure E4-3].

## 2.4. Summary

The European yield model is widely used to determine the **characteristic load-carrying capacity** of connections with dowel-type fasteners. This model is based on the yield model from Johansen [29] who considered equilibrium in the ultimate limit state to compose formulas for the characteristic capacity of timber-to-timber connections. The capacity is dependent on the timber member thicknesses, the embedment strength, the fastener diameter, and the yield moment of the fastener. The EYM is a modified version of Johansen's yield model in which equations for steel-to-timber connections, the rope effect, and a correction factor (pre-factor) are included. The latter can lead to an inaccurate prediction of the characteristic connection capacity. The correction factor is included for the failure modes in which two plastic hinges develop. It is, however, not present for the failure modes with one plastic hinge, even though this equation also contains the yield moment of the fastener.

Steel-to-timber connections with **multiple shear planes** can be decomposed to determine their load-bearing capacity. The inner- and outer timber members are considered separately, and the sum of their capacities is assumed to be equal to the capacity of the complete connection. A requirement for

this approach is that the failure modes in the different members are kinematically compatible. The load-bearing capacity of a fastener in individual timber members is dependent on the member thickness and the yield moment of the dowel. When the member thickness increases, the ductile failure modes, in which plastic hinges develop, will be governing. In practice, generally, these ductile modes are preferred, but limited member dimensions might not allow for these modes to govern the capacity.

The yield models pre-assume failure of the connection by embedment failure or a combination of embedment failure and the development of plastic hinges. However, for connections with multiple fasteners, **brittle failure** modes should also be considered because they can cause premature failure. The possible brittle failure modes are splitting, row shear, block shear, net tensile failure, and plug shear. Splitting is considered in EC5 by a formula prescribing the effective number of fasteners in a row. The effective number of fasteners is dependent on the number of fasteners in a row, the spacing between these fasteners, and their diameter. Block- and plug shear are added as an informative appendix in EC5 (2004). In the new EC5 [1], it is mandatory to consider all possible brittle failure modes for multi-fastener connections.

The European norm EN26891 prescribes how to perform a test to determine the **load-slip behaviour** of a connection with mechanical fasteners. This test procedure is used for the determination of the load-bearing capacity of a connection but also its stiffness. For the stiffness of a connection, a distinction is made between three parameters. In the first parameter, the initial slip modulus $k_i$, joint settlement is included. In the second, the slip modulus $k_s$, the initial slip is excluded. It is the slope of the secant line drawn between 10 and 40% of the estimated ultimate load. In the third stiffness parameter, the effect of joint settlement/initial slip is eliminated by performing an unloading-reloading cycle. The corresponding elastic stiffness, referred to as the elastic modulus $k_e$, can then be determined. In the test procedure, loading up to 40% of the estimated load-carrying capacity is considered to be a good representation of the maximum connection force under serviceability loading. Correspondingly, the applied load to determine stiffness is dependent on the estimated characteristic connection capacity. How to estimate this capacity is not prescribed in the procedure, even though this may affect the test results.

EC5 prescribes a formula to determine the **stiffness $K_{ser}$** for a connection with dowel-type fasteners and predrilled holes. Its value is dependent on the diameter of the fastener and the mean density of the timber. $K_{ser}$ is analogous to the stiffness parameter $k_s$ in EN26891. The formula gives a stiffness value per fastener per shear plane. The derivation of the formula is briefly shown in Ehlbeck and Larsen [11]. It is found that the formula is composed using test data from nailed (2-8mm nails) timber-to-timber connections. Several assumptions are made in the establishment of the formula. One of them is that failure is governed by the mode in which two plastic hinges per shear plane develop. This assumption might be probable for nailed connections considering the relatively high slenderness, however, for fasteners with a larger diameter, different steel grade, and/or other member thickness this failure mode may not be so evident. Ehlbeck and Larsen used data from laboratory tests on nailed timber-to-timber connections and fitted a formula on the instantaneous deformation $u_{inst}$ at approximately 40 percent of the load-carrying capacity (0.4R). The equation for the instantaneous stiffness $K_{ser,inst}$ is thereafter established by dividing 40% of $F_{est}$ by the formula for the instantaneous slip. Correspondingly, $K_{ser,inst}$ is found to be analogous to $k_i$ in EN26891, which would only be equal to $k_s$ if there is no initial slip. However, Dubas [10] found that connections with fasteners with predrilled holes always show some initial slip. Since $K_{ser}$ does not include the initial slip, this should be accounted for separately. In current EC5 [20], such an initial slip is only prescribed for bolted connections. This is done because the initial slip due to hole clearance in the timber is significantly more than the initial slip that can be found in timber-to-timber connections with tight-fitted fasteners.

<div style="text-align: right; font-size: 3em;">3</div>

# Stiffness Modelling

## 3.1. Introduction

In the previous chapter, it has been discussed that the current stiffness formula from EC5 is insufficient to accurately represent the stiffness of all types of timber connections. In this chapter, it is explored how a better estimation of the stiffness of steel-to-timber connections can be made. A beam-on-foundation (BOF) model of a single dowel connection is made to analyse its slip modulus $k_s$ for comparison with $K_{ser}$. Essential in BOF modelling is a good representation of the embedment behaviour. A model to represent embedment parallel to the grain is discussed in the first section. After the single-dowel connection, test data of multi-dowel connections is analysed. The parameters influencing the stiffness of a connection with slotted-in steel plates and numerous dowels are identified by studying the test data. An engineering model that could be used to predict the stiffness of a large-scale connection is discussed. At last, possible idealizations of the load-slip behaviour of large timber connections are presented.

## 3.2. Modelling of the embedment behaviour

To determine the characteristic capacity of a single-dowel connection, the European yield model (EYM) can be used. The equations from EYM are established based on equilibrium in the ultimate limit state in which the connection geometry, yield moment, and embedment strength are considered. Under serviceability loading, the maximum embedment stress will not be reached or is only reached locally. Therefore, to analyse the stiffness of a single-dowel connection, it is important to know how the embedment stress progresses. A typical stress-displacement relationship for a dowel loaded parallel to the grain is shown in figure 3.1.
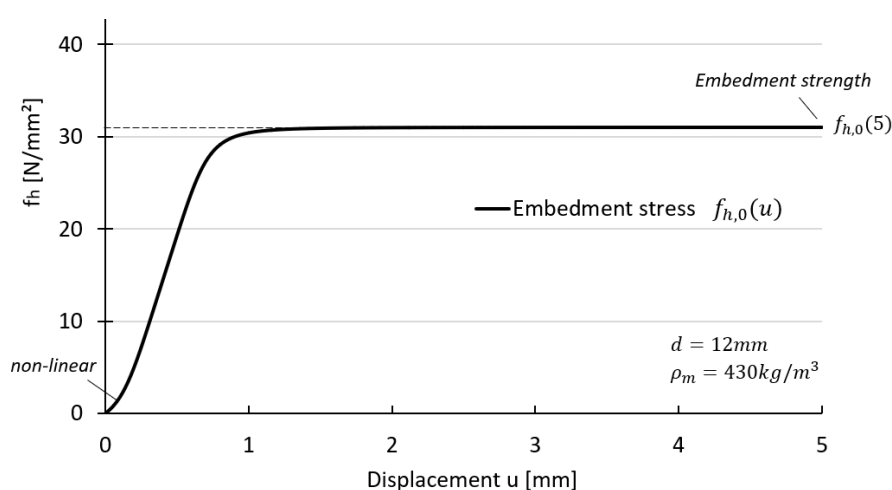


**Figure 3.1:** Typical embedment behaviour of a dowel loaded parallel to the grain; example.

Schweigler et al. [46] reviewed a wide range of possible parametrization equations to represent

embedment behaviour. Sauvat [45] proposed a function for the foundation modulus $k_f$, which represents the slope of the embedment curve. This function, taken as represented in Lemaître et al. [33], is the trigonometric function shown in equation 3.1.

$$k_f(u) = (-a_3 \cdot (arctan(((u \cdot a_6) + a_4)^{a5} + a_1) + a_2)) \tag{3.1}$$

The parameters $a_1$ and $a_5$ determine the shape of the trigonometric function. Initial slip can be considered by adjustment of parameter $a_4$. Parameters $a_2$ and $a_3$ can be coupled to other parameters in combination with the elastic ($k_{f,el}$) and plastic ($k_{f,pl}$) foundation moduli. The last parameter, $a_6$ can be found by solving equation 3.2 at a dowel displacement of 5mm. The parameter ensures that the ultimate embedment strength corresponds to the expected embedment strength.

$$\int k_f(u)du = f_h(u) \tag{3.2}$$

Lemaître et al. [33] suggest the following values and expressions for the model parameters of a fastener loaded parallel to the grain :

$$
\begin{aligned}
a_1 &= 2 \\
a_2 &= \frac{(k_{f,el} \cdot (\pi/2) - k_{f,pl} \cdot arctan(a_1))}{k_{f,pl} - k_{f,el}} \\
a_3 &= \frac{-k_{f,el}}{arctan(a_1) + a_2} \\
a_4 &= 0 \text{ (initial slip) or} \leq 0 \text{ (with initial slip)} \\
a_5 &= 4 \\
a_6 &= \text{set by fitting for } f_h(5mm)
\end{aligned}
\tag{3.3}
$$

For timber connections loaded parallel to the grain, the plastic foundation modulus $k_{f,pl}$ is equal to zero. Based on embedment data from literature [31] [26] [43], the elastic foundation modulus $k_{f,el}$ is estimated to be approximately $49kN/mm^3$ for a 12mm dowel loaded parallel to the grain. The embedment tests show good agreement on this value, even though the mean density of the test specimens varies. This suggests that the correlation between the embedding stiffness (parallel to the grain) and the density of softwood specimens is weak. In the embedment tests, the initial slip, which is dependent on the non-linear part of the stress-displacement relationship, is observed to be approximately 0.1mm. This can be incorporated in the model by adjustment of parameter $a_4$.

The embedding model is illustrated using an example. The embedment strength is calculated using equation 2.10, a mean density of 430 $kg/m^3$, and a dowel diameter of 12mm. This gives an embedment strength of $31MPa$. The model parameters proposed by Lemaître et al. (equations 3.3) are taken. The parameters $a_4$ and $a_6$ are fitted to be -1.64 and 4.05 to account for an initial slip of 0.1mm. In figure 3.2 the modelled foundation modulus and the corresponding development of the embedment strength are shown.
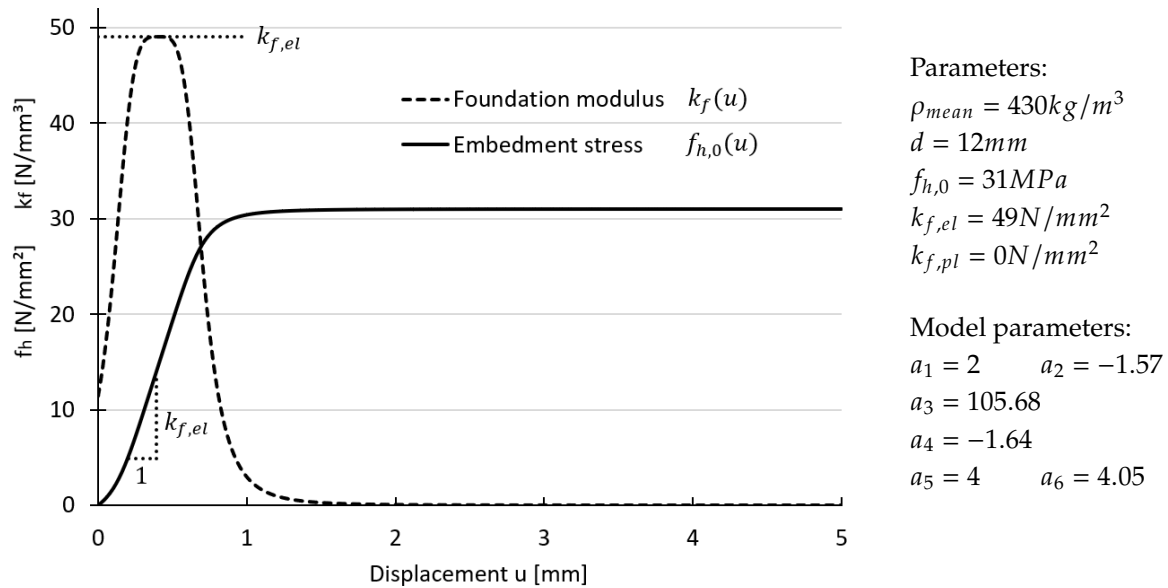
**Figure 3.2:** Graphical illustration of the embedding model for a 12mm dowel in softwood loaded parallel to the grain; example.

## 3.3. Single-dowel connection

It has been widely reported [44] [41] [37] that the stiffness formula prescribed by EC5 (equation 2.24) is not accurate for timber connections with dowel and slotted-in steel plates. This can be explained by the assumptions made in the derivation of the formula, as discussed in section 2.3.4. The deviation between the formula and the stiffness obtained from tests is reported to be significant already for a single-dowel connection [41] [37]. In this section, the deviation of the EC5 formula from the expected stiffness is researched for a typical timber connection with a slotted-in steel plate and a single dowel. The slip modulus is estimated using Beam On Foundation (BOF) modelling. The dowel is modelled as an elastic beam on a non-linear elastic foundation. The foundation, i.e. the supporting springs, represents the embedment behaviour of the timber. The model used to represent the embedment behaviour has been discussed in section 3.2.

The dimensions of the analysed double shear connection are taken in accordance with the small specimens tested in Malo et al. [37]. The modelled side member thickness is 50mm instead of the 51mm in the tested specimens, which is chosen to be able to model the supports with exactly 5mm in between. The geometry of the symmetric single-dowel connection is shown in figure 3.3. The steel plates are 10mm thick and the dowels have a diameter of 12mm. On both sides of the steel plate, there is a gap of 1.5mm to allow for easy assembly of the connection. The dowels are tight-fitted in the predrilled timber holes. The initial slip caused by clearance in the steel plates is not considered. To clarify, this means that the dowel is in direct contact with the timber and the steel plate when the load is applied.
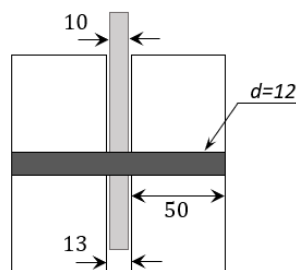


**Figure 3.3:** Dimensions of the single-dowel connection in double shear.
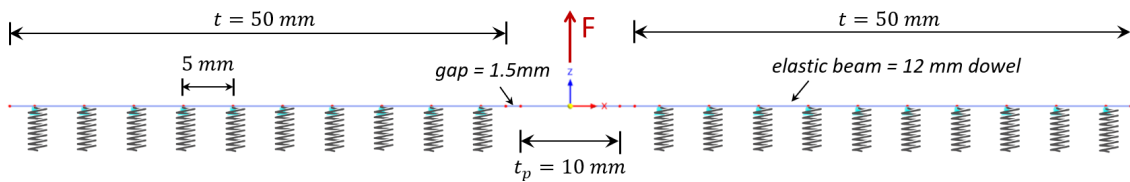
**Figure 3.4:** Beam on Foundation (BOF) model corresponding to the single dowel connection in figure 3.3.

The schematization of the BOF model of the single-dowel connection is shown in figure 3.4. The stiffness of the modelled springs is related to the embedment behaviour. The embedding behaviour previously shown in figure 3.2 is incorporated. The force-displacement diagram of the springs is established by multiplying the embedment stress with the contact area that the spring represents. The springs are placed 5mm apart and the dowel diameter is 12mm. Correspondingly, the contact area of each spring is equal to $60mm^2$. In the model, the force-displacement behaviour of the spring is discretized using displacement increments of 0.02mm, between which the model components are linearized. This methodology is adopted from Lemaître et al. [33]. Based on their sensitivity study, they recommend applying a minimum distance of 0.4d between the springs. In addition, this distance should not be larger than the diameter of the dowel [8]. The modelled force-displacement diagram of the springs is shown in figure 3.5
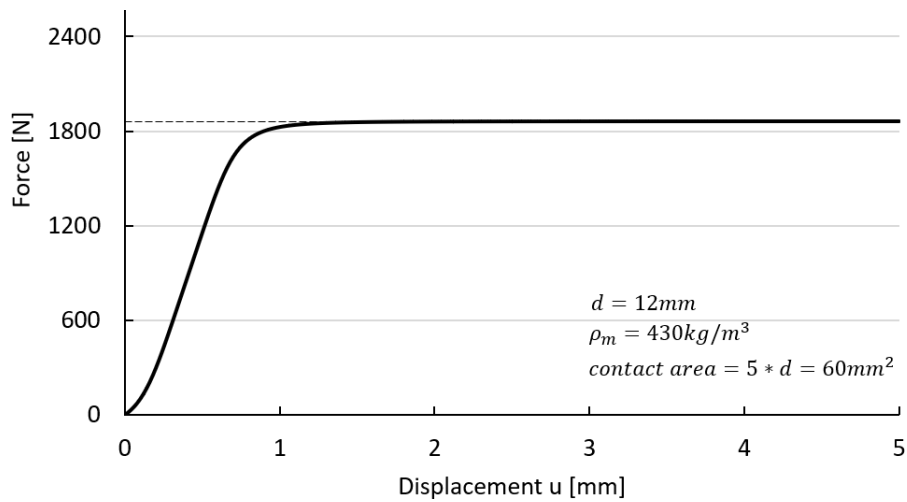


**Figure 3.5:** Force-displacement diagram of the modelled springs.

To estimate the stiffness of the connection using the BOF model, loads are applied to the slotted-in steel plate and the displacement is determined. The applied loads are 10 and 40% of the characteristic capacity, which is calculated according to Johansen's equations (section 2.2.1). The embedment strength is calculated using equation 2.10. The mean density is $430kg/m^3$. High-strength steel (hss) dowels with a yield strength of 755MPa were used. For hss dowels is it most accurate to calculate the yield moment using equation 2.11 from theory [43]. For the single-dowel connection, failure is found to be governed by failure mode g in which one plastic hinge per shear plane develops (see figure 2.1 for FM g). The characteristic capacity is estimated to be 26.5kN. To evaluate stiffness under serviceability loading, the displacements corresponding to loads 0.1R (2.65kN) and 0.4R (10.62kN) are determined. The results are shown in figure 3.6.
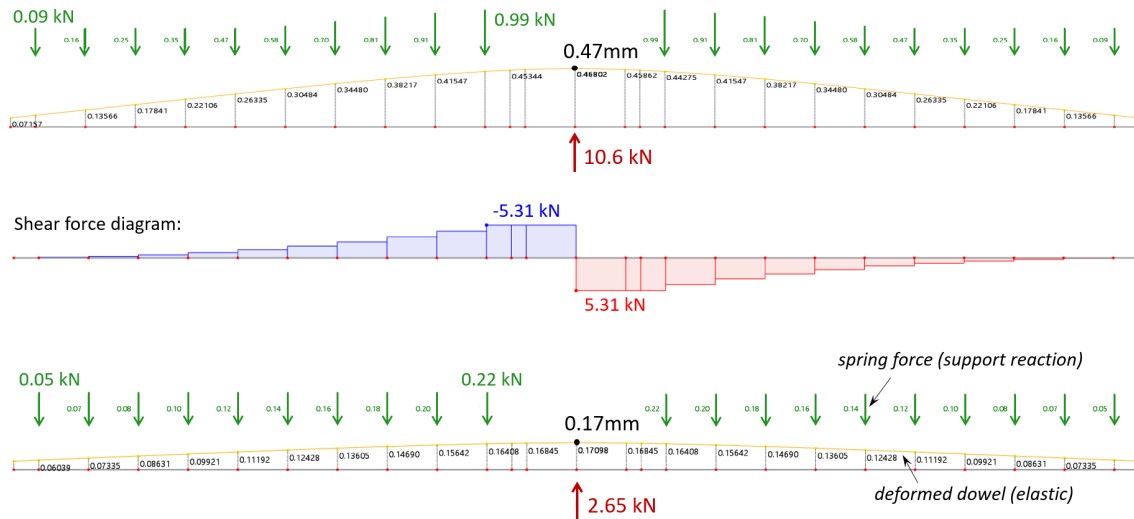
**Figure 3.6:** Results from the BOF model; elastic deformation of the dowel, spring forces, and the deformation in the middle of the steel plates at loads 0.1R and 0.4R respectively.

The slip modulus $k_{s,BOF}$ of the single dowel connection is calculated with equation 3.4. The slip modulus is calculated to be 26.8kN/mm. The double shear connection is symmetric, and thus the estimated stiffness per shear plane is 13.4kN/mm. Equation 2.24 from EC5 predicts a stiffness of 9.3kN/mm per shear plane for this connection. The difference is most likely due to the larger dowel diameter and member thickness than considered in the derivation of $K_{ser}$. In the BOF model, a perfect interaction between the dowel and the timber is considered. In tests and practice, however, the slip modulus for a single dowel connection can have a large scatter because it is sensitive to the production quality of the connection [43].

$$k_{s,BOF} = \frac{0.4R - 0.1R}{u_{0.4R} - u_{0.1R}} \tag{3.4}$$

where $k_{s,BOF}$ = slip modulus determined using BOF model [$kN/mm$], R = characteristic capacity of the connection, and $u$ = displacement obtained from BOF model [$mm$].

Malo et al. [37] did not evaluate the slip modulus of their tested connections. Instead, they determined the elastic unloading-reloading stiffness. To evaluate this stiffness, they applied a different loading protocol, shown in figure B.4 in the Appendix, than prescribed by EN26891 (figure 2.13). The assessed stiffness is most comparable to the elastic modulus $k_e$ from EN26891, shown in figure 2.15. However, $k_e$ is evaluated by performing only one loading cycle, while Malo et al. reported that multiple unloading-reloading cycles had to be performed before they stabilized and the plots appeared on top of each other. For the single-dowel tests by Malo et al., the average stiffness of the unloading-reloading cycles in tension, compression, and alternating load is 22.89$kN/mm$ (per shear plane). This value is significantly higher than the initial stiffness of 13.4$kN/mm$ obtained from the BOF model. The difference is likely to be caused by various non-linear effects, like densification of the timber around the hole edge [41]. This suggests that even under serviceability loading, plastic deformation of the timber will occur. This phenomenon and the effect of dowel misalignment are extensively discussed by Reynolds et al. [41].

The difference in initial- and elastic stiffness also becomes evident from embedment tests in which a loading cycle has been performed. Sandhaas [43] performed such embedment tests for 12mm hss dowels. The obtained stress-displacement graphs are shown in figure 3.7. The tests show significant variation in initial slip and foundation modulus $K_s$. On the contrary, the elastic foundation modulus $K_e$ shows good agreement for all the performed tests. Furthermore, the values for $K_e$ are notably higher in comparison to $K_s$.
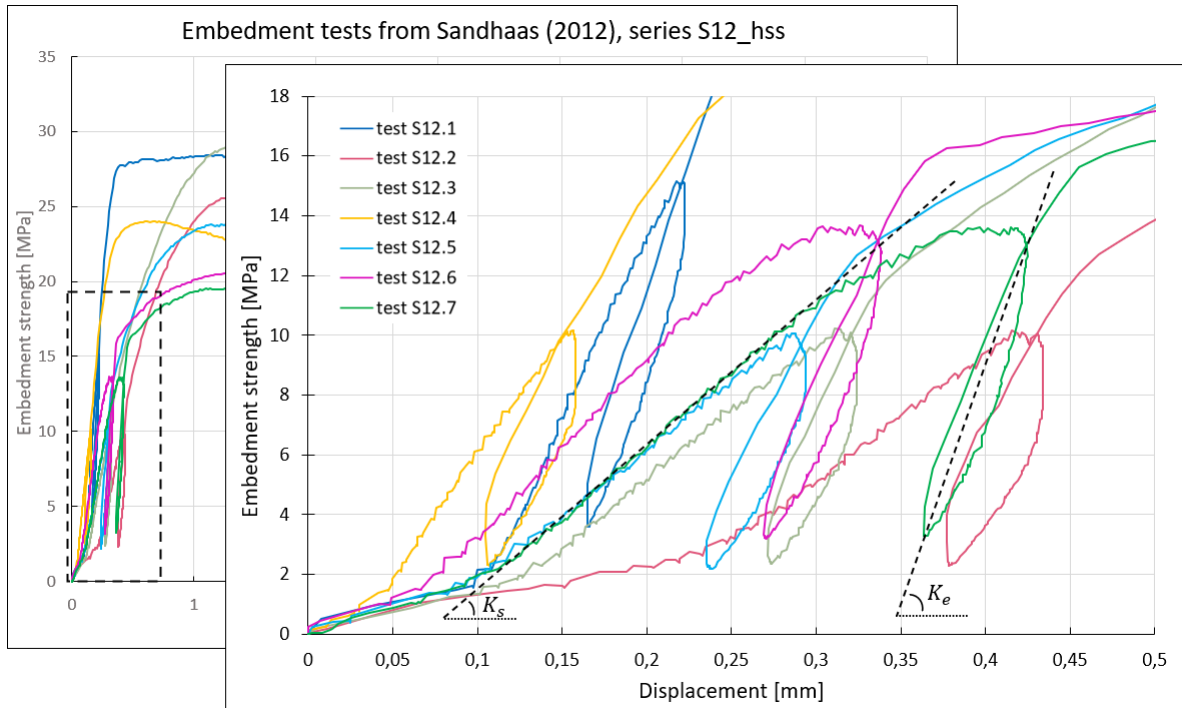
**Figure 3.7:** Embedment tests with 12mm hss dowels in spruce. Source: the figures are generated from data shared by C. Sandhaas. They are zoomed-in versions of Figure A-28 in her PhD thesis [43].

In the formula for $K_{ser}$ in EC5 (equation 2.24), the dowel slenderness, i.e. the ratio between dowel diameter and timber member thickness, is not considered. To research if the timber member thickness influences the stiffness, the side member thickness from the single-dowel connection shown in figure 3.3 is varied. Thicknesses of 50, 75, 100, and 125mm are considered. The impact on stiffness is analysed using BOF modelling. Only one-half of the connection is modelled, which is possible because it is symmetric. A support that prevents the rotation of the dowel at the location of the steel plate is placed at the symmetry plane. The obtained elastic deformation for $t_1$=50 and 75mm at an applied load of 0.4R is shown in figure 3.8. A more elaborate illustration of the BOF model can be found in figure B.1 in Appendix B.1. The obtained results are listed in table 3.1.
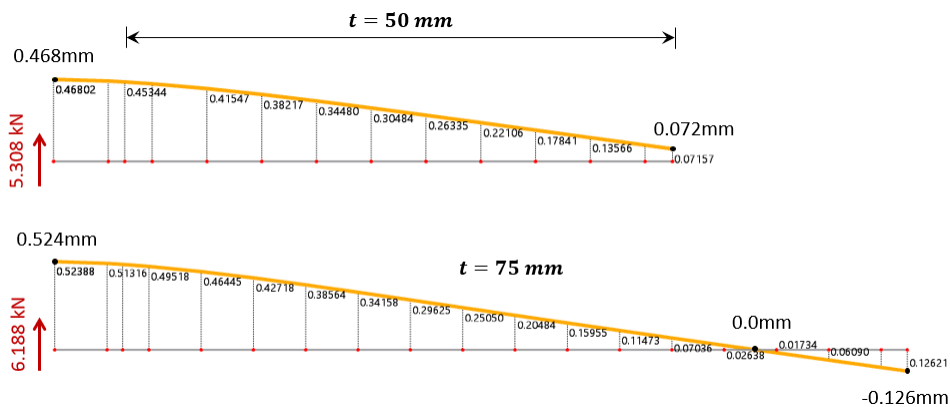


**Figure 3.8:** Displacements obtained from the BOF model for $t_1$ = 50 and 75mm at an applied load of 0.4R.

**Table 3.1:** Comparison of stiffness for different side member thicknesses using BOF model. Values are expressed per shear plane within the double-shear single-dowel connection.

| $t_1$ [mm] | $F_{v,Rk}$ [kN] | FM (fig. 2.1) | 0.4R [kN] | 0.1R [kN] | $u_{0.4}$ [mm] | $u_{0.1}$ [mm] | $k_{s,BOF}$ [kN/mm] |
|---|---|---|---|---|---|---|---|
| 50 | 13.27 | g | 5.308 | 1.327 | 0.468 | 0.171 | 13.40 |
| 75 | 15.47 | g | 6.188 | 1.547 | 0.524 | 0.190 | 13.92 |
| 100 | 18 | h | 7.2 | 1.8 | 0.572 | 0.207 | 14.79 |
| 125 | 18 | h | 7.2 | 1.8 | 0.562 | 0.202 | 15.04 |
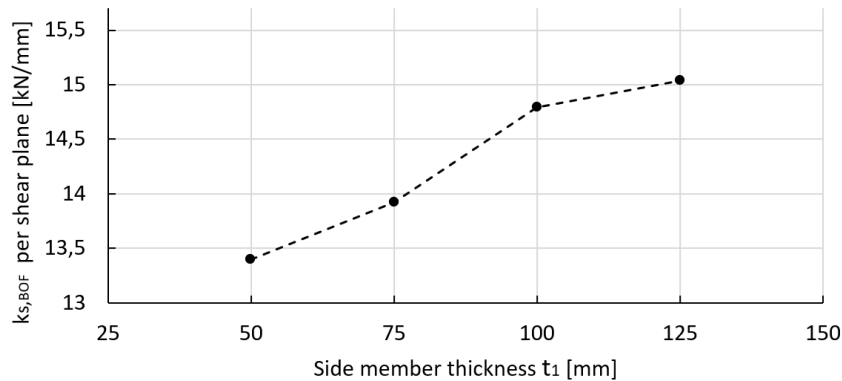


**Figure 3.9:** Relation between slip modulus $k_s$ and side member thickness.

From the results, graphically shown in figure 3.9, it can be concluded that the side member thickness does impact the stiffness. The slip modulus becomes higher when the member thickness increases. For the analysed connection, a doubling of the side member thickness (from 50mm to 100mm) would result in an increase in stiffness per shear plane of approximately 10%. Figure 3.8 shows that for $t_1$=50mm, all displacements are in the same direction. For the connections with larger side member thicknesses, the direction of the displacement will vary depending on the considered position. The influence of the timber member thickness on connection stiffness is also discussed by Jockwer & Jorissen [27] and Lemaître et al. [33]. Jockwer and Jorissen identified this relationship based on many tests of timber-to-timber connections with varying side member thicknesses.

## 3.4. Multi-dowel connection

Timber connections with slotted-in steel plates are commonly used within stability trusses to connect the members. Numerous dowels are applied to connect the steel plates and the timber members. These dowels are regularly continuous, which makes their assembly challenging when multiple steel plates are used. Oversized holes in the steel plates are present to ensure the smooth assembly of the dowels. In this section, the stiffness of multi-dowel connections is analysed. The aim is to be able to make a better estimation of the stiffness of large steel-to-timber connections. First, connections with multiple dowels in a row are studied. Thereafter, connections with multiple dowels in a row and multiple rows of dowels are investigated.

### 3.4.1. Multiple fasteners in a row

Jorissen [30] discussed the effect of the number of fasteners in a row and the spacing in between on the connection strength. He conducted tests on bolted timber-to-timber connections and found that the strength per fastener is reduced as the number of fasteners in a row increases. Based on his research, equation 2.17 has been adopted in EC5.

$$n_{ef} = n^{0.9} \cdot \sqrt[4]{\frac{a_1}{13d}} \qquad \text{(2.17 revisited)}$$

Jorissen also found a lower stiffness than $K_{ser}$ in EC5 (equation 2.24) suggests for the connections with multiple bolts. He mentioned that the reduction in stiffness, as the number of fasteners increases, is

mainly due to the hole clearance in the timber members. Because of this clearance, the fasteners will be activated sequentially as the connection displacement increases. After a certain displacement, all fasteners will contribute to resisting the applied force, however, the load will not be distributed equally amongst the fasteners. The sequential activation of the fasteners causes a step-wise load-slip curve up to the point where all fasteners are situated against the timber. The displacement of the fasteners under serviceability loading might be less than that required to 'activate' all fasteners. In that case, the number of effective fasteners, contributing to the connection stiffness, will be less than the actual number of fasteners. Jorissen proposed equation 3.5 to account for the reduction in stiffness, caused by clearance, for multiple bolted timber-to-timber connections. The equation suggests that the stiffness per shear plane is only 30% of that obtained if the equation from EC5 is used.

$$k_{ser} = k_{bolt} \cdot \frac{\rho_k^{1.5} \cdot d}{20} = 0.3 \cdot \frac{\rho_k^{1.5} \cdot d}{20} \tag{3.5}$$

where $k_{ser}$ = slip modulus [$N/mm$], $k_{bolt}$ = multiplication factor for bolted connections, $d$ = fastener diameter [$mm$], and $\rho_k$ = characteristic density of timber [$kg/m^3$].

In dowelled timber connections with slotted-in steel plates, the holes in the steel plates are regularly oversized for smooth assembly. Sandhaas [43] conducted tests on steel-to-timber connections with one slotted-in steel plate in which an oversize of 0.5mm has been used for the holes in the steel plate. Figure 3.10 shows the load-slip curves for the tested softwood specimens with one, three, and five 12mm hss dowels. It can be observed that the curves show better agreement as the number of dowels increases. The large variation for the single dowel tests is likely the effect of the initial position of the dowel within the hole in the steel plate and the quality of the predrilled holes in the timber. The latter may influence the initial embedment behaviour and, as a consequence, the initial slip. In the load-slip curve with three dowels, the initial slip is larger in comparison to the single-dowel tests. In addition, the first part of the curve is relatively flat, followed by a fairly linear course.
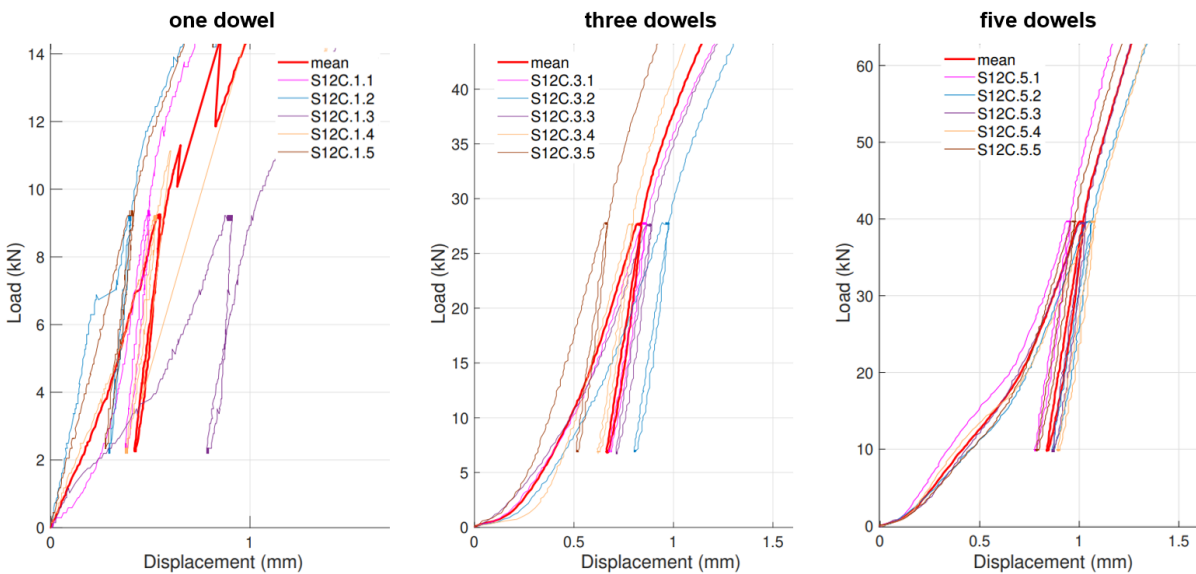


**Figure 3.10:** Load-slip curves from tests on connections with one slotted-in steel plates and one, three, and five 12mm hss dowels in a row. Source: the figures are generated from data shared by C. Sandhaas. They are zoomed-in versions of Figures B-28, B-29, and B-30 in her PhD thesis [43].

The load-slip curves of the tests with five dowels, in figure 3.10, show good agreement. The initial part of the curve (up to 40kN) shows a stepwise behaviour, which is likely due to the sequential activation of the dowels. The five-dowel connections show a linear load-slip behaviour from approximately 20kN. The linear behaviour between 20 and 40kN can be interpreted as the stiffness after various non-linear processes have occurred. The unloading-reloading procedure eliminates all the non-linear effects that are present when the connection is first loaded. Consequently, the linear elastic modulus $k_e$ is expected to be higher and linear, which is confirmed by observing the graph.

Sandhaas [43], Malo et al. [37], and Reynolds et al. [41] all conducted tests on timber connections with slotted-in steel plates in softwood specimens. Malo et al. and Reynolds et al. performed loading sequences specifically meant to analyse the unloading-reloading stiffness of the connections. Their loading protocols can be found in Appendix B.2. In both test procedures, the connections are loaded up to 40% of the estimated characteristic capacity and dowels are installed sequentially. Correspondingly, multiple tests have been performed on the same specimen with varying numbers of dowels.

    Sandhaas [43] her research mainly focussed on the connection capacity, for which she applied the loading protocol according to EN26891. In accordance with this procedure, a loading cycle is performed from which the elastic modulus $k_e$ can be determined. Sandhaas did not report on this elastic modulus in her thesis. To determine the elastic stiffnesses of the tested connections, the recorded load-slip graphs of the tests have been requested. Sandhaas shared the test data, which could then be used to estimate the elastic stiffness of the tested connections.

The elastic stiffness from tested connections with one to five (12mm) dowels in a row is collected. In all tests, the distance between the fasteners in a row is equal to 5d (60mm). The connection parameters and loading procedures accessory to the tests can be found in Appendix B.2. The elastic stiffnesses from the tests are shown in figure 3.11. The stiffness (y-axis) is expressed per dowel per shear plane.
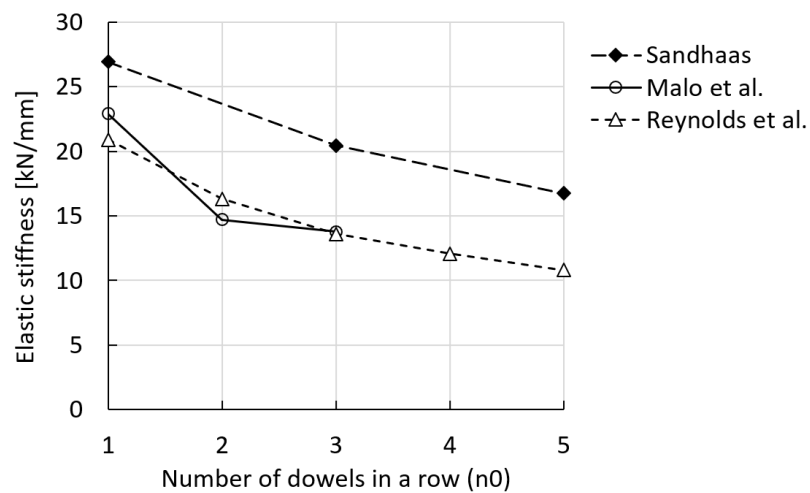


**Figure 3.11:** Elastic stiffness of connection tests with a slotted-in steel plate and one to five 12mm dowels in a row. Sources: Sandhaas [43], Malo et al. [37], and Reynolds et al. [41].

From figure 3.11, it can be observed that the tests from Sandhaas show higher elastic stiffness values in comparison to the tests performed by the other researchers. This might partly be explained by the higher density and the larger side member thicknesses (see table B.1 in Appendix B.2 for the parameters). The difference in stiffness is also expected to be caused by the smaller hole clearance in the steel plates in the connections from Sandhaas. The clearance is equal to 0.5mm whereas this is 1mm in the tests from the other researchers. The hole clearance in the steel plates is considered to be the main cause for the significant reduction of stiffness as the number of dowels in a row increases. The effective number of dowels contributing to the (elastic) stiffness of the connection, is expected to be higher when the clearance in the steel plates is less. As for the hole clearance in the timber, the dowels are tight-fitted, i.e. hole diameter is the same as the dowel diameter, in all tests.

    Another factor that might cause a difference in the compared elastic stiffnesses is the fitting method. Malo et al. and Reynolds et al. utilized all information from the performed cycles to fit a linear line, whereas, the formula (equation 2.23) prescribed by EN26891 is used to estimate the elastic modulus $k_e$ for the tests performed by Sandhaas. Furthermore, Sandhaas deliberately chose to perform the loading cycles at lower loads ($< 40\%$ of $F_{est}$) to prevent any damage to the specimen. This is done to prevent any damage in the first loading loop because her research mainly focused on the ultimate load-carrying capacity of the connections. The reduced loading level might have affected the elastic modulus. More information about the differences between the performed tests can be found in Appendix B.2.

The effective number of fasteners that contribute to the stiffness of a multi-dowel connection can be calculated with equation 3.6.

$$n_{ef} = \frac{k_{multiple}}{k_{single}} \tag{3.6}$$

where $n_{ef}$ = effective number of dowels, $k_{multiple}$ = stiffness (per shear plane) of the multi-dowel connection, and $k_{single}$ = stiffness (per shear plane) of the single-dowel connection.

Malo et al. [37] composed a model that can be used to estimate the elastic stiffness of a connection with dowels and slotted-in steel plates. In their model, the connection stiffness is dependent on the number of dowels. The model is based on the tests they performed, from which it became clear that, as the number of dowels in a row increases, the stiffness per dowel per shear plane decreases. For the effective number of dowels in a row, they proposed equation 3.7. In their complete model, the number of dowel rows is also considered to cause a reduction of stiffness. This will be discussed in the next section.

$$n_{ef} = 0.3 + 0.7e^{\frac{1-n_0}{2}} \tag{3.7}$$

$$n_{ef} = n_0{}^x \tag{3.8}$$

where $n_{ef}$ = effective number of dowels in a row, $n_0$ = actual number of dowels in a row (from 1 up to 10), and $x$ = exponent (0-1).

The form of another possible formula for the effective number of dowels is shown in equation 3.8. If the exponent is set equal to 0.9 the formula is similar to that prescribed by EC5 for the effective number of dowels in a row with respect to load-carrying capacity (equation 2.17). The effective number of dowels in a row, determined using the elastic stiffness from test data previously shown in figure 3.11, is plotted in figure 3.12. In addition, possible formulas representing the effective number of dowels in a row are plotted in this figure. The prediction equations are plotted for up to 10 dowels in a row.
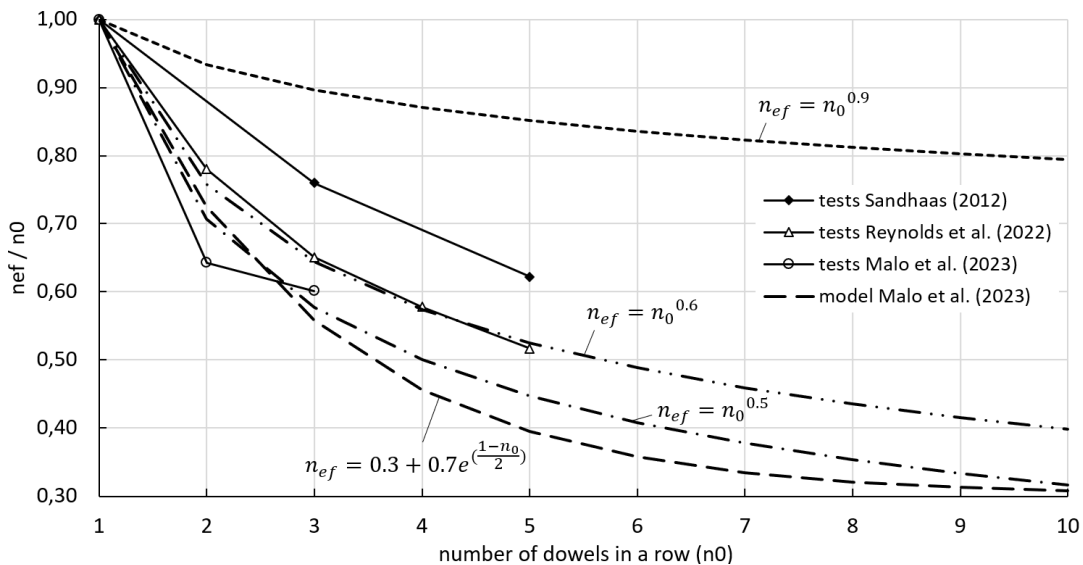


**Figure 3.12:** Effective number of dowels in a row (nef) for the elastic stiffness as a function of the number of dowels in a row (n0).

## 3.4.2. Group-effect

Malo et al. [37] performed tests on timber connections with dowels and slotted-in steel plates to evaluate their stiffness. The aim of their research was to quantify the serviceability stiffness of connections with numerous dowels. The study is designed specifically for connections in the context of trusses in multi-storey buildings. The researchers based the geometries and materials used for testing on the connections used in the Mjøstårnet building.

Three small-scale specimens and one large-scale specimen were used to perform multiple tests. They performed multiple loading cycles to determine the elastic stiffness of the connections. Based on the results, the researchers composed a model that can be used to estimate the connection stiffness of large-scale connections with 12mm dowels and softwood members. Equation 3.9 is the proposed 'engineering model' that can be used for connections with dowels loaded either parallel or perpendicular

to the grain.  The loading direction in relation to the grain orientation is found to have a significant impact on the stiffness and should therefore be considered.  The model is coupled to the stiffness $k_{ser}$ calculated with the formula from EC5 (equation 2.24).

$$K_{ser,mod} = k_{ser} \cdot m \cdot n_{spd} \cdot n_0 \cdot (q_{0,1} + q_{0,2}e^{\frac{1-n_0}{r_0}}) \cdot n_{90} \cdot (q_{90,1} + q_{90,2}e^{\frac{1-n_{90}}{r_{90}}}) \qquad (3.9)$$

$K_{ser,mod}$ = serviceability stiffness of a multi-dowel connection with slotted-in steel plates [$kN/mm$].

$k_{ser}$ = slip modulus per dowel per shear plane according to equation 2.24 (steel-to-timber) from EC5 [$kN/mm$].

$m$ = factor that accounts for the error made by $k_{ser}$ for a single dowel.

$n_{spd}$ = number of shear planes per dowel.

$n_0$ = number of dowels along the grain.                          $n_{90}$ = number of dowels perpendicular to the grain.

$q_{0,1}$, $q_{0,2}$, and $r_0$ = govern the non-dimensional asymptotic decrease for a row of dowels along the grain.

$q_{90,1}$, $q_{90,2}$, and $r_{90}$ = govern the non-dimensional asymptotic decrease for a row of dowels perpendicular to the grain.

Unloading-reloading cycles were performed to estimate the elastic stiffness of the tested connections. For a single dowel connection, this stiffness is reported to be much higher than $k_{ser}$.  In the model, the parameter $m$ accounts for this difference.  For a single-dowel connection with a 12mm dowel and timber with a mean density of $430kg/m^3$, the stiffness according to EC5 is 9.3kN/mm per shear plane. For the same connection in which the dowel is loaded parallel to the grain, Malo et al. measured an average elastic stiffness of 22.89kN/m per shear plane.  To account for this difference, parameter $m$ is approximately 2.5, meaning that the measured elastic stiffness for a single dowel connection is two and a half times higher than $k_{ser}$.  In equation 3.9, the expressions within brackets incorporate the decaying stiffness dependent on the number of dowels parallel and perpendicular to the grain.  At last, the parameter $n_{spd}$ (the effective number of shear planes) can be used to consider the effect of unequal stiffness of inner and outer timber members.

For this thesis, we are particularly interested in the group effect of dowels loaded parallel to the grain.  An important conclusion from the study by Malo et al. is that for an equal number of dowels parallel to the grain, the stiffness per dowel will be reduced when the number of dowels perpendicular to the grain increases.  The recommended model parameters for large-scale connections loaded parallel to the grain are listed in figure 3.13.  For the determination of these parameters, the researchers put the most emphasis on the domain with numerous dowels (>10).  Therefore, the model is expected to be mainly applicable to large timber connections.  The part of the model that accounts for the decaying, as a function of the number of dowels, is graphically illustrated in figure 3.13.



Plotted equation:

$$f(n_0, n_{90}) = (q_{0,1} + q_{0,2}e^{\frac{1-n_0}{r_0}}) \cdot (q_{90,1} + q_{90,2}e^{\frac{1-n_{90}}{r_{90}}})$$

Parameters:

$q_{0,1} = q_{90,1} = 0.3$

$q_{0,2} = q_{90,2} = 0.7$

$r_0 = 2 \qquad r_{90} = 4$

$m = 2.5$
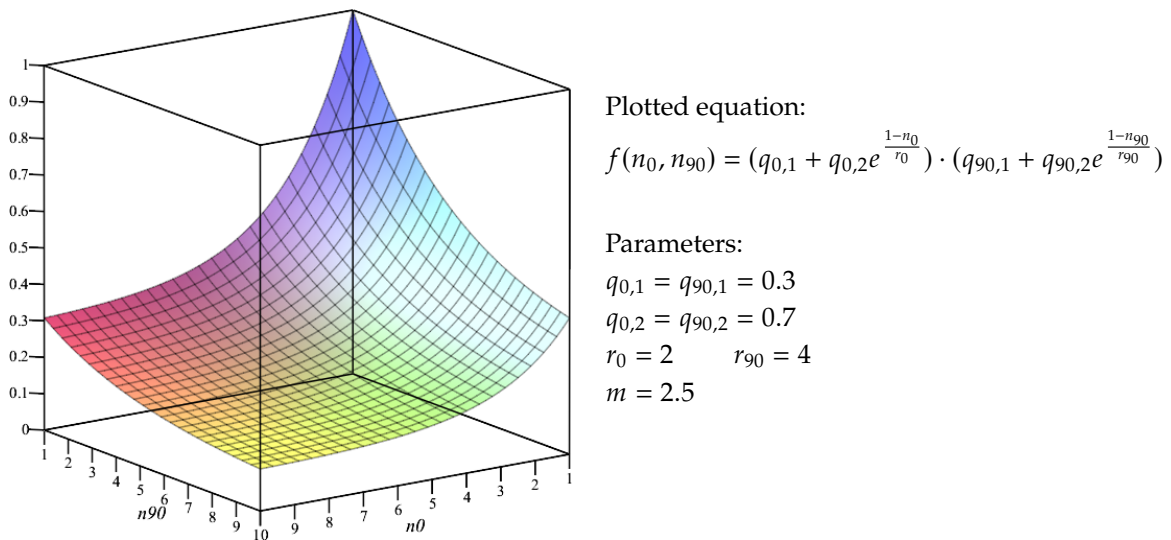
**Figure 3.13:** Graphical representation of the average relative stiffness dependent on dowels in the two directions and model parameters for 12mm dowels loaded parallel to the grain. Source: the figure is based on [37, Fig. 24], the parameters are taken from [37, Tab. 5].

Note that the parameters in figure 3.13 are determined such that the effective number of shear planes (parameter $n_{spd}$) should be taken equal to the actual number of shear planes. The researchers, however, mentioned that for more widespread application of the model, it is probably wise to consider $n_{spd}$ separately. More information about the effective number of shear planes in dowel-type connections with multiple shear planes can be found in Bocquet et al. [8]. Equations 3.10 and 3.11 show the model including the recommended parameters.

$$K_{ser,mod} = 2.5k_{ser} \cdot n_{spd} \cdot n_0 \cdot (0.3 + 0.7e^{\frac{1-n_0}{2}}) \cdot n_{90} \cdot (0.3 + 0.7e^{\frac{1-n_{90}}{4}}) \tag{3.10}$$

$$K_{ser,mod} = k_e \cdot n_{spd} \cdot n_0 \cdot (0.3 + 0.7e^{\frac{1-n_0}{2}}) \cdot n_{90} \cdot (0.3 + 0.7e^{\frac{1-n_{90}}{4}}) \tag{3.11}$$

where $k_e$ = elastic stiffness per dowel per shear plane for a single-dowel connection [$kN/mm$], $n_{spd}$ = number of shear planes, $n_0$ = number of dowels along the grain, and $n_{90}$ = number of dowels perpendicular to the grain.

The stiffness obtained from tests and by using the engineering model for the large-scale connections from Malo et al. [37] are shown in figure 3.15. The geometry of the tested large-scale connections is shown in figure 3.14. A maximum of five dowels in a row were tested. The researchers observed that the stiffness approaches an asymptotic value as the number of dowels in a row increases. This is one of the principles adopted in the model parameters accounting for the decaying stiffness behaviour. The asymptotic values for the tested top- and middle large-scale connections are shown in figure 3.15. The figure shows that the middle connection has a higher stiffness in comparison to the top connection. According to the proposed model, this difference is solely caused by the number of dowels perpendicular to the grain. The middle connection has five dowel rows, whereas the top connection has seven rows of dowels. However, it is noteworthy that their dowel pattern differs, which might also have an effect.
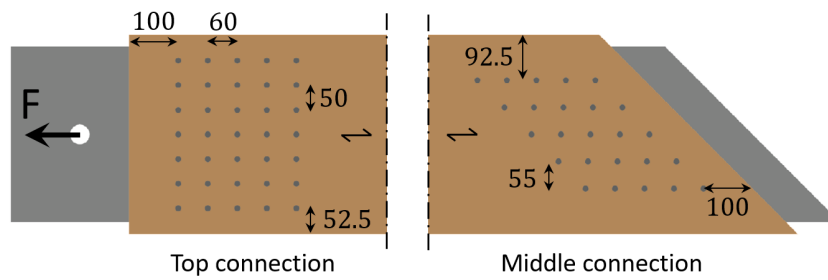


**Figure 3.14:** Geometry of the large-scale connections tested by Malo et al. Based on [37, Fig. 6].
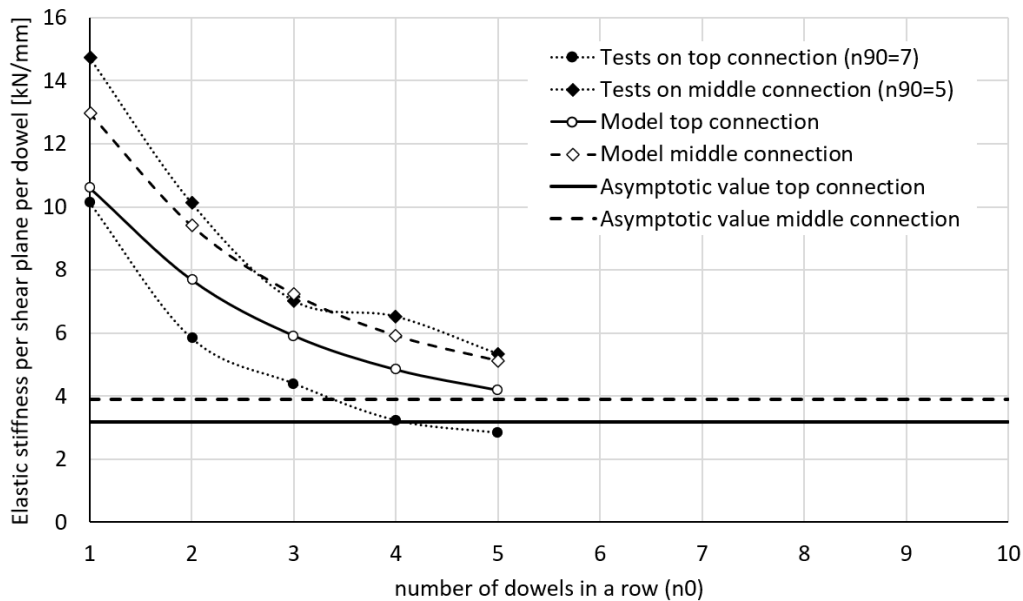


**Figure 3.15:** Elastic stiffness of the large-scale connections from Malo et al. [37]. Based on [37, Fig. 22].

Malo et al. [37] verified their model by comparing it with the measured connection stiffness of the large-scale connections. A comparison between the connection stiffness according to the proposed model, the measurements and according to EC5 is shown in table 3.2. In addition to the connections from Malo et al., a 35-dowel connection with similar geometry is tested by Reynolds et al. [41]. The stiffness of this connection is also estimated using the proposed model. This is an interesting verification of the model because several parameters differ in comparison to the top- and middle large-scale connections from Malo et al.

First and foremost, for the 35-dowel connection from Reynolds et al., the mean density is measured to be $378kg/m^3$ which is expected to reduce the stiffness of the connection since the embedment strength is lower. Second, the number of shear planes is more. Three slotted-in steel plates with a thickness of 8mm are used. Furthermore, the timber member sizes differ. The inner timber members are thinner (80mm) than the outer members (108mm). Last, the 12mm dowels have a lower steel grade (S355) which is not expected to influence the elastic bending behaviour of the dowels, however, it does reduce the characteristic capacity calculated according to Johansen's Yield Model (section 2.2.1). When 10 and 40% of this capacity are considered to represent serviceability loading conditions, the applied forces will be less, under the condition that failure modes with plastic hinges govern the connection capacity, in comparison to a connection with hss dowels. The amount of applied load might affect the connection stiffness, but its influence is expected to be little. It is also noteworthy to mention that Reynolds et al. performed fewer unloading-reloading cycles. This is important because Malo et al. specifically mentioned that the load-slip curves appeared on top of each other after performing multiple unloading-reloading cycles.

The stiffness of the 35-dowel connection is estimated using equation 3.11 and the elastic stiffness of the single-dowel connection reported by Reynolds et al. [41]. To clarify, the model is coupled to the elastic unloading-reloading stiffness, measured by Reynolds et al., for a single dowel connection. For this connection, the mean value of the elastic stiffness per shear plane is reported to be 20.9kN/mm. The estimated elastic stiffness of the 35-dowel connection can be read from table 3.2.

**Table 3.2:** Comparison of the elastic stiffness from measurements, analytical model (equation 3.11), and EC5 (equation 2.24) of large steel-to-timber connections.

| Connection | Stiffness per dowel per sp [kN/mm] | | Parameters | | | Elastic stiffness [kN/mm] | | |
|---|---|---|---|---|---|---|---|---|
| | $K_{ser}$ EC5 | Measured | $n_{spd}$ | $n_0$ | $n_{90}$ | Measured | Model | EC5 |
| Top [37] | 9.304 | 22.89 | 4 | 5 | 7 | 540 | 586 | 1303 |
| Middle [37] | 9.304 | 22.89 | 4 | 5 | 5 | 522 | 512 | 930 |
| 35 dowels [41] | 7.669 | 20.90 | 6 | 7 | 5 | 846 | 819 | 1610 |

From table 3.2 it can be concluded that the stiffness estimated using the model from Malo et al. shows good agreement with the measured values. This is not only the case for their tested connections, but also for the 35-dowel connection tested by Reynolds et al. In figure 3.16 the three large-scale connections are plotted within the graphical representation of the decaying part of the model. In addition, the computed reduction factor, which can be interpreted as the effective number of dowels, is shown. This factor is the ratio between the elastic stiffness of the large timber connection expressed per dowel per shear plane and the elastic stiffness for a single-dowel connection (also per shear plane). The computed factors are 0.18, 0.22, and 0.187, thus, the elastic stiffness per dowel per shear plane of these large connections is estimated to be approximately one-fifth of the stiffness from a single dowel connection.

**Top:** $f(n_0, n_{90}) = f(5,7) = 0.180$
**Middle:** $f(5,5) = 0.220$
**35-dowels:** $f(7,5) = 0.187$
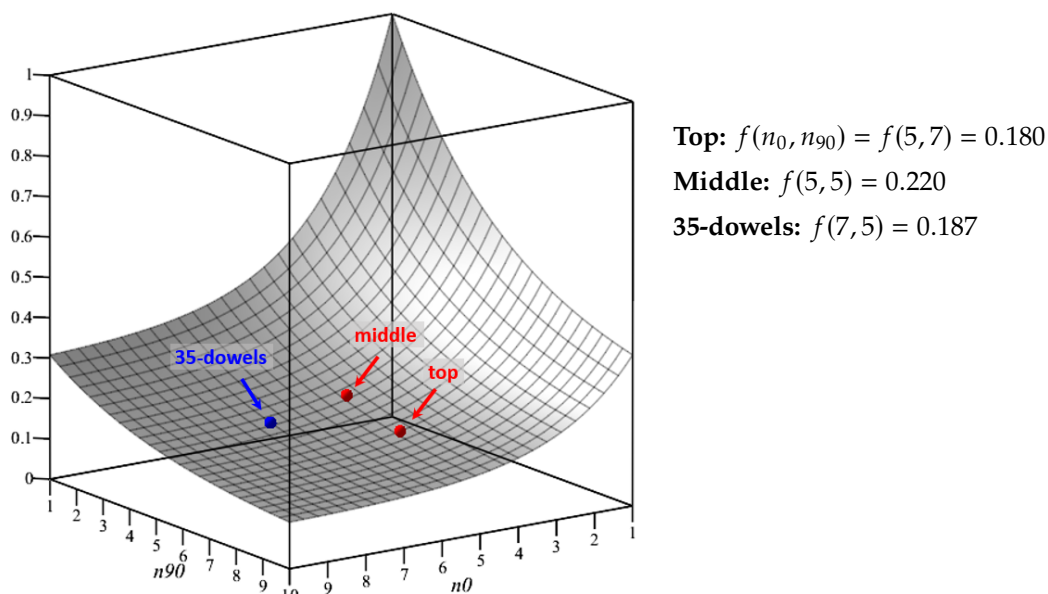
**Figure 3.16:** Points showing the stiffness reduction factor for the connections used in the verification of the model. The figure is based on [37, Fig. 24].

### 3.4.3. Initial slip

Manufacturing- and construction tolerances can influence both the load-carrying capacity and the stiffness of a multi-dowel connection. They include effects like misalignment of the holes, variation of the hole diameters, and the initial position of the fasteners [30]. Reynolds et al. [41] researched the stiffness and initial slip of multi-dowel timber connections with slotted-in steel plates. Based on tests, they found that the oversized holes in the steel plates, commonly used in practice to allow for easy assembly, impact the load-slip behaviour of a multi-dowel connection. The initial position of the fasteners in the holes in the steel plates will cause the dowels to be activated, i.e. contribute to load-carrying capacity and stiffness, sequentially. Some dowels will be situated against the steel plate when assembled, whereas others will be on the opposite side of the holes. For the latter, the dowel only contributes to the stiffness after a displacement equal to the oversize of the hole in the steel plate has been bridged. The effect of manufacturing and construction tolerances on the behaviour of a group of fasteners in a steel-to-timber connection is illustrated in figure 3.17.



**(a)** Timber member(s).
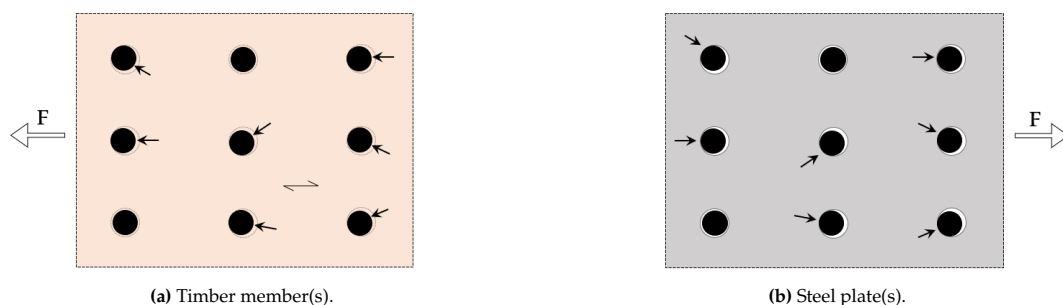


**(b)** Steel plate(s).

**Figure 3.17:** Example of a steel-to-timber connection with non-activated and activated (and some oblique loaded) dowels within a large group at a displacement equal to half of the hole clearance in the steel plates.

Reynolds et al. [41] tested a softwood specimen with large timber connections (with equal geometry) on both sides of the specimen. The connections, shown in figure 3.19 have 35 dowels and three slotted-in steel plates. In their paper, Reynolds et al. plotted the load-slip behaviour of the full specimen, i.e. with the slip of two connections. This plot has been digitized and adjusted such that it shows the load-slip behaviour for a single 35-dowel connection. This load-slip curve and the linear fitted stiffnesses are shown in figure 3.18. In the connections, 12mm dowels are used and the steel holes are 13mm. Thus, an

oversize/hole clearance in the steel plate of 1mm is present.
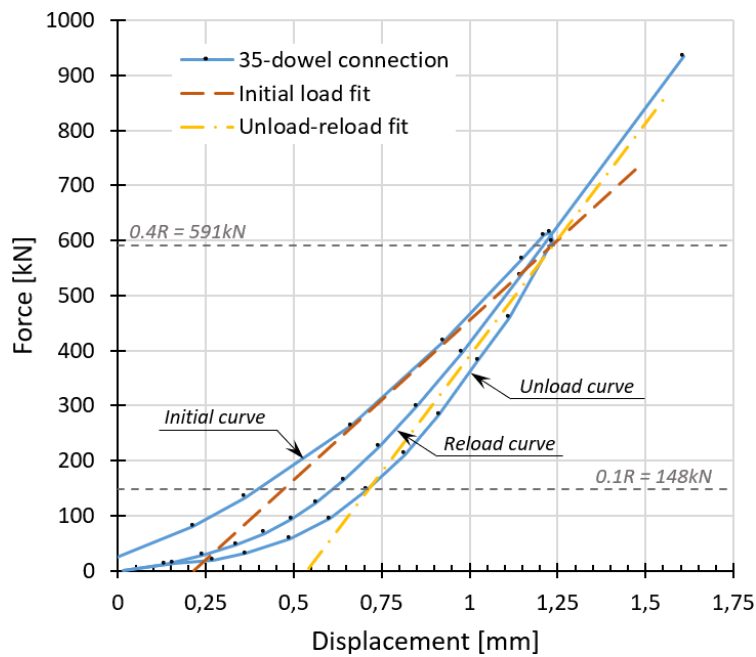


**Figure 3.18:** Load-slip curve of the 35-dowel connection tested by Reynolds et al. Based on [41, Fig. 11].
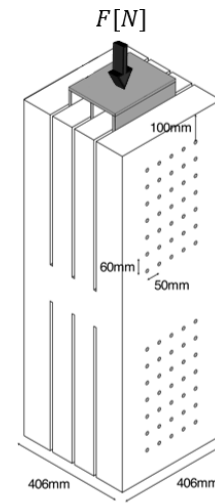
**Figure 3.19:** Test specimen with two 35-dowel connections [41, Fig. 1].

Figure 3.18 shows that the unload-reload stiffness of the connection is higher in comparison to the initial stiffness. The reload curve shows a smooth increase from 0 up to 591kN, which is 40% of the estimated load-carrying capacity of the connection. Note that this curve does not yet exhibit a linear trajectory after exceeding a load of 0.1R (10% of $F_{est}$). Rather, the curve is linear from a load of approximately 300kN which corresponds to 20% of $F_{est}$. This shows that it is not accurate to presume that the connection stiffness is linear after 10% of $F_{est}$. The non-linear initial part of the curve is caused by the hole clearance in the steel plates and the corresponding sequential activation of the dowels. Using the 10/40 criterion for $k_e$ from EN26891 [22] will give a lower stiffness than the unload-reload stiffness determined by Reynolds et al. This suggests that the 10/40 criterion is not suitable for determining the elastic stiffness of these types of large steel-to-timber connections. Similar to Reynolds et al., Malo et al. [37] also used a different approach to make a fit on the load-slip behaviour of their tested connections. They utilized all information from the performed cycles and used the method of least squares to make a linear fit. Based on their observations, Reynolds et al. propose to idealize the load-slip behaviour of large steel-to-timber connections by two parameters: the zero-stiffness region and the unload-reload stiffness. This representation is illustrated in figure 3.20.
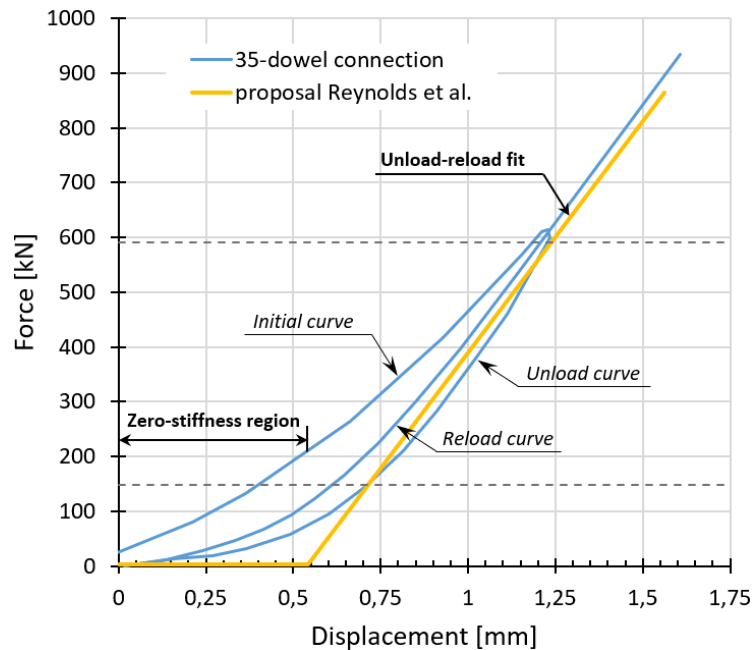
**Figure 3.20:** Proposal by Reynolds et al. for the idealization of the load-slip curve. Based on [41, Fig. 11].

All data on the load-slip curve between 10 and 40% of the estimated failure load is used to make the unload-reload fit in figure 3.20. The zero-stiffness region is defined as the intersection between this fit and zero force. For the tested 35-dowel connections, the unload-reload stiffness is 846kN/mm and the zero-stiffness region is 0.55mm. The latter is caused by the hole clearance in the steel plates in combination with various non-linear processes [41]. Mainly plastic deformation around the hole in the timber is responsible for the non-reversible hole opening that causes the zero-stiffness region.

### 3.4.4. Tri-linear idealization

The proposal from Reynolds et al. [41] to idealize the load-slip behaviour of a connection into a zero stiffness region followed by the unload-reload stiffness has been discussed in the previous section. This idealization greatly simplifies the load-slip behaviour before the connection reaches its elastic stiffness. In this section, two possible tri-linear idealizations to represent the load-slip behaviour are discussed. The reason for this is that, in practice, some connections will be loaded by a low force and the approach from Reynolds et al. might overestimate their local displacement. The idealizations are based on two different lines of thought:

- **Tri-linear idealization 1**: the first part of the curve (Region 1/R1) is the initial slip of the connection. This region, with zero stiffness, is the result of non-reservable deformation caused by densification around the timber holes. The load-slip behaviour is presumed to exhibit its linear elastic stiffness from the point at which the load is 0.1R (Region 3). Last, a linear line between the end of R1 and the beginning of R3 is drawn in which the connection exhibits a low stiffness, i.e. lower than the elastic stiffness in R3.

- **Tri-linear idealization 2**: this idealization presumes that the load-slip behaviour will be linear from the point where a displacement equal to the hole clearance in the steel plates has occurred. The initial slip region (R1) and R2 are determined in the same manner as discussed in Idealization 1. Note that in this second idealization, the stiffness in R2 is higher in comparison to idealization 1. Furthermore, the elastic stiffness trajectory will be present after a much higher force.

Illustrations of both tri-linear idealizations, for the 35-dowel connection from Reynolds et al. [41], are shown in figure 3.21. These are merely examples, and more large-scale tests are necessary to establish accurate load-slip relationships. Reynolds et al. mentioned that even for connections with fasteners that do not require hole clearance in the steel plates, significant irreversible deformation of the timber will occur. Based on the embedment tests in Reynolds et al. [40] they estimated that this non-reversible deformation can be up to 0.45mm. This is determined by back-calculation of the difference in the initial

and unload-reload stiffness of tests with 12mm screws. More tests under serviceability loading are required to quantify this value. The amount of irreversible deformation will depend on the level of the load and the number of dowels. The irreversible deformation in the 35-dowel connection is estimated by the difference in the slip between the intersection of the initial- and the unload-reload stiffness fit with zero-force (x-axis). This will give a value of 0.33mm, as can be determined from figure 3.18. This value is taken for the initial slip (region 1) in figure 3.21. This initial slip will also be present if there is no hole clearance in the steel plates. In the second region, the dowels are activated, i.e. contributing to the stiffness, sequentially which is due to the hole clearance in the steel plates.
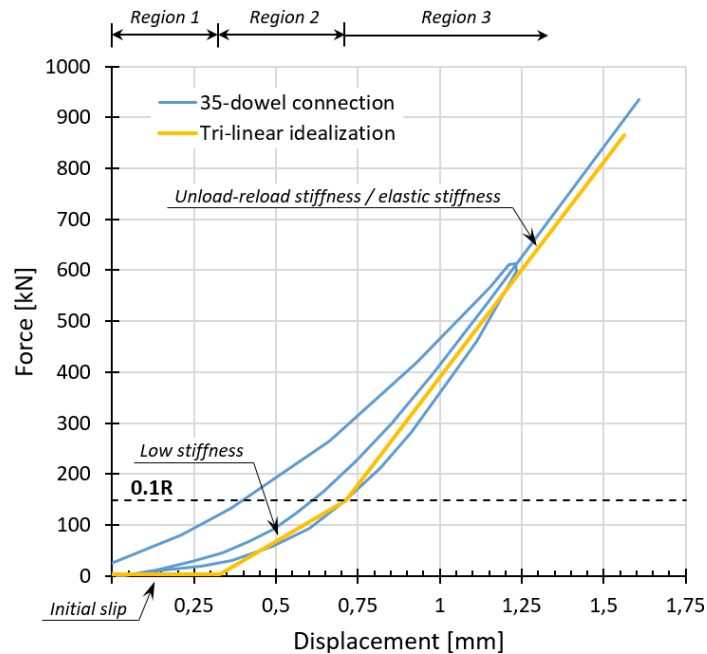


(a) Tri-linear idealization 1: dependent on the applied force (percentage of $R/F_{est}$).
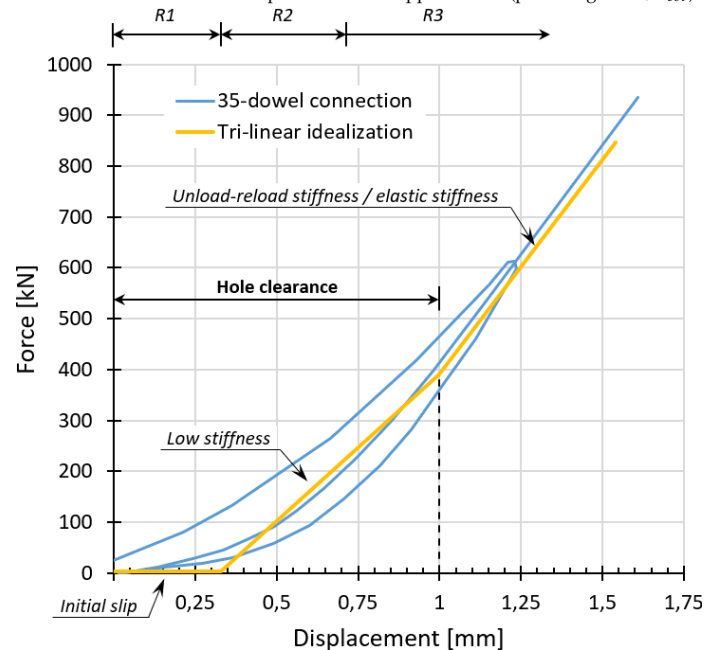


(b) Tri-linear idealization 2: dependent on the hole clearance in the steel plates.

**Figure 3.21:** Example of two tri-linear idealizations to represent the load-slip curve of a large steel-to-timber connection. Source: the idealizations are illustrated in the load-slip curve of the 35-dowel connection from Reynolds et al. [41]. The figures are based on Figure 11 from their paper.

Tri-linear idealizations, like the examples shown in figure 3.21, are meant to better represent the load-slip behaviour before the elastic stiffness is present. These idealizations can be useful to estimate the slip of connections that are exposed to relatively low loads. In the context of timber stability trusses, this is expected to be the case for connections in the upper part of the structure. It is likely that repeated cyclic loading and alternation between tension and compression results in more plastic deformation around the timber holes, which results in a larger initial slip. Such "fully reversed" loading cycles were applied in the tests by Malo et al. [37]. It would be interesting to analyse the load-slip curve corresponding to their large-scale tests. Unfortunately, this graph or information about the amount of initial slip is not shared in their paper. When connections are loaded in cycles but not alternating between tension or compression, it might be necessary to consider different load-slip behaviour for loading in tension and compression. It is expected that the stiffness of a connection loaded in tension is lower in comparison to compression. This can be concluded from the reported stiffness values of the small-scale specimens in Malo et al. [37]. Jorissen [30] also mentioned this difference and discussed that the reason for this is the distinct stress contours.

## 3.5. Summary

**Beam On Foundation (BOF)** modelling is a useful method for the estimation of the stiffness of timber connections. In such a numerical model, the fastener is modelled as an elastic beam and the supporting springs represent the embedment behaviour of the timber. An advantage of this approach is that it allows for detailed modelling of embedment behaviour. Connections with different types of loading angles e.g. parallel and perpendicular to the grain, embedding stiffnesses related to the timber material properties, and non-linear behaviour can be considered by simply adjusting the embedment curves. An extensive review of parametrization equations that can be used to mimic embedment behaviour can be found in Schweigler et al. [46].

A mathematical expression is used to imitate the **embedment behaviour** of a 12mm dowel loaded parallel to the grain. The dowel initially has a low embedment stiffness, which increases non-linearly as the displacement increases. After the dowel has undergone a certain displacement, the embedding stiffness becomes linear. This stiffness is referred to as the elastic embedding stiffness $k_{f,el}$. Several embedment tests are taken from the literature to estimate this stiffness value for 12mm dowels in softwood loaded parallel to the grain. From these embedment tests, the initial slip i.e. the displacement corresponding to the non-linear part is also estimated. This information is then used in the BOF model.

A **BOF model** of a steel-to-timber connection with a single dowel and two shear planes is made in a finite element program. The dowel is modelled as an elastic beam with its actual (circular) cross-section. A non-linear load-displacement curve is assigned to the supporting springs, representing the timber embedment. The slip modulus obtained from the BOF model $k_{s,BOF}$ is found to be higher than the value obtained using the formula prescribed by EC5. The side member thickness is varied to analyse whether this affects the stiffness. It is found that the stiffness (per shear plane) increases when the side members become thicker. The effect of side member thickness (or dowel slenderness) on connection stiffness is currently not considered in the $K_{ser}$ formula. In this chapter, the effect of member thickness on stiffness has been studied using BOF modelling. In literature, this dependency is also mentioned by several authors who analysed test data [27] [33].

The geometry of the modelled single-dowel connection is based on the small specimens used in Malo et al. [37] who measured the **unloading-reloading stiffness** of timber connections with 12mm dowels and slotted-in steel plates. This stiffness is found to be much higher in comparison to the initial stiffness. From observing test data, it became clear that the initial stiffness is very sensitive to production quality. Correspondingly, the unloading-reloading stiffness might be a more representative parameter for the stiffness of connections, since the effect of various non-linear processes is not included. The displacement caused by the settlement of the connection, however, should be accounted for.

Malo et al. [37] applied cyclic loading on timber connections with dowels and slotted-in steel plates to measure their serviceability stiffness. An important conclusion from their study is the reduction in stiffness related to the number of dowels parallel and perpendicular to the grain. Based on the test results, they proposed an **engineering model** to estimate the elastic (unloading-reloading) stiffness of

large timber connections. The accuracy of the model is verified using tests on large-scale connections. The application of this model is currently limited to 12 mm dowels. The model is made in a multiplicative way such that it allows for the inclusion of other effects on stiffness, like the effective number of shear planes [37].

The stiffness of a **group of dowels** is found to be sensitive to the oversized holes in the steel plates because it causes sequential activation of the dowels. Reynolds et al. [41] proposed to idealize the load-slip behaviour of a large steel-to-timber connection by a "zero-stiffness region" followed by the unloading reloading stiffness. The "zero-stiffness region" is created by the hole clearance in the steel plate and non-linear influences like the plastic deformation of the timber.

At last, it is shown that the load-slip behaviour of a large timber connection could be represented using a **tri-linear idealization** of the curve. Two possible idealizations have been discussed (see figure 3.21). In both approaches, the first region of the curve has zero stiffness due to hole opening/densification of the timber as a result of various non-linear effects, i.e. construction- and manufacturing tolerances and non-linear embedment. In the second region, the dowels are activated sequentially due to the hole clearance in the steel plates. The corresponding 'low' stiffness represents the connection stiffness up till the elastic stiffness is reached. The size of the low-stiffness region can be related to the amount of load or the amount of displacement. The slope of the third and last part of the load-slip curve is equal to the elastic stiffness, which may be estimated using the discussed engineering model proposed by Malo et al. [37].

# Part II
## Modelling

# 4

# Case Study: Mjøstårnet

## 4.1. Introduction

To analyse the effect of the load-slip behaviour of connections within a stability truss on SLS design, a study is performed using a finite element model (FEM). The truss in the short facade of Mjøstårnet is used as a case for this study. In this chapter, the design of the building and the FEM model are discussed. In addition, the model is analysed to provide insight into the structural behaviour. The model is established using design rules from Eurocodes and information provided by SWECO Norway (*M. A. Bjertnæs, personal communication, March 2023*). It is chosen to model the stability truss in 2D, but second-order effects are considered.

## 4.2. Building design

Mjøstårnet is built as a symbol of sustainable design, using timber as the main material. The building is located in Brummendal, Norway and is made using local resources, suppliers, and materials. The building accommodates offices, apartments and hotel rooms. At the top of the structure, a pergola is placed. This structure was redesigned in a later stadium of the project because the engineers were challenged to increase the architectural top of the building. The pergola is meant to give an impression of the frame structure used within the building. At completion, the architectural top was located at a height of 85.4m.
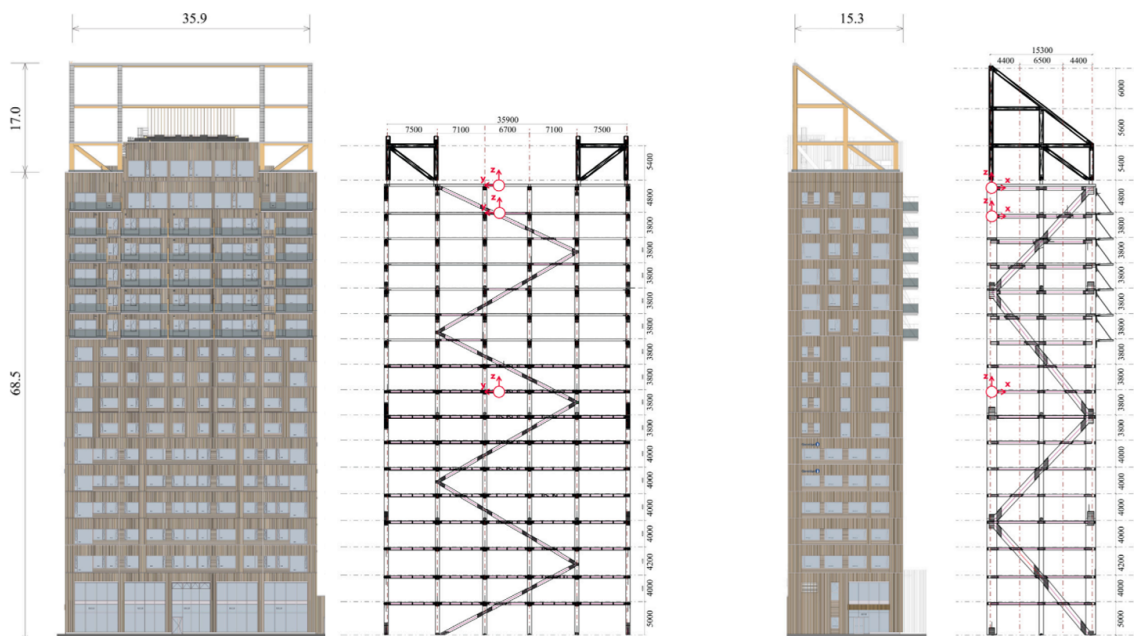


**Figure 4.1:** Mjøstårnet building and frame structure; front- and side view. Adapted from [52, Fig. 1 & Fig. 5a].

The engineering of Mjøstårnet is done by Sweco Norway using the design rules from Eurocodes. Moelven Limtre was responsible for the supply and installation of the structural components [4]. The building's geometry and an impression of the frame structure are shown in figure 4.1.

### 4.2.1. Stability trusses

The building is stabilized by four glulam trusses which are located at the perimeter of the building. In the short direction of the building, four large diagonal members, spanning multiple stories, are present. These are attached to large columns, which form the truss chords, located in the corners of the building. Correspondingly, the diagonals in the short frame span over the full width of the structure. They are of notable size because they have to provide stability within a relatively small width. In the wide facades, the stability trusses consist of six diagonals of smaller size. The corresponding columns, which act as chords, are not at the corner of the building.

**Material**

The glulam elements are of class GL30c, with the exemption of the bottom sections of the corner columns. These sections are of class GL30h. Using standard values for the E-modulus and the densities is considered appropriate for analysing the serviceability behaviour of a timber truss [32]. The properties are in accordance with EN14080 [16] and can be read from table 4.1. The GL30c members consist of lamella with different characteristics. The outer lamellas are of strength class T22, and the inner lamella T15. For the connections, the properties of T15 lamella should be used because most of the dowels will be located in the inner section of the member [37]. The properties of T15 and T22 lamella are shown in table 4.2.

**Table 4.1:** Material properties glulam timber; EN14080 [16].

| Property | Symbol | GL30c | GL30h | Units |
|---|---|---|---|---|
| Bending Strength | $f_{m;k}$ | 30 | 30 | $N/mm^2$ |
| Tensile Strength | $f_{t;0;k}$ | 19.5 | 24 | $N/mm^2$ |
|  | $f_{t;90;k}$ | 0.5 | 0.5 | $N/mm^2$ |
| Compression Strength | $f_{c;0;k}$ | 24.5 | 30 | $N/mm^2$ |
|  | $f_{c;90;k}$ | 2.5 | 2.5 | $N/mm^2$ |
| Shear Strength | $f_{v;k}$ | 3.5 | 3.5 | $N/mm^2$ |
| Shear Modulus | $G_{mean}$ | 650 | 650 | $N/mm^2$ |
| Density | $\rho_k$ | 390 | 430 | $kg/m^3$ |
|  | $\rho_{mean}$ | 430 | 480 | $kg/m^3$ |
| Modulus of Elasticity | $E_{0;mean}$ | 13000 | 13600 | $N/mm^2$ |
|  | $E_{0,05}$ | 10800 | 11300 | $N/mm^2$ |
|  | $E_{90;mean}$ | 300 | 300 | $N/mm^2$ |

**Table 4.2:** Properties for boards/planks for glued laminated timber; EN14080 [16] and EN338 [23].

| Class of boards | $f_{t,0,I,k}[N/mm^2]$ | $E_{t,0,I,mean}[MPa]$ | $\rho_{I,k}[kg/m^3]$ | $\rho_{I,mean}[kg/m^3]$ |
|---|---|---|---|---|
| T15 | 15 | 11500 | 360 | 430 |
| T22 | 22 | 13000 | 390 | 470 |

For the glulam members with strength class GL30c, the characteristic density will be used for strength verifications. A mean density of $430\ kg/m^3$, which is the mean value for timber planks T15, will be used for the estimation of the connection capacities and stiffness.

### 4.2.2. Floors

The seven highest floors (including the roof) are made out of concrete and have a thickness of 300mm. Concrete floors are applied to increase the self-weight of the building, which was necessary to meet serviceability requirements [52]. The other floors are made out of prefabricated timber elements. A typical floor plan, including approximate dimensions, is shown in figure 4.2.
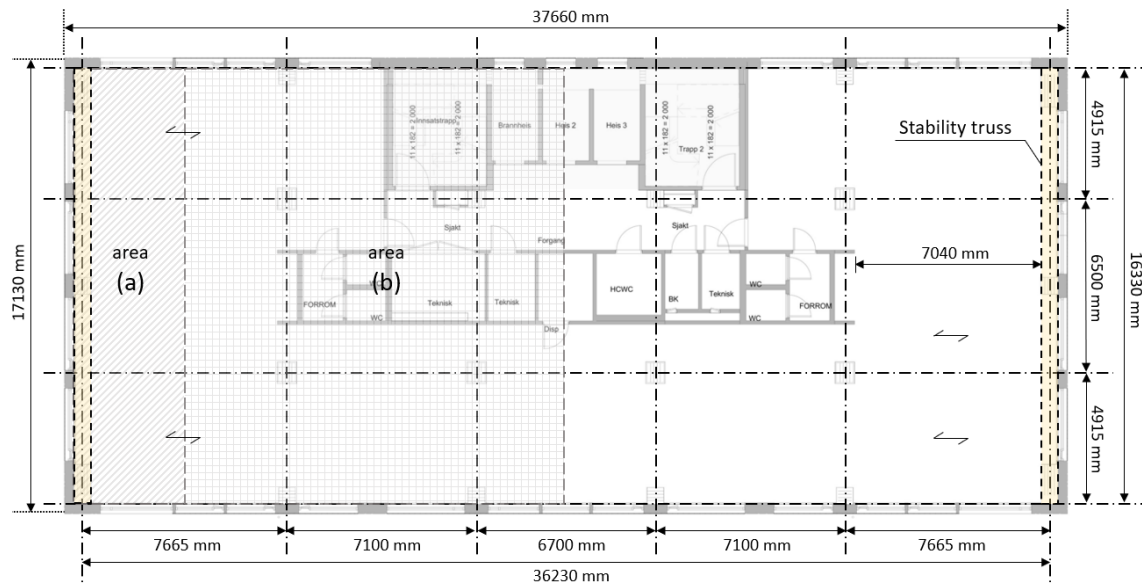
**Figure 4.2:** Typical floor plan (office floor) with approximate dimensions. Adapted from [38, id: 44852]

**Concrete Floors**

The concrete floors are supported by timber glulam (GL30c) beams. Because of the large weight of these floors, the supporting beams are larger in comparison to the supporting beams on timber floors. The 300mm layer of reinforced concrete has a density of $2400 kg/m^3$.

**Timber Floors**

The timber floors consist of decks referred to as the "Trä8 floor system", a design developed by Moelven [3]. These decks are prefabricated and can span up to 8 meters. This floor system is lightweight and uses less wood in comparison to CLT flooring. Because of its low weight, acoustics and vibrations are important design criteria. Moelven has done many tests to verify the system's performance [3]. In Mjøstårnet, the wooden decks span up to 7m and the average width is 2.6m. After installation on-site, a layer of 50mm concrete screed is placed on top. The total thickness of the timber floors is 360mm [52].

## 4.2.3. Truss connections

The truss members are connected with slotted-in steel plates and dowels. The steel plates are most commonly 12mm thick and of steel grade S355. Four steel plates are applied, and continuous dowels are used. The dowels have a diameter of 1mm and a steel grade EN 1.4418 with properties in accordance with EN 10088-3 [15]. The dowels are heat-treated martensitic stainless steel with a yield strength of 755MPa. The holes in the steel plates have a diameter of 13mm, which is 1mm larger than the diameter of the dowel. This is done to ensure smooth assembly of the connections on-site.

**Figure 4.3:** Assembly of a truss connection [38, id: 42180].

The steel plates and dowels are embedded at least 85mm to protect them in case of a fire. The minimum embedment depth can be determined using the simplified reduced cross-section method from Eurocode 1995-1-2 [21]. Furthermore, intumescent fire strips are placed in gaps and slots that expand when exposed to high temperatures [3]. These measurements are taken to ensure sufficient strength of the connections in case of a fire. A three-dimensional image of a truss connection between a corner column and diagonals is shown in figure 4.4. In figure 4.5, a typical geometry of a connection with steel plates slotted in a diagonal member is shown.
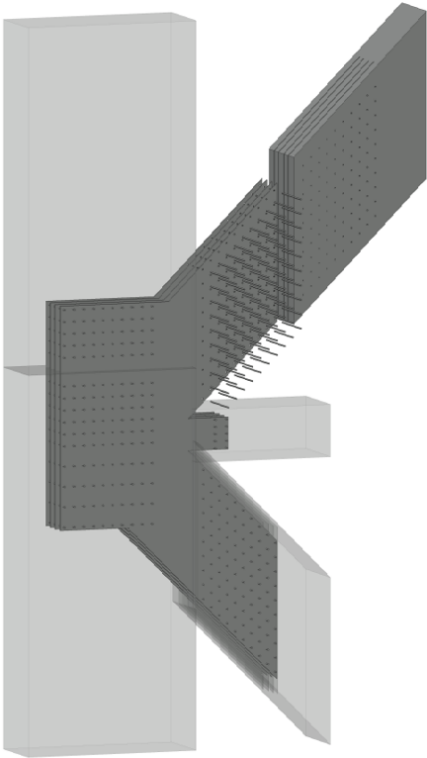


**Figure 4.4:** Truss connection.
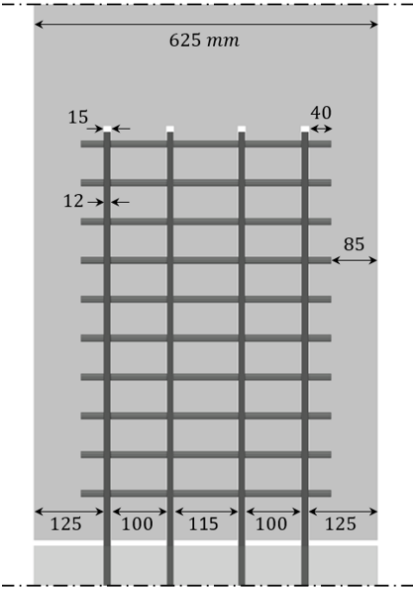


**Figure 4.5:** Typical connection geometry.

## 4.3. Designation of the truss parts

The stability truss located in the short direction of the Mjøstårnet building is studied in this thesis. Names are assigned to the truss members and their connections. These will be used throughout this thesis to refer to specific parts. The adopted designations are shown in figure 4.6.



**(a) Connections**.

**(b) Members**.
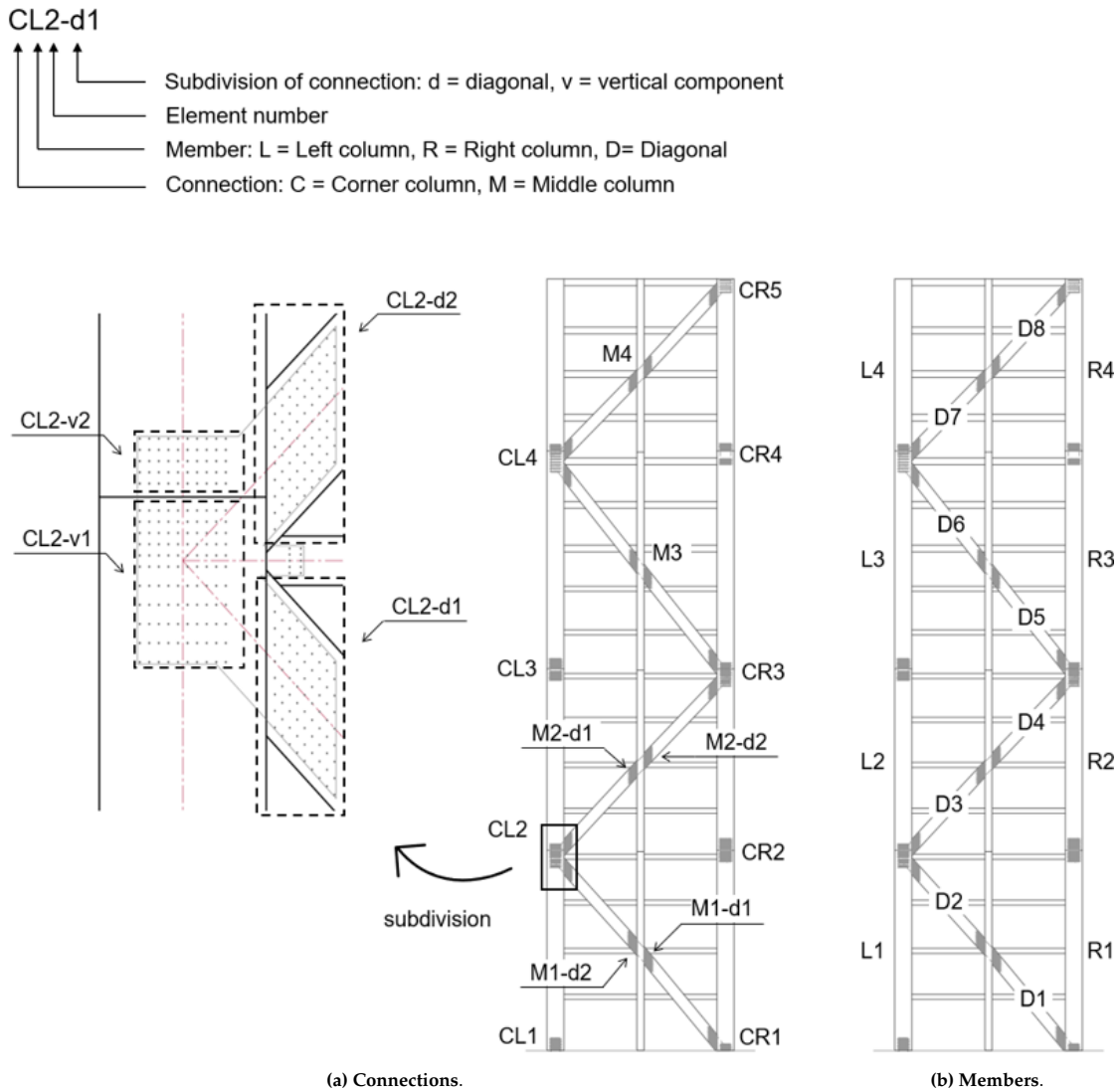
**Figure 4.6:** Designation of the truss parts.

## 4.4. Finite element model

A 2D finite element model (FEM) of Mjøstårnet's stability frame, located in the short facade of the building, is made. It is chosen to simplify the Mjøstårnet building by not modelling the pergola located at the top because it has no structural purpose. The frame is modelled in RFEM6 [49]. Because the building is rectangular and symmetric, the structural behaviour of the modelled stability frame is assumed to be similar to a 3D model. Second-order effects are included by modelling an additional frame. The translation of Mjøstårnet's stability system into a 2D frame model is graphically shown in figure 4.7.
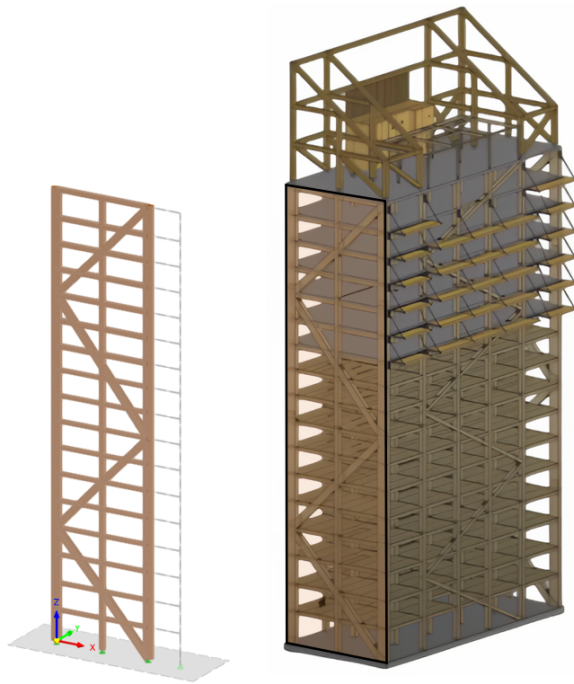
**Figure 4.7:** Modelled frame and its actual location in the Mjøstårnet building. Adapted from [50].
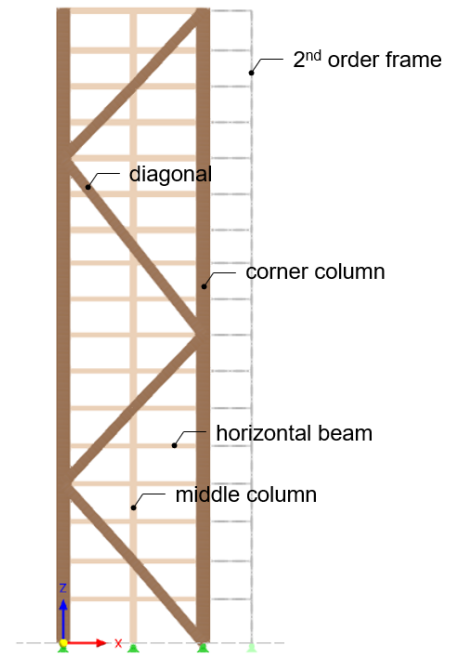
**Figure 4.8:** Adopted names for the members within the modelled frame.

The adopted reference names for the different types of modelled members are shown in figure 4.8. In this figure, the truss structure, consisting of diagonals and corner columns, is emphasized. When spoken of the "frame", the structure including all timber members is referred to. To clarify, these are the truss members, the mid-column, and the horizontal beams. The terms "truss" and "frame" are used throughout the remainder of this thesis. An impression of the considered building (including dimensions) is shown in figure 4.9a. In figure 4.9b the corresponding structural system is shown.
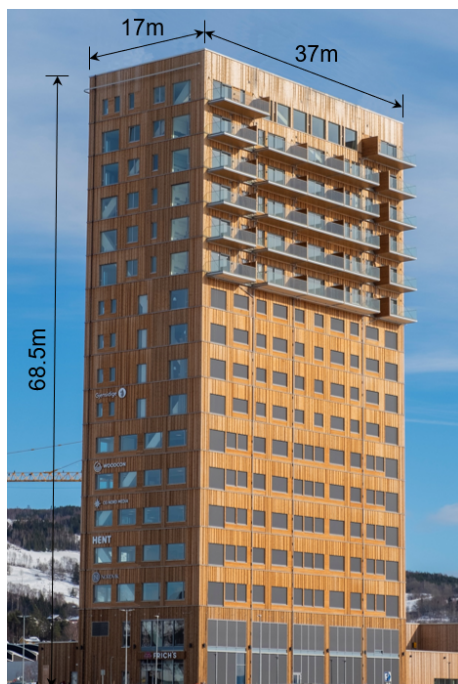


**(a) Building and dimensions.** Adapted from [38, id: 44496].
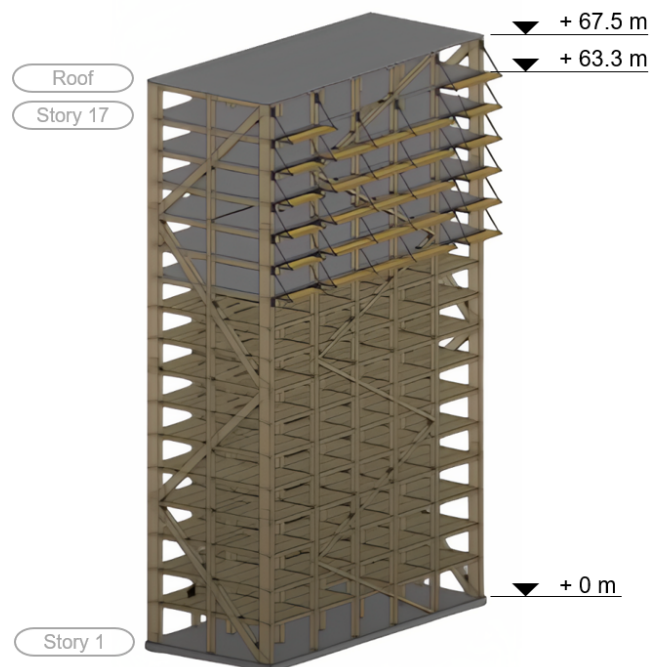
**(b) Structural system.** Adapted from [50].

**Figure 4.9:** Impression of the adjusted/simplified Mjøstårnet building.

In figure 4.9b, the respective heights of the two upper floors (roof and floor 17) are shown. These floors are important with respect to the maximum accelerations, which will be used later in the assessment of the dynamic comfort requirement.

### 4.4.1. Geometry and member dimensions

The geometry of the frame is obtained from detailed drawings provided by SWECO Norway. The global dimensions and member sizes incorporated in the FE model are shown in figure 4.10 and table 4.3 respectively.



**(a)** Global dimensions.　　　**(b)** Modelled members.　　　**(c)** Mechanical model.
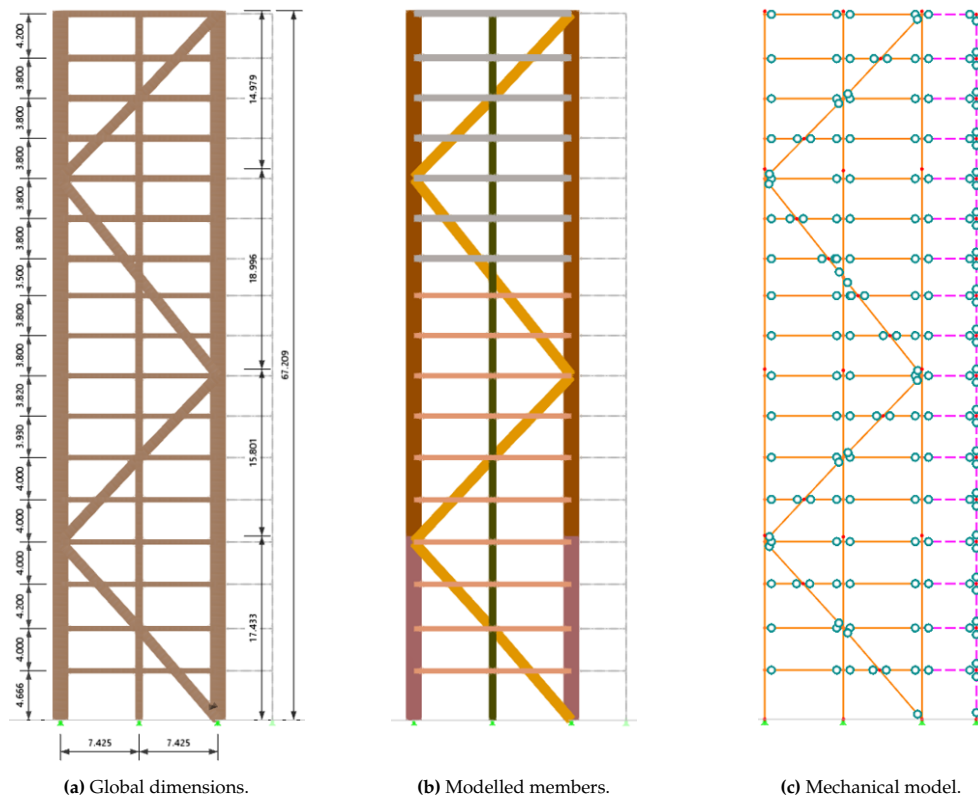
**Figure 4.10:** RFEM model of the stability frame.

**Table 4.3:** Strength class and dimensions of the frame members.

| Member | Strength Class | Dimension [mm] | Color (fig. 4.10b) |
|---|---|---|---|
| Corner columns (bottom section) | GL30h | 625 x 1485 | |
| Corner columns | GL30c | 625 x 1485 | |
| Middle columns | GL30c | 625 x 630 | |
| Beams (concrete floors) | GL30c | 625 x 585 | |
| Beams (timber floors) | GL30c | 625 x 439 | |
| Diagonals | GL30c | 625 x 990 | |

### 4.4.2. Loads and load-combinations

The permanent loads are estimated using the information provided by SWECO Norway and literature about the Mjøstårnet project. The variable loads, wind loads, and load combinations are in accordance with Eurocodes. In the 2D model, some of the floor loads are directly transferred to the horizontal beams that are part of the stability frame. This area is highlighted in figure 4.2 by the letter (a). The second-order loads are determined using area (b) illustrated in the same figure. The loads on this area are placed as point loads on the modelled 2nd order frame at each floor.

**Permanent loads**

The permanent loads consist of the self-weight of the floors, the internal partitions, and the facade cladding. The roof and the six upper floors are made out of 300mm concrete. The self-weight of these floors is taken to be $8kN/m^2$. The timber "Trä8 system" decks are applied on the other floors. Including the top layers, the weight of these decks is approximately $2kN/m^2$. The facade's weight is $1kN/m^2$ and the internal partition is $0.5kN/m^2$ [52].

**Table 4.4:** Permanent loads.

| Permanent Load | Value | Unit |
|---|---|---|
| Facade | 1.0 | $kN/m^2$ |
| Concrete floors | 8.0 | $kN/m^2$ |
| Timber floors | 2.0 | $kN/m^2$ |
| Internal partitions | 0.5 | $kN/m^2$ |

The self-weight of the frame structure is incorporated by activating the self-weight of the modelled members in RFEM. A strength class is assigned, and the program calculates the self-weight using the corresponding mean density.

**Variable loads**

The variable loads are dependent on the function of the storey. Floors 0 to 3 function as office space. The floors above function as hotel rooms and apartments for residents. The variable loads are taken in accordance with EN1991-1-1 [18].

**Table 4.5:** Variable loads.

| Type | Category | Floor | Variable load | Factor $\psi_0$ |
|---|---|---|---|---|
| Roof (terrace) | - | 17 | $4.0 \, kN/m^2$ | 0 |
| Residential / Hotel | A | 4 - 16 | $2.0 \, kN/m^2$ | 0.7 |
| Office | B | 0 - 3 | $3.0 \, kN/m^2$ | 0.7 |

**Wind load**

Wind loading is determined using EC1991-1-4 [19]. The static wind pressure at the top of the building is equal to approximately $1.13kN/m^2$, corresponding to a fundamental basic wind speed of 22 $m/s$. The factor $c_{pe}$ for the wind pressure is 0.8 and for wind suction 0.66. The structural factor ($c_s c_d$) is taken to be equal to 1. The width of the wide facade is estimated to be approximately 37 meters. Half of the force caused by the wind on this facade is assumed to enter the stability system. This is because the same truss is located in the facade on the other side of the building. The static wind load at the bottom of the building will be lower than at its top. To account for this, the wind loading is divided into four parts. For each column section, a different distributed wind load is applied. The distributed loads are calculated using the static wind load at the top of each section in accordance with EC1991-1-4. A graphical presentation of the modelled wind load is shown in figure 4.11.
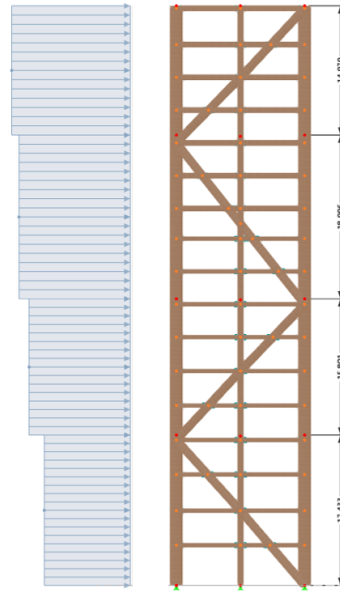
**Figure 4.11:** Wind load.

**Load combinations**

Load combinations are dependent on the consequence class of the structure. For tall structures with high consequences for loss of human life, consequence class CC3 is prescribed by Eurocode 1990 [17]. For this consequence class, the factor of actions ($K_{FI}$) is equal to 1.1. The corresponding design combinations to verify the strength of the members (ULS) are shown in equation 4.1 and 4.2. Equation 4.3 can be used to check the static equilibrium of the structure.

$$[6.10a] \quad 1.49G + \sum_{i \geq 1} 1.65\psi_{0,i}Q_{k,i} \tag{4.1}$$

$$[6.10b] \quad 1.32G + 1.65\psi_{0,1}Q_{k,1} + \sum_{i \geq 1} 1.65\psi_{0,i}Q_{k,i} \tag{4.2}$$

$$0.9G + 1.65\psi_{0,1}Q_{k,1} \tag{4.3}$$

The $\psi$-factors account for combinations of actions. Because Mjøstårnet is located in Norway, their values are taken from the Norwegian National Annex (NS:2016) corresponding to EC1990. For wind loads $\psi_0 = 0.6$. To reduce the computational time of the FEM model, the number of design equations is limited, and only the governing combinations are kept. To verify the deflections of the structure, the SLS characteristic load combination is used. For the dynamic/modal analyses, three (mass) combinations are considered. The load combinations (LC's) for ULS and SLS design incorporated in the model are listed in table 4.6.

**Table 4.6:** Load combinations applied in the FE model.

| Name | Type | Combination |
|------|------|-------------|
| LC1 and LC2 | ULS | 0.9G + 1.65Wind (left and right) |
| LC3 and LC4 | ULS (6.10a) | 1.49G + 0.99Wind (left and right) + 1.16Q |
| LC5 and LC6 | ULS (6.10b) | 1.32G + 1.65Wind (left and right) + 1.16Q |
| LC7 and LC8 | SLS (characteristic) | 1.0G + 1.0Wind (left and right) + 0.7Q |
| LC9 and LC10 | SLS (characteristic) | 1.0G + 1.0Wind (left and right) |
| LC11 | SLS (modal analysis) | 1.0G |
| LC12 | SLS (modal analysis) | 1.0G + $Q_{est}$* |
| LC13 | SLS (modal analysis) | 1.0G + 0.3Q ($\psi_2 = 0.3$) |

*$Q_{est}$ is the estimated actual life load according to Tulebekova et al. [52].

### 4.4.3. Connections

In practice, vertical trusses are commonly modelled with pinned connections without any additional adjustments [36] [52]. This will be referred to as **approach 1**. The stiffness of the connections could be accounted for by either applying springs at the nodes (**approach 2**) or by reducing the cross-sectional area of the members at the location of the connections. The latter method has previously been applied in sensitivity studies of Treet and Mjøstårnet [53] [39]. In this approach, the reduced cross-section is related to the dimensions of the connected member rather than the actual stiffness of the connections. This methodology was used because the stiffness of the large-scale connections is uncertain. According to the current EC5, the (initial) stiffness of the large-scale connections can be calculated using the formula for $K_{ser}$ (equation 2.24) and multiplying this value by the number of fasteners and shear planes. This suggests that the stiffness of a group of fasteners is equal to the sum of the stiffness of an individual fastener. However, in the literature review, it has been discussed that this is not the case.



**(a)** Actual connection [52, Fig. 12a].    **(b)** Reduced cross-section [52, Fig. 12b].    **(c)** Pinned members (RFEM model).
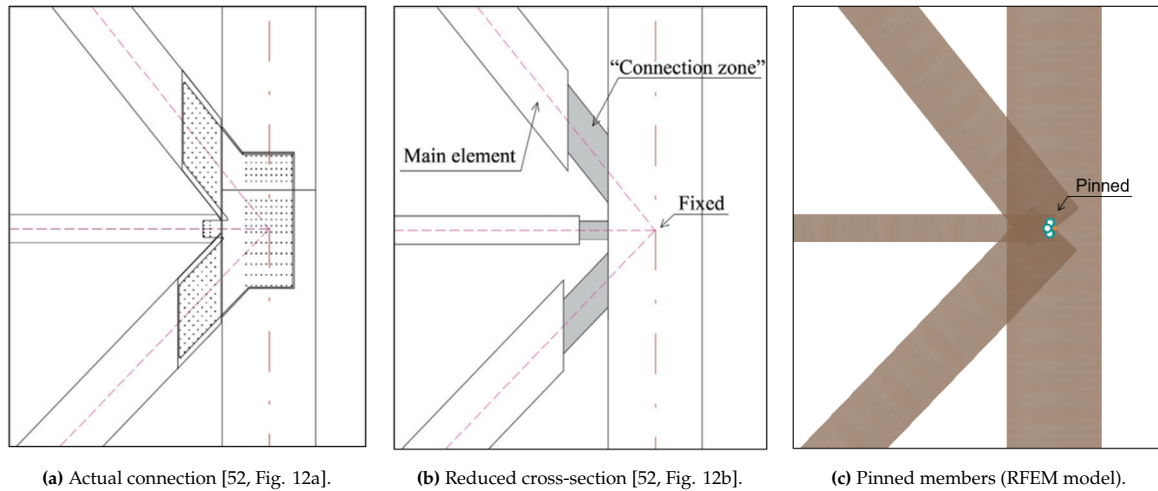
**Figure 4.12:** Modelling of diagonal connections.

**Diagonal elements**

A typical diagonal connection (at the bottom diagonal) consists of 10 rows of dowels with 10 dowels in each row, i.e. a total of 100 dowels, and 4 slotted-in steel plates. According to current EC5, the connection stiffness then becomes $K_{ser}$ multiplied by 800. For a mean density of 430 $kg/m^3$ and a dowel diameter of 12mm, $K_{ser}$ (per dowel and shear plane) is equal to $9.304kN/mm$. Multiplying this value with 800 gives a total connection stiffness of approximately $7443kN/mm$. This value could be incorporated into the FEM model by means of an axial stiffness assigned to the hinge at the end of the member (**approach 2**). The length of the diagonal connection is approximately 1060mm. The axial stiffness of this (timber) part can be calculated with equation 4.5. This gives a stiffness of $7588kN/mm$ which is almost exactly the same as the computed $K_{ser}$. Based on this, one can understand why engineers would therefore decide to adopt the simplistic modelling approach 1.

$$\Delta l = \frac{F \cdot l}{E \cdot A} \tag{4.4}$$

$$k = \frac{E \cdot A}{l} \tag{4.5}$$

where $\Delta l$ = the extension of the member, $F$ = section force, $l$ = length of the member, $E$ = elastic modulus, $A$ = cross-section area, and $k$ = the equivalent stiffness of a (member) section.

In the FE model, the truss members intersect at the point where their centre lines meet. This means that the end node of the diagonal member is located in the middle of the column it is connected to (see figure 4.12c). Thus, the modelled member is longer than the actual diagonal member. The axial elastic stiffness of the slotted-in steel plates inside the column can be considered accounted for if the 'extra' length of the diagonal timber member has similar stiffness as the steel plates. Whether replacing the steel plates

inside the column with a timber section is representative will depend on their stiffness ratios. In the studied truss, the cross-sectional (cs) area of the four slotted-in steel plates with a thickness of 12mm is equal to $39360mm^2$. Correspondingly, the stiffness ratio (EA) of these plates and a timber diagonal element of equivalent length is approximately 1.03 (see table 4.7). This means that the axial stiffness of the steel plates slotted in the columns is accounted for with sufficient accuracy when replaced by a timber cross-section of the connected diagonal.

**Table 4.7:** Axial stiffness (EA) of the steel plates and diagonal timber members.

| Element | E-modulus $[MPa]$ | (cs) Area $[mm^2]$ | EA $[N]$ |
|---|---|---|---|
| 4 slotted-in steel plates ($t = 12mm$) | 210.000 | 39.360 | $8266 \cdot 10^6$ |
| GL30c diagonal member ($625x990mm$) | 13.000 | 618.750 | $8044 \cdot 10^6$ |

When the EA ratio between the connected timber member and the slotted-in steel plates is not close to 1, the elastic stiffness of the steel plates could be accounted for by a more detailed approach. The length of the slotted-in steel plates inside the corner- and middle columns can be estimated using the width of the column in combination with the angle of the connected diagonal. When a diagonal is connected to the column under an angle $\theta$, the length of the steel plate inside the column can be calculated using equation 4.6. This simple relationship is based on the assumption that there is force equilibrium at the point where the centre lines of the members meet. Meaning that the oblique part of the steel plate is under full axial load up till this point. This force is then responsible for the elastic elongation of the steel plates.

$$l_{SPc} = \frac{0.5 \cdot w_{column}}{cos(\theta)} \tag{4.6}$$

where $l_{SPc}$ = length of the steel plates inside the column, $w_{column}$ = column width, and $\theta$ = angle of the diagonal member.

In equation 4.6, the length of the slotted-in steel plate, and correspondingly its stiffness, is dependent on the width of the column. Because the width of the corner- and middle columns differs, the length of the steel plates will not be the same. Figures 4.13 and 4.14 illustrate how the length of the part of the steel plates inside the columns is determined. In figure 4.13 the grey marked area shows the figurative (oblique) slotted-in steel plate. The actual plate inside the corner columns is one large piece which is indicated by the grey contour lines in the figure.



**(a)** Connection in the RFEM model.

**(b)** Steel plate slotted inside the column.
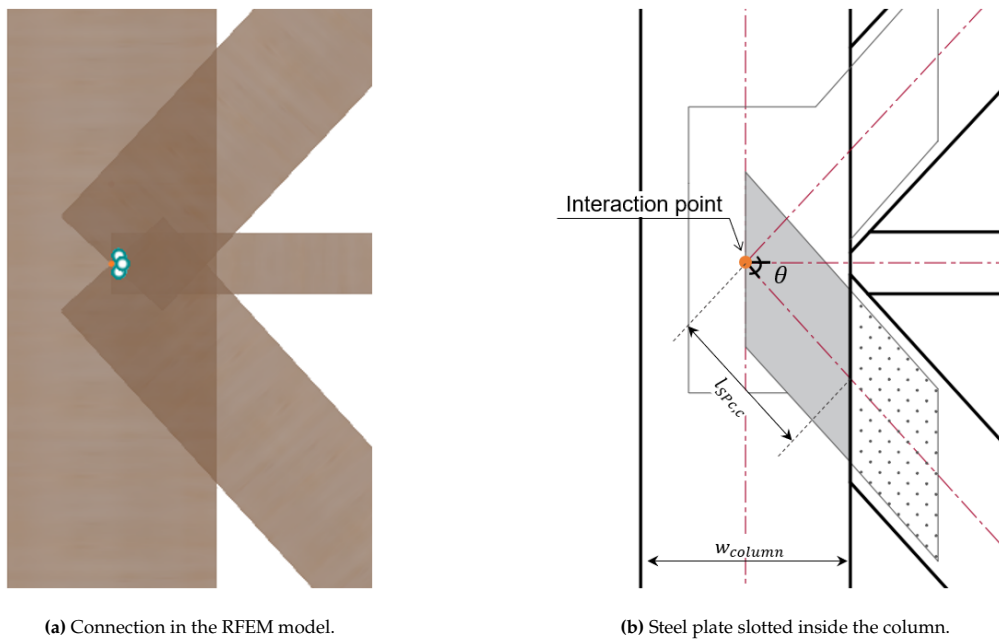
**Figure 4.13:** Estimation of the length of the slotted-in steel plates inside the corner columns.

**(a)** Connection in RFEM model.

**(b)** Steel plate slotted inside the column.
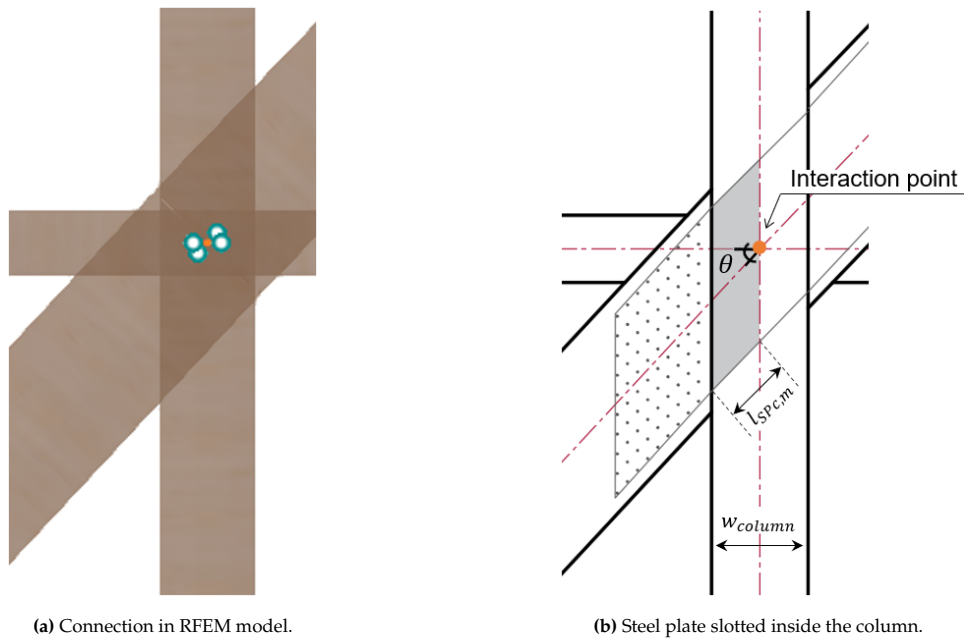
**Figure 4.14:** Estimation of the length of the slotted-in steel plates inside the middle columns.

### Vertical component

The diagonals are connected to the corner columns by means of a large group of dowels inside the columns. This dowel group is highlighted in figure 4.15 and will be referred to as the 'vertical component'. At these connections, two diagonals connect, one of which will be loaded in tension while the other will be loaded in compression. This vertical component of these diagonal forces is a force either upward or downward, depending on the direction of the wind load. Equilibrium at the node is made by transferring this force to the corner column by means of the large group of dowels inside the column. An example of nodal equilibrium at such a connection is shown in figure 4.16.
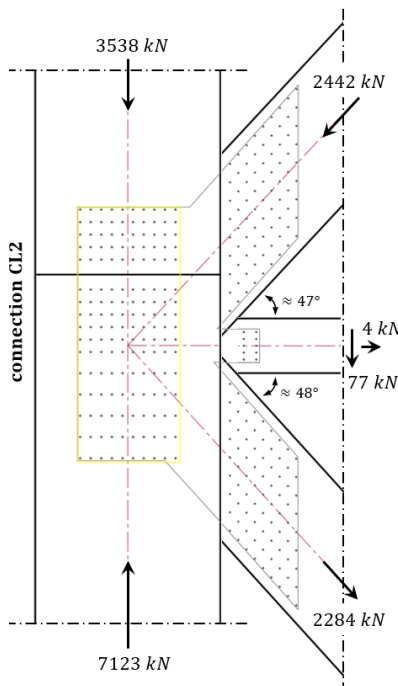


**Figure 4.15:** Truss connection CL2 between diagonals and corner column.
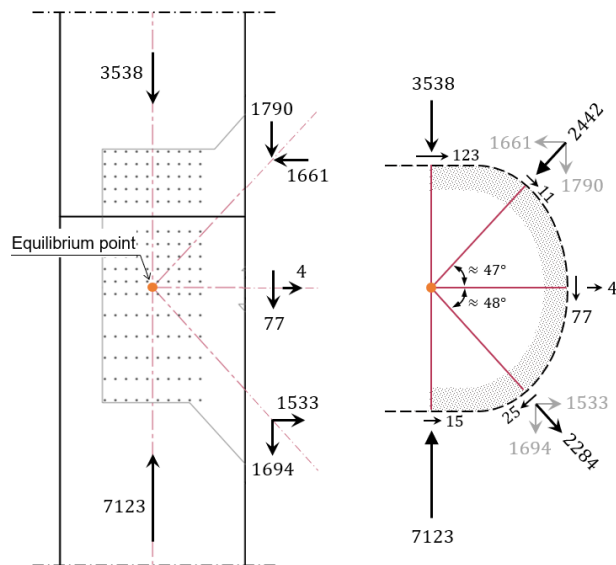


**Figure 4.16:** Example of (nodal) equilibrium of forces in connection CL2 and load combination 8 (LC8).

To account for the (vertical) stiffness of the dowel group inside the corner columns, a small stiff element is modelled. A shear stiffness can be specified within the node at the end of the stiff element where it connects to the diagonals. The modelled element has a length of just 1mm and is shown in figure 4.17a. In figure 4.17b the corresponding mechanics scheme is shown. This approach assures that only the vertical forces coming from the diagonals will cause vertical displacement. This is necessary because the difference in vertical force between two column sections is transferred by contact pressure, not by the dowel group.



(a) Modelling approach in RFEM model.

(b) Mechanics-scheme (including nodal springs and forces in LC8).
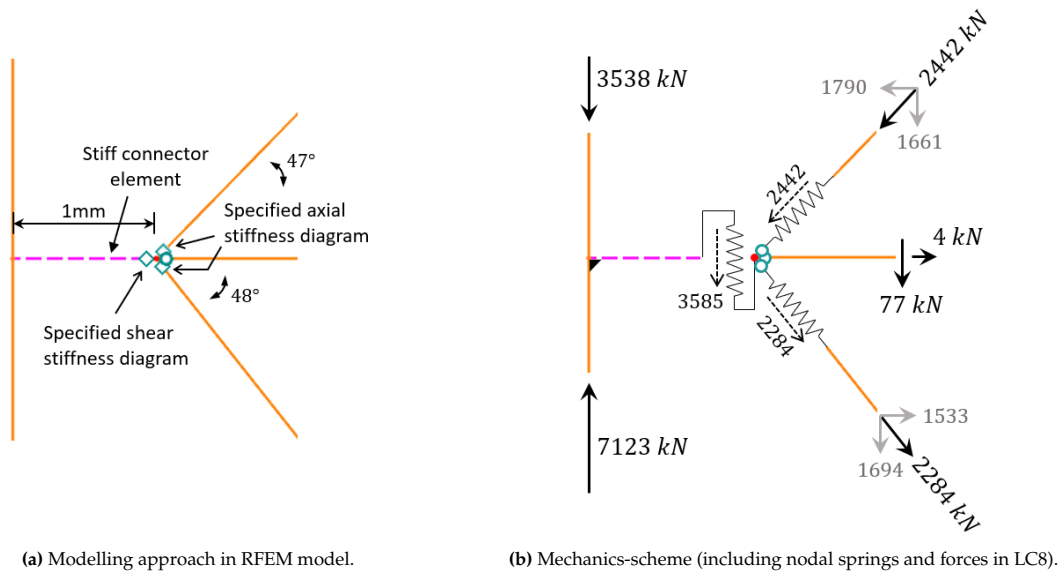
**Figure 4.17:** Modelling of the connection between diagonals and corner column in which the stiffnesses can be specified in the nodes; connection CL2 is used for this example.

### 4.4.4. Foundation stiffness

Reed and Wiig [39] studied the effect of multiple design parameters on the natural frequencies of the Mjøstårnet building. They identified the most significant parameters and concluded that the axial stiffness of the diagonal connections and the vertical foundation stiffness had the largest impact on the natural frequency of the building. This thesis's main focus is on the effect of the stiffness of the truss connections on serviceability requirements, i.e. deflections and dynamic behaviour. However, the influence of the foundation stiffness will also be briefly analysed in the sensitivity study. The results can be used for comparison with those obtained by Reed and Wigg. This is an interesting comparison because they made a 3D model of the building in Abaqus.

In the RFEM model, the vertical foundation stiffness is modelled by assigning a stiffness to the supports located at the bottom of the columns. The building's foundation consists of circular steel piles with a length of 30 meters. At this depth, the piles make contact with the bedrock. The piles have a diameter of 400mm and a thickness of 12.5mm. The pile head is a 2-meter-thick concrete slab which connects the foundation piles to the bottom of the (above-ground) structure. Based on this data, Tulebekova et al. [52] expect the foundation to be eminently stiff. Therefore, they chose to apply pinned supports, i.e. no vertical springs, in their numerical model which they used to study the dynamic behaviour of the building. Ellis [14] researched the accuracy of the prediction methods for the natural frequencies of buildings. By studying measured mode shapes of tall buildings, he concluded that the effect of the dynamic soil-structure interaction can be reasonably omitted since its effect on the overall dynamic response is little.

### 4.4.5. Modal analysis

The natural frequencies of the building can be estimated using the Model Analysis add-on that is built-in in the RFEM software [49]. The software performs a natural vibration analysis of the modelled structure. The results of the iterative calculation are the natural frequencies and the corresponding mode shapes. The natural frequencies are computed using the mass and the stiffness of the structure. Therefore, accurate modelling of the mass, including the point loads placed on the 2nd-order frame, is

important. For the modal analysis, permanent loads and (part of the) variable loads are converted into a mass. This conversion of mass is graphically shown in figure 4.18. Note the mass difference between the concrete- and timber floors, shown in the figure.



<div align="center">(a) At the concrete floors.                              (b) At the timber floors.</div>
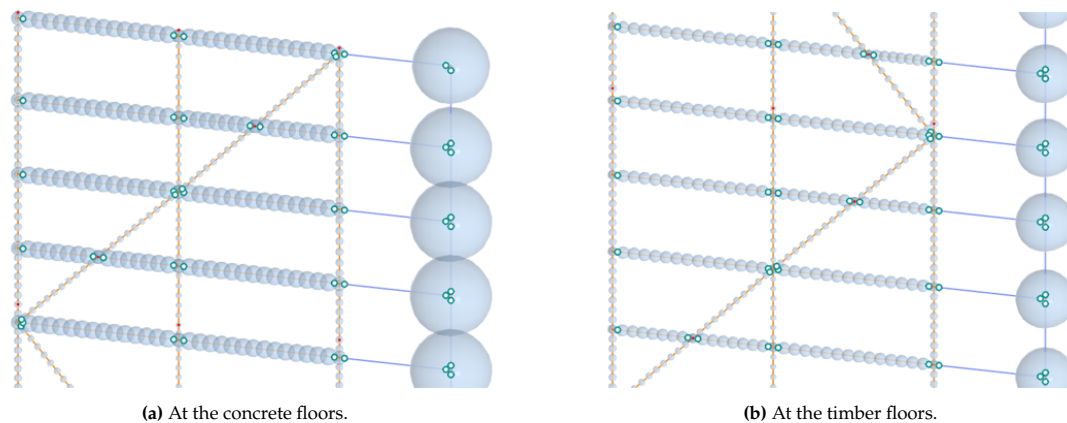
**Figure 4.18:** Loads computed into mass to perform the modal analysis.

Since the variable loads will partly be translated into mass, it is relevant to discuss what part of the variable load should be considered. In Eurocode 0 [17], the frequent load combination gives the lowest total load. In this combination, the variable load is multiplied by a factor ($\psi_2$) of 0.3. This multiplication factor can be an overestimation of the actual life load when the building is in service. Based on the architectural layout of the floor plans, Tulebekova et al. [52] estimated the 'actual' variable load of the Mjøstårnet building. Their estimated variable loads ($Q_{est}$) are considered in a separate load case. At last, a load case in which only the permanent loads are transformed into mass is considered. An overview of the load cases and the applied multiplication factors are shown in table 4.8.

**Table 4.8:** Multiplication factors for variable load in the considered mass combinations.

| (Mass) Combination | tag | Office [$3kN/m^2$] | Hotel [$2kN/m^2$] | Apartment [$2kN/m^2$] |
|---|---|---|---|---|
| $1.0G$ | LC11 | 0 | 0 | 0 |
| $1.0G + Q_{est}$ | LC12 | 0.05 | 0.11 | 0.17 |
| $1.0G + 0.3Q$ | LC13 | 0.3 | 0.3 | 0.3 |

It is expected that the three load cases, shown in table 4.8, will have little varying results. This is mainly because of the low value for the variable loads in comparison to the permanent loads. This is particularly due to the high self-weight of the concrete floors. In the design of another building, for example, a multi-storey timber building without concrete floors, the different load cases will cause more deviation between the results. Therefore, it is important to make a contemplated decision about the considered mass when analysing the dynamic response of a timber building. Based on the estimation of the variable load for Mjøstårnet made by Tulebekova et al. it seems appropriate to state that a live load partition factor of 0.1, i.e. 10% of the variable load, is a proper value. The outcome might be conservative, but this is considered to be better than overestimating the participating variable load, which is likely the case when applying the frequent combination (live load partition factor = 0.3) from EC0.

## 4.5. Preliminary study

The forces within the members and connections obtained from the RFEM model are briefly discussed to create familiarity with the design. To verify the accuracy of the model, the capacities of the members and connections are checked according to the design rules from Eurocodes. The necessary information i.e. geometries, materials etc. are provided by SWECO and taken from literature. Some small deviations in comparison to the actual structure are expected because a simplified version of the Mjøstårnet building is considered (see figure 4.9). The stability frame is modelled in 2D with an additional frame structure to account for second-order effects. This second-order frame has no weight, pinned connections, and point

loads are placed at each storey to represent the mass of part of the building. In the estimations of these point loads, some simplifications are made. For example, the weight of the inner columns is estimated as if it has a uniform cross-section throughout the building's height. In the actual building, however, the dimensions of these inner columns differ depending on the floor [34, Table 1]. Such simplifications are not expected to have a large impact on the global behaviour of the structure. Because of the translation into a 2D system, it is considered necessary to determine the forces in ULS and perform the design checks (according to Eurocodes) for the members and connections.

### 4.5.1. Truss members

The dimensions and the strength classes of the truss members are listed in table 4.3. The truss members have uniform dimensions, i.e. the cross-section of the bottom member is the same as the top member. In the ultimate limit state (ULS), the left corner column has the highest loads in both tension and compression. When the structure is loaded by the wind coming from the left, the column is loaded in tension. On the right side of the structure, the bottom two column sections have similar forces. This is due to the diagonals spanning over multiple storeys. The diagonal members are loaded both in compression and tension, dependent on the direction of the wind. The force in the lower diagonals is much higher in comparison to the upper diagonals. The maximum member forces under ULS loading are shown in figure 4.19 In figure 4.20 the most heavily loaded members are highlighted. Unity Checks (UC's) are performed on all truss members. The result can be found in table C.2 in Appendix C. The highest obtained values are; 0.60 for the left corner column under compression, and 0.57 for the bottom diagonal under tension. Thus, the truss members are easily meeting their strength requirements.
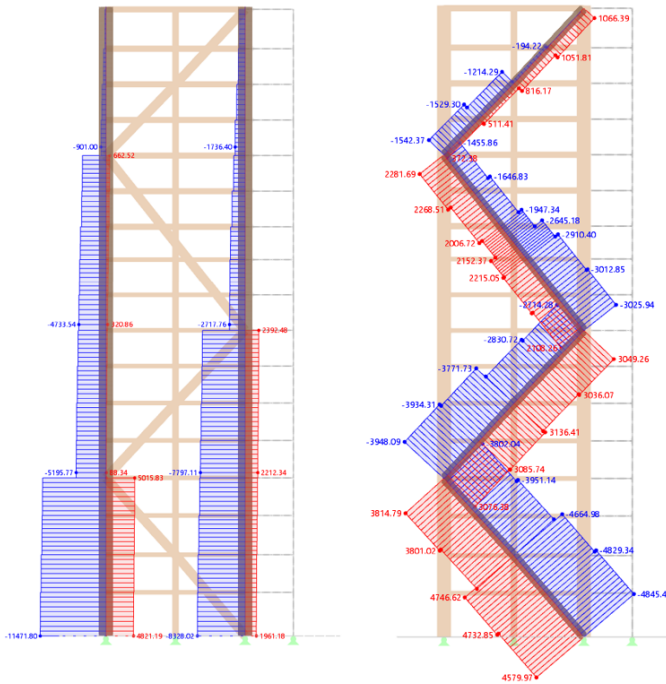


**Figure 4.19:** ULS forces in the truss members (red=tension).   **Figure 4.20:** Heaviest loaded members.
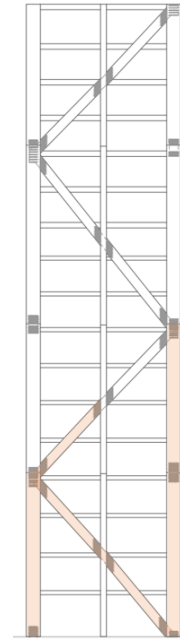
Under SLS design loads, the member force distribution is very similar to that shown in figure 4.19, but the force in each member is lower. Tension will still occur at the lower left column section. The loads in the diagonals will alternate between compression and tension. Table C.4 shows that the SLS force in the diagonal members is fluctuating at about 60% of the ULS force for all diagonals. This ratio is dependent on the proportion of permanent load in relation to the variable loads. In addition, a high consequence class (here CC3) will also affect this ratio. The obtained member forces from the model under SLS loads are shown in figure C.2 in Appendix C.

### 4.5.2. Truss connections

An overview of the connections within the modelled truss can be found in figure 4.6a. In the actual truss, the number of dowels in the upper diagonal connections is less in comparison to the diagonal connections in the bottom diagonal members. The difference in the number of dowels, design capacity, and estimated stiffness can be read from table 4.9. The stiffness is estimated using the engineering model discussed in section 3.4.2. Note that because of the difference in the number of dowels, the estimated stiffness of the upper connections is less in comparison to the lower ones. This might affect the serviceability behaviour of the structure, which will be researched further in the sensitivity study.

The timber member thicknesses and fastener spacing are estimated from drawings provided by Sweco Norway. A typical geometry of a diagonal connection is shown in figure 4.5. Information about the material properties can be found in design codes and in the literature. The timber properties were taken from EN14080 [16]. The yield strength of the dowels is 755MPa [52], corresponding to grade EN1.4418 in accordance with EN10088-3 [15]. For these high-strength steel (hss) dowels, the formula for the yield moment from theory (equation 2.11) is most accurate [43]. The connections between the highlighted members in figure 4.20 are the most important because these are exposed to the highest loads. Correspondingly, the connections at the bottom of the truss govern their design.

**Table 4.9:** Non-uniform diagonal connections.

| **Connections** (fig. 4.6a) | **Nr. of dowels** | **Design capacity** | $\mathbf{K_{ser,mod}}$ (eq. 3.10) |
|---|---|---|---|
| CR1-d1, M1-d1, M1-d2 | 10 x 10 =100 | 5362 kN | 2141 kN/mm |
| CL2-d1, CL2-d2, M2, CR3-d1, CR3-d2 | 9 x 9 =81 | 4995 kN | 1861 kN/mm |
| M3, CL4-d1, CL4-d2, M4, CR5-d1 | 8 x 8 =64 | 3993 kN | 1613 kN/mm |

The characteristic- and design capacities of the diagonal connections are calculated using Johansen's yield model (YM), the European yield model (EYM), and block shear according to Annex A in current EC5. An overview of the results can be found in table C.5 in Appendix C. It is concluded that block shear governs the capacity of the bottom (100-dowel) diagonal connections. For the other diagonal connections, the yield models are governing their capacity. Johansen's YM is considered to be more accurate because in the EYM a correction factor of 1.15 is incorporated in the calculation of the characteristic capacity. This factor causes a difference in the estimated load-bearing capacity using EYM in comparison to YM. More information about this can be found in the literature review (chapter 2).

The highest calculated unity check is 0.90 governed by block shear. It can be concluded that the capacity of the timber connections is much more critical in comparison to the strength of the timber members. In the last column of table C.5, the ratio between the characteristic connection capacity and the maximum occurring SLS force has been determined. This is relevant to see whether the range of 10% to 40% of the estimated characteristic connection capacity is a representative value for the force under serviceability loading. The 10/40 criterion is commonly used when reporting the stiffness of tested connections. The computed ratio lies between 9% and 38%, therefore, the range 10-40% of $F_{est}$ can be regarded as accurate for this truss structure.

In the RFEM model, the load-slip behaviour of the connections is incorporated by specifying a load-slip diagram in the nodes. An example of the modelled connection will be briefly discussed to verify that the model works as expected. Connection CL2 (see fig. 4.6a) is taken for this example. At this connection, two diagonals and a horizontal beam are attached to the left column. The forces at the connection, under LC8, are drawn in figure 4.21. When converting the diagonal forces into a horizontal and vertical component, it can be verified that the forces are in equilibrium. The vertical component of the diagonal forces is transferred to the column by means of a shear force in the small stiff modelled element.
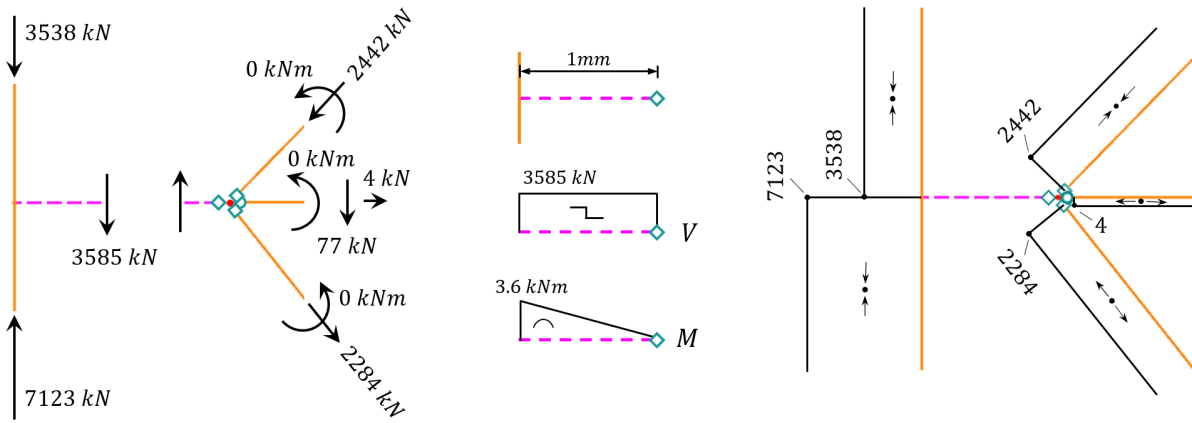
**Figure 4.21:** Forces in modelled connection CL2. From RFEM model in LC8.

In figure 4.21 the diagonals have an axial force of 2442kN (compression) and 2284kN (tension). These forces will cause the local displacement in accordance with the specified load-slip diagram. The specified diagram, representing the load-slip behaviour of the diagonal connections, is shown in figure 4.22a. The diagram consists of an initial slip of 0.6mm followed by the estimated elastic stiffness of $2141kN/mm$ (from table 4.9). This load-slip behaviour is specified both when loaded in tension and compression. The diagonal forces are plotted into this graph and the corresponding slip can be determined. From the report generated by RFEM, the nodal displacement can be read. Because the nodal displacement gives the same value as the expected axial slip, drawn in figure 4.22a, it is verified that the approach is working as intended. The same verification can be done for the vertical component. In the example from figure 4.21, a force of 3585kN is transferred through shear by the stiff element. The specified load-slip diagram, representing the dowel group inside the column, is shown in figure 4.22b. The initial slip is 0.6mm and the stiffness of this dowel group is specified to be $3425kN/mm$. A local displacement of 1.63mm can be read from the diagram. Note that the slip in relation to the shear force is specified. Thus, in this example, the node will displace downward.



**(a)** Diagonals CL2-d1 and CL2-d2.



**(b)** Vertical component CL2-v.
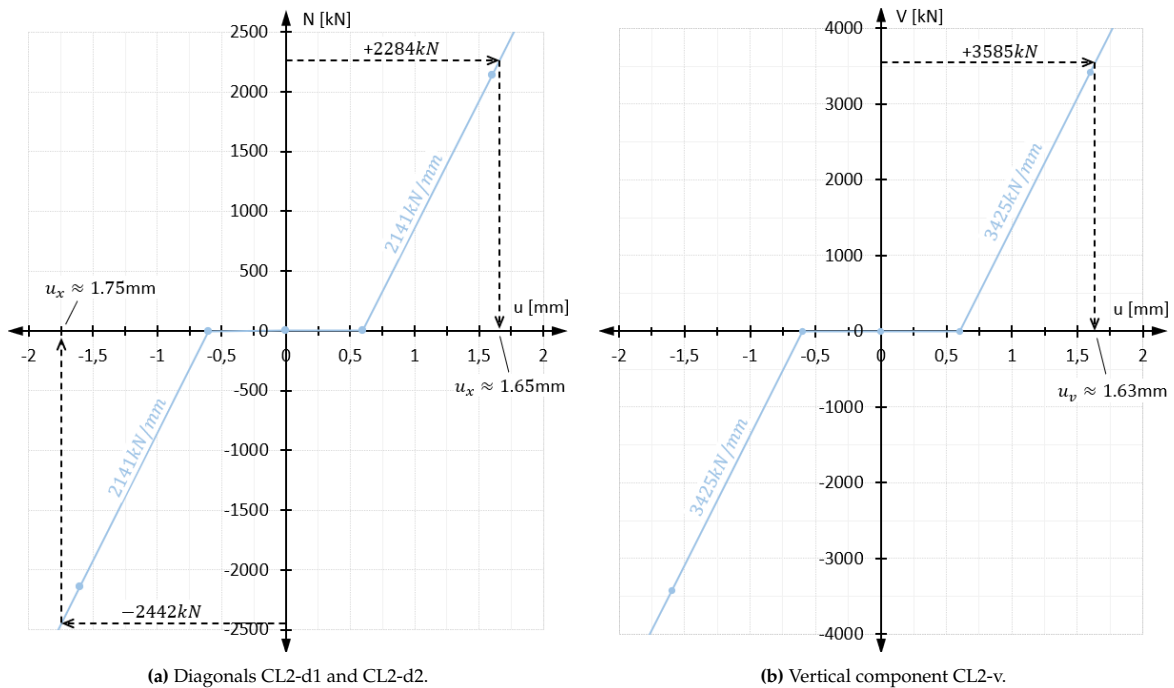
**Figure 4.22:** Load-slip diagrams and local deformations corresponding to the connection forces under LC8.

# 5

# Sensitivity Study

## 5.1. Introduction

In this chapter, the sensitivity of multiple parameters on the maximum displacements and the natural frequency of the structure is researched. The main objective is to quantify the influence of the truss connections. In addition to the connections, the vertical foundation stiffness is studied by adjusting the spring stiffness of the supports. The modelling of the diagonal connections and their vertical component require more detailed modelling. An explanation of the modelling approach used to study the influence of the connections is provided in the concerning section. In all the models, with the exemption of the models used to study the influence of the foundation stiffness, pinned supports are applied.

## 5.2. Vertical stiffness of the foundation

The stiffness of the foundation is commonly taken conservatively in FE models to assure structural strength and stability. When taking the same conservative approach to studying dynamic behaviour, this might lead to an overestimation of the dynamic response. Therefore, to accurately estimate this response, an adjusted model may be required. For example, Tulebekova et al. [52] analysed the dynamic response of Mjøstårnet. In their study, they used measurements of modal shapes to update their numerical modal. They expressed the accuracy of the model in terms of the agreement of its modal shape with actual measurements. In their numerical model, they used pinned supports and thus omitted the vertical stiffness of the foundation. For the vertical springs, a stiffness range from $1*10^6$ up to $6*10^6 kN/m$ is considered. In addition, rigid supports are applied to showcase the effect of this modelling choice on the displacement and natural frequency. In the studied model, the beam- and diagonal connections are modelled as pinned without any additional adjustments (approach 1, see section 4.4.3).
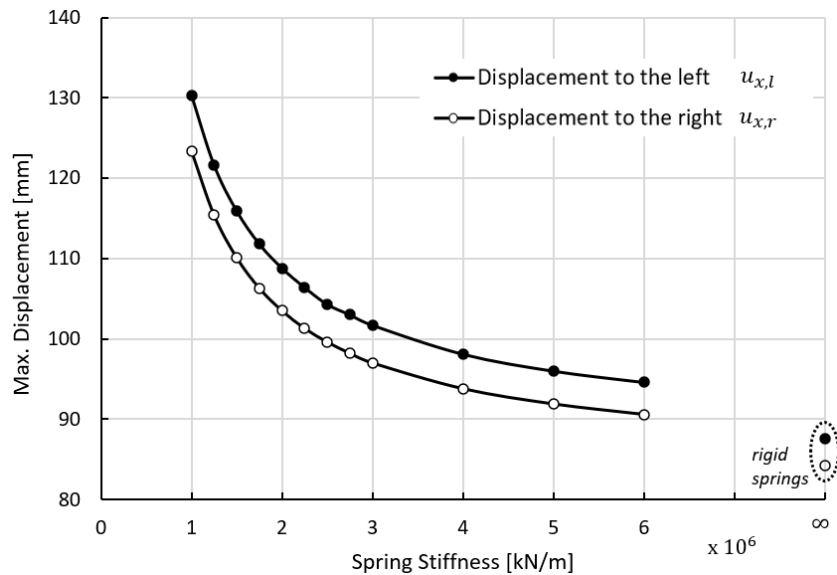
**Figure 5.1:** Maximum displacement as a function of the vertical foundation stiffness.

In figure 5.1 the displacements are plotted against the stiffness of the vertical springs. Displacement towards the right- and the left are plotted. The difference between these displacements is related to the asymmetric truss in which the diagonals span over multiple storeys. Especially in the low stiffness range, the effect of the foundation stiffness on displacement is strong. The graph shows an exponential decrease in displacement with an increase in spring stiffness. The effect of applying rigid springs also becomes evident by comparing it to the obtained displacement when applying springs of $6 * 10^6 kN/m$. The displaced shapes are shown in figure 5.2.
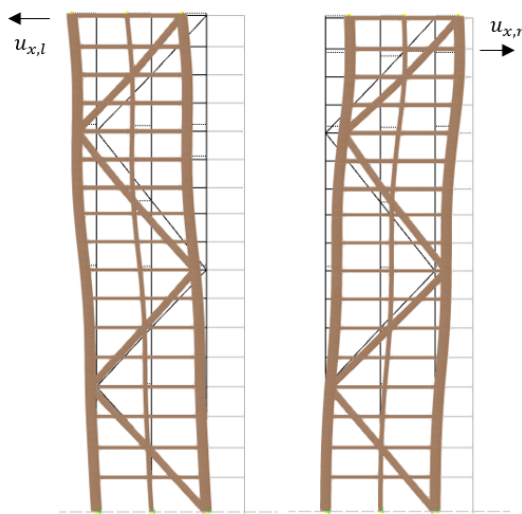


**Figure 5.2:** Static displacements.                              **Figure 5.3:** Mode shape.
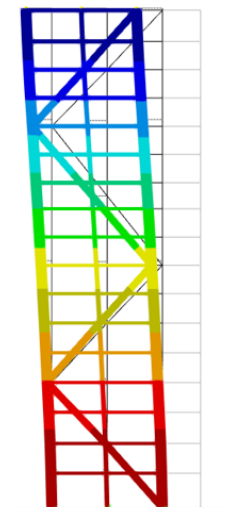
The mode shape of the structure is shown in figure 5.3. In figure 5.4, the influence of the vertical spring stiffness on the natural frequency is shown. This natural frequency corresponds to the first translational mode. Three load/mass combinations are considered (see table 4.8). The difference in computed natural frequency between these load cases is not large. This is due to the high permanent weight of the concrete floors in relation to the variable loads. Similar to the displacements, the natural frequency is most significantly influenced in the lower stiffness range. However, as previously discussed in section 4.4.4, it is likely most accurate to apply pinned supports when analysing the dynamic response of the building [14] [52]. Figure 5.4 shows that the natural frequency when applying rigid springs will differ

substantially in comparison to those obtained in the lower stiffness range.
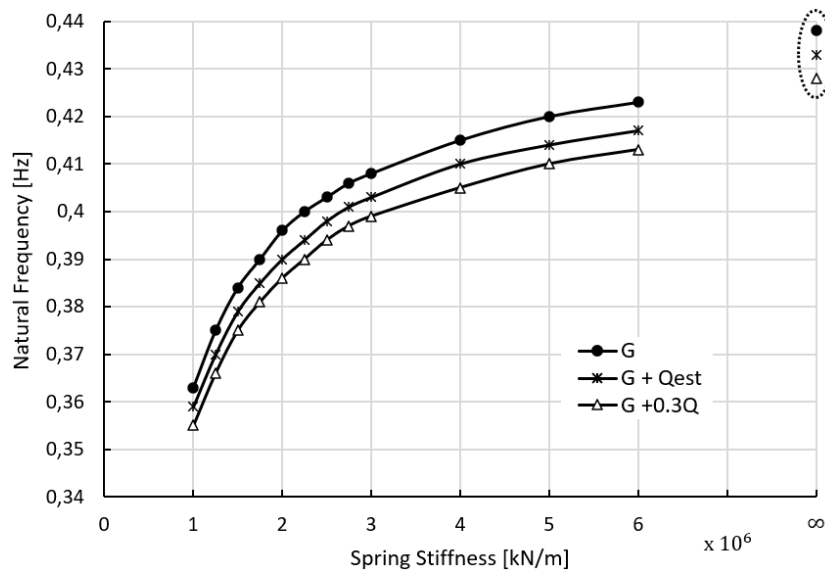


**Figure 5.4:** Natural frequency as a function of the vertical foundation stiffness.

## 5.3. Rotational stiffness of the horizontal beam connections

In practice, connections are commonly modelled as pinned. This is also the case for the connection between the horizontal beams and the columns. Previous studies into the dynamic behaviour of Mjøstårnet [39] [52] concluded that it might be appropriate to assign rotational stiffness to these connections. However, the elastic rotational stiffness of these timber connections is unknown. To analyse their effect, the most extreme cases, namely applying either pinned or stiff connections, are considered. Note that this concerns only the beam-column connections within the modelled 2D frame structure. In the actual building, these connections are also present outside the stability frame, i.e. in the column-beam structure applied throughout the building. If the rotational stiffness of all these beam-column connections were considered, which requires a 3D model, the effect of this parameter on the serviceability behaviour of the building will be greater. The results for the two extreme cases are shown in table 5.1. In the studied model, the diagonal connections are pinned without any additional adjustments.

**Table 5.1:** Pinned versus stiff horizontal beam connections.

|  | Natural frequency [Hz] | | | Max. displacement [mm] | |
|---|---|---|---|---|---|
|  | $1.0G$ | $G + Q_{est}$ | $G + 0.3Q$ | $u_{x,l}$ | $u_{x,r}$ |
| **pinned** | 0.438 | 0.433 | 0.428 | 87.6 | 84.2 |
| **stiff** | 0.441 | 0.435 | 0.431 | 86.8 | 79.2 |

The results in table 5.1 show a small difference in the computed natural frequency between the model with pinned and stiff connections. As for the displacement, the difference is most significant towards the right. This is because the rotational stiff connections prevent large bending deformation in the column. The horizontal beams are expected to have a much larger bending resistance in comparison to the rotational capacity of the connections. Correspondingly, it seems most accurate to simply model these connections as pinned.

## 5.4. Axial stiffness of the diagonal connections

To research the sensitivity of the axial stiffness of the diagonal connections, we want to be able to easily adjust the stiffness. This is achieved by subdividing the diagonal elements into parts and alternating the E-modulus of the modelled diagonal member. The approach is explained in detail in the first subsection. In the second subsection, the results are presented.

### 5.4.1. Modelling approach

In the RFEM model, members are modelled as rods to which properties are assigned. As a consequence, the members intersect at their centrelines. For the diagonal members, this means that they have a greater length in the model than in the actual structure. The 'extra' length causes the stiffness of the modelled diagonal element to be lower. An argument can be made that this could be considered to take into account the elastic stiffness of the steel plates and the stiffness of the connections. This approach, in which the modelled members are pinned without additional adjustments, has been discussed in section 4.4.3 and is referred to as approach 1. In the same section, approach 2, in which the connection stiffness is considered separately and assigned to the nodes, is discussed. This approach is applied in this sensitivity study.

To enable analysis of the diagonal connection stiffness, the diagonal elements are subdivided into parts representing the steel plates slotted in the columns, the dowelled connections, and the timber member. The term 'element' is used when referring to all parts. Subdivision of the diagonal element is shown in figure 5.5. Note that the steel plates slotted in the columns do not have equal lengths on the two sides of the element. This is because the middle column has a smaller width in comparison to the corner column. The term 'diagonal connection' is used to refer to the ends of the actual timber member. In this region, the steel plates are slotted in the timber diagonal member. Correspondingly, the stiffness of these parts will be the sum of the elastic deformation of the steel plates slotted in the diagonal, the deformation of the timber in this region, and the deformation of the dowels that transfer the load between the steel plates and the timber diagonal.
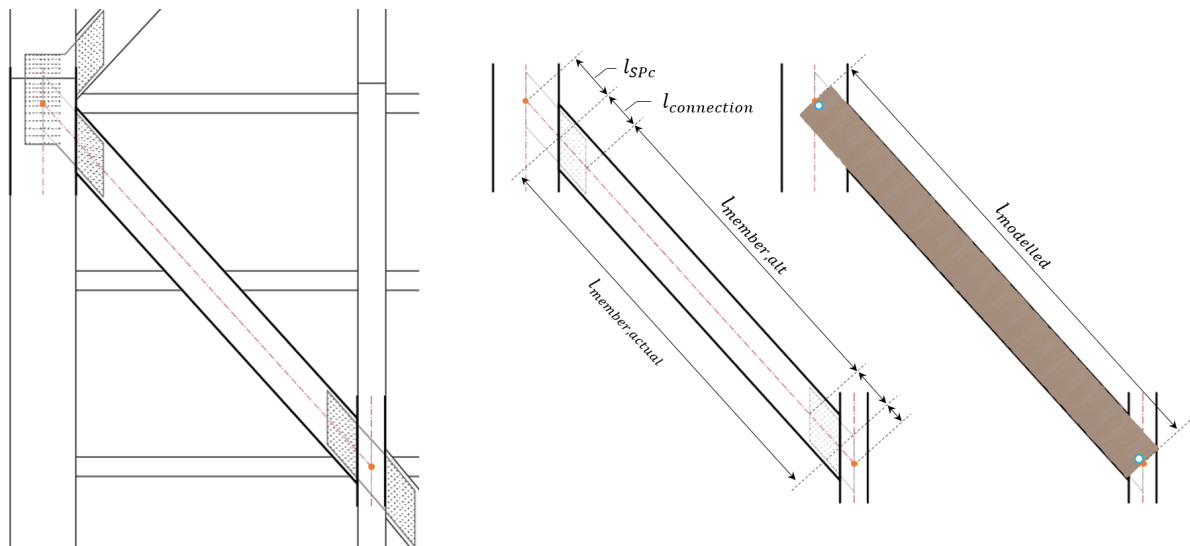


**Figure 5.5:** Subdivision of a diagonal element.

A more detailed image of the subdivided diagonal element is shown in figure 5.6. Each part can be represented by a spring. The stiffness of the diagonal element can be considered as the equivalent of these springs, which are placed in series.
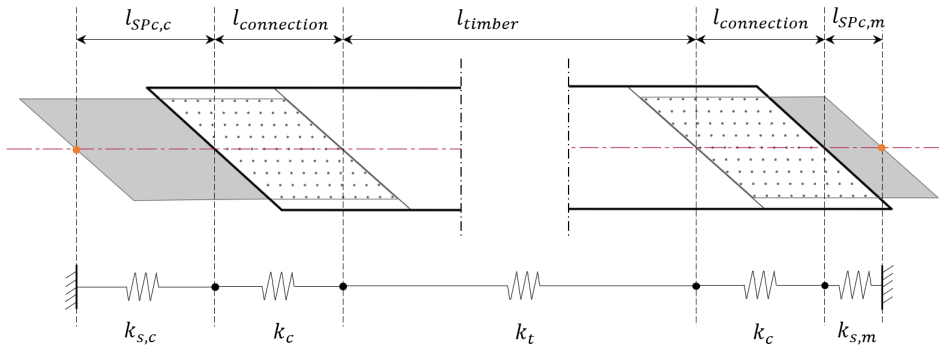
**Figure 5.6:** Translation of diagonal element into a series of springs.

The length of the connection ($l_{connection}$) is dependent on the connection geometry. Equation 5.1 shows how this length is computed in this study. The length of the steel plates inside the columns ($l_{SPc,c}$ and $l_{SPc,m}$) can be related to the width of the columns. This has been discussed in section 4.4.3. The length of the remaining timber member ($l_{timber}$) can be calculated using equation 5.2.

$$l_{connection} = a_3 + (n_0 - 1) \cdot a_1 + 30 \tag{5.1}$$

where $l_{connection}$ = length of the diagonal connection, $a_3$ = end spacing parallel to the grain, $n_0$ = number of dowels in a row (parallel to the grain), and $a_1$ = dowel spacing parallel to the grain.

$$l_{timber} = l_{modelled} - 2 \cdot l_{connection} - l_{SPc,c} - l_{SPc,m} \tag{5.2}$$

where $l_{timber}$ = length of the remaining diagonal timber member, $l_{modelled}$ = length of the modelled diagonal rod, $l_{SPc,c}$ = length of the steel plate slotted-in the corner column, and $l_{SPc,m}$ = length of the steel plate slotted-in the middle column.

After subdivision of the diagonal element, the stiffness of each of the parts is determined. The elastic stiffness of the steel plates (inside the columns) and the remaining timber member are computed using equation 4.5. All the properties used for the computations are listed in table 5.2. The properties of the diagonal elements will differ slightly throughout the structure. To avoid having to model each element separately, average values are taken. Because the length and angle of the modelled diagonal rods are very similar, this simplification will not cause significantly different results.

$$k = \frac{E \cdot A}{l} \tag{4.5 revisited}$$

where $k$ = the elastic stiffness, $E$ = elastic modulus, $A$ = cross-section area, and $l$ = length of the part.

**Table 5.2:** Properties of the diagonal elements.

| Property | Symbol | Value | Unit | Note |
|---|---|---|---|---|
| Average length of the modelled diagonals | $l_{modelled}$ | 11204 | $mm$ | |
| Average angle of the modelled diagonals | $\theta$ | 48 | ° | |
| Length of steel plates inside corner column | $l_{SPc,c}$ | 1110 | $mm$ | equation 4.6 |
| Length of steel plates inside middle column | $l_{SPc,m}$ | 471 | $mm$ | equation 4.6 |
| End spacing parallel to the grain | $a_3$ | 130 | $mm$ | |
| Dowel spacing parallel to the grain | $a_1$ | 100 | $mm$ | |
| Number of dowels parallel to the grain | $n_0$ | 10 | - | |
| Length of the connection (zone) | $l_{connection}$ | 1060 | $mm$ | equation 5.1 |
| Length of the timber member | $l_{timber}$ | 7503 | $mm$ | equation 5.2 |
| Mean E-modulus of the timber (GL30c) | $E_t$ | 13000 | $MPa$ | EN14080 [16] |
| Area of the timber diagonal | $A_t$ | 618750 | $mm^2$ | |
| E-modulus of the steel plates | $E_s$ | 210000 | $MPa$ | |
| Thickness of slotted-in steel plates | $t_{SP}$ | 12 | $mm$ | |
| Height of slotted-in steel plates | $h_{SP}$ | 820 | $mm$ | |
| Area of the 4 slotted-in steel plates | $A_s$ | 39360 | $mm^2$ | $t = 12mm$ |

For springs placed in series, equation 5.3 can be used to compute the equivalent stiffness of the springs.

$$\frac{1}{k_{eq}} = \frac{1}{k_1} + \frac{1}{k_2} + \dots \tag{5.3}$$

The aim is to be able to specify the connection stiffnesses in the nodes (at the ends of the diagonal rod) within the FE model. Therefore, the stiffness of the diagonal element without accounting for the connection stiffnesses must be determined. To clarify, the equivalent stiffness of the timber member and the steel plates inside the columns on both sides of the element should be accounted for by the altered stiffness of the modelled diagonal member. The equivalent stiffness is computed according to the formula shown in equation 5.4.

$$k_{eq,model} = (\frac{1}{k_{s,c}} + \frac{1}{k_{s,m}} + \frac{1}{k_t})^{-1} \tag{5.4}$$

where $k_{eq,model}$ = the equivalent stiffness, $k_{s,c}$ = stiffness of the steel plates inside the corner column, $k_{s,m}$ = stiffness of the steel plates inside the middle column, $k_t$ = stiffness of the remaining timber member.

Since the length of the diagonal rods in the FE model remains the same, it is chosen to alter their E-modulus to incorporate the equivalent stiffness. The altered E-modulus is determined using the ratio between the equivalent stiffness, calculated using equation 5.4, and the stiffness of the modelled diagonal member. This is shown in equation 5.5.

$$E_{alt} = \frac{k_{eq,model}}{k_{modelled}} \cdot E_t \tag{5.5}$$

where $E_{alt}$ = the altered E-modulus, $k_{eq,model}$ = the equivalent stiffness, $k_{modelled}$ = stiffness of the modelled diagonal timber member, and $E_t$ = E-modulus of the timber member.

The computed stiffnesses are listed in table 5.3 as well as the altered E-modulus for the diagonal rods. For the latter, the mean length and the mean angle of the modelled diagonals (see property table 5.2) are used. This means that all modelled diagonals are assigned the same altered E-modulus.

**Table 5.3:** Computed stiffnesses and altered E-modulus.

| Computed property | Symbol | Value | Unit | Note |
|---|---|---|---|---|
| Stiffness of the modelled timber member | $k_{modelled}$ | 718 | $kN/mm$ | equation 4.5 |
| Stiffness of the steel plates inside corner column | $k_{s,c}$ | 7446 | $kN/mm$ | equation 4.5 |
| Stiffness of the steel plates inside middle column | $k_{s,m}$ | 17549 | $kN/mm$ | equation 4.5 |
| Stiffness of the (remaining) timber member | $k_t$ | 1072 | $kN/mm$ | equation 4.5 |
| Equivalent stiffness | $k_{eq,model}$ | 890 | $kN/mm$ | equation 5.4 |
| Altered E-modulus | $E_{alt}$ | 16109 | $MPa$ | equation 5.5 |

The altered E-modulus from table 5.3 is assigned to the modelled timber diagonal members. This value accounts for the elastic stiffness of the remaining timber member and the steel plates placed inside the columns to which the diagonals are connected. The stiffness of the diagonal connections can now be assigned to the nodes. This allows for a simple and accurate study of the influence of diagonal connection stiffness on serviceability behaviour. The results of this sensitivity study are discussed in the next section.

## 5.4.2. Results

The axial stiffness of the diagonal connections is plotted against the maximum displacements in figure 5.7. The graph shows a steep decrease in displacement in the low stiffness range. In the higher stiffness range, the effect is less.
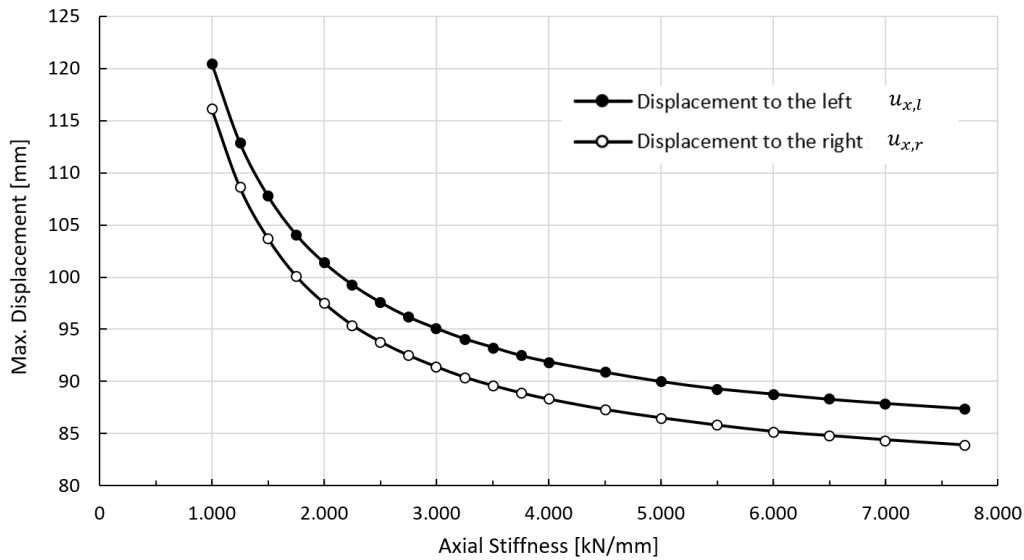
**Figure 5.7:** Maximum displacement as a function of the axial stiffness of the diagonal connections.

From figure 5.7 it becomes evident that to limit the maximum displacement, one should aim to avoid a low stiffness of the diagonal connections. If the structure does not meet its displacement requirement, the engineer could choose to increase the diagonal connection stiffness. In figure 5.8, the impact of the diagonal connection stiffness on the natural frequency is plotted. Similarly to the displacement, the effect is largest in the low-stiffness range. The natural frequency increases with higher stiffness.
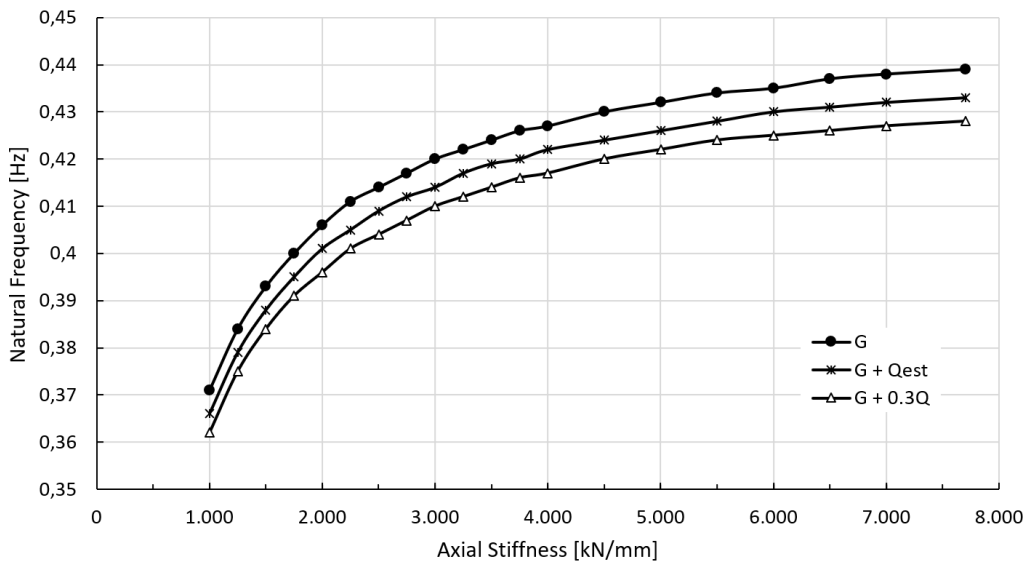


**Figure 5.8:** Natural frequency as a function of the axial stiffness of the diagonal connections.

For the 100-dowel diagonal connections, the elastic stiffness estimated with equation 3.10 is equal to 2141kN/mm. To study how sensitive the serviceability behaviour is to changes in the connection parameters, some examples are considered. The number of dowels is kept the same, but the timber grade is changed. In addition, the effect of changing the number of steel plates by adding or subtracting one plate is considered. The variants are listed in table 5.4

Table 5.4: Adjusted parameters and corresponding estimated elastic stiffness of the diagonal connections; examples.

| Name | SP* | strength class | $\rho_{\text{mean}}$ [$kg/m^3$] | $K_{\text{ser,mod}}$ (eq. 3.10) |
|------|-----|----------------|-------------------|------------------|
| GL30c (current) | 4 | GL30c | 430 | $2141 kN/mm$ |
| GL20h | 4 | GL20h | 370 | $1709 kN/mm$ |
| GL20h + 3SP's | 3 | GL20h | 370 | $1282 kN/mm$ |
| GL32h | 4 | GL32h | 490 | $2604 kN/mm$ |
| GL32h + 5SP's | 5 | GL32h | 490 | $3255 kN/mm$ |

*number of slotted-in steel plates.

In figure 5.9, the estimated elastic stiffnesses corresponding to the different diagonal connections are drawn. It shows that with small adjustments, the maximum displacement can be changed significantly. If the displacement requirements were not met in the initial design, increasing the stiffness of the diagonal connections can be an effective way to reduce the displacements. If the requirements are still not met when applying relatively easy adjustments, like those presented in this example, a designer would have to consider increasing the number of dowels or changing the dimensions of the timber members. The former is purposely not done for this example because the engineering model (equation 3.10) used to estimate the elastic stiffness of the diagonal connections is assumed to only provide a good estimation for a number of dowels up to 100.
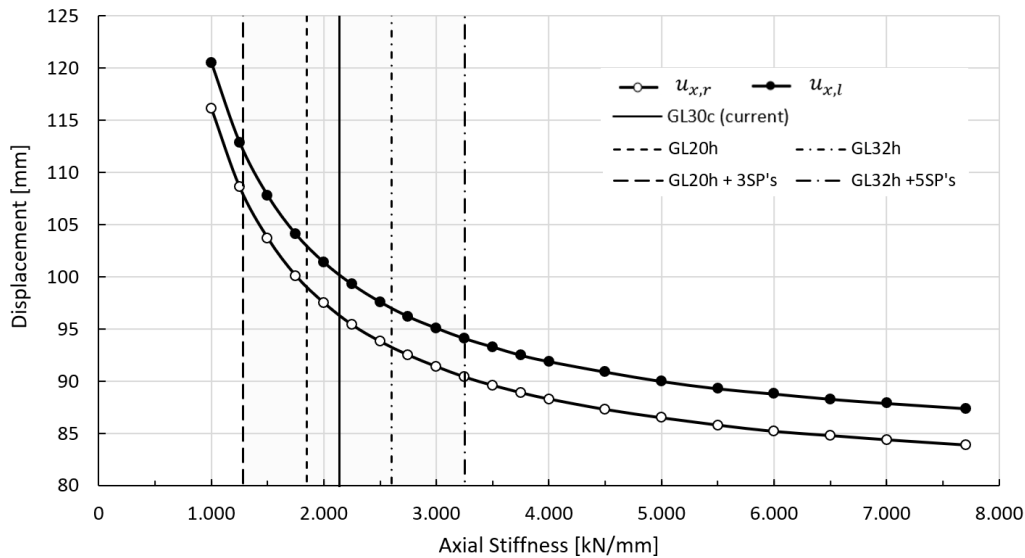


Figure 5.9: Effect of changing the diagonal connection parameters on the maximum displacement.

The maximum displacements, corresponding to the examples listed in table 5.4, can be read from table 5.5. Furthermore, the changes in natural frequency are presented. The percentages in the table indicate the change in comparison to the diagonal connection that is actually applied in the structure.

Table 5.5: Change in max. displacement and natural frequency due to adjusted stiffness of the diagonal connections.

| Name | $K_{\text{ser,mod}}$[kN/mm] | $u_{x,l}$[mm] | $f_1$[Hz]$(G + Q_{est})$ |
|------|----------------|----------|------------------|
| GL30c (current) | 2141 | 100 | 0.404 |
| GL20h | 1709 (-20.2%) | 103 (+3%) | 0.398 (-1.5%) |
| GL20h + 3SP's | 1282 (-40.1%) | 112 (+12%) | 0.380 (-5.9%) |
| GL32h | 2604 (+21.6%) | 97 (-3%) | 0.410 (+1.5%) |
| GL32h + 5SP's | 3255 (+52.0%) | 94 (-6%) | 0.417 (+3.2%) |

the percentages indicate the change in comparison to the current connection (GL30c).

## 5.5. Initial slip of the diagonal connections

In the previous paragraph, the influence of the elastic stiffness of the diagonal connections has been discussed. Before the connections reach their elastic stiffness, they will undergo some local displacement. This phenomenon, referred to as the initial slip or zero-stiffness region, has been discussed in section 3.4.3. The most simplistic way to model the load-slip behaviour of the connection is to divide it into two parts; an initial slip and the elastic stiffness. The RFEM model has been built such that the load-slip behaviour of the connections can be assigned in the nodes by means of a diagram. The diagram assigned to the diagonal connections is shown in figure 5.10. The initial slip will not affect the natural frequency of the structure, therefore, only the effect on maximum (global) displacement is discussed in this section.
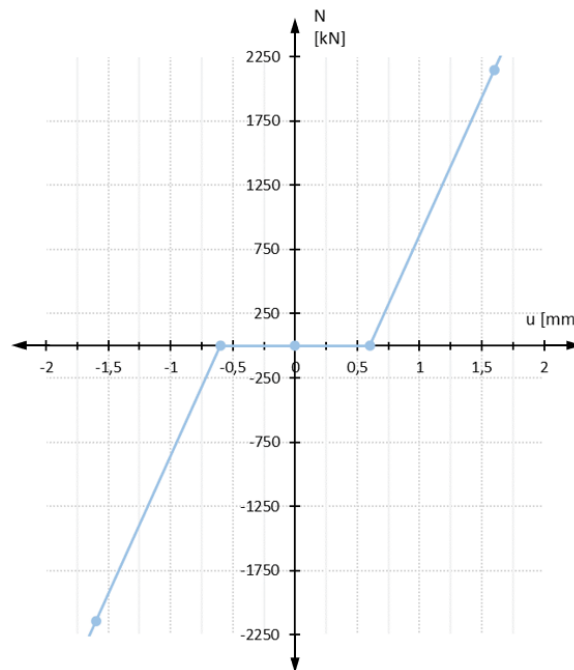


**Figure 5.10:** Load-slip diagram assigned to the nodes at the ends of the modelled diagonal members.

The initial slip in figure 5.10 is equal to 0.6mm. The initial slip of a large connection with a hole clearance in the steel plates of 1mm is expected to be around 0.5 - 0.6mm. This approximation is based on the load-slip graph of the large specimen tested by Reynolds et al. [41] which has been presented and discussed in section 3.4.3. Reynolds et al. obtained a zero-stiffness region of 0.55mm for their 35-dowel softwood connections. This value is estimated by fitting an elastic stiffness and reading the point at which this linear fit intersects with zero force (the x-axis). They concluded their research by stating that densification around the timber holes opens them up, and thereby, increases the zero-stiffness region. In their test on the large specimen, only one unloading-reloading cycle is performed.

The diagonal connections in Mjøstårnet's truss will be repeatedly loaded in cycles and alternate between tension and compression. The connections in the bottom of the truss will be exposed to the highest normal forces. It could be that the zero-stiffness region in these bottom connections becomes larger due to cyclic exposure with loads close to 40% of $F_{est}$. In addition, long-term effects, like creep, might enlarge the zero-stiffness region even more. The diagonal connections in the upper part of the truss will not be exposed to loads close to $0.4F_{est}$, therefore, the initial slip in these connections is expected to be lower in comparison to the bottom connections. Assuming a local initial displacement of 0.6mm for all diagonal connections is considered to be a suitable and conservative approach. To quantify the effect of the initial slip, a range from 0 up to 0.7mm is studied. The elastic stiffness of the diagonal connections is fixed at 2141kN/mm. The results are plotted in figure 5.11.
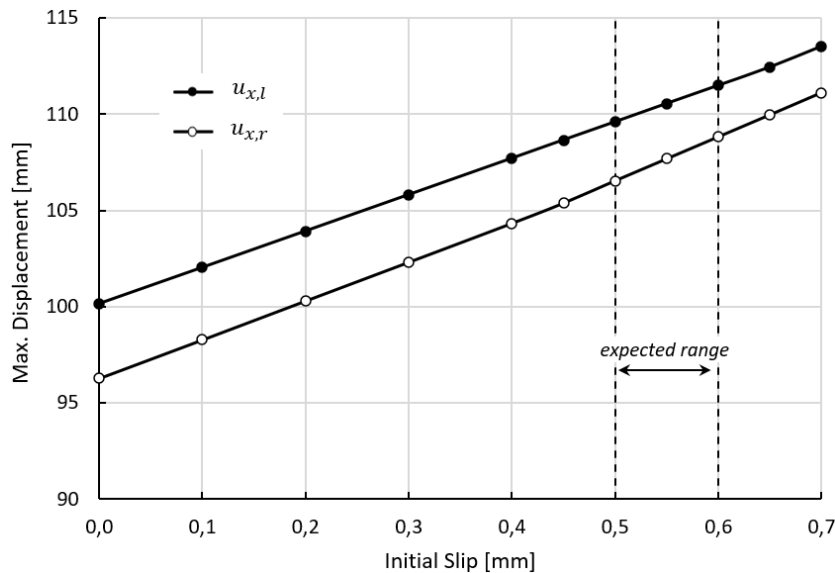
**Figure 5.11:** Maximum displacement as a function of initial slip of the diagonal connections.

A linear relation between the maximum displacement and the initial slip is found, as shown in figure 5.11. The maximum displacement of the structure increases as a result of the increasing local slip in the diagonal connections. The figure shows that the difference between not considering the slip (0mm) and applying the expected slip is very significant. Correspondingly, it is important to verify the global displacement of a structure taking into account the initial slip of the diagonal connections.

### 5.5.1. Tri-linear idealizations

In section 3.4.4 from the literature review, it has been discussed that the load-slip behaviour of a large timber connection with slotted-in steel plates could be idealized by splitting it into three parts. Two possible tri-linear idealizations have been proposed. These idealizations are meant to provide a more accurate estimation of the slip in the initial part of the load-slip curve. This is relevant for connections that are exposed to low loads. In the context of a stability truss, this concerns the connections in the upper diagonals.

Reynolds. et al. [41] proposed to subdivide the load-slip curve into a zero-stiffness region followed by an elastic stiffness. This approach is here referred to as 'linear' and the corresponding diagram is shown in figure 5.10. In figure 5.12a, the first tri-linear idealization of the axial load-slip behaviour of the diagonal connections is shown. Herein, the elastic stiffness is present from the point where the connection reached 10% of $F_{est}$. For the 100-dowel diagonal connection, the characteristic failure load is estimated to be 7591kN. Block shear governs this failure, as can be read from table C.5. 10% of $F_{est}$ is then equal to 759kN. For the initial slip due to non-reversible deformation, a value of 0.3mm is applied.

Tri-linear idealization 2 is shown in figure 5.12b. In this diagram, the elastic stiffness is present after the local displacement is equal to the hole clearance in the steel plate, which is 1mm. The initial slip is 0.3mm. Note that the two tri-linear idealizations do not differ very much in this case. That is because at 10% of $F_{est}$ the local displacement is expected to be approximately equal to 1mm.

(a) Tri-Linear Idealization 1.                    (b) Tri-Linear Idealization 2.
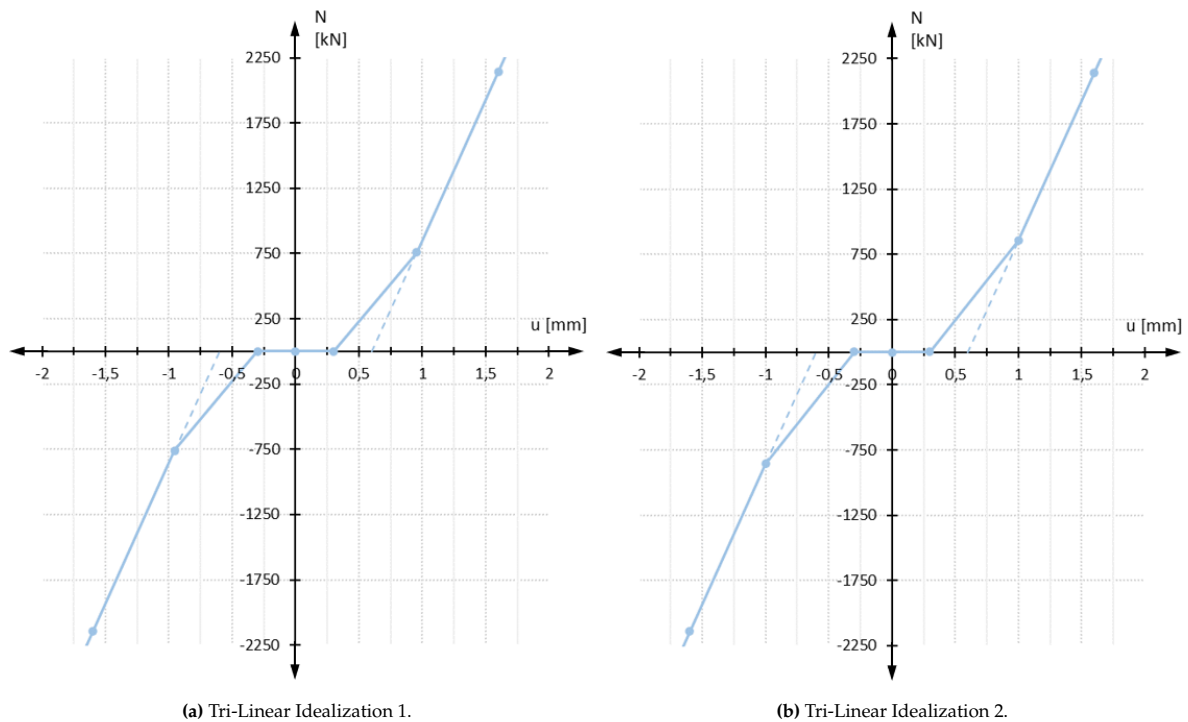
**Figure 5.12:** Modelled load-slip relationships for the diagonal connections.

The obtained maximum displacements when applying the tri-linear idealizations in comparison to using the linear idealization for the diagonal connections are shown in table 5.6. Note that only the displacements are compared because the natural frequency will not be affected by the idealization of the low-stiffness region of the curve. The results show that the difference in maximum global displacement is little. Therefore, it is advised to model the load-slip behaviour of the diagonal connections according to the linear approach. This approach is most simple and only requires the addition of a local initial slip to the elastic stiffness.

**Table 5.6:** Comparison of results for the three idealizations.

|  | Max. displacement [mm] | |
|---|---|---|
|  | $u_{x,l}$ | $u_{x,r}$ |
| **Linear** | 111.48 | 108.82 |
| **Tri-Linear 1** | 112.25 | 108.52 |
| **Tri-Linear 2** | 112.23 | 108.40 |

### 5.5.2. Non-uniform connection geometry

The geometry of the diagonal connections at the bottom member has been considered to be (uniformly) applied at every diagonal connection throughout the height of the structure. This connection has 10 dowels in a row and 10 rows of dowels, i.e. 100 dowel connection. In the actual design, however, the number of dowels in the diagonal connections will decrease towards the top of the structure. The number of dowels is 100 (10x10), 81 (9x9), and 64 (8x8) respectively. This design choice will result in a less stiff structure. Consequently, the displacements are expected to increase, and the natural frequency is expected to be lowered. The size of the diagonal members does not change with height.

To research the impact of lowering the number of dowels towards the top of the structure, the non-uniform connections are considered in a separate model. In this model, the adjusted E-modulus is the same for all diagonal members (same value as for uniform connections). In actuality, when the number of dowels in a row decreases, the length of the connection will also decrease (see equation 5.1). A change from 10 to 9 dowels in a row will result in a decrease in the connection zone of 100mm which is the spacing in between dowels parallel to the grain. Correspondingly, the timber member length will increase by 200mm when the connection length is reduced on both sides of the member. The

timber diagonal member length is large i.e. 11.2m on average, thus, the change in adjusted E-modulus is negligible. Therefore, the E-modulus of the modelled diagonal members in the non-uniform models is kept at 16109MPa (see table 5.3). The applied connection stiffnesses, for the non-uniform model, can be read from table 4.9. The load-slip behaviours are idealized using the linear approach with a zero-stiffness region of 0.6mm. The results are shown in table 5.7.

**Table 5.7:** Comparison of results for uniform and non-uniform diagonal connection geometry.

|  | Natural Frequency [Hz] | | | Max. Displacement [mm] | |
| --- | --- | --- | --- | --- | --- |
|  | $1.0G$ | $G + Q_{est}$ | $G + 0.3Q$ | $u_{x,l}$ | $u_{x,r}$ |
| **Uniform** | 0.409 | 0.403 | 0.399 | 111.48 | 108.82 |
| **Non-Uniform** | 0.403 | 0.398 | 0.394 | 113.98 | 111.32 |

The results for the non-uniform geometry of the diagonal connection applied in the actual stability truss in the Mjøstårnet building do not deviate much from those from the uniform model. The maximum displacements increase by 2.5mm and the natural frequency decreases slightly, as can be read from table 5.7. The preliminary study into the connection capacities, from which the results are shown in table C.5, showed that the UC's of the upper diagonal connections are low. This suggests that, with respect to strength, the applied number of dowels could have been even lower. One has to bear in mind, however, that applying numerous different connection geometries requires more engineering work. Therefore, it seems best to design the connections at the bottom and apply the required geometry uniformly throughout the stability truss.

## 5.6. Vertical components

When the diagonal forces are decomposed, it becomes evident that there is a residual vertical force that must be transferred to the corner columns to create equilibrium. The vertical components of the diagonal forces enter the steel plates and are transferred to the timber columns by means of a large group of dowels. An image of such a connection is shown in figure 4.15. In this figure, the dowel group which transfers the vertical component to the column is highlighted in yellow. In this connection, there are 10 rows of dowels perpendicular to the grain and 16 dowels in each row (parallel to the grain).

At three locations within the truss, a connection between two diagonals and a corner column can be found (connection CL2, CR3, and CL4 in figure 4.6a). The number of dowels inside the column at connection CL4 is slightly less compared to the other two vertical components. Connection CL2 is located between two column sections with different strength classes (the bottom left section is GL30h). Correspondingly, the dowels located in this bottom section will have a higher stiffness. For the sensitivity study, the vertical stiffnesses of the three connections are taken to be equal. A stiffness range of 1000 - 6000kN/mm is considered. The modelling approach will be explained further in the next section. The elastic (axial) stiffness of the diagonal connections has been given a value of 2141kN/mm with an initial slip of 0.6mm.

### 5.6.1. Modelling approach

To be able to assign stiffness to the dowel group inside the columns, a stiff element with a size of 1mm is modelled. This has been discussed in section 4.4.3 and is shown in figure 4.17. A shear stiffness diagram is specified at the node at the end of this element. The transferred force can be determined from the FE model. This can be done by either decomposing the forces inside the diagonals or by analysing the jump of the force inside the corner column at the point where equilibrium is made with the diagonal forces. This jump will be highest in the connection located lowest in the truss (connection CL2). Under serviceability loading, the vertical component of the connection located in the upper section of the truss (CL4) is relatively small. Therefore, it is studied whether tri-linear idealization 2 gives significantly different results in comparison to simple linear idealization. The difference is found to be negligible, and thus, it is chosen to apply the linear idealization. The modelled load-slip behaviour is shown in figure 5.13. For all three connections that have a vertical component, an initial slip of 0.6mm is given, followed by an elastic stiffness.

**(a)** General linear idealization.

**(b)** Example; diagram for elastic stiffness of 4000kN/mm.
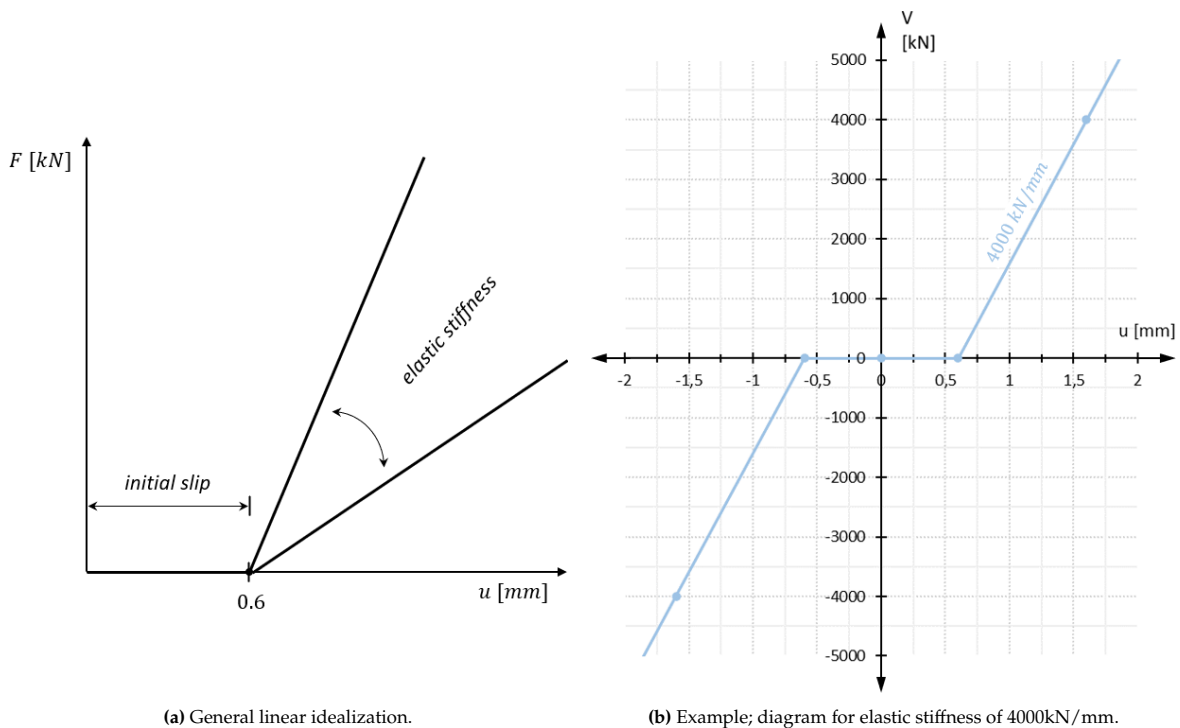
**Figure 5.13:** Modelled load-slip relationships for the vertical components.

## 5.6.2. Results

The influence of the stiffness of the dowel group inside the corner columns on displacement is shown in figure 5.14. Similar to the diagonal connections, the curve starts with a steep decrease and gradually becomes more flat. The displacements when not accounting for the slip of the vertical component of the connection are also shown in the figure for comparison. It can be seen that stiff connections result in a lower displacement. The difference is significant, especially compared to the displacements corresponding to a low connection stiffness.
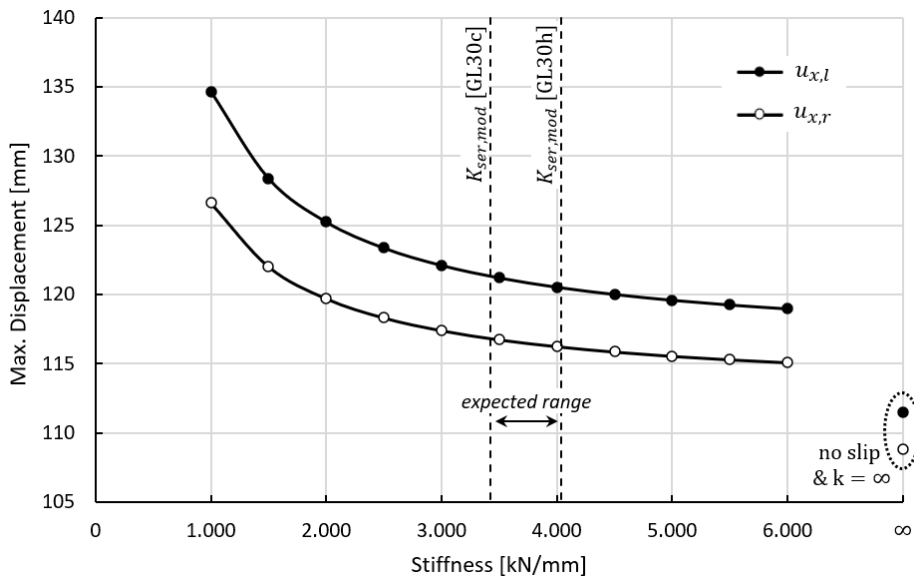


**Figure 5.14:** Maximum displacement as a function of the stiffness of the vertical component.

In figure 5.14, the expected range of the actual stiffness of the vertical components is shown. A range is provided because connection CL2 is in between two column sections that have different strength

classes. Equation 3.9, for the estimation of the elastic stiffness, is composed for up to (10 x 10) 100 dowels. However, as previously discussed and shown in figure 3.15, the stiffness per dowel per shear plane of the tested large-scale connections seemed to approach an asymptotic value. This asymptotic value is used to extrapolate, and thereby, estimate the connection stiffness for the connections with (10 x 16) 160 dowels. The influence of the connection stiffness on the natural frequency is shown in figure 5.14. As the stiffness increases, the curve flattens out. There is, however, still a notable difference between the highest stiffness considered and not accounting for the vertical component, i.e. infinite stiffness.
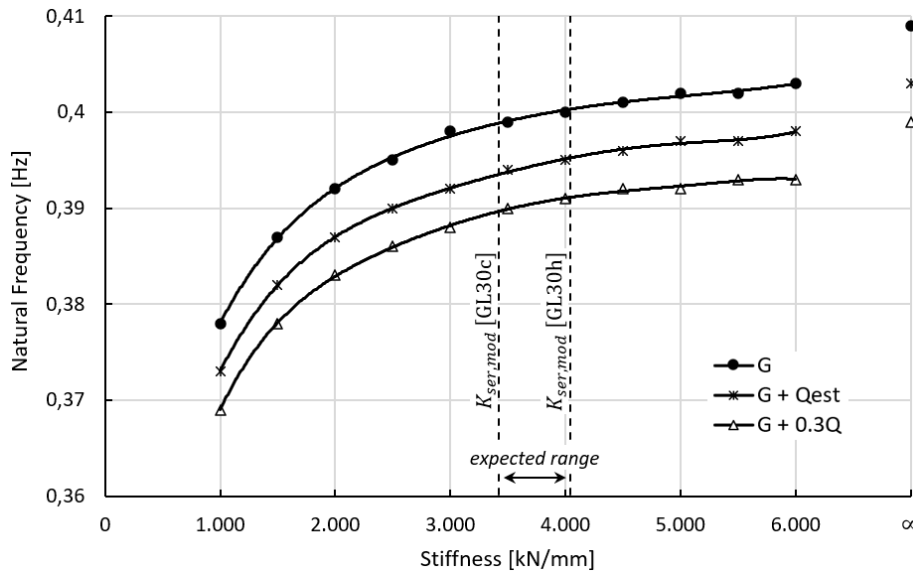


**Figure 5.15:** Natural frequency as a function of the stiffness of the vertical component.

## 5.7. Connection to the foundation

The bottom sections of the corner columns are connected to the foundation using slotted-in steel plates inside the columns. Connection CL1 will be loaded in tension under serviceability loading. This tension force occurs in load-combination 7 (LC7) and LC9 and will cause an uplift of the column. Consequently, the horizontal displacements at the top of the structure will increase.

In the studied model, the load-slip relationship of the diagonal connections is fixed with an initial slip of 0.6mm and an elastic stiffness of 2141kN/mm. The vertical components of connections CL2, CR3, and CL4 are given an initial slip of 0.6mm followed by an elastic stiffness of 3425kN/mm. The elastic stiffness of the column-foundation connection is estimated using the engineering model from section 3.4.2. The column connection has 100 dowels and the member is of strength class GL30h, which has a mean density of $480 kg/m^2$. Using equation 3.10, the elastic stiffness of the column-foundation connection is estimated to be 2525kN/mm. To be able to incorporate the connection stiffness within the node, the E-modulus of the modelled column member is adjusted. This approach is the same as discussed in section 5.4.1 for the diagonal connections. The length of the bottom column section is 17433mm and the length of the connection is 1045mm. The mean value of the E-modulus for GL30h is 13600MPa. The computed altered E-modulus is 14467MPa. This adjustment enables us to specify the load-slip diagram, representing the connection behaviour, within the node at the bottom of the column section.

The tension force in the connection to the foundation in LC7 and LC9 is higher than 10% of the estimated connection capacity. Therefore, an initial slip of 0.6mm followed by the elastic stiffness is applied. The modelled diagram is shown in figure 5.16. Note that the load-slip behaviour of the connection is present when it is loaded in tension. In compression, the load is transferred by contact pressure. There is a stiffness value assigned to compressive loading, but this is only to compensate for the altered E-modulus discussed above.
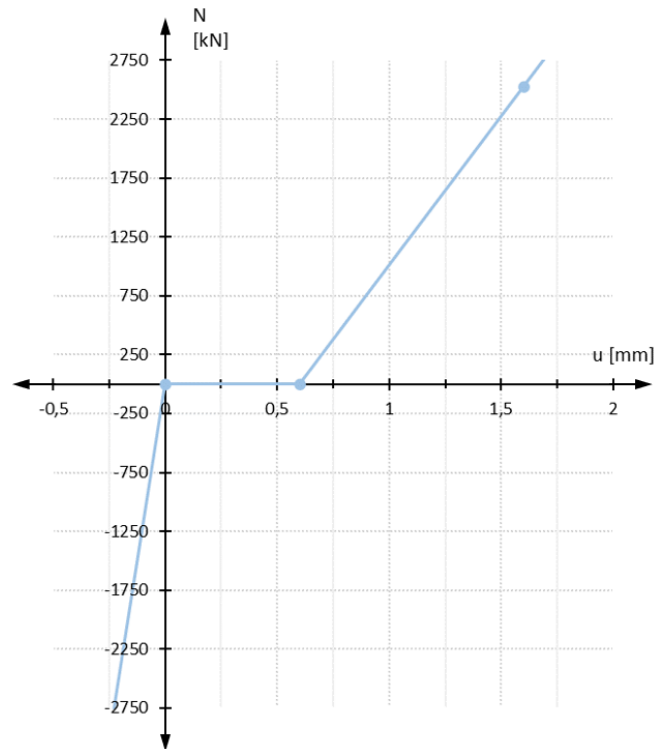
**Figure 5.16:** Load-slip diagram of the connection to the foundation.

The increase of the maximum displacement towards the right, when accounting for the column-foundation connection, is shown in table 5.8. This amplification is the result of the tension force that occurs in LC7 and LC9. At the top of the structure, the displacement increases by 4-5mm (depending on the considered LC). The amplification is significant, therefore, the slip of this connection should be accounted for in the design. Ideally, tension at the bottom of the truss is prevented, but for tall structures, this will be difficult to avoid.

**Table 5.8:** Amplification of displacement when considering the load-slip behaviour of the connection to the foundation.

|  | LC | Tension [kN] | $u_{x,r}$ [mm] |
|---|---|---|---|
| **Base Model** | 7 | 1381 | 116.83 |
|  | 9 | 1791 | 117.13 |
| **Incl. connection** | 7 | 1363 | 121.11 |
| **to foundation** | 9 | 1769 | 122.15 |

For the modelled structure in which all the expected load-slip diagrams for the connections are incorporated, the displacement towards the left is 121.4mm. This displacement is comparable with the computed displacement towards the right ($u_{x,r}$=122.15mm) when accounting for the local slip of the column-foundation connection under tension.

## 5.8. Conclusions

The following parameters are found to have a significant influence on the serviceability behaviour of the structure:

- The (oblique) diagonal connections. These are located at the ends of the diagonal members. They connect the diagonal members to the corner- and middle columns.
- The vertical components i.e. the dowel groups inside the corner columns at the points where two diagonals are attached. Here, the vertical component of the diagonal force is transferred to the column.

- The vertical stiffness of the foundation.

For the three parameters listed above, their effect on both the natural frequency and maximum displacement is highest in the region with low stiffnesses. The curves flatten as the considered stiffness increases. The natural frequency increases with increasing stiffness, whereas, the displacements will decrease.

A linear idealization of the load-slip behaviour of the connections is found to be sufficiently accurate for all considered connections. This idealization consists of an initial slip followed by the elastic stiffness of the connection. For connections that will be exposed to low force, this idealization might slightly overestimate local displacements. For these connections, tri-linear idealizations are expected to be more accurate. However, this requires more discreet modelling and more tests should be done to obtain accurate values for the three regions in these idealizations. In the context of the analysed stability truss, applying tri-linear idealizations had a negligible influence on its serviceability behaviour. Therefore, it is advised to use a simple linear relationship for all the truss connections.

The initial slip of a connection does not affect the natural frequency of the structure. Thus, when the dynamic response of the building is considered, only the elastic stiffness of the connections would have to be specified within the nodes. The local displacements, that occur before a connection reaches its elastic stiffness, have a significant influence on the global displacement of the structure. The initial slip in the diagonal connections, in particular, greatly amplifies the displacement. This is because there are numerous of these connections within the truss.

It is also important to consider the connection between the corner column and the foundation. When this connection is loaded in tension, the local displacement will amplify the displacement at the top of the structure. Compression is transferred by contact, which needs to be accounted for when specifying the load-slip diagram of the connection in the node.

6

# Variant Study

## 6.1. Introduction

In this chapter, alternative designs for the structural system are considered. This is meant to provide structural engineers with information about the effect of preliminary design decisions. The focus is on the change of serviceability behaviour that the variants might have as a result of changing the number of connections and their geometries. The goal of the variant study is to support the decision-making process in the preliminary design stage of a project.

## 6.2. Variants

The four variants shown in figure 6.1 are researched. A short description of the variants A up to D is given below.

- **Variant A**: The truss members are changed from timber grade GL30c to GL30h.
- **Variant B**: The diagonals span over 3 storeys instead of 4.
- **Variant C**: Cross bracing is applied.
- **Variant D**: The width of the stability structure is increased by 50%.
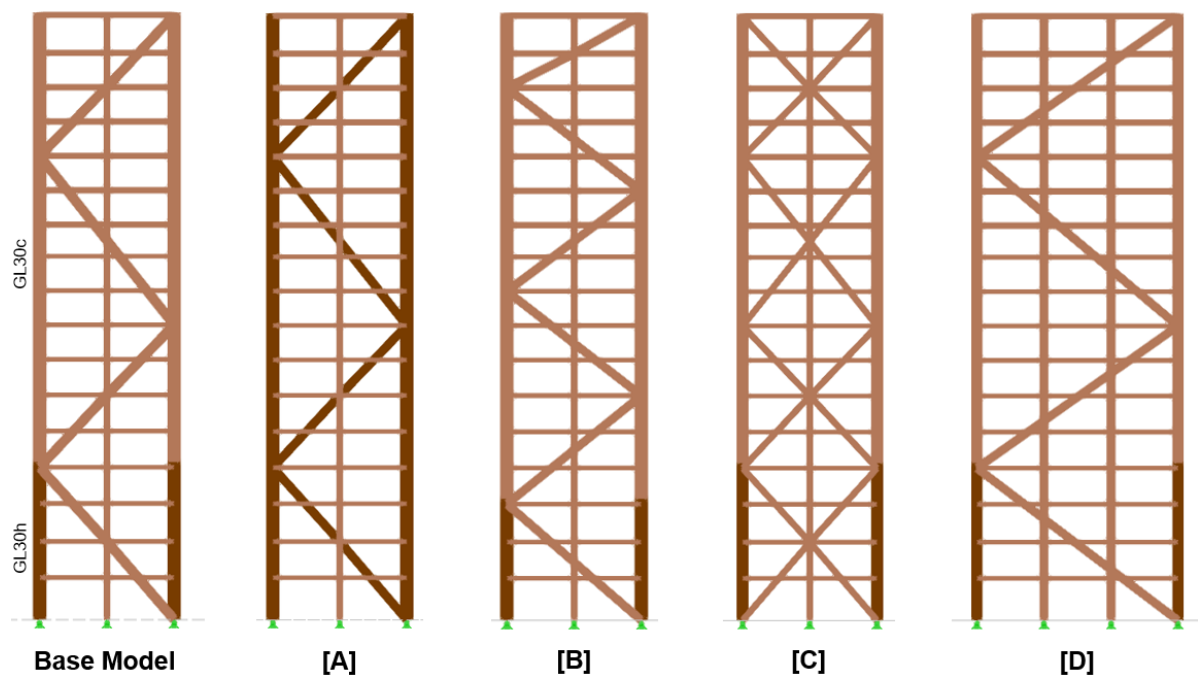


**Figure 6.1:** Overview of the modelled variants.

To make a fair comparison between the variants, the unity checks (UC's) for the diagonal- and column members at the bottom of the structure are aimed to be as close as possible to those from the base model. This means that the cross-sectional area of the timber members is scaled accordingly. The width of each truss member remains equal to 625mm, thus only the member heights are adjusted. For each variant, a model with pinned members without any additional adjustments (approach 1) and a model in which connection stiffnesses are considered (approach 2) are studied. This allows for a comparison between the two modelling approaches. The vertical foundation stiffness is not considered, correspondingly, the supports are pinned.

In modelling approach 2, the behaviour of the connections is incorporated by specifying the load-slip diagram in the nodes. The E-modulus of the modelled diagonal members is altered, as previously discussed in section 5.4.1, to enable this. The elastic connection stiffnesses are computed using equation 3.10. The modelled load-slip behaviour of the connections consists of an initial slip of 0.6mm followed by elastic stiffness. The diagrams are specified for the diagonal connections, the vertical component i.e. the dowel group inside the corner columns, and the connection between the corner columns and the foundation.

The connection geometry of the vertical components and the column-foundation connection are the same for all variants, with the exemption of variant A. The vertical component has a higher stiffness in variant A because of the higher timber grade. For this variant, the elastic stiffness of the vertical component is estimated to be 4040kN/mm. The estimated elastic stiffness for the other variants is 3425kN/mm. The modelled load-slip diagram of the column-foundation connection is shown in figure 6.2b. The elastic stiffness is 2525kN/mm when loaded in tension and compression is transferred through contact. The altered E-modulus of the bottom column section is 14467MPa. This value is the same for all variants, except for variant B in which the length of the lower column section has changed.



(a) Vertical component for all variants except A.          (b) Column-foundation connection for all variants.
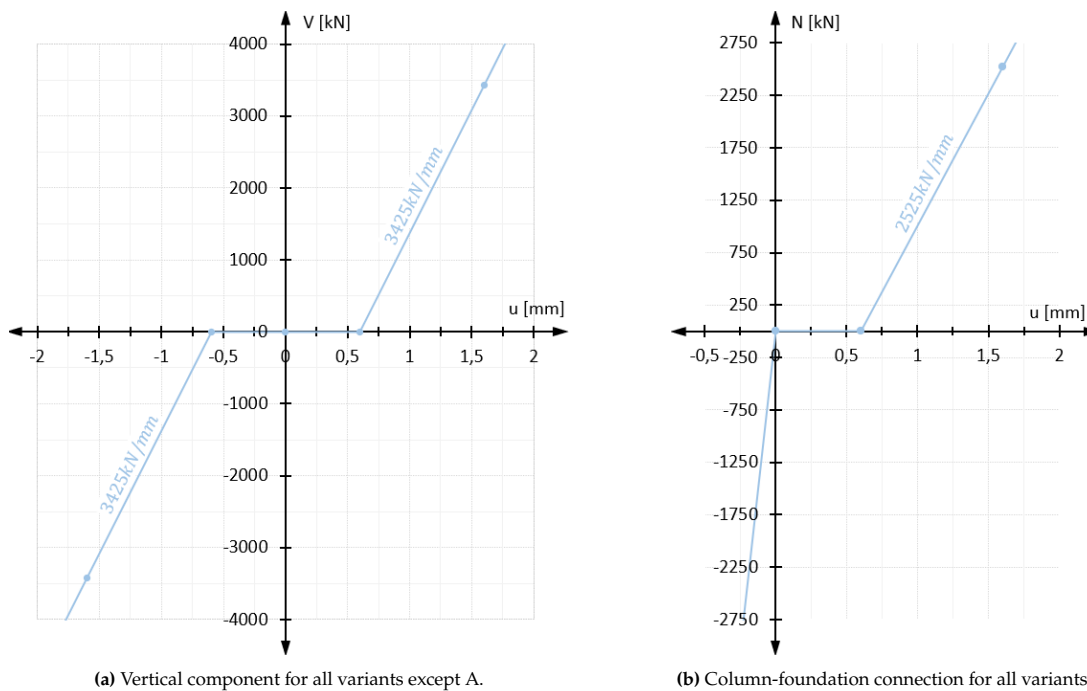
**Figure 6.2:** Applied load-slip diagrams.

The load-slip diagram of the diagonal connections differ for each variant. As previously mentioned, the member dimensions are scaled to keep their UC's approximately the same. This is also done for the design capacity of the governing diagonal connections. The geometry of the connections is adjusted to keep the UC similar to that in the base model. When the height of the diagonal members is adjusted, this will have an effect on the dowel geometry. The steel parts are kept to be embedded at least 85mm to satisfy the fire criteria. The geometries of the diagonal connections are uniform throughout the height of the truss. To clarify, the upper connections have the same geometry as the governing ones at the bottom of the structure.

In the following subsections, each variant is discussed separately. The considered properties are mentioned, and the dynamic response and maximum displacements obtained using modelling approaches 1 and 2 are presented. A modal analysis is performed which gives the natural frequency as well as the corresponding mode shape. Mass combination $G + Q_{est}$ (see table 4.8) is considered in the modal analysis. The calculation provided in EC1991-1-4 [19] is used to estimate the building's accelerations. This analytical approach makes use of numerous parameters related to the building's geometry and wind conditions. The effective mass per unit area is provided by Sweco Norway (*M. A. Bjertnæs, personal communication, July 2023*). In the calculations, a structural damping of 1.5% is considered for all variants with the exemption of variant D. The accelerations at floor 17 are computed. This floor is located at a height of +63.3m which is indicated in figure 4.9b.

### 6.2.1. Base model

The properties related to the diagonal elements in the base model are previously shown in table 5.2. For the variants, only changes in properties with respect to the properties listed in this table will be mentioned. Two FE models are drawn up using the two different approaches. In the base model with approach 2, the E-modulus of the diagonal members is altered to 16109MPa (see table 5.3) and the elastic stiffness of the 10x10 dowel diagonal connections is 2141kN/mm. The obtained dynamic responses and displacements are presented in table 6.1.

**Table 6.1:** Results for the base model.

| Modelling approach | Dynamic response | | Max. displacement [mm] | |
|---|---|---|---|---|
| | $f1[Hz]$ | $A[m/s^2]$ | $u_{x,l}$ | $u_{x,r}$ |
| **Approach 1** | 0.433 | 0.0654 | 87.6 | 84.2 |
| **Approach 2** | 0.393 (-10.2%) | 0.0731 (+11.8%) | 122.2 (+45.1%) | 121.1 (+43.8%) |

### 6.2.2. Variant A

The strength class of all the truss members is changed to GL30h. Consequently, the stiffness of the members increases. Furthermore, the elastic stiffness of the connections increases because of the higher mean density. For this variant, the member dimensions and connection geometries are kept the same as the base model. This is done because the geometry of the truss is unchanged. The properties that differ in comparison to the base model are listed in table 6.2.

**Table 6.2:** (altered) Properties in variant A.

| Property | Symbol | Value | Unit | Note |
|---|---|---|---|---|
| GL30h | $E_{mean}$ | 13600 | $MPa$ | |
| | $\rho_{mean}$ | 480 | $kg/m^3$ | |
| Diagonal connections | $K_{ser,mod}$ | 2525 | $kN/mm$ | equation 3.10 |
| Vertical components | $K_{ser,mod}$ | 4040 | $kN/mm$ | equation 3.10 |
| Altered E-modulus | $E_{alt}$ | 16721 | $MPa$ | equation 5.4 |

The computed dynamic responses and displacements are shown in table 6.3. Note that the results are comparable with the values from the base model (see table 6.1). The most significant difference is the lower displacement for approach 2, which is to be expected when the stiffness of the truss increases.

**Table 6.3:** Results for variant A.

| Modelling approach | Dynamic response | | Max. displacement [mm] | |
|---|---|---|---|---|
| | $f1[Hz]$ | $A[m/s^2]$ | $u_{x,l}$ | $u_{x,r}$ |
| **Approach 1** | 0.434 | 0.0653 | 86.8 | 83.3 |
| **Approach 2** | 0.403 (-7.1%) | 0.0711 (+8.9%) | 115.8 (+33.4%) | 115.9 (+39.1%) |

### 6.2.3. Variant B

For this variant, the angle of the diagonal elements is lowered. The elements now span 3 storeys, with the exemption of the upper two diagonals. Because the upper diagonals differ, their properties are

computed separately. The dimensions of the diagonal members and their connections are changed. The height of the bottom corner column sections (with timber grade GL30h) is less, as can be seen in figure 6.1. The altered E-modulus of the lowest section of the left corner column is now 14747MPa. All altered properties related to the diagonal elements are listed in table 6.4.

**Table 6.4:** (altered) Properties in variant B.

| Property | Symbol | Value | Unit | Note |
|---|---|---|---|---|
| Diagonal member | b x h | 625x 848 | $mm$ | $A = 530.000mm^2$ |
| Diagonal connections | $n_{90}$ | 8 | - | $a_2 = 85mm$ |
| | $n_0$ | 9 | - | $a_1 = 100mm$ |
| | $K_{ser,mod}$ | 1541 | $kN/mm$ | equation 3.10 |
| | $l_{connection}$ | 960 | $mm$ | equation 5.1 |
| | $h_{SP}$ | 635 | $mm$ | $(n_{90} - 1)a_2 + 40$ |
| | $A_s$ | 30480 | $mm^2$ | 4 SP's ($t = 12mm$) |
| Model parameters 1 | $l_{modelled}$ | 9481 | $mm$ | average length |
| (lower diagonals) | $\theta$ | 39 | $^\circ$ | average angle |
| | $l_{SPc,m}$ | 405 | $mm$ | equation 4.6 |
| | $l_{SPc,c}$ | 955 | $mm$ | equation 4.6 |
| | $l_{timber}$ | 6201 | $mm$ | equation 5.2 |
| | $E_{alt}$ | 16080 | $MPa$ | equation 5.4 |
| Model parameters 2 | $l_{modelled}$ | 9846 | $mm$ | average length |
| (2 upper diagonals) | $\theta$ | 28 | $^\circ$ | average angle |
| | $l_{SPc,m}$ | 357 | $mm$ | equation 4.6 |
| | $l_{SPc,c}$ | 841 | $mm$ | equation 4.6 |
| | $l_{timber}$ | 5318 | $mm$ | equation 5.2 |
| | $E_{alt}$ | 16597 | $MPa$ | equation 5.4 |

The computed dynamic responses and displacements are shown in table 6.5. The difference in results obtained by modelling approaches 1 and 2 has increased. This is because the number of connections, in comparison to the base model, has increased.

**Table 6.5:** Results for variant B.

| Modelling approach | Dynamic response | | Max. displacement [mm] | |
|---|---|---|---|---|
| | $f1[Hz]$ | $A[m/s^2]$ | $u_{x,l}$ | $u_{x,r}$ |
| **Approach 1** | 0.435 | 0.0639 | 85.8 | 81.5 |
| **Approach 2** | 0.383 (-12%) | 0.0743 (+16.3%) | 131.1 (+52.8%) | 128.4 (+57.6%) |

## 6.2.4. Variant C

In variant C, cross bracing is applied. The member forces in this truss are different from those with single braces. To keep the UC's comparable, both the dimensions of the diagonals and corner columns are adjusted. Tension will now occur in the connection to the foundation at both the left- and right-corner columns. This tension force will, however, be lower in comparison to the base model. The E-modulus of both column sections is adjusted (both to 14467 MPa), and the load-slip behaviour of the connections to the foundations is specified in the node at the bottom of these sections. The additional altered properties are listed in table 6.6.

**Table 6.6:** (altered) Properties in variant C.

| Property | Symbol | Value | Unit | Note |
|---|---|---|---|---|
| Corner column | b x h | 625 x 1320 | $mm$ | $A = 825.000 mm^2$ |
| Diagonal member | b x h | 625 x 635 | $mm$ | $A = 396.875 mm^2$ |
| Diagonal connection | $n_{90}$ | 6 | - | $a_2 = 85 mm$ |
| | $n_0$ | 10 | - | $a_1 = 100 mm$ |
| | $K_{ser,mod}$ | 1284 | $kN/mm$ | equation 3.10 |
| Model parameters | $l_{SPc,c}$ | 986 | | equation 4.6 |
| | $l_{timber}$ | 7627 | $mm$ | equation 5.2 |
| | $h_{SP}$ | 465 | $mm$ | $(n_{90} - 1)a_2 + 40$ |
| | $A_s$ | 22320 | $mm^2$ | 4 SP's ($t = 12 mm$) |
| | $E_{alt}$ | 15779 | $MPa$ | equation 5.4 |

The results are shown in table 6.7. Note that the maximum displacement to the left and right are equal because the structure is symmetric. Even though the number of connections increases in comparison to the base model, the maximum displacements are lower (for approach 2). This is because the stiffness of the structure increased due to a larger number of diagonal members. Consequently, the natural frequency increases and the maximum acceleration decreases.

**Table 6.7:** Results for variant C.

| Modelling approach | Dynamic response | | Max. displacement [mm] | |
|---|---|---|---|---|
| | $f1[Hz]$ | $A[m/s^2]$ | $u_{x,l}$ | $u_{x,r}$ |
| **Approach 1** | 0.443 | 0.0626 | 80.7 | 80.7 |
| **Approach 2** | 0.410 (-7.4%) | 0.0687 (+9.7%) | 113.5 (+40.6%) | 113.5 (+40.6%) |

## 6.2.5. Variant D

In this last variant, the width of the structure is increased by 50%. Consequently, the point loads applied on the second-order frame are increased by the same percentage. The diagonals span over the same number of storeys as the base model, but their angle will be lowered due to the larger width. A middle column is added and the dimensions of the corner columns, middle columns, and diagonals are changed. The compression force in the middle columns increased, therefore, their width is also increased to keep their UC's similar to those in the base model. For the calculation of the accelerations, a damping of 1.9% is used. Furthermore, the mass per unit area is increased by 50%. Because of the additional middle column, the length of the diagonal elements between two middle columns and between a mid-column and a corner column will differ. Correspondingly, two altered E-modules for the modelled diagonal members are computed. All properties are listed in table 6.8.

**Table 6.8:** (altered) Properties in variant D.

| Property | Symbol | Value | Unit | Note |
|---|---|---|---|---|
| Corner column | b x h | 1115 x 625 | $mm$ | $A = 696.875 mm^2$ |
| Middle column | b x h | 860 x 625 | $mm$ | $A = 537.500 mm^2$ |
| Diagonal | b x h | 842 x 625 | $mm$ | $A = 526.250 mm^2$ |
| Diagonal connection | $n_{90}$ | 8 | - | $a_2 = 85 mm$ |
| | $n_0$ | 9 | - | $a_1 = 100 mm$ |
| | $K_{ser,mod}$ | 1541 | $kN/mm$ | equation 3.10 |
| Model parameters | $l_{connection}$ | 960 | $mm$ | equation 5.1 |
| | $h_{SP}$ | 635 | $mm$ | $(n_{90} - 1)a_2 + 40$ |
| | $A_s$ | 30480 | $mm^2$ | 4 SP's ($t = 12mm$) |
| | $l_{modelled}$ | 9291 | $mm$ | average length |
| | $\theta$ | 37 | ° | average angle |
| | $l_{SPc,m}$ | 538 | $mm$ | equation 4.6 |
| | $l_{SPc,c}$ | 698 | $mm$ | equation 4.6 |
| | $l_{timber}$ | 6295, 6135 | $mm$ | for $E_{alt,m}$ and $E_{alt,c}$ respectively (eq. 5.2) |
| | $E_{alt,m}$ | 16223 | $MPa$ | for member between mid. columns |
| | $E_{alt,c}$ | 16199 | $MPa$ | between mid. and corner columns |

The results are shown in table 6.9. The displacements, when accounting for the connection stiffnesses, are much higher in comparison to the results obtained from approach 1. Because of the increased width, the number of connections increased as well, which explains the large difference in displacement for modelling approaches 1 and 2. The accelerations are low in comparison to the previously discussed variants. This is largely due to the increased mass (per unit of area) of the building in the direction of the considered mode.

**Table 6.9:** Results for variant D.

| Modelling approach | Dynamic response | | Max. displacement [mm] | |
|---|---|---|---|---|
| | $f1 [Hz]$ | $A [m/s^2]$ | $u_{x,l}$ | $u_{x,r}$ |
| **Approach 1** | 0.421 | 0.0404 | 61.8 | 62.4 |
| **Approach 2** | 0.360 (-14.5%) | 0.0483 (+19.6%) | 103.9 (+68.1%) | 105.6 (+69.2%) |

## 6.3. Conclusions

It can be concluded that the difference in serviceability behaviour between the two approaches is significant for each of the researched variants. It is considered insufficient to analyse the building's maximum displacement using the simplistic approach 1. Incorporating the elastic stiffness of the connections (approach 2) lowers the global stiffness of the structure. Consequently, the natural frequency decreases and the maximum displacements increase. The latter is amplified even more due to the initial slip that occurs before the connections reach their elastic stiffness.

The difference in the obtained maximum displacements between the two modelling approaches becomes more as the number of connections increases. This can be concluded by comparing the amplification in displacements for the variants with more connections (Variants B & D) to the displacements of the other variants. The larger difference in displacement between modelling approaches 1 and 2 is due to the significant local displacement that occurs at each connection. Limiting the number of connections within the truss could therefore be necessary to limit the global maximum displacements.

The serviceability behaviour of variant B is found to be worse than the base model. As a consequence of lowering the angle of the diagonals, the number of diagonals increased. Correspondingly, the number of connections increased as well. This resulted in an increase in both maximum acceleration and displacements.

The serviceability behaviour of variants A, C, and D improved in comparison to the base model. However, the improvements for variants A and C are small. Variant D, by far, showed the most improvement. For

this variant, the difference in maximum displacement obtained using the two modelling approaches is high (68.1% and 69.2% increase in displacement). The natural frequency, which is dependent on the system's stiffness and the modelled mass, is lower in comparison to other variants. The related peak accelerations are much lower, which is mainly due to the increased mass per unit area. This shows that increasing the mass of the building is more effective than increasing its stiffness for reducing the peak acceleration.

# 7

# Results

## 7.1. Introduction

The results obtained from the sensitivity- and variant study are presented in this chapter. First, the influence of the truss connections on maximum displacement and natural frequency, obtained from the sensitivity study, is discussed. Thereafter, the peak accelerations and maximum displacements for the base model are computed with the two different modelling approaches and compared. Last, the serviceability behaviour of the modelled variants is presented.

## 7.2. Sensitivity study

Three parameters are found to have a significant influence on the serviceability behaviour of the structure. One of them is the vertical stiffness of the foundation. The sensitivity of the model to this parameter is studied, but in successive models, pinned supports are applied. The load-slip behaviour of two types of connections influence the serviceability behaviour of the truss significantly. The first, referred to as diagonal connections, are highlighted in figure 7.1a. The second, referred to as the vertical component, is the dowel group inside the corner column at the point where two diagonals attach. The vertical component of the force from the diagonals is transferred to the column through this connection. This group of dowels is highlighted in figure 7.1b.



**(a)** The (oblique) dowel group inside the diagonal members (**diagonal connections**).

**(b)** The dowel group inside the corner columns (**vertical component**).
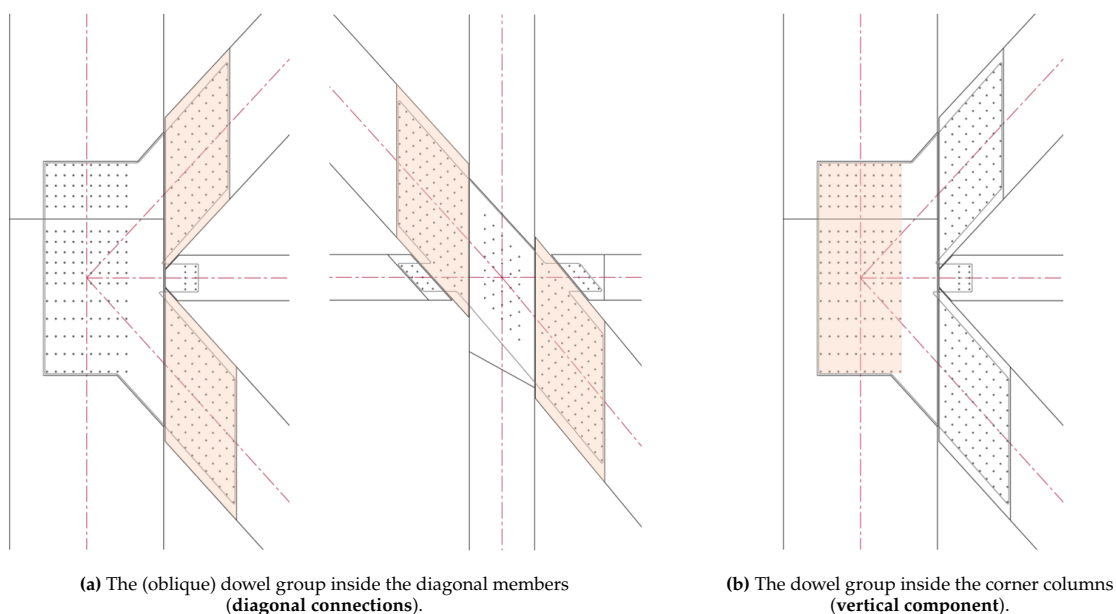
**Figure 7.1:** Truss connections that have a significant influence on the serviceability behaviour.

The load-slip behaviour of a connection can be idealized as linear or tri-linear. In the former, the connection is assigned an initial slip followed by elastic stiffness. In a tri-linear idealization, a low stiffness is specified in the region before the elastic stiffness. In most connections within the truss, the local displacement will surpass the low-stiffness region because of the high loads. Only the connections located at the top of the truss might exhibit a displacement in the low-stiffness region. The difference in results when accounting for this is found to be negligible. Thus, a simple linear idealization is considered accurate enough to make a sound estimation of both natural frequency and displacements.

The displacement and natural frequency as a function of the axial stiffness of the diagonal connections is shown in figure 7.2. Because of the high axial loads and the presence of many of these connections, they have a considerable effect on the serviceability behaviour of the truss. It can be seen that the effect is most significant in the lower stiffness region. The natural frequency, for the loading combination with the estimated variable load, varied from 0.366Hz for the lowest stiffness (1000kN/mm) up to 0.433 HZ for the highest stiffness (7702kN/mm). The connection will, however, not have a stiffness anywhere close to this upper value. The stiffness of the 100 dowel connection is estimated to be around 2141kN/mm. At this stiffness value, the natural frequency and displacements are sensitive to small changes in stiffness. The decrease in displacement between the lowest- and highest diagonal connection stiffness is 38%. This is only due to the difference in elastic stiffness. This does not yet include the initial slip within these connections. When adding an initial slip of 0.6mm, the displacements at the top increase by approximately 12mm, i.e. an increase of 11% (left) and 13% (right) respectively.

**Table 7.1:** Results for the upper- and lower bound of the stiffness of the diagonal connections.

| elastic stiffness | | natural frequency | $u_{x,l}[mm]$ | $u_{x,r}[mm]$ |
|---|---|---|---|---|
| min. | 1000 kN/mm | 0.366 Hz | 120.5 | 116.1 |
| max. | 7702 kN/mm | 0.433 Hz (+18.3%) | 87.4 (-37.9%) | 83.9 (-38.4%) |



**Figure 7.2:** Influence of the elastic stiffness of the diagonal connections on the max. displacement and natural frequency. Adjusted versions of figures 5.7 and 5.8.

In Mjøstårnet's truss, the number of dowels is lower in the diagonal connections at the top of the structure compared to the bottom. This is possible because the diagonal forces in the upper part of the structure are lower. The effect of applying such a non-uniform connection geometry throughout the truss has been studied. The reduced number of dowels caused a decrease in global stiffness. Correspondingly, the natural frequency slightly decreased (-1.3%) and the displacement increased by approximately 2.2%. Applying even fewer dowels in the upper connections would have been possible. This would then lead to a larger difference in results. In relation to serviceability design requirements and for simplicity, it is considered best to apply a uniform design of the connections throughout the truss.

The influence of the stiffness of the vertical components on the maximum displacements and natural frequency is shown in figure 7.3. A similar trend as for the diagonal connections can be observed, however, the effect is less. This is because this connection is present at three locations within the truss, whereas there are many more diagonal connections. The investigated range is an elastic stiffness of

1000 - 6000 kN/mm. The actual stiffness is expected to be somewhere in the middle of this range. Not accounting for the stiffness of these connections is also considered by investigating a case in which the connections are modelled to be stiff. The difference in maximum displacements between the model with the lowest considered stiffness (1000kN/mm) and the model in which the elastic stiffness of these connections is not considered are 17.2% ($u_{x,l}$) and 14.1% ($u_{x,r}$) respectively. The stiffness of the vertical component also influences the natural frequency, which increases as the connection becomes stiffer. The results show that the stiffness of these connections can have a significant influence on the serviceability behaviour of the structure and, therefore, should be considered when modelling a stability truss.

**Table 7.2:** Results for the upper- and lower bound of the stiffness of the vertical component.

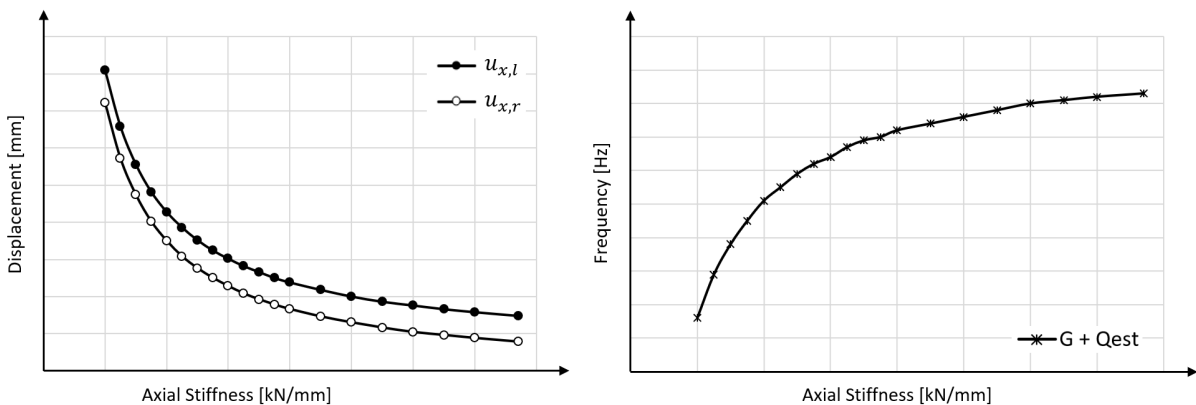| elastic stiffness | | natural frequency | $u_{x,l}[mm]$ | $u_{x,r}[mm]$ |
|---|---|---|---|---|
| min. | 1000 kN/mm | 0.373 Hz | 134.7 | 126.6 |
| max. | 6000 kN/mm | 0.398 Hz (+6.7%) | 119.0 (-11.7%) | 115.1 (-9.1%) |
| stiff | $\infty$ | 0.403 Hz (+8.0%) | 111.5 (-17.2%) | 108.8 (-14.1%) |
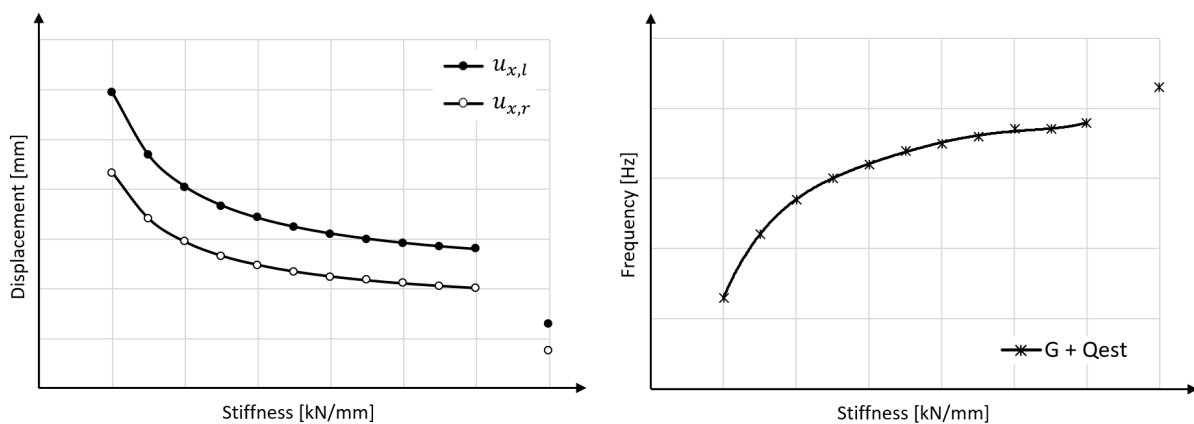


**Figure 7.3:** Influence of the elastic stiffness of the vertical component on the max. displacement and natural frequency. Adjusted versions of figures 5.14 and 5.15.

The influence of the rotational stiffness of the horizontal beam connections is also investigated. Two extreme cases were considered; pinned and stiff connections. The influence of these connections within the truss is found to be little. Only the displacements towards the right showed a significant decrease (-5.9%) when applying stiff connections. In the actual structure, the connections will be semi-rigid. With current knowledge, a good estimation of this elastic rotational stiffness is not achievable. Therefore, it is best to simply model these connections as pinned.

It is also found that, under serviceability load, tension can occur at the connection between the left corner column and the foundation. This will cause local displacement, which results in an increase of maximum displacement of approximately 5mm (+4.3%) at the top of the structure. In the Mjøstårnet building, a lot of weight is added. Consequently, there is only significant tension in the bottom corner column sections. If the self-weight of the building were lower, the tension force at the foundation would become higher and tension might even occur at multiple column connections, i.e. also in between column sections. Tension, especially under serviceability loading, should be avoided as much as possible. When it occurs, the effect of the local deformation on the maximum displacement should be considered. Compression, between column sections and the foundation, is transferred by contact and will not cause any additional displacement.

In addition to the influence of the connections, the vertical stiffness of the foundation is analysed. This parameter is found to have a significant influence on both the natural frequency and the maximum displacements. A range of $1 \cdot 10^6$ - $6 \cdot 10^6$ kN/m and a stiff foundation are considered. The actual stiffness of the foundation is unknown, but based on data from the literature, it is expected to be fairly stiff. The difference between the lower bound stiffness and a stiff foundation is an increase of 20.6% for

the natural frequency and a decrease of up to 48.7% in displacement. Correspondingly, foundation stiffness can play a significant role in meeting serviceability requirements. Careful consideration of its influence in an early stage of the design might therefore be necessary. The result of the upper and lower bounds and the trend lines are shown below. Note that the amount of influence and the observed trends are comparable with that of the diagonal connections. When studying the dynamic response of a tall building, the soil-structure interaction is expected to be little. Therefore, using a stiff foundation (pinned supports) is considered to give a good estimation of the natural frequency. The static displacement due to the foundation stiffness, however, must be considered by using the expected foundation stiffness.

**Table 7.3:** Results for the upper- and lower bound of the stiffness of the foundation.

| elastic stiffness | | natural frequency | $u_{x,l}[mm]$ | $u_{x,r}[mm]$ |
|---|---|---|---|---|
| min. | $1 \cdot 10^6$ kN/m | 0.359 Hz | 130.3 | 123.4 |
| max. | $6 \cdot 10^6$ kN/m | 0.417 Hz (+16.2%) | 94.6 (-37.7%) | 97 (-27.2%) |
| stiff | $\infty$ | 0.433 Hz (+20.6%) | 87.6 (-48.7%) | 84.2 (-46.6%) |
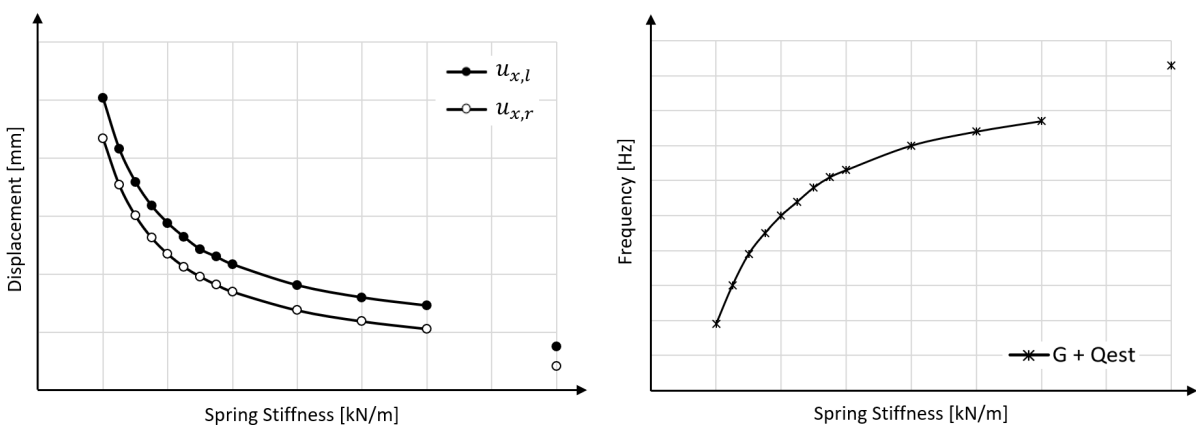


**Figure 7.4:** Influence of the vertical foundation stiffness on the max. displacement and natural frequency. Adjusted versions of figures 5.1 and 5.4.

## 7.3. Comparison of the modelling approaches

Two modelling approaches have been considered for studying the serviceability behaviour:

- **Approach 1**: Pinned truss members with no additional adjustments.
- **Approach 2**: Pinned truss members with the load-slip behaviour of connections specified in the nodes at the ends of the modelled members.

The first approach speaks for itself. The information used for the second approach is explained briefly below. For the estimation of the elastic stiffness, which is incorporated in the model, equation 3.10 is used. This formula gives a much lower stiffness for a group of dowels in comparison to equation 2.24 from EC5. This is because, in the latter, no group effect on stiffness is accounted for. Furthermore, $K_{ser}$ ($k_s$ in EN26891, see figure 2.15) is not considered to be an appropriate stiffness parameter for the prediction of the stiffness of large timber connections applied in stability trusses. This is because the connections will be loaded in cycles and alternate between tension and compression. Therefore, the elastic stiffness ($k_e$ in EN26891) is considered to be a much more representative parameter.

The hole clearance in the steel plates causes an initial slip of the connection. This initial slip is defined as the amount of slip up to the intersection between the elastic stiffness and zero force. For dowelled connections, the hole clearance in the steel plate is commonly 1mm larger than the diameter of the dowels. Based on the literature study, the corresponding initial slip, caused by various non-linear influences, is estimated to be approximately 0.6mm. This initial slip does not affect the natural frequency of the structure. The following elastic stiffnesses are applied in the model in which the load-slip behaviour of the connections is incorporated (approach 2):

- Diagonal connections (10x10 dowels): 2141kN/mm.
- Vertical component (16 x 10 dowels): 3425kN/mm. Estimated using the asymptotic value for the number of dowels in a row and using a mean density of $430kg/m^3$ corresponding to GL30c, which is considered conservative for connection CL2v (see fig. 4.6a) since the bottom corner column section is timber class GL30h.
- Connection to the foundation (CL1 in fig. 4.6a, 10x10 dowels): 2525kN/mm [GL30h]. This elastic stiffness is only present when loaded in tension, compression is transferred through contact.

In the following subsections, the obtained maximum displacements and peak accelerations will be presented. The results will be compared to those obtained using modelling approach 1.

### 7.3.1. Maximum displacement

For the base model in which approach 2 is implemented, the displacements at the top of the structure are determined to be 121.5mm and 122.2mm, to the left and right, respectively. In comparison to the model in accordance with approach 1, the maximum displacements increased by 39.5% (from 87.6mm to 122.2mm). Note that in approach 1, the largest displacement is towards the left ($u_{x,l}$) whereas in approach two it is towards the right ($u_{x,r}$). The large increase in displacement towards the right is because the slip in the connection to the foundation, when loaded in tension, is incorporated in modelling approach 2. The difference in global displacement between the two modelling approaches shows the significant effect of the truss connections.

**Table 7.4:** Maximum displacements for the base model using the two different modelling approaches.

|              | Max. displacement [mm] | |
|--------------|-----------------|-----------------|
|              | $u_{x,l}$       | $u_{x,r}$       |
| **Approach 1** | 87.6            | 84.2            |
| **Approach 2** | 121.5 (+38.7%)  | 122.2 (+45.2%)  |

The displacement criterion of $h/500$ imposes that the structure is allowed to displace 137mm. The maximum displacement obtained from the base model in which approach 2 is incorporated is 122.2mm. It is expected that, when including the vertical foundation stiffness, the displacements will exceed the imposed limit. Correspondingly, the foundation must be very stiff to meet the displacement criterion. The static displacement shape of the modelled structure is shown in figure 7.5.
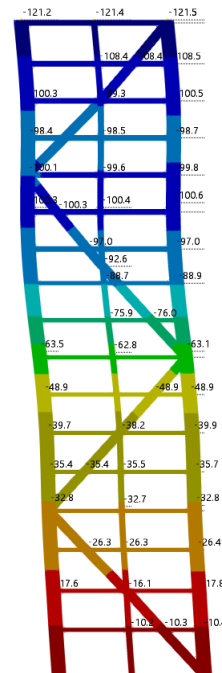


**Figure 7.5:** Static displacement leftward $u_{x,l}$[mm] (approach 2).

To present the effect of the initial slip and elastic stiffness of the diagonal connections and the vertical components on displacement, they are incorporated individually in the model. The results for each of the models are shown in table 7.5. A specification of the included parameters is provided for each of the listed models. The column chart shown in 7.6 corresponds to the table.

**Table 7.5:** Maximum displacements for each of the modelled connection parameters.

| Load-slip diagram specified in the model | | Displacement $u_{x,l}$ | Increase* |
|---|---|---|---|
| pinned connections | | 82.5 mm | - |
| diagonal connections | only 0.6mm initial slip | 94.5 mm | +12 mm (+14.5%) |
| | only k=2141kN/mm | 100.1 mm | +17.6 mm (+21.3%) |
| | 0.6mm slip followed by k=2141kN/mm | 112.2 mm | +29.7 mm (36%) |
| vertical components | only 0.6mm initial slip | 86.7 mm | +4.2 mm (+5.1%) |
| | only k=3425kN/mm | 87.5 mm | +5.0 mm (+6.1%) |
| | 0.6mm slip followed by k=3425kN/mm | 91.7 mm | +9.3 mm (+11.2%) |
| everything included (approach 2) | | 121.5 mm | +39 mm (+47.3%) |

In all the models $E_{alt}$ of the diagonal members is 16107MPa, therefore, model pinned connection $\neq$ approach 1.
*increase in displacement with respect to the model with pinned connections.
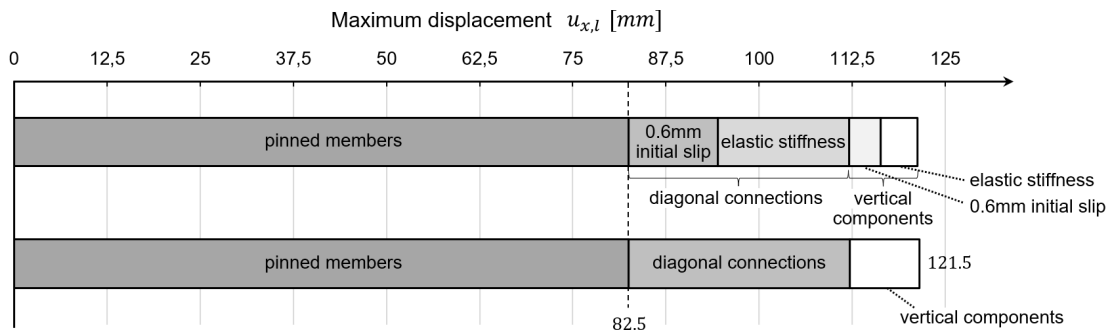


**Figure 7.6:** Column chart; effect of the connection parameters on maximum displacement.

Figure 7.6 shows that the elastic stiffness of the diagonal connections has the most effect on the maximum displacement of the structure. The initial slip of 0.6mm for the diagonal connection is the second most influential. In addition, the results show that the load-slip behaviour of the diagonal connections causes approximately 3/4 of the overall increase in global displacement due to the connections. Whereas, the vertical components are responsible for 1/4th of the increase. The difference is because there are many more diagonal connections in comparison to vertical components in the studied truss.

## 7.3.2. Peak accelerations
The mode shapes obtained from the modal analysis and the procedure from EN1991-1-4 [19] are used to determine the peak accelerations at the top floor. A damping of 1.5% is used, which is the estimated damping based on measurements on the Mjøstårnet building performed by Tulebekova et al. [52]. The peak accelerations are determined for floor 17 which is at a height of +63.3m (indicated in figure 4.9b). The mode shape corresponding to the first natural frequency is shown in figure 7.7.
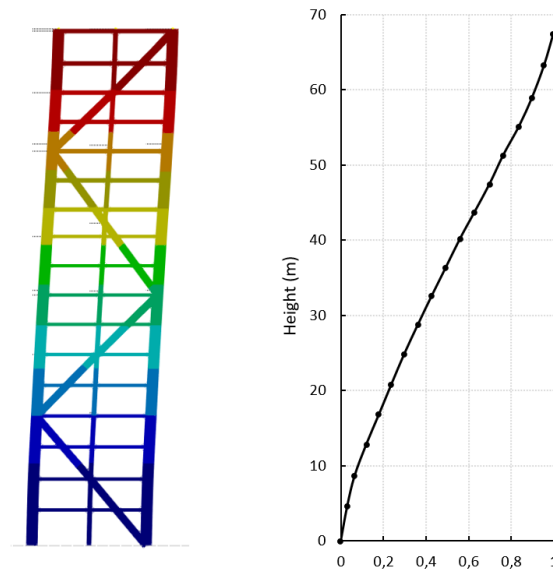
**Figure 7.7:** Mode shape (approach 2).

The peak accelerations are determined for three cases:

1. With the natural frequency ($f_1$) and mode shape obtained from the model with pinned members (approach 1). $f_1 = 0.433 Hz$.
2. With $f_1$ and mode shape (fig. 7.7) obtained from the base model in which approach 2 is applied. $f_1 = 0.393 Hz$
3. Using the measured frequency of the Mjøstårnet building from literature [52]. $f_1 = 0.493 Hz$

In figure 7.8 the results for the three cases are plotted in the ISO 10137 curve. In approach 2, the connection stiffnesses are accounted for. These reduce the global stiffness of the structure which causes a shift of the point, in comparison to approach 1, towards the upper left. This point, indicated by the number 2, is further away from meeting the criterion for residences. The measured frequency of 0.493Hz is notably higher than the frequencies obtained from the FE models. As can be seen in figure 7.8, this causes a shift towards the lower right. In all cases, the criteria set for residences are not met. The case in which the measured frequency is considered, however, is close to meeting the recommended value.
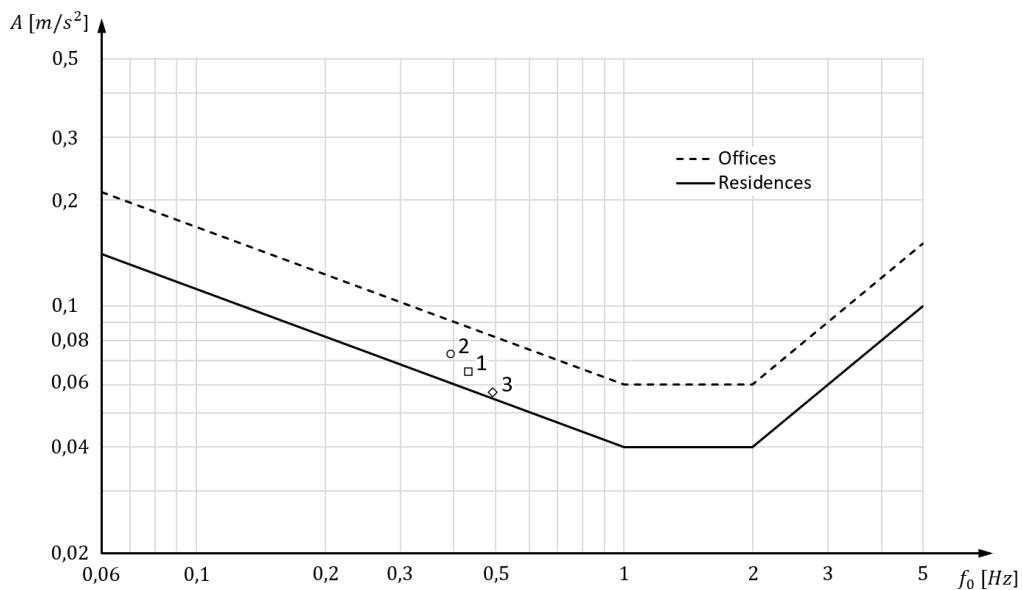


**Figure 7.8:** Results for cases 1,2, and 3 plotted in the ISO 10137 curve [2].

## 7.4. Variant study

The base models, discussed in the previous section, show that the maximum displacements are critical and the recommended (dynamic) comfort criteria, related to the peak accelerations at the top floor, are not met. To analyse how changes in the structural system can improve serviceability behaviour, several variants are studied. The variants A to D have been discussed in chapter 6. In this section, the results, i.e. maximum displacements and peak accelerations, of each variant are compared.

### 7.4.1. Maximum displacement

An overview of the computed maximum displacements is shown in figure 7.9. For each variant, the displacements towards the right and left are shown. Furthermore, the results from both approaches 1 and 2 are plotted for comparison. The percentages indicate the difference in displacement between the two approaches. The percentages can be interpreted as the increase in global displacement due to the load-slip behaviour of the truss connections.
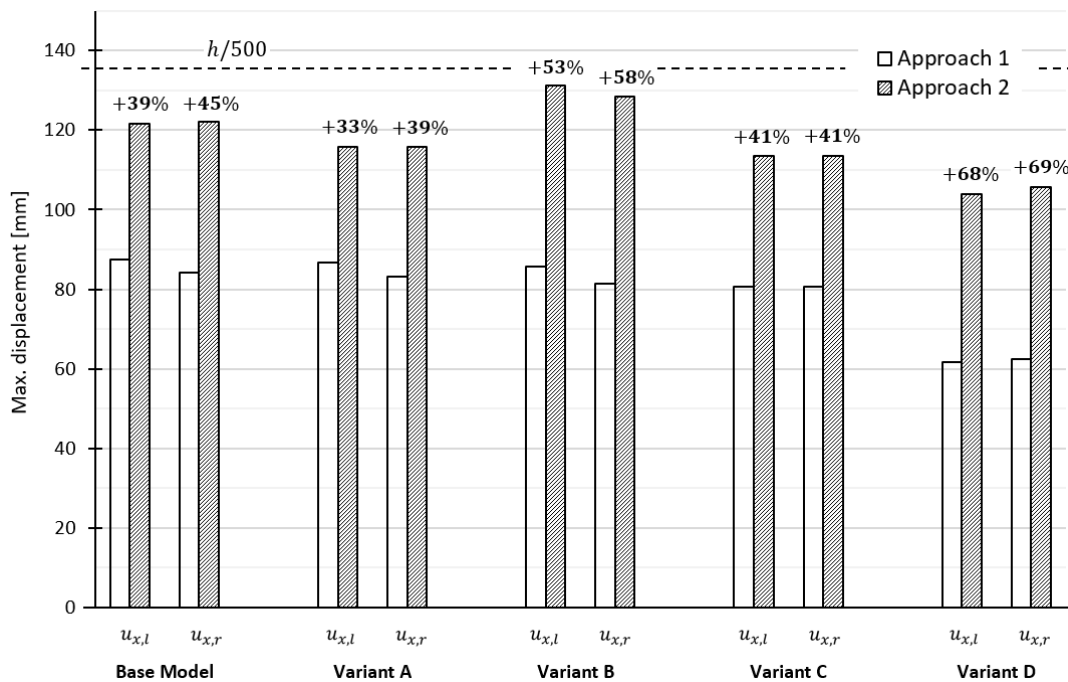


**Figure 7.9:** Maximum displacements for each variant.

Figure 7.9 shows that, for all variants, it is important to consider the load-slip behaviour of the truss connections because they significantly amplify the maximum displacement of the structure. When the number of connections is more (Variant B and D) the difference between the two approaches increases. All variants are within the prescribed limit of $h/500$, however, the foundation stiffness is not incorporated in these models. Thus, most variants depend on a stiff foundation to stay below the displacement limit. Variant D, in which the structure is widened, shows the most improvement in comparison to the base model.

### 7.4.2. Peak accelerations

The peak accelerations at the top floor are computed for each variant. The values of the mode shapes at floor 17 (at a height of +63.3m) are retrieved from the FE models. These in combination with the calculation from Eurocode (EN1991-1-4) are used to determine the peak accelerations. The models in which the load-slip behaviour of the truss connections is included (approach 2) are considered for comparison. The results are plotted in figure 7.10. The base model is indicated with a black dot.
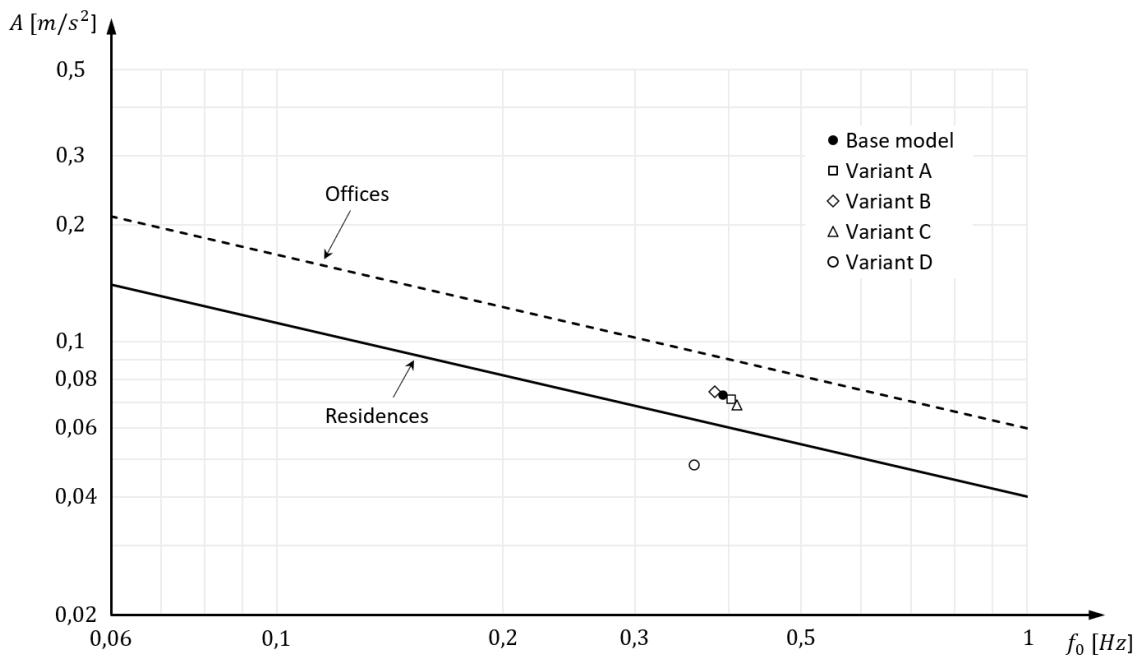
**Figure 7.10:** Dynamic response of the variants plotted in ISO 10137 curve [2].

Figure 7.10 shows that variants A, B, and C show little improvement in the dynamic response of the structure. For these variants, the requirement for residences is not met, just like the base model. Variant D shows much improvement in comparison to the base model. In this variant, the building width increased by 50%, and consequently, the mass per unit area also increased by 50%. In addition, the applied damping is 1.9%, whereas the damping is 1.5% for the other variants and the base model. The damping causes a relatively small reduction in acceleration. The increased mass is primarily responsible for the great reduction in peak acceleration in comparison to the base model. This shows the large effect of the mass of the building on its dynamic response.

# Part III
## Research Outcome

# 8
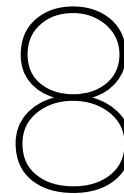
# Discussion

## 8.1. Introduction

This thesis started with a literature review in which the limitations of the current design rules have been pointed out. Thereafter, the stiffness of connections with dowels and slotted-in steel plates has been researched more in-depth. A 2D finite element model of the stability system from the Mjøstårnet building is made in the modelling part. A method to incorporate the load-slip behaviour of the truss connections into the FE model is developed. In this approach, the connection behaviour is specified within the nodes at the ends of the members. A sensitivity study focused on the serviceability stiffness of the truss connections has been performed using this model. At last, several variants of the structure have been considered to develop recommendations for design. The results of these studies are shown in the previous chapter. In this chapter, the interpretation, application, and limitations of the research are discussed.

## 8.2. Interpretation of the results

The literature review shows that the current design rules provided in EC5 are unsuitable for the serviceability design of structures with large timber connections. The slip modulus $K_{ser}$ is not an accurate predictor for the stiffness of these connections. An elastic stiffness parameter should be used instead. Due to hole clearance inside the steel plates, some slip will occur before the connection reaches its elastic stiffness. Reynolds et al. [41] proposed to idealize the load-slip behaviour of these connections by a zero-stiffness region followed by elastic stiffness. This idealization is shown for their large-scale tested connection in figure 3.20.

In this thesis, the idealization of the load-slip behaviour of large timber connections by splitting it into three parts has also been discussed. This is referred to as a tri-linear idealization, and the three parts are the following:

- Region 1: timber hole opening which is non-reversible deformation.
- Region 2: sequential activation of the dowels due to the hole clearance in the steel plates.
- Region 3: the elastic stiffness of the connection.

Two possible idealizations are presented based on observing the measured load-slip response of the 35-dowel connection from Reynolds et al. [41, Fig. 11]. It should be possible to establish a relationship between the load level and the slip, which is partly dependent on the hole clearance in the steel plates. An example of two general idealizations is shown in figure 8.1.

**(a) tri-linear idealization 1:** dependent on load level.          **(b) tri-linear idealization 2:** dependent on hole clearance.
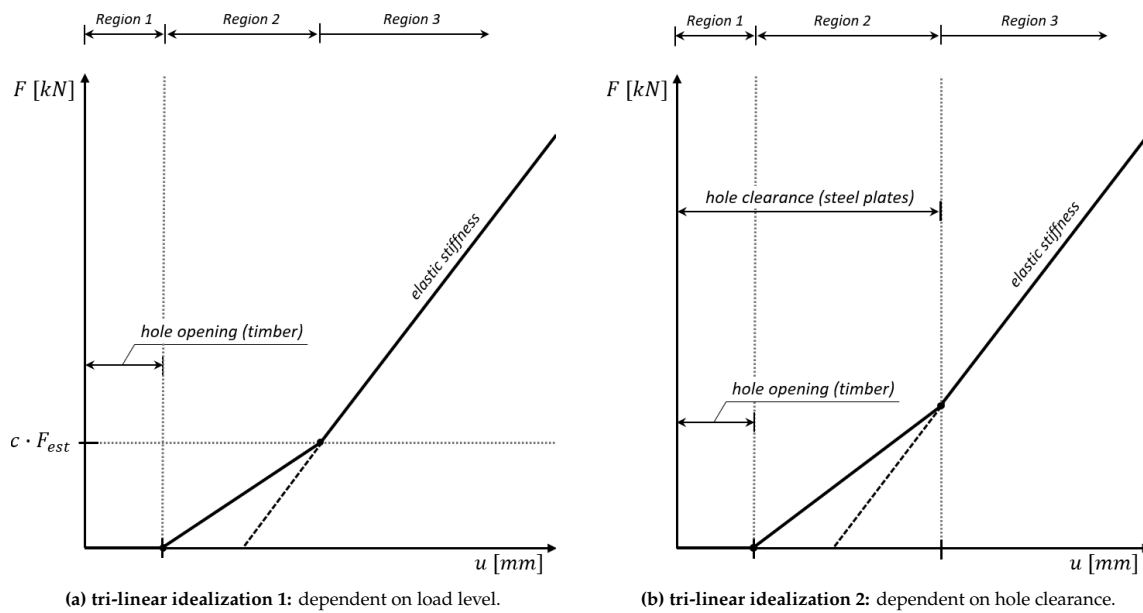
**Figure 8.1:** Example of generalized tri-linear idealizations to represent the load-slip behaviour of large timber connections with multiple slotted-in steel plates, numerous dowels, and clearance in the holes in the steel plates.

In the tri-linear idealization shown in figure 8.1a, the point at which the connection reaches its elastic stiffness is related to the load level. This idealization is based on the 10%/40% approach used for the estimation of connection stiffness according to EN26891 [22]. However, for these connections, it is not considered appropriate to assume that they exhibit linear load-slip from $0.1F_{est}$. The load-slip curve of the 35-dowel connection tested by Reynolds et al. [41], shown in figure 3.19, for example, has a linear reload curve from approximately 20% of $F_{est}$. That is why a factor $c$ is shown in the general tri-linear idealization 1, shown in figure 8.1a. The value of this factor would be dependent on the hole clearance in the steel plates. More tests of large steel-to-timber connections are required to establish such a relationship. In the second general tri-linear idealization, shown in figure 8.1b, the point at which the connection reaches its elastic stiffness is directly related to the hole clearance in the steel plates. This idealization is based on the assumption that all dowels will contribute to the elastic stiffness once a displacement equal to the hole clearance has occurred.

The tri-linear idealizations provide an explanation for the load-slip behaviour of the large timber connections commonly used in glulam trusses. Region 2 in these curves is caused by sequential activation of the dowels, which is present due to the hole clearance in the steel plates. This means that if the hole clearance is eliminated, for instance by applying self-drilling dowels, the region would disappear. Correspondingly, this would effectively reduce the local displacement in the connections. In addition, the elastic stiffness of the connection is also expected to be higher when all dowels are tight-fitted into the steel plates. That is because sequential activation of the dowels is considered to be largely responsible for a great reduction in the elastic stiffness of the connection. The difference in the idealized load-slip behaviour for connections with and without clearance is illustrated in figure 8.2.

**(a)** with clearance.  **(b)** without clearance.

**Figure 8.2:** Difference in idealized load-slip behaviour for connections with and without hole clearance in the steel plates.

Figure 8.2 shows that elimination of the hole clearance in the steel plates changes the load-slip behaviour of the truss connections. As a consequence of the decreased local displacement, the global displacement of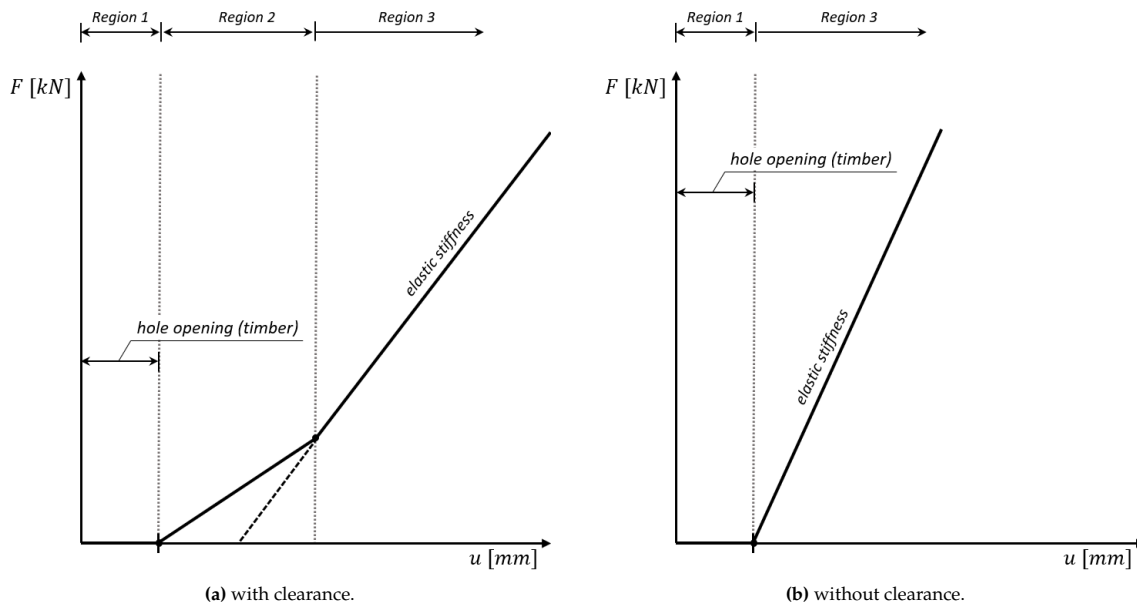 the structure will decrease. In addition, the higher elastic stiffness will stiffen the structure, which causes the natural frequency to increase. The load-slip behaviour of a connection, before it reaches its elastic stiffness, is only considered to be important for the prediction of local displacement when the connection is exposed to low loads. In the context of a stability truss, most connections will be exposed to high loads, and thus their slip will be in the elastic stiffness region. Therefore, a simple load-slip diagram consisting of an initial slip followed by the elastic stiffness is sufficiently accurate for the prediction of the displacement of a stability truss. For the prediction of the dynamic response, only the elastic stiffness is relevant because an initial slip will not affect the global stiffness of the truss.

The serviceability performance of multi-storey timber buildings generally governs their design. The load-slip behaviour of large timber connections was unexplored, and as a result, timber structures are commonly modelled as a system of pinned members without any additional adjustments. The results discussed in section 7.3 show that this modelling approach is insufficient for the design of timber buildings that are stabilized by trusses. The behaviour of the truss connections should therefore be considered when modelling the structure.

The sensitivity study showed that the stiffness of the truss connections affects both the maximum displacements and the natural frequency of the structure. The diagonal connections have the most influence, followed by the vertical component. The effect is highest at the lower stiffness values, and the curves flatten out as their stiffness increases. This is shown in figures 7.2 and 7.3. It shows that avoiding the lower stiffness region can be important to make the structure meet its serviceability requirements.

The variant study showed that most adjustments resulted in little improvement in the serviceability behaviour. The maximum displacements decreased slightly, in comparison to the base model, for most variants. The number of diagonal connections in variants B and D is greater than in other variants. This caused a larger difference in the obtained maximum displacements using modelling approaches 1 and 2. This shows that limiting the number of connections can be important in relation to meeting displacement criteria. The change in peak accelerations, for most variants, is found to be small. The exemption to this is variant D in which the structure is widened. By widening the structure, the mass per unit area in the direction of the analysed mode increased by 50%. This is the only case in which the equivalent mass has been changed. The results showed a large reduction in the peak accelerations. Consequently, this is the only variant that met the dynamic response requirements from ISO 10137 for

residences. The criterion is even met by a large margin. This showed the importance of the building's mass in limiting the accelerations.

The importance of the added mass, in the form of concrete floors, to have the Mjøstårnet building meet the comfort criteria, has also been emphasized in literature [3]. This also speaks to the consequences related to an inaccurate estimation of the mass of the building. Overestimation of the building's mass, which is commonly done for ultimate limit state design to be on the safe side, will lead to an underestimation of the accelerations. In the modal analysis performed in this thesis, three mass combinations are studied (see table 4.8). This showed that using the frequent load combination from Eurocode results in a higher mass in comparison to the estimation made based on the architectural floor plan. Consequently, when using the frequent load combination, the accelerations are likely to be underestimated. The use of a live load partition factor of 0.1, i.e. 10% of the variable load, is considered to be more appropriate.

The effect of the load-slip behaviour of the truss connections on the maximum displacement is large. The local displacement in the connections is caused by an initial slip in combination with the elastic stiffness. All the local displacements in the truss connections add up, causing the global horizontal displacements of the structure to increase. The difference in maximum displacement, when accounting for the load-slip behaviour of the connections, becomes clear from the comparison between modelling approaches 1 and 2, discussed in section 7.3. For the base model, the maximum displacement obtained using approach 2 is approximately 40% higher in comparison to approach 1. The natural frequency obtained using approach 2 is approximately 9% lower in comparison to approach 1. The errors made in the prediction of the natural frequencies of buildings are commonly quite large [14]. A difference in natural frequency of 9% is small considering the uncertainty associated with other factors like the mass, material stiffnesses, and the effect of non-structural elements. Therefore, the simple approach 1 provides a very reasonable estimate. Approach 2, however, is not much more complex and would only require a proper estimation of the elastic stiffness of the connections. If an acceptable estimation can be made, it is advised to at least analyse the difference in natural frequency obtained using approach 2, especially when the elastic stiffness of the connections is low and there are many connections within the truss. The elastic stiffness of the connections can be increased by eliminating the hole clearance in the steel plates. If the hole clearance is eliminated and, thus, the elastic stiffness of the connections is estimated to be high, the natural frequency obtained using approach 1 will likely be close to the value obtained using approach 2.

The natural frequency of the base model, in which the load-slip behaviour of the connections is considered, is approximated to be 0.393Hz. A natural frequency of 0.433 is obtained from the FE model in which approach 1 is implemented. Sweco, the structural engineering firm for the Mjøstårnet building, estimated the natural frequency of the first translation mode to be 0.370Hz [3]. In their estimation, they included a value for the vertical stiffness of the foundation. When the building was completed, field measurements of accelerations have been carried out. Based on the obtained data, the frequency for the first mode is determined to be approximately 0.493Hz [52]. The significant difference between the structural FE models and the measurements is most probably primarily caused by non-structural elements. This is presumed because Tulebkova et al. [52] made a FE model of the Mjøstårnet building in which the non-structural elements are included, and from their model, they were able to obtain natural frequencies close to the measurements. The non-structural elements will increase the stiffness of the building and thereby increase its natural frequency. Images of the non-structural elements in the Mjøstårnet building are shown in figure 8.3.
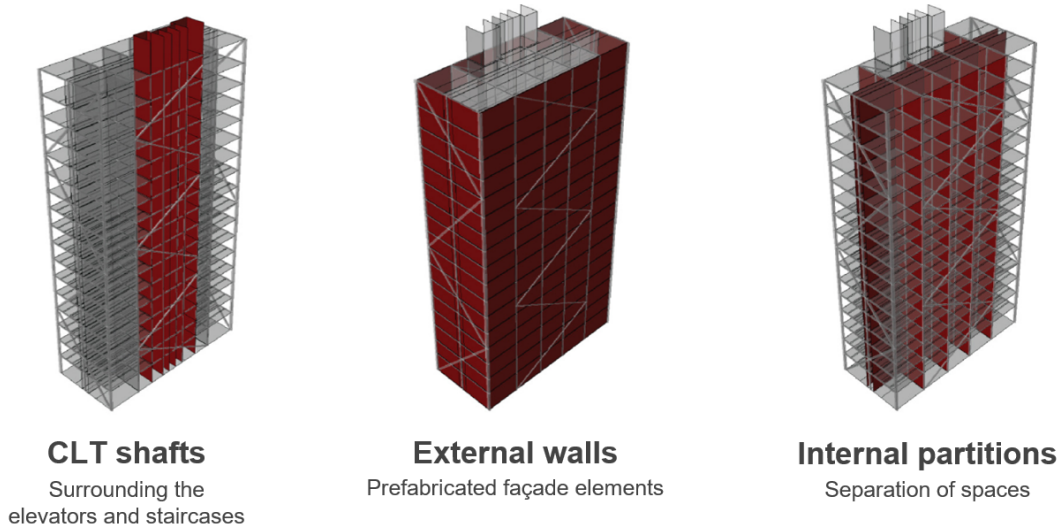
**CLT shafts**
Surrounding the
elevators and staircases

**External walls**
Prefabricated façade elements

**Internal partitions**
Separation of spaces

**Figure 8.3:** Non-structural elements in Mjøstårnet. Adjusted from [52, Fig. 2].

## 8.3. Application

In the FE model of a truss structure, the modelled members intersect at their centre lines. This makes the length of the modelled diagonal timber members larger than those present in the actual truss. To account for the load-slip behaviour of the diagonal connections, an engineer could incorporate this by specifying a diagram in the end nodes of the modelled diagonal rods. This can be considered as a conservative approach. For a more accurate estimation, the stiffness of the modelled diagonal members can be adjusted. This is possible because the stiffness of the diagonal connections is now specified in the end nodes, thus, the part of the diagonal member equal to the length of the connections can be considered to be removed from the modelled member.

In this thesis, the stiffness of the modelled diagonal members is increased by altering their E-modulus. This approach has been discussed in section 5.4.1. To determine the stiffness of the diagonal elements, they are split into parts. These parts are the steel plates inside the columns, the diagonal connections, and the (remaining) timber member (see figure 5.6). The altered E-modulus only represents the stiffness of the steel plates and the timber member since the connection stiffness is incorporated in the end nodes. The approach can be simplified if the stiffness per unit of length ($EA$) of the diagonal timber member, and the slotted-in steel plates are comparable. Because then, only the length of the connections has to be subtracted to alter the E-modulus. In the studied truss, the EA of the timber diagonals and the slotted-in steel plates inside the columns are similar (see table 4.7). In that case, the E-modulus of the modelled diagonals can be altered using equation 8.1. When the length of the connections is equal at both ends, equation 8.1 is the same as equation 8.2.

$$E_{alt} = \frac{l_{modelled}}{(l_{modelled} - l_{connection1} - l_{connection2})} \cdot E_t \tag{8.1}$$

$$E_{alt} = \frac{l_{modelled}}{(l_{modelled} - 2 \cdot l_{connection})} \cdot E_t \tag{8.2}$$

$E_{alt}$ = Altered E-modulus for the modelled diagonal members.

$l_{modelled}$ = Length of the modelled diagonal member (see figure 5.5).

$l_{connection}$ = Length of the connection zone (numbers 1 and 2 refer to the connections at both ends of the diagonal member).

$E_t$ = E-modulus of the diagonal timber member.

Removing the connection zones, by altering the E-modulus of the diagonal members, allows for specifying the connection behaviour at the end nodes, without being unnecessarily conservative. The same approach can be used to incorporate the load-slip behaviour of the connection between corner columns and the foundation. This is only considered necessary when this connection is exposed to tension under serviceability loading. Even with the extra mass, in the form of concrete floors, applied in the researched case (Mjøstårnet building), a tension force is still present in this connection (see fig.

C.3). The load-slip behaviour of the connection to the foundation should be specified with care because compression forces are transferred through contact.

To account for the load-slip behaviour of the vertical component i.e. the dowel group inside the corner columns that transfers the vertical component of the diagonal forces to the column, a different approach is used. A small stiff element is modelled, at which end the load-slip behaviour of this connection could be specified by means of a nodal shear diagram (see figure 4.17). This assures that only the vertical component of the diagonal forces is transferred by the dowel group. This is necessary because a compression force between column sections is transferred through contact and not by the connection between the sections. Correspondingly, these columns can be considered continuous unless the connection between sections will be exposed to tension.

The most simple way to idealize the load-slip behaviour of a large timber connection is by specifying an initial slip followed by an elastic stiffness. Based on research by Reynolds et al. [41] applying an initial slip of approximately 0.6mm for large-scale steel-to-timber connections in which the hole clearance in the steel plates is 1mm is considered an appropriate value. In addition to the hole clearance, non-linear processes like densification of the timber around the hole edge occur, which influence the amount of initial slip. The 0.6mm initial slip can be specified for all truss connections, which is assumed to be a conservative approach because the connections higher up in the truss are exposed to load lower than 40% of $F_{est}$. Correspondingly, the initial slip in these connections is expected to be lower.
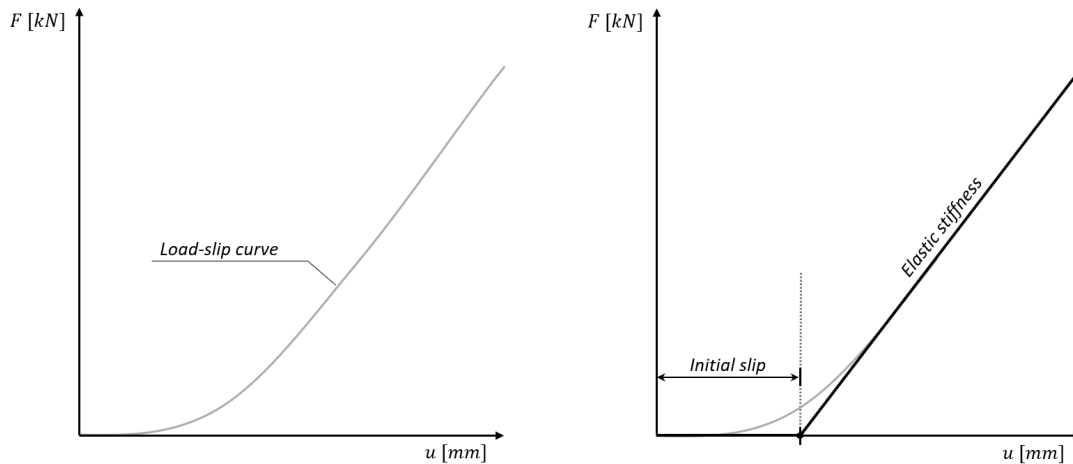
**Figure 8.4:** Idealization of the load-slip curve of a large timber connection with multiple slotted-in steel plates, numerous dowels, and clearance in the holes in the steel plates.

## 8.4. Limitations

It is assumed that the permanent loads on the structure are modelled sufficiently accurate. Inaccurate modelling of the mass can cause an underestimation of the dynamic response of the structure. Information about the mass of the structural systems is provided by Sweco Norway and taken from literature. The finite element model is verified by observing the maximum forces in the truss members and by performing the unity checks for the members and their connections. The structure's natural frequency is determined by performing a modal analysis within the 2D FE model. An Excel sheet with the procedure from EN1991-1-4 [19] is drawn up to calculate the peak accelerations. The equivalent mass per unit area estimated by Sweco is used in the calculations.

In the calculation of the peak accelerations, a damping of 1.5% is taken for the base model, which is based on measurements done on the Mjøstårnet building [52]. For the researched variants A, B, and C, the same damping of 1.5% is taken in the calculations. For variant D, a damping of 1.9% is considered. The damping of this variant is expected to be larger as a consequence of the increased width of the structure. This assumption is based on the measured damping of 2.3% for the translational mode in the long direction [52]. The cause of the significantly larger damping in the long direction in comparison to the short direction is uncertain. The total viscous damping of the timber truss is dependent on the material damping in the glulam members and the structural damping in the dowelled connections [36].

In addition, the non-structural elements might also influence the damping. To what extent each of these parameters influences the overall damping is currently unknown. Investigation of the damping has not been a part of this research. Since the damping is likely greatly dependent on the number of dowelled connections in the truss, the actual damping might differ slightly for each of the researched variants.

For the studies that required an estimation of the elastic stiffness of the connections, it is assumed that the estimations are reasonably accurate. For the prediction of the elastic stiffness of the connections, the engineering model from Malo et al. [37] is used with the parameters that the researchers proposed. This model is assumed to give a good estimation of the behaviour of the connections applied in Mjøstårnet since the same timber grade, dowel size (12mm), and hole clearance in the steel plates (1mm) are used in the tested connections. The tested connections, however, are smaller and the number of tests is few. Consequently, there is no guarantee that the prediction is close to perfect. In the performed sensitivity study, a large range of connection stiffnesses has been considered. The effect that an under- or overestimation of the elastic stiffness would have on the displacements and the natural frequency can be read from the produced figures. Mainly in the high connection stiffness region, the effect of an error in the estimation of the elastic stiffness would be minimal. If the connection stiffness is in the lower part of the considered range, the effect of a small deviation in stiffness on the maximum displacements of the structure can be substantial.

# 9

# Conclusions and Recommendations

The aim of this thesis has been to research the influence of the stiffness of large timber connections on the serviceability behaviour of multi-storey timber buildings with glulam stability trusses and to provide guidance for modelling and design. The main research question is:

*"To what extent does the stiffness of timber connections with dowels and slotted-in steel plates influence the serviceability behaviour of multi-storey timber buildings with glulam stability trusses?"*

## 9.1. Conclusions

A finite element model of a glulam stability frame has been made and the influence of the connections on serviceability behaviour of the structure is analysed. A modelling approach that allows for the specification of load-slip diagrams in the modelled nodes is developed. The load-slip behaviour of the truss connections is found to significantly influence the maximum displacements and, to a lesser extent, the natural frequency of the structure. Therefore, the connection behaviour should be incorporated into numerical models in order to accurately predict the serviceability behaviour of a multi-storey timber building that is stabilized using glulam trusses.

The connections between diagonal- and column members are identified as most influential with respect to the serviceability behaviour of the investigated building. A distinction has been made between diagonal connections and vertical components. The effect of the former is found to be larger because there are many of these connections within the stability truss. The load-slip behaviour of the truss connections is idealized as an initial slip followed by its elastic stiffness. To what extent the truss connections influence the serviceability behaviour is found to be dependent on the amount of initial slip and the elastic stiffness of the diagonal connections and the vertical components. The initial slip causes an increase in the maximum horizontal displacement of the structure. The elastic stiffness will influence both the maximum displacements and the natural frequency. To study the sensitivity of the serviceability behaviour in relation to the elastic stiffness of the connections, a stiffness range has been considered. The maximum displacements are found to decrease exponentially as the elastic stiffness increases. This showed that avoiding a low elastic stiffness can be critical for meeting the displacement criterion. The natural frequency is found to increase as the elastic stiffness of the connections increases. Similar to the displacements, the effect of a small change in stiffness is largest in the lower stiffness region.

Two modelling approaches have been compared. In the first (approach 1), the truss members are pinned with no further adjustments. In the second (approach 2), the load-slip behaviour of the connections is incorporated by specifying a load-slip diagram at the end nodes of the modelled members. The E-modulus of the diagonal members is altered to enable this. Furthermore, small stiff elements are modelled to be able to incorporate the stiffness of the vertical component. The modelled load-slip behaviour of the truss connections consists of an initial slip followed by their elastic stiffness. For the base model in which approach 2 is implemented, the maximum displacement is 40% higher in comparison to that obtained from the model with approach 1. For the researched variants in which the

number of truss connections increased, the difference is larger (up to 69% for variant D). This shows that the maximum horizontal displacement is highly dependent on the number of truss connections. The applied estimated elastic stiffness and the initial slip in the truss connections cause a significant difference in displacement between modelling approaches 1 and 2. An initial slip of 0.6mm has been considered, and the elastic stiffness is estimated using an empirical equation. The elastic stiffness of the truss connections is estimated to be much lower than Eurocode 5 suggests. The elastic stiffness per dowel per shear plane is found to decrease as the number of dowels in the connection increases. The significant group effect is likely primarily due to the hole clearance in the steel plates. This clearance causes sequential activation of the dowels which, in combination with non-linear processes like densification of the timber around the hole edge, results in a great reduction in the elastic stiffness of the large timber connections. The most effective measurement to lower the global displacement caused by the truss connections would, therefore, be to eliminate the hole clearance. This would reduce the initial slip and increase the elastic stiffness of the connections.

The connection parameters that cause the increase in the maximum horizontal displacement, which are the initial slip and elastic stiffness of the diagonal connections and the vertical components, are studied individually. This showed that, for the researched structure, the elastic stiffness of the diagonal connections has the most effect on the displacement. The initial slip of the diagonal connections has been identified as the second most influential. For the base model, the complete load-slip behaviour of the diagonal connections is responsible for approximately 76% of the total increase in displacement caused by the truss connections. The other 24% is caused by the local slip of the vertical components. This difference is because there are many more diagonal connections within the truss in comparison to vertical components. The local slip in the connection with the foundation can also cause an increase in maximum global displacement, but only when it is loaded in tension.

The effect of the load-slip behaviour of the truss connections on the natural frequency is found to be less in comparison to the effect on maximum displacements. For the base model in which approach 2 is implemented, the natural frequency is 9% lower in comparison to the model with approach 1 (from 0.433Hz to 0.393Hz). The corresponding peak accelerations increased by 12% (from $0.0654m/s^2$ to $0.0731m/s^2$). The global stiffness of the structure decreased when accounting for the elastic stiffness of the truss connections. The initial slip in the connections does not affect the natural frequency because it does not change the global stiffness of the structure. The dynamic response of variants in which the connection behaviour is incorporated (approach 2) is analysed for comparison. The researched variants, with the exemption of variant D, had similar natural frequencies as the base model. Correspondingly, variants A to C did not show a large difference in the dynamic response of the structure. The peak accelerations varied from $0.0687m/s^2$ to $0.0743m/s^2$. Thus, the maximum change in acceleration in comparison to the base model is just 6%. The errors in the prediction of the natural frequency due to factors other than the stiffness of the connections, like the mass of the building and the effect of non-structural elements on the global stiffness, are expected to be much larger. The effect of non-structural elements became evident from the comparison between the natural frequency obtained from the FE models with measurements. The measured natural frequency of 0.493Hz is 25% higher in comparison to that obtained from the FE model in which approach 2 is implemented ($f = 0.393Hz$). The effect of the mass is clearly shown by the researched variant D for which the peak accelerations are determined to be $0.0483m/s^2$ which is 34% lower than the acceleration from the base model. It can be concluded that the effect of the elastic stiffness of the truss connections on the dynamic response of the building is relatively small. Therefore, both modelling approaches are considered to be sufficiently accurate for the prediction of the dynamic response of the building.

The formula for the slip modulus $K_{ser}$ from the current EC5 is not an accurate predictor for the stiffness of large timber connections with dowels and slotted-in steel plates. Three main issues are identified in the context of these connections within stability trusses:

1. An elastic stiffness parameter should be used instead of the slip modulus $K_{ser}$.
2. The design rules do not account for a reduction in stiffness for a group of dowels.
3. The initial slip due to the hole clearance in the steel plates is not clearly prescribed.

## 9.2. Recommendations for modelling and design

First and foremost, for the design of timber connections with slotted-in steel plates and dowels in glulam trusses, used to stabilize multi-storey timber buildings, it is recommended to apply a hole clearance in the steel plates as little as practically possible. The ideal would be to drill the holes, with a diameter equal to the diameter of the dowels, through both the timber and the steel plates and then install the dowels on-site. Another option would be to use self-drilling dowels. The practical application of both of these assembly procedures is questionable, especially for large connections with multiple slotted-in steel plates. Furthermore, it is advised to keep the number of connections within the glulam stability trusses to the required minimum. The (local) slip in each of the truss connections will coincide with an increase in the global horizontal displacement of the complete structure. Finally, it is important that the compression forces inside the columns are transferred between column sections and to the foundation, by contact.

Based on this research, several recommendations can be made regarding the numerical modelling of multi-storey timber buildings that are stabilized with glulam trusses. First and foremost, it is important to emphasize that there is a difference in the modelling approach for ULS and SLS design. It is not recommended to use one model (with the same parameters) for both purposes because in-calculated safety in ULS design can result in inaccurate predictions of the serviceability behaviour. Modelling recommendations for SLS design are provided here. Diagonal truss members can be modelled as pinned under the condition that they are primarily loaded in their axial direction. The columns can be modelled as continuous, but the engineer should carefully analyse whether tension at the connection to the foundation or between column sections will occur under service loads. For the horizontal beams that are part of the frame but not part of the stability truss, their connection with the columns may be modelled as pinned.

For the determination of the maximum displacements of the structure, the axial load-slip behaviour of the diagonal connections should be considered. It is recommended to idealize their behaviour as an initial slip followed by its elastic stiffness. This can be specified by means of a diagram in the end nodes of the modelled diagonal members. Optionally, the E-modulus of the modelled diagonal member can be altered to account for the fact that the length of the modelled diagonal member is larger than the length of the actual timber member. The stiffness of the vertical component can also be incorporated into the model, but this requires more modelling effort. If the number of truss connections that have a vertical component is limited, only accounting for the load-slip behaviour of the diagonal connections will provide a decent estimation of the maximum displacements in the early stage of the design.

For a first prediction of the dynamic response of the building, the truss members can simply be modelled as pinned without any further adjustments (previously referred to as approach 1). Furthermore, pinned supports can be applied under the columns because the dynamic ground structure interaction is most likely negligible. Finally, an accurate estimation of the mass is considered to be highly important. An overestimation of the mass can result in an underestimation of the dynamic response of the building. In ULS design, masses are commonly rounded up to be on the conservative side. The designer should prevent the same mass from being used for the prediction of the dynamic response. That is why it is recommended to compose separate models for SLS design. Another option would be to incorporate different loads and conditions in one model, but this may lead to confusion.

## 9.3. Recommendations for future studies

The stiffness of steel-to-timber connections with dowel-type fasteners should be investigated further. A focus point should be to develop a deeper understanding of the effect that the hole clearance in the steel plates has on the load-slip behaviour of large timber connections. In particular, quantification of the group effect on elastic stiffness is considered to be necessary to ensure the proper design of modern timber structures.

In the context of multi-storey timber buildings that are stabilized using glulam trusses, developing a better understanding of the parameters that influence its damping will be a valuable contribution to the prediction of the dynamic response of these buildings.

The research conducted in this thesis could be followed up by making a 3D FE model. This model can then be used to study multiple vibration modes, i.e. translational modes in both directions and

torsional mode. Furthermore, the mass can be modelled more precisely, which allows for studying how sensitive the dynamic response of the building is to variation in mass. Finally, non-structural elements can be modelled which are expected to have a significant influence on the global stiffness of the building. Studying their effect on serviceability behaviour can provide a lot of practical insight.

# Literature and Other sources

[3] R. Abrahamsen. "Mjøstårnet – Construction of an 81 m tall timber building". In: *Internationales Holzbau-Forum (IHF)*. 2017.

[4] R. Abrahamsen. "Mjøstårnet - 18 storey timber building completed". In: *Internationales Holzbau-Forum (IHF)*. 2018.

[5] R. Abrahamsen and K. Malo. "Structural Design and Assembly of "Treet" - A 14-storey Timber Residential Building in Norway". In: *New Zealand Timber Design*. 2014.

[6] H.J. Blaß, A. Bienhaus, and V. Krämer. "Effective bending capacity of dowel-type fasteners". In: *Proceedings of CIB-W18 Meeting 33*. KIT Holzbau und Baukonstruktionen, 2000, paper 33-7–5.

[7] H.J. Blaß and C. Sandhaas. *Timber Engineering - principles for design*. KIT Scientific Publishing, 2017. ISBN: 3731506734.

[8] J.F. Bocquet, R. Lemaître, and T. Bader. "Design recommendations and example calculations for dowel-type connections with multiple shear planes". In: *Design of Connections in Timber Structures: A State-of-the-Art Report*. Shaker Verlag, 2018, pp. 241–295.

[9] A. Brunauer. "The practical design of dowel-type connections in timber engineering structures according to EC5". In: *International Conference on Connections in Timber Engineering - From Research to Standards*. Institute of Timber Engineering and Wood Technology, 2017, pp. 6–14.

[10] P. Dubas, E. Gehri, and T. Steurer. In: *Einführung in die Norm SIA 164 (1981) - Holzbau*. Baustatik und Stahlbau, ETH Zürich, 1981.

[11] J. Ehlbeck and H.J. Larsen. "Eurocode 5-Design of timber structures: Joints". In: *International Workshop on Wood Connectors*. Forest Products Society, 1993, pp. 9–23.

[12] J. Ehlbeck and H. Werner. "Untersuchungen über die Tragfähigkeit von Stabdübelverbindungen". In: *European Journal of Wood and Wood Products*. Vol. 46. Springer, 1988, pp. 281–288.

[13] J. Ehlbeck and H. Werner. "Softwood and hardwood embedding strength for dowel-type fasteners". In: *Proceedings of the CIB-W18 meeting 25*. KIT Holzbau und Baukonstruktionen, 1992, paper 25-7–2.

[14] B.R. Ellis. "An Assessment of the Accuracy of Predicting the Fundamental Natural Frequencies of Buildings and the Implications Concerning the Dynamic Analysis of Structures." In: *Proceedings of the Institution of Civil Engineers*. Vol. 69. 3. 1980, pp. 763–776.

[26] I. Glišović, B. Stevanović, and T. Kočetov-Mišulić. "Embedment test of wood for dowel-type fasteners". In: *Wood Research*. Vol. 57. 2012, pp. 639–650.

[27] R. Jockwer and A. Jorissen. "Load-deformation behaviour and stiffness of lateral connections with multiple dowel type fasteners". In: *Proceeding to the 5th INTER Meeting*. KIT Holzbau und Baukonstruktionen, 2018, paper 51-7–7, 141–158.

[28] R. Jockwer and A. Jorissen. "Stiffness and Deformation of Connections with Dowel-Type Fasteners". In: *Design of Connections in Timber Structures: A State-of-the-Art Report by COST Action FP1402*. Shaker Verlag, 2018, pp. 95–126.

[29] K.W. Johansen. "Theory of timber connections". In: *International Association of Bridge and Structural Engineering*. Vol. 9. 1949, pp. 249–262.

[30] A.J.M. Jorissen. "Double shear timber connections with dowel type fasteners". PhD thesis. University of Technology Delft, 1998.

[31] V. Karagiannis, C. Málaga-Chuquitaype, and A.Y. Elghazouli. "Modified foundation modelling of dowel embedment in glulam connections". In: *Construction and Building Materials*. Vol. 102. Elsevier, 2016, pp. 1168–1179.

[32] P. Landel and A. Linderholt. "Reduced and test-data correlated FE-models of a large timber truss with dowel-type connections aimed for dynamic analyses at serviceability level". In: *Engineering structures 260: 114208*. Vol. 260. Elsevier, 2022.

[33] R. Lemaitre et al. "Beam-on-Foundation Modelling as an Alternative Design Method for Timber Joints with Dowel-Type Fasteners: Part 2: Modelling Techniques for Multiple Fastener Connections". In: *Proceeding to the 6th INTER Meeting*. KIT Holzbau und Baukonstruktionen, 2019, paper 52-7–9, 175–190.

[34] H. Liven and R. Abrahamsen. "Mjøstårnet: The World's Tallest Timber Building". In: *World Conference of Timber Engineering (WCTE 2023)*. 2023, pp. 4209–4214.

[35] P. van der Lugt. *Tomorrow's Timber (Lüning edition)*. Jeroen van Oostveen, 2020. URL: https://tomorrows-timber.com/.

[36] K. Malo, R. Abrahamsen, and M.A. Bjertnaes. "Some structural design issues of the 14-storey timber framed building "Treet"in Norway". In: *European Journal of Wood and Wood Products*. 2016.

[37] K. Malo et al. "Serviceability Stiffness of Timber Connections with Dowels and Slotted-in Steel Plates". In: *World Conference on Timber Engineering (WCTE 2023)*. 2023, pp. 1136–1145.

[38] Moelven. *Mjøstårnet - Press release*. 2019. URL: https://mediabank.moelven.com/mediaroom.html?keywords=Mjostarnet&company=MoelvenLimtreAS.

[39] D.H. Reed and L.H. Wiig. "A Parametric Study of Tall Timber Buildings". Master thesis. Norwegian University of Science and Technology (NTNU), 2020.

[40] T. Reynolds, R. Harris, and C. Wen-Shao. "Viscoelastic embedment behaviour of dowels and screws in timber under in-service vibration". In: *European Journal of Wood and Wood Products*. Vol. 71. 5. 2013, pp. 623–634.

[41] T.P.S. Reynolds et al. "Stiffness and slip in multi-dowel timber connections with slotted-in steel plates". In: *Engineering Structures 268: 114723*. Vol. 268. Elsevier, 2022.

[42] Rothoblaas. *Plates and Connectors for Timber*. 2020.

[43] C. Sandhaas. "Mechanical behaviour of timber joints with slotted-in steel plates". PhD thesis. University of Technology Delft, 2012.

[44] C. Sandhaas and J.W.G. van de Kuilen. "Strength and stiffness of timber joints with very high strength steel dowels". In: *Engineering Structures*. Vol. 131. 2017, pp. 394–404.

[45] N. Sauvat. "Resistance d'assemblages de type tige en structure bois sous chargements cycliques complexes." PhD thesis. Université Blaise Pascal-Clermont- Ferrand II, 2001.

[46] M. Schweigler et al. "Parameterization equations for the nonlinear connection slip applied to the anisotropic embedment behavior of wood". In: *Composites Part B: Engineering*. Vol. 142. Elsevier, 2018, pp. 142–158.

[47] M. Schweigler et al. "Embedment test analysis and data in the context of phenomenological modeling for dowelled timber joint design." In: *Proceedings of the INTER Meeting 52*. KIT Holzbau und Baukonstruktionen, 2019, paper 52-07–8.

[48] R. Smith. "Deflection limits in tall buildings—are they useful?" In: *Structures Congress 2011*. 2011, pp. 515–527.

[49] Dlubal Software. *RFEM 6: FEM Structural Analysis Software*. 2023. URL: https://www.dlubal.com/en.

[50] Wood Solutions. *Mjøstårnet, an 18-storey mixed use full-timber building - insights from the design, fire testing and construction*. 2020. URL: https://www.woodsolutions.com.au/webinars/woodsolutions-tuesday-webinars/mjostarnet-18-storey-mixed-use-full-timber-building.

[51] H. Svatoš-Ražnjević, L. Orozco, and A. Menges. "Advanced Timber Construction Industry: A Review of 350 Multi-Storey Timber Projects from 2000–2021". In: *Buildings 12(4): 404*. Vol. 12. 2022.

[52] S. Tulebekova et al. "Modeling stiffness of connections and non-structural elements for dynamic response of taller glulam timber frame buildings". In: *Engineering Structures 261: 114209*. Vol. 261. 2022.

[53] I. Utne. "Numerical Models for Dynamic Properties of a 14 Storey Timber Building". Master thesis. Norwegian University of Science and Technology (NTNU), 2012.

# Standards

[1]     prEN1995-1-1 (pre-norm). *Eurocode 5: Design of timber structures*. European Committee for Standardization (CEN), Informal enquiry, Apr. 2023.

[2]     ISO 10137. *Basis for design of structures - Serviceability of buildings and walkways against vibrations.* International Organization for Standardization (ISO), Geneva, 2007.

[15]   EN10088-3. *Stainless steels - Part 3 : Technical delivery conditions for semi-finished products, bars, rods, wire, sections and bright products of corrosion resisting steels for general purposes*. European Committee for Standardization (CEN), Brussels, 2014.

[16]   EN14080. *Glued laminated timber and glued solid timber - Requirements*. European Committee for Standardization (CEN), Brussels, 2013.

[17]   EN1990. *Eurocode 0: Basis of structural design*. European Committee for Standardization (CEN), Brussels, 2002.

[18]   EN1991-1-1. *Eurocode 1: Actions on structures - Part 1-1: General actions - Densities, self-weight, imposed loads for buildings*. European Committee for Standardization (CEN), Brussels, 2002.

[19]   EN1991-1-4. *Eurocode 1: Actions on structures - Part 1-4: General actions - Wind actions*. European Committee for Standardization (CEN), Brussels, 2005.

[20]   EN1995-1-1. *Eurocode 5: Design of timber structures - Part 1-1: General - Common rules and rules for buildings*. European Committee for Standardization (CEN), Brussels, 2004.

[21]   EN1995-1-2. *Eurocode 5: Design of timber structures - Part 1-2: General - Structural fire design*. European Committee for Standardization (CEN), Brussels, 2004.

[22]   EN26891. *General principles for the determination of strength and deformation characteristics*. European Committee for Standardization (CEN), Brussels, 1991.

[23]   EN338. *Structural timber - Strength classes*. European Committee for Standardization (CEN), Brussels, 2016.

[24]   EN383. *Determination of embedment strength and foundation values for dowel type fasteners*. European Committee for Standardization (CEN), Brussels, 2007.

[25]   EN409. *Determination of the yield moment of dowel type fasteners*. European Committee for Standardization (CEN), Brussels, 2009.

# Appendices

<div align="right">

# A

</div>
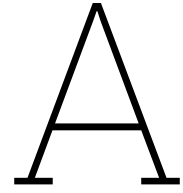
# Timber Connection Design

## A.1. Fastener spacing and edge & end distances

The minimum fastener spacings are prescribed in EC5. The spacing is dependent on the type of fastener. Table A.1 shows the prescribed minimum spacing for dowels. Note that the spacing is dependent on the grain angle. In figure A.1, the spacing is illustrated.

**Table A.1:** Minimum spacings and edge/end distances for dowels in EC5 [20, Table 8.5].

| Spacing or distance | Angle | Minimum spacing or end/edge distance |
|---|---|---|
| $a_1$ (parallel to grain) | $0° \leq \alpha \leq 360°$ | $(3 + 2|\cos \alpha|)d$ |
| $a_2$ (perpendicular to grain) | $0° \leq \alpha \leq 360°$ | $3d$ |
| $a_{3,t}$ (loaded end) | $-90° \leq \alpha \leq 90°$ | $\max(7d; 80mm)$ |
| | $90° \leq \alpha \leq 150°$ | $\max((a_{3,t}|\sin \alpha|)d; 3d)$ |
| $a_{3,c}$ (unloaded end) | $150° \leq \alpha \leq 210°$ | $3d$ |
| | $210° \leq \alpha \leq 270°$ | $\max((a_{3,t}|\sin \alpha|)d; 3d)$ |
| $a_{4,t}$ (loaded edge) | $0° \leq \alpha \leq 360°$ | $\max((2 + 2\sin \alpha)d; 3d)$ |
| $a_{4,c}$ (unloaded edge) | $0° \leq \alpha \leq 360°$ | $3d$ |



(a) Spacing between fasteners.

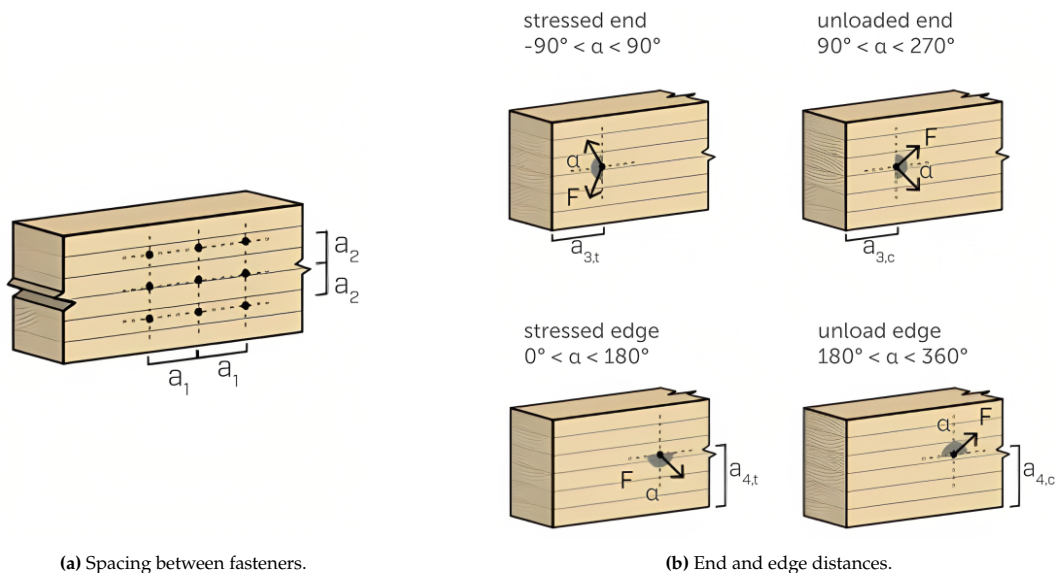(b) End and edge distances.

**Figure A.1:** Fastener spacing [42, p. 57].
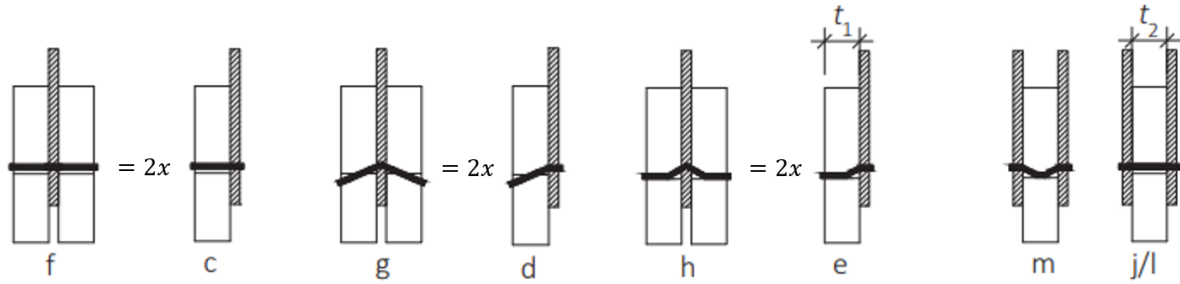
## A.2. European yield model
### A.2.1. Failure modes



**Figure A.2:** Failure modes for double shear steel-to-timber connections with thick plates (t ≥d). Adapted from [7, Figure E2-9].

**(c/f)** $$f_{h,k}t_1d \qquad \text{(A.1)}$$

**(l)** $$0.5f_{h,k}t_2d \qquad \text{(A.2)}$$

**(d/g)** $$f_{h,k}t_1d \cdot \left(\sqrt{2 + \frac{4M_{y,Rk}}{f_{h,k}dt_1^2}} - 1\right) + \frac{F_{ax,Rk}}{4} \qquad \text{(A.3)}$$

**(m)** $$2.3\sqrt{M_{y,Rk}f_{h,k}d} \qquad \text{(A.4)}$$

**(e/h)** $$2.3\sqrt{M_{y,Rk}f_{h,k}d} + \frac{F_{ax,Rk}}{4} \qquad \text{(A.5)}$$

where $f_{h,k}$ = characteristic embedment strength [MPa], $t_1$ = side member thickness [mm], $t_2$ = middle member thickness [mm], $d$ = fastener diameter [mm], and $M_{y,Rk}$ = characteristic yield moment of the fastener [Nmm].

**Rope effect:** $$\frac{F_{ax,Rk}}{4} \qquad \text{(A.6)}$$

with a minimum value of:

- Round nails 15%
- Screws 100%
- Bolts 25%
- Dowels 0%

### A.2.2. Correction factor (pre-factor)
Failure modes e/h and m for steel-to-timber connections contain a correction factor. This factor accounts for the partial safety approach related to the material factor for steel. Notable is that no factor is assigned to failure mode d even though the yield moment of the steel fastener is present in the equation [7, p.356]. The derivation process leading to the correction factor for failure modes in which two plastic hinges develop is shown:

$k_{mod} = 0.9$, $\gamma_{M,steel} = 1.1$, and $\gamma_{M,timber} = 1.3$

$$
\begin{aligned}
F_{v,Rd} &= 2.3\sqrt{M_{y,Rd} \cdot f_{h,d} \cdot d} \\
&= 2.3\sqrt{\frac{M_{y,Rk}}{\gamma_{M,steel}} \cdot \frac{f_{h,k} \cdot k_{mod}}{\gamma_{M,timber}} \cdot d} \qquad \text{(A.7)} \\
&= 2.3\sqrt{\frac{M_{y,Rk}}{1.1} \cdot \frac{f_{h,k} \cdot 0.9}{1.3} \cdot d} \quad = 0.7933 \cdot F_{v,Rk}
\end{aligned}
$$

Eurocode 5 procedure to calculate the design value excluded the partial safety factor for steel:

$$F_{v,Rd} = F_{v,Rk} \cdot \frac{k_{mod}}{\gamma_{M,timber}} = F_{v,Rk} \cdot \frac{0.9}{1.3} = 0.6923 \cdot F_{v,Rk} \qquad (A.8)$$

**Correction factor** (pre-factor):

$$\frac{0.7933}{0.6923} = 1.146 \approx 1.15 \qquad (A.9)$$

## A.3. Testing procedure and terminology in EN26891

EN26891 [22] prescribes the European testing procedure for timber connections. The loading protocol is shown in figure A.3 and the corresponding idealized load-slip curve is shown in figure A.4. Below the figures, the terminologies related to the measurement points are listed.
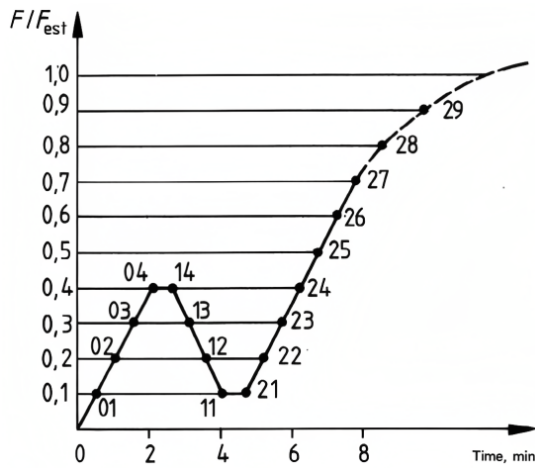


**Figure A.3:** Loading protocol.
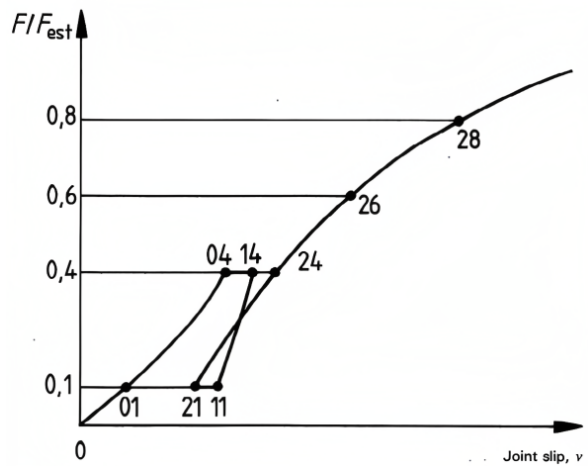


**Figure A.4:** Idealized load-slip curve.

Terminology and calculations related to measurements:

1)  Maximum load                  $F_{max}$

2)  Estimated maximum load        $F_{est}$

3)  Initial slip                  $v_i = v_{04}$

4)  Modified initial slip         $v_{i,mod} = \frac{4}{3} \cdot (v_{04} - v_{01})$

5)  Joint settlement              $v_s = v_i - v_{i,mod}$

6)  Elastic slip                  $v_e = \frac{2}{3} \cdot (v_{14} + v_{24} - v_{11} - v_{21})$

7)  Initial slip modulus          $k_i = \frac{0.4 \cdot F_{est}}{v_i}$

8)  Slip modulus                  $k_s = \frac{0.4 \cdot F_{est}}{v_{i,mod}}$

9)  Slip at 0.6 $F_{max}$         $v_{0.6}$

10) Modified slip at 0.6 $F_{max}$  $v_{0.6,mod} = v_{0.6} - v_{24} + v_{i,mod}$

11) Slip at 0.8 $F_{max}$         $v_{0.8}$

12) Modified slip at 0.8 $F_{max}$  $v_{0.8,mod} = v_{0.8} - v_{24} + v_{i,mod}$

## A.4. Embedment tests by Ehlbeck and Werner

Elhbeck and Werner [13] performed numerous embedment tests on both softwood- and hardwood specimens. Fasteners with different diameters are tested, and fasteners are loaded at a grain angle of 0 ° and 90 °. For the softwood specimens with fasteners loaded parallel to the grain, 360 tests were performed. The fitted regression line is shown in figure A.5.
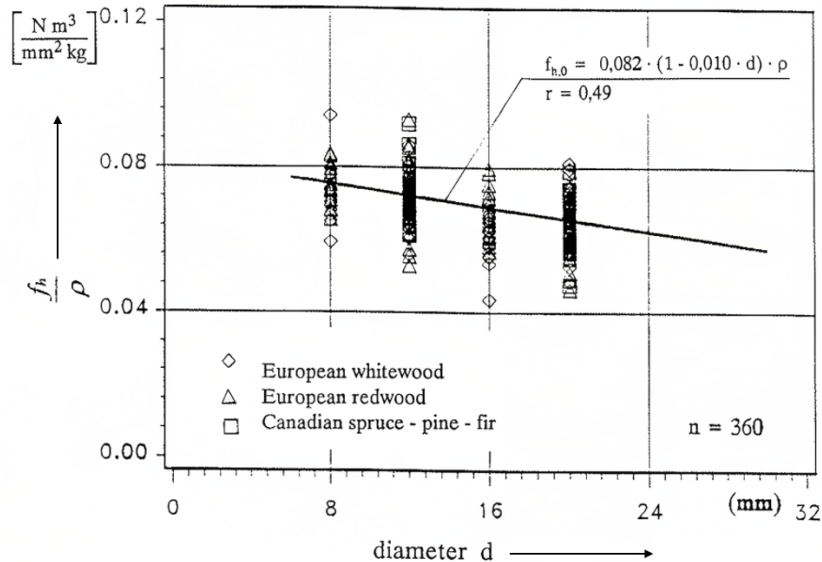


**Figure A.5:** Regression analysis on embedment tests from Ehlbeck and Werner [13, Fig. 2].

## A.5. Stiffness formulas from different design codes

Jockwer and Jorissen [28] compared the stiffness formulas adopted in several design codes. The formulas, from three design codes; EC5, DIN1051, and SIA265, are presented in this section.

Eurocode 5 (2004): European standard

Two formulas are adopted in current EC5 [20] for connections with dowel-type fasteners. One formula is for dowel-type fasteners with predrilled holes and the other for nails without pre-drilling. The formulas are shown in table A.2. For steel-to-timber connections, $K_{ser}$ may be multiplied by two. Clearance should be added separately.

**Table A.2:** Formulas for stiffness $K_{ser}$ in EC5.

| fastener type | timber-to-timber |
|---|---|
| dowels | |
| bolts without clearance | $\dfrac{\rho_m^{1.5} \cdot d}{23}$ |
| screws | |
| nails (with predrilling) | |
| nails (without predrilling) | $\dfrac{\rho_m^{1.5} \cdot d^{0.8}}{30}$ |

DIN 1052 (2008): former German standard

Table A.3 shows the stiffness formula for fasteners in timber-to-timber and steel-to-timber (value x2) connections. For bolts with clearance, a slip of 1mm should be added.

**Table A.3:** Stiffness formulas in DIN1052 (2008).

| fastener type | |
|---|---|
| dowels | |
| bolts without clearance | $\dfrac{\rho_k^{1.5} \cdot d}{20}$ |
| screws | |
| nails (with predrilling) | |
| nails (without predrilling) | $\dfrac{\rho_k^{1.5} \cdot d^{0.8}}{25}$ |

SIA 265 (2012): Swiss standard
The formulas in table A.4 are for fasteners loaded parallel to the grain and moisture content class 1.

**Table A.4:** Stiffness formulas in SIA 265 (2012).

| fastener type | timber-to-timber | steel-to-timber |
|---|---|---|
| dowels | | |
| bolts without clearance | $3 \cdot \rho_k^{0.5} \cdot d^{1.7}$ | $6 \cdot \rho_k^{0.5} \cdot d^{1.7}$ |
| screws | | |
| nails (with predrilling) | | |
| nails (without predrilling) | $60 \cdot d^{1.7}$ | $120 \cdot d^{1.7}$ |

# A.6. Derivation of the formula for Kser

In Ehlbeck and Larsen [11] the background of the current stiffness formulas for $K_{ser}$, adopted in Eurocode 5 [20], is briefly discussed. The equations in EC5 and the formulas provided by Elbeck and Larsen differ slightly. This can be seen by comparing the formulas in table A.2 and A.5.

**Table A.5:** Stiffness for single shear connections from Ehlbeck and Larsen [11, Table 6].

| fastener type | timber-to-timber | steel-to-timber |
|---|---|---|
| dowels | $\dfrac{\rho_k^{1.5} \cdot d}{20}$ | $\dfrac{\rho_k^{1.5} \cdot d}{30}$ |
| screws with $d \geq 8mm$ | | |
| nails (with predrilling) | $\dfrac{\rho_k^{1.5} \cdot d}{20}$ | $\dfrac{\rho_k^{1.5} \cdot d}{20}$ |
| screws with $d < 8mm$ | | |
| nails (without predrilling) | $\dfrac{\rho_k^{1.5} \cdot d^{0.8}}{25}$ | $\dfrac{\rho_k^{1.5} \cdot d^{0.8}}{25}$ |

The equations in table A.5 are established with empirical data from many tests. From this data, the instantaneous deformation at approximately 40% of the maximum load-carrying capacity is estimated. 40 percent of the maximum force is a generally accepted measurement point for stiffness under serviceability loads (SLS). On test data from **predrilled nailed timber-to-timber** connections, equation A.10 was fitted.

$$u_{inst} = 40 \cdot \frac{d^{0.8}}{\rho_k} \tag{A.10}$$

The loading at which the slip $u_{inst}$ is present is 40% of the maximum capacity (R), hence, $F_{ser} = 0.4R$. Therefore, the instantaneous stiffness can be determined with equation A.11.

$$K_{ser,inst} = \frac{F_{ser}}{u_{inst}} = \frac{0.4R}{u_{inst}} \tag{A.11}$$

According to Ehlbeck and Larsen, the load-carrying capacity of nailed timber-to-timber connections is most frequently governed by failure mode f. The formula for this failure mode is shown in equation A.12.

$$R = \sqrt{\frac{2\beta}{1+\beta}} \cdot \sqrt{2M_{y,Rk}f_{h,k}d}$$

$$= \sqrt{2M_{y,Rk}f_{h,0,k}d} \quad \text{(for } \beta = 1)$$

(A.12)

$\beta$ = grain angle

For the embedment strength, equation 2.9 is used. This equation is repeated for convenience:

$$f_{h,0,k} = 0.082(1 - 0.01d) \cdot \rho_k$$

(2.9 revisited)

For the yield moment of the nails (with $f_{y,k} \approx 600N/mm^2$), equation 2.14 is used. This formula was provided in the previous Eurocode 5 (1995) before the adoption of the formula (equation 2.12) proposed by Blaß et al. [6]. Equation 2.14 from the old EC5, used in the derivation by Ehlbeck and Larsen, is repeated:

$$M_y = 180d^{2.6}$$

(2.14 revisited)

Next, the embedding strength and the yield moment formulas are filled in equation A.12:

$$R = \sqrt{2M_{y,Rk}f_{h,0,k}d}$$

$$= \sqrt{2 \cdot (180d^{2.6}) \cdot (0.082(1 - 0.01d) \cdot \rho_k) \cdot d}$$

$$= \sqrt{360 \cdot (0.082(1 - 0.01d) \cdot \rho_k) \cdot d^{3.6}}$$

(A.13)

$$= \sqrt{29.52(1 - 0.01d) \cdot \rho_k \cdot d^{3.6}} \quad \approx \sqrt{0.3(100 - d) \cdot \rho_k \cdot d^{3.6}}$$

$$R = \sqrt{29.52(1 - 0.01d) \cdot \rho_k \cdot d^{3.6}}$$

(A.14)

Last, equation A.14 for the characteristic maximum load-bearing capacity and equation A.10 for the instantaneous slip are filled in equation A.11 to obtain a formula for the instantaneous stiffness:

$$K_{ser,inst} = \frac{0.4R}{u_{inst}}$$

$$= \frac{0.4(\sqrt{29.52(1 - 0.01d) \cdot \rho_k \cdot d^{3.6}})}{40 \cdot \frac{d^{0.8}}{\rho_k}}$$

(A.15)

$$= \frac{\rho_k^{1.5} \cdot d}{100} \cdot \sqrt{\frac{29.52}{100}} \cdot \sqrt{(100 - d)}$$

$$K_{ser,inst} \approx \frac{0.543}{100} \cdot \sqrt{(100 - d)} \cdot \rho_k^{1.5} \cdot d$$

(A.16)

The root term in equation A.16 is removed to simplify the formula. In Elhbeck and Larsen [11] it is mentioned that this simplification for nails 2 to 8mm leads to equation A.18. However, filling in d=15.31 results in the 1/20, as can be seen in A.17. It is rather unclear what assumptions are taken by Elhbeck and Larsen in the simplification of equation A.16. Ehlbeck and Larsen do mention that on the basis of further research, they came up with the stiffness values shown in table A.5. It could be that they made small changes, for instance, to make the formulas more generally applicable. Note that in table A.5 the equations for timber-to-timber connections with small fasteners (d<8mm) and for larger fasteners, i.e. dowels and screws d>8mm, are the same.

$$K_{ser,inst} = \frac{0.543}{100} \cdot \sqrt{(100 - d)} \cdot \rho_k^{1.5} \cdot d$$

$$= \frac{0.543}{100} \cdot \sqrt{(100 - 15.31)} \cdot \rho_k^{1.5} \cdot d \tag{A.17}$$

$$\approx \frac{1}{20} \cdot \rho_k^{1.5} \cdot d$$

$$K_{ser,inst} \approx \frac{\rho_k^{1.5} \cdot d}{20} \tag{A.18}$$

The result is the formula for stiffness shown in equation A.18. This is the same formula as previously shown in table A.5 for dowels, screws and nails in timber-to-timber connections. The other formulas in the table are likely derived using the same procedure. This suggests that Ehlbeck and Larsen used a different formula for the instantaneous displacement for steel-to-timber connections. The formula for $K_{ser}$ in EC5 (equation 2.24) is very similar to the formula derived in Elhbeck and Larsen (equation A.18). When replacing the characteristic density with the mean density, the equation from EC5 is obtained. This is shown below.

$$K_{ser,inst} = \frac{\rho_k^{1.5} \cdot d}{20} \quad \text{and} \quad \rho_k = \frac{\rho_m}{1.1} \quad \longrightarrow \quad K_{ser,inst} \approx \frac{\rho_m^{1.5} \cdot d}{23} = K_{ser,EC5}$$

The same derivation procedure can be repeated for **non-predrilled nails in timber-to-timber** connections. For non-predrilled nails, the equation for the embedment strength ($f_{h,0,k}$) and the initial displacement ($u_{inst}$) differ from those for predrilled nails. The pre-assumed failure mode (R) and the yield moment ($M_{y,Rk}$ are the same. The procedure is briefly repeated for timber-to-timber connections non-predrilled nails:

$$K_{ser,inst} = \frac{F_{ser}}{u_{inst}} = \frac{0.4R}{u_{inst}} \tag{A.19}$$

$$u_{inst} = 60 \cdot \frac{d^{0.8}}{\rho_k} \tag{A.20}$$

$$f_{h,0,k} = 0.082 \cdot \rho_k \cdot d^{-0.3} \tag{A.21}$$

$$R = \sqrt{2M_{y,Rk}f_{h,0,k}d} \quad \text{(for } \beta = 1\text{)} \tag{A.22}$$

$$M_y = 180d^{2.6} \tag{A.23}$$

Filling in A.20 up to A.23 in equation A.19 gives:

$$K_{ser,inst} = \frac{0.4R}{u_{inst}}$$

$$= \frac{0.4(\sqrt{29.52 \cdot \rho_k \cdot d^{3.3}})}{60 \cdot \frac{d^{0.8}}{\rho_k}} \tag{A.24}$$

$$K_{ser,inst} \approx \frac{\rho_k^{1.5} \cdot d^{0.85}}{27.61} \tag{A.25}$$

$$K_{ser,inst} = \frac{\rho_k^{1.5} \cdot d^{0.85}}{27.61} \quad \text{and} \quad \rho_k = \frac{\rho_m}{1.1} \quad \longrightarrow \quad K_{ser,inst} \approx \frac{\rho_m^{1.5} \cdot d^{0.85}}{32.67} \tag{A.26}$$

For nails with diameter 2- 8 mm, equation A.26 is approximately equal to the formulation in EC5 (for nails without predrilling). Note that the power term differs.

$$K_{ser,EC5} = \frac{\rho_m^{1.5} \cdot d^{0.8}}{30} \approx K_{ser,inst} = \frac{\rho_m^{1.5} \cdot d^{0.85}}{32.67} \qquad \text{(for nails 2-8mm)}$$

Ehlbeck and Larsen ultimately proposed the stiffness formula shown in table A.5. The following approximate formula for nailed connections without predrilled holes is present in the table:

$$K_{ser,inst} = \frac{\rho_k^{1.5} \cdot d^{0.8}}{25} \tag{A.27}$$

Note that in equation A.27 the power term for the fastener diameter changed in comparison to equation A.25. It may be that this is done to simplify the formula, but the actual reason for this change is unknown.

# B

# Stiffness Modelling

## B.1. BOF modelling of a single dowel

To research the effect of the timber member thickness on the slip modulus $k_s$, BOF modelling is used. Four different member thicknesses; 50, 75, 100, and 125mm are considered. Equation B.1 is used to determine the slip modulus. Figure B.1 shows the dowel deformation for three member thicknesses at a load of 0.4R.

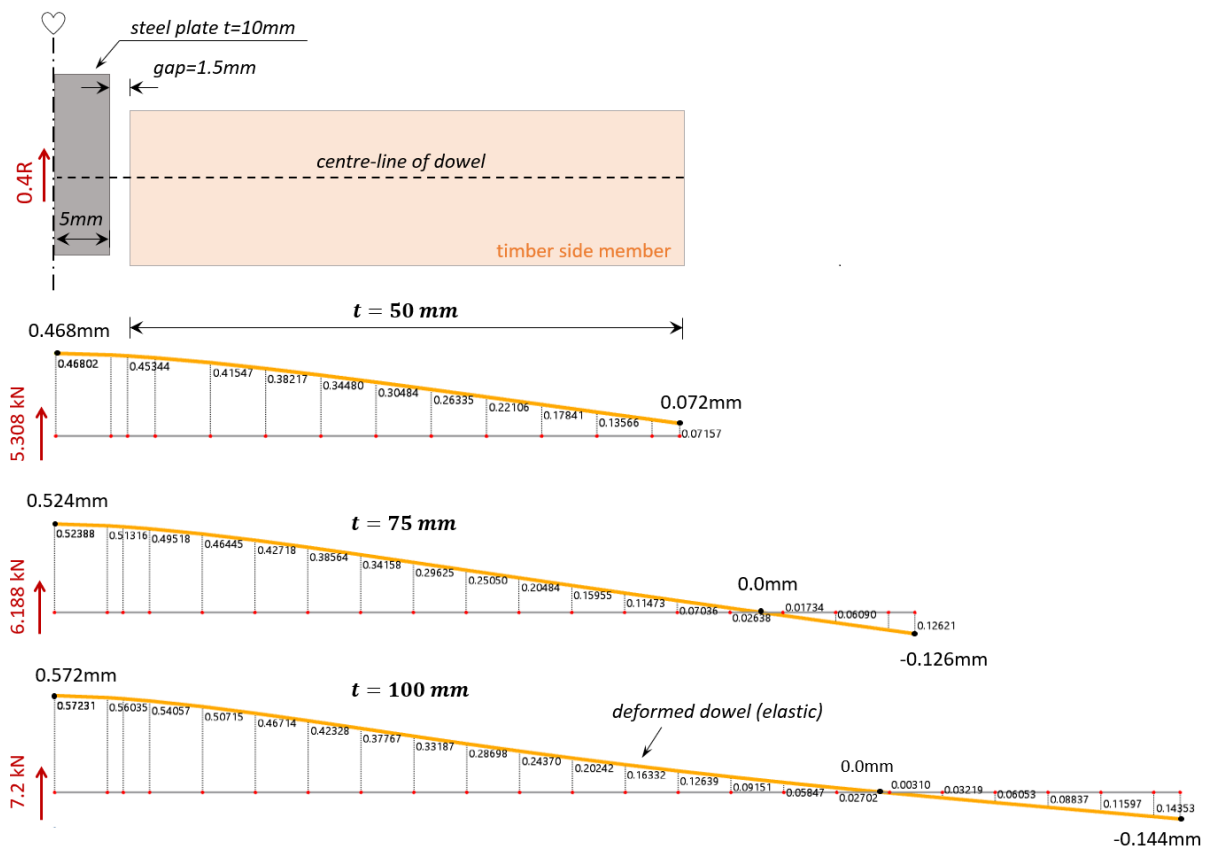$$k_{s,BOF} = \frac{0.4R - 0.1R}{u_{0.4R} - u_{0.1R}} \tag{B.1}$$



**Figure B.1:** Elastic dowel deformation for different side members thicknesses (load=0.4R).

113

## B.2. Comparison of test data

Sandhaas [43], Malo et al. [37], and Reynolds et al. [41] conducted tests on timber connections with slotted-in steel plates and dowels. Several tests are similar, which allows for comparison. It is, however, important to point out the differences that may affect the measured stiffness. In the compared tests, 12mm dowels are used, one slotted-in steel plate i.e. two shear planes, and softwood specimens. The number of dowels in a row is one up to five. The spacing between dowels (in a row), for all tests, is 60mm corresponding to 5d, i.e. five times the dowel diameter, which is the minimum-required spacing prescribed by EC5 (see table A.1). The connection parameters of the performed tests are shown in table B.1.

**Table B.1:** Connection parameters of the tests.

| Tests from: | side member thickness | mean density | steel plates | dowels | hole clearance in steel plates |
|---|---|---|---|---|---|
| Sandhaas | 91 $mm$ | 458 $kg/m^3$ | S690 (12 $mm$) | hss (~609 $MPa$) | 0.5 $mm$ |
| Malo et al. | 51 $mm$ | 430 $kg/m^3$ | S355 (12 $mm$) | hss (755 $MPa$) | 1 $mm$ |
| Reynolds et al. | 70 $mm$ | 378 $kg/m^3$ | S355 (8 $mm$) | mild S355 (355 $MPa$) | 1 $mm$ |

In the next sections, the loading procedures, tested specimens, and determination methods for stiffness are presented individually for each of the three experiments.

### B.2.1. Sandhaas

Sandhaas [43] used the test protocol from EN26891, which is shown in figure 2.13. An image of the tested specimens, with one, three, and five dowels in a row, is shown in figure B.2.
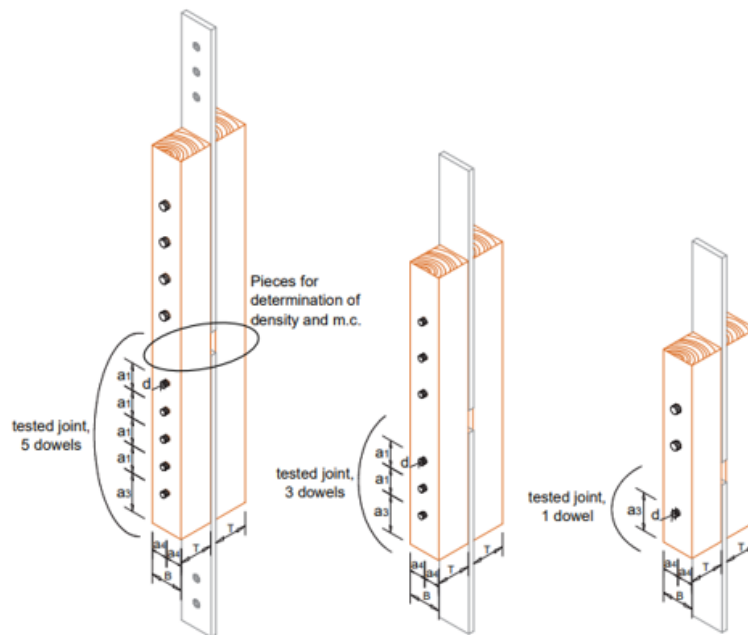


**Figure B.2:** Test specimens [43, Figure 7-1].

Sandhaas mentioned the following about the applied load: "In this research, usually a lower value than 40% of $F_{est}$ was chosen for the big specimens as any damage in the first loop that serves to settle the specimens should be avoided"[43, p. 177]. The load-slip behaviour measured for the softwood specimens with five hss dowels is shown in figure B.3. It can be observed that the applied loads for the unloading-reloading cycles are lower than 10% and 40% of the measured characteristic connection capacity. It could be that this affects the measured elastic stiffness.

**Figure B.3:** Load-slip curve of spruce specimens with five 12mm hss dowels. Sandhaas [43, Figure B-30].

The elastic stiffness of the tests has been determined using the data shared by Sandhaas (*C. Sandhaas, personal communication, May 2023*). For each test, the elastic modulus is determined in accordance with the EN26891 [22]. The elastic reloading cycle is used to determine the elastic modulus ($k_e$) using equation 2.23.
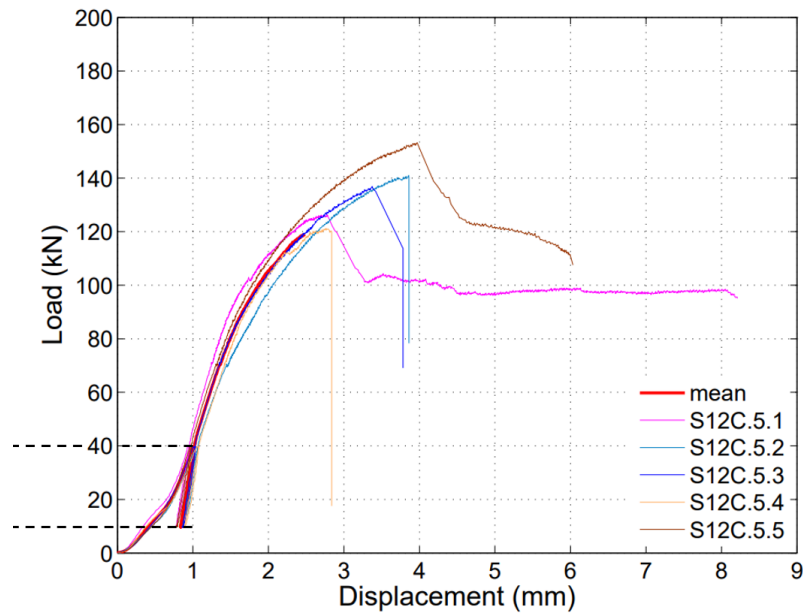
$$k_e = \frac{0.4 \cdot F_{est}}{v_e} \quad \text{where} \quad v_e = \frac{2}{3} \cdot (v_{14} + v_{24} - v_{11} - v_{21}) \qquad \text{(2.23 revisited)}$$

Tests on softwood specimens with one, three, and five hss dowels in a row have been performed. For each number of dowels, five tests have been conducted. For the estimation of the elastic stiffness, the mean values of each of the test series are used.

## B.2.2. Malo et al.

Malo et al. [37] mention the following about their test procedure: "The tests were performed by sequentially installing an additional row of dowels along the grain, starting from the ends of the connections" [37, p.1139]. The loading procedure is shown in figure B.4 and the geometry of the tested connections are shown in figure B.5 and B.6.
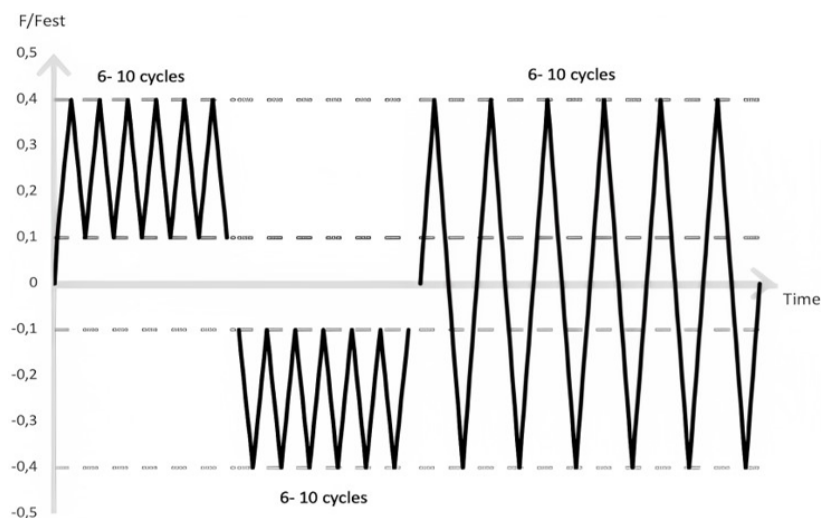


**Figure B.4:** Loading protocol [37, Figure 11].
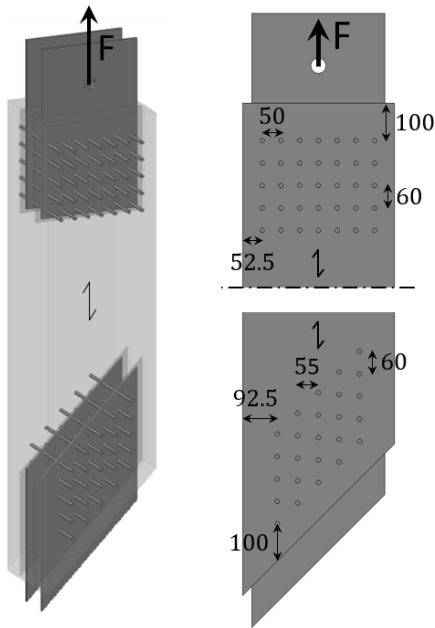
**Figure B.5:** Large scale specimen.



**Figure B.6:** Small-scale specimens [37, Figure 3].

The method of least squares has been used to fit a linear line on the stable unloading-reloading cycles. Correspondingly, the information from multiple cycles is used to obtain the fit. This approach can lead to different stiffness values depending on the choice of points, and therefore, the points should be chosen with care. Figure B.7 shows the linear fit on tension- and compressive cycles utilizing the points indicated by pink dots.
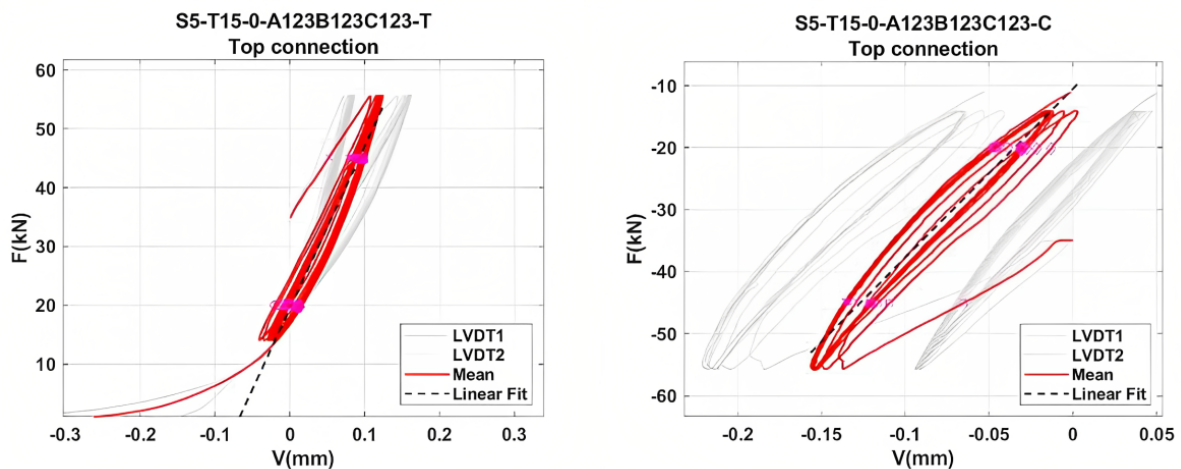


**Figure B.7:** Linear fit using the method of least squares; tension cycle (left) and compressive cycle (right) [37, Fig. 12&13].

## B.2.3.  Reynolds et al.

Reynolds et al. [41] mention the following about their test procedure: "For each specimen, a force–displacement diagram for the tension and compression loading was recorded for each of the five tests, as the dowels are added one by one"[41, p. 6]. The loading sequence is shown in figure B.8 and an image of the tested medium specimen is shown in figure B.9.
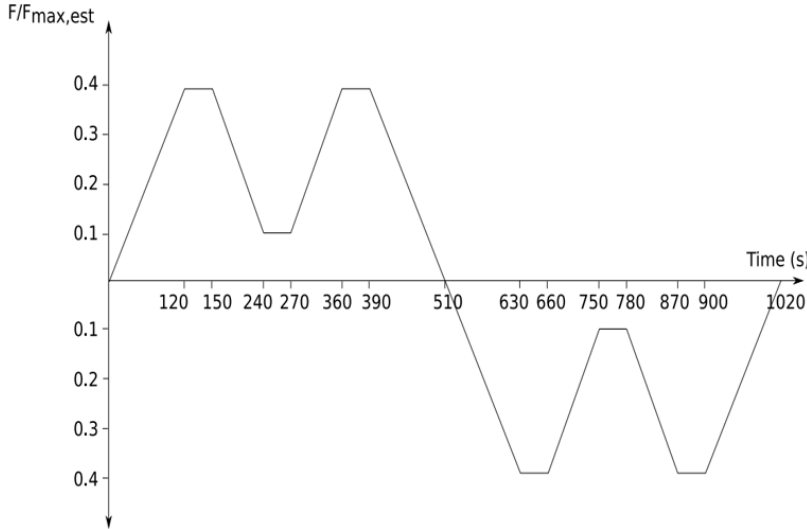
**Figure B.8:** Loading sequence [41, Fig. 3].
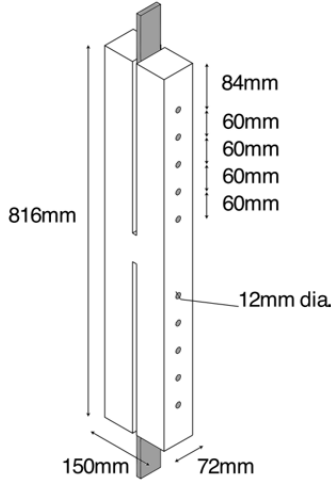


**Figure B.9:** Medium specimen [41, Fig. 1].

Reynolds et al. determined the 'unload-reload' stiffness utilizing all the data on the load-slip curve between 10 and 40% of the estimated failure load. The obtained linear fits on the load-slip curve of a single dowel- and large specimen are shown in figure B.10.
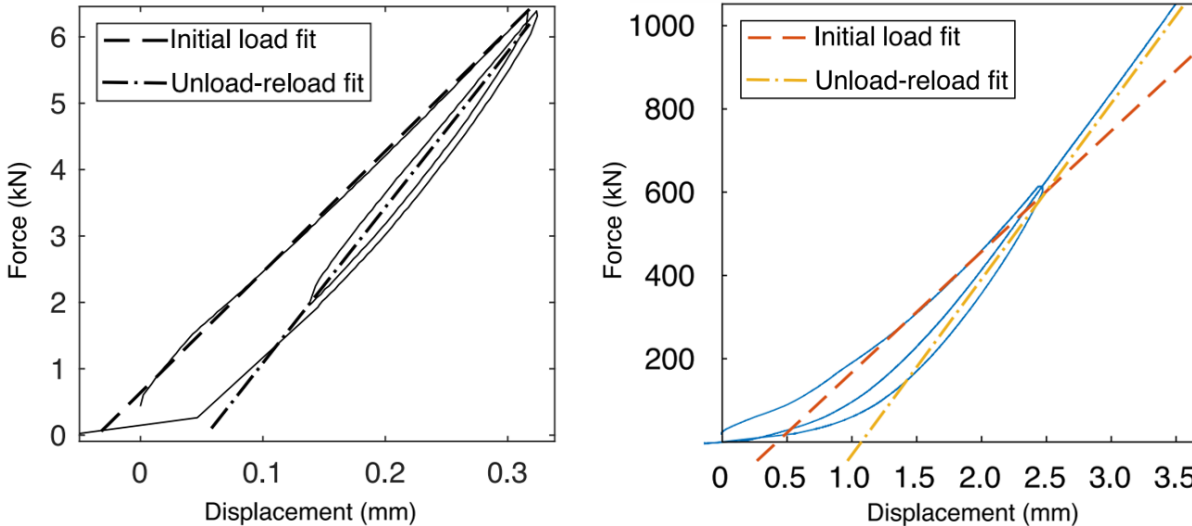


**(a)** Single 12mm dowel [41, Fig. 8].



**(b)** 35-dowel softwood specimen [41, Fig. 11].

**Figure B.10:** Linear fits on the load-slip curves of the tested specimens.

# C
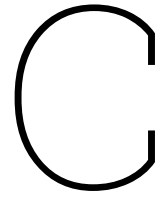
# Case Study: Mjøstårnet

## C.1. Preliminary study

The stability system in the short facade of Mjøstårnet is complex. Therefore, it has been chosen to analyse the modelled structure before the models are used to perform the sensitivity- and variant study. The results of the preliminary study are presented in this chapter. The calculations are performed using the design checks from the current EC5 (2004).

### C.1.1. Identification of members and connections

The truss parts, consisting of members and connections between these members, are named such that they can easily be referred to. The designation of all the parts is illustrated in figure 4.6.



**(a) Connections**.

**(b) Members**.
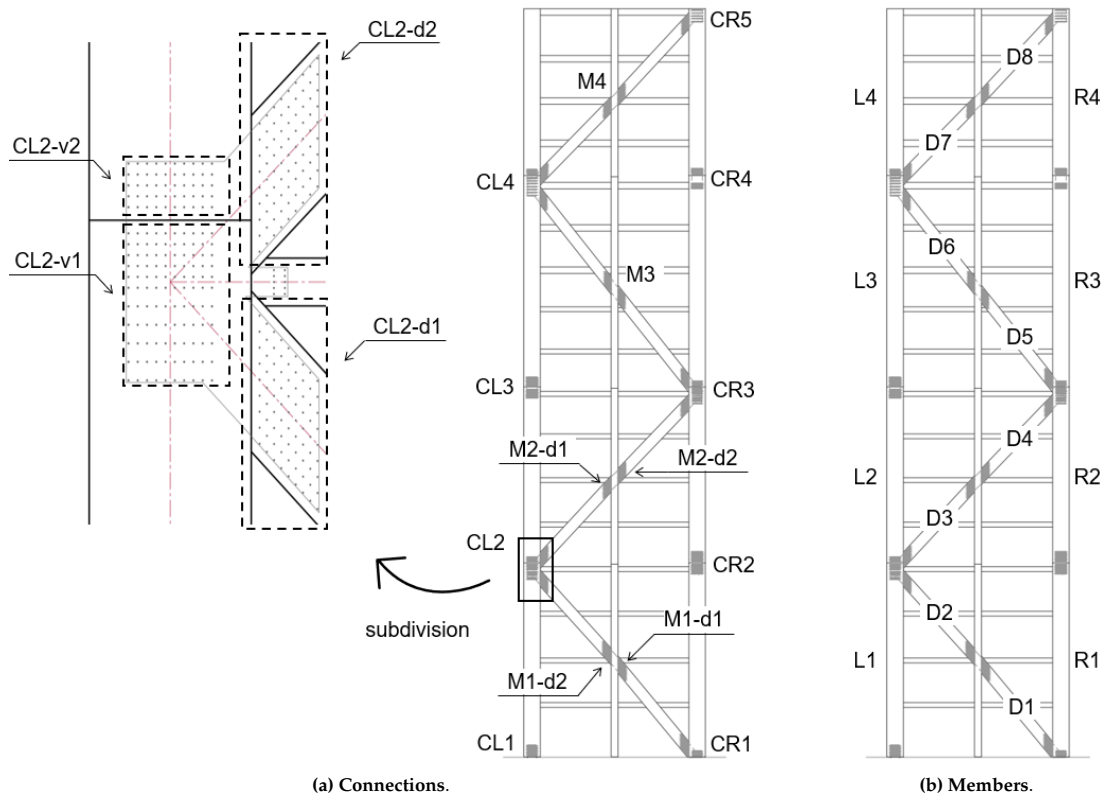
**Figure 4.6** revisited; Designation of the truss parts.

## C.1.2. Geometry of the truss connections

Legend:

- n = total number of dowels
- n0 = number of dowels parallel to the grain
- a1 [mm] = dowel spacing parallel to the grain
- n90 = number of dowels perpendicular to the grain
- a2 [mm] = dowel spacing perpendicular to the grain

**Table C.1:** Geometries of the truss connections.

| Member | Connection | n | n0 | a1 | n90 | a2 | Connection | n | n0 | a1 | n90 | a2 |
|---|---|---|---|---|---|---|---|---|---|---|---|---|
| L1 | CL1 | 100 | 10 | 100 | 10 | 85 | CL2-v1 | 110 | 11 | 100, 170 | 10 | 85 |
| L2 | CL2-v2 | 50 | 5 | 100 | 10 | 85 | CL3-v1 | 70 | 7 | 120 | 10 | 100 |
| L3 | CL3-v2 | 70 | 7 | 120 | 10 | 100 | CL4-v1 | 80 | 8 | 120, 200, 260 | 10 | 85 |
| L4 | CL4-v2 | 50 | 5 | 100 | 10 | 85 | - | - | - | - | - | - |
| R1 | CR1-v | 50 | 5 | 100 | 10 | 85 | CR2-v1 | 80 | 8 | 120 | 10 | 100 |
| R2 | CR2-v2 | 80 | 8 | 120 | 10 | 100 | CR3-v1 | 110 | 11 | 100, 170 | 10 | 85 |
| R3 | CR3-v2 | 50 | 5 | 100 | 10 | 85 | CR4-v1 | 50 | 5 | 120 | 10 | 100 |
| R4 | CR4-v2 | 50 | 5 | 120 | 10 | 100 | CR5-v | 50 | 5 | 120 | 10 | 100 |
| D1 | CR1-d | 100 | 10 | 100 | 10 | 85 | M1-d1 | 100 | 10 | 100 | 10 | 85 |
| D2 | M1-d2 | 100 | 10 | 100 | 10 | 85 | CL2-d1 | 81 | 9 | 100 | 9 | 98 |
| D3 | CL2-d2 | 81 | 9 | 100 | 9 | 98 | M2-d1 | 81 | 9 | 100 | 9 | 98 |
| D4 | M2-d2 | 81 | 9 | 100 | 9 | 98 | CR3-d1 | 81 | 9 | 100 | 9 | 98 |
| D5 | CR3-d2 | 81 | 9 | 100 | 9 | 98 | M3-d1 | 64 | 8 | 100 | 8 | 112 |
| D6 | M3-d2 | 64 | 8 | 100 | 8 | 112 | CL4-d1 | 64 | 8 | 100 | 8 | 112 |
| D7 | CL4-d2 | 64 | 8 | 100 | 8 | 112 | M4-d1 | 64 | 8 | 100 | 8 | 112 |
| D8 | M4-d2 | 64 | 8 | 100 | 8 | 112 | CR5-d | 64 | 8 | 100 | 8 | 112 |

## C.1.3. Unity checks of the truss members

The forces from the RFEM model are used to perform the design checks. The buckling of the compressive members is also checked, but not shown in this table. The truss members are regularly connected to horizontal beams, which greatly reduces their buckling length. Correspondingly, the members met the buckling requirements. The members are also checked on buckling in the absence of these buckling supports, and it was found that the buckling resistance is then too low. This means that intermediate supports are necessary. The bending and shear forces in the truss members are small and do not change the values of the unity checks significantly when they are accounted for. Therefore, the unity checks, listed in table C.2, are performed using the axial forces only.

Table C.2: Unity checks of the truss members.

| Member | Strength class | Area $A [mm^2]$ | Max. compr. force (-) $N_{c,0,d}$ [kN] | Max. tension force (+) $N_{t,0,d}$ [kN] | max. compr. stress $\sigma_{c,0,d}$ [N/mm²] | max. tensile stress $\sigma_{t,0,d}$ [N/mm²] | UC (c) | UC (t) |
|---|---|---|---|---|---|---|---|---|
| L1 | GL30h | 928125 | 11472 | 5016 | 12.36 | 5.40 | 0.60 | 0.33 |
| L2 | GL30c | 928125 | 5196 | 321 | 5.60 | 0.35 | 0.33 | 0.03 |
| L3 | GL30c | 928125 | 4734 | 663 | 5.10 | 0.71 | 0.30 | 0.05 |
| L4 | GL30c | 928125 | 901 | 0 | 0.97 | - | 0.06 | - |
| R1 | GL30h | 928125 | 8328 | 2212 | 8.97 | 2.38 | 0.43 | 0.14 |
| R2 | GL30c | 928125 | 7797 | 2393 | 8.40 | 2.58 | 0.50 | 0.19 |
| R3 | GL30c | 928125 | 2718 | 0 | 2.93 | - | 0.17 | - |
| R4 | GL30c | 928125 | 1736 | 0 | 1.87 | - | 0.11 | - |
| D1 | GL30c | 618750 | 4845 | 4747 | 7.83 | 7.67 | 0.46 | 0.57 |
| D2 | GL30c | 618750 | 3966 | 3815 | 6.41 | 6.17 | 0.38 | 0.46 |
| D3 | GL30c | 618750 | 3948 | 3136 | 6.38 | 5.07 | 0.38 | 0.38 |
| D4 | GL30c | 618750 | 3049 | 2844 | 4.93 | 4.60 | 0.29 | 0.34 |
| D5 | GL30c | 618750 | 3026 | 2215 | 4.89 | 3.58 | 0.29 | 0.27 |
| D6 | GL30c | 618750 | 1953 | 2282 | 3.16 | 3.69 | 0.19 | 0.27 |
| D7 | GL30c | 618750 | 1542 | 520 | 2.49 | 0.84 | 0.15 | 0.06 |
| D8 | GL30c | 618750 | 203 | 1066 | 0.33 | 1.72 | 0.02 | 0.13 |

Table C.3: Member properties; design stresses corresponding to table C.2.

| | tensile strength | | compr. strength | |
|---|---|---|---|---|
| | characteristic $f_{t,0,g,k}$ [Mpa] | design $f_{t,0,g,d}$ [Mpa] | characteristic $f_{c,0,g,k}$ [Mpa] | design $f_{c,0,g,d}$ [Mpa] |
| GL30h | 24 | 16.62 | 30 | 20.77 |
| GL30c | 19.5 | 13.50 | 24.5 | 16.96 |

$k_{mod} = 0.9$, $\gamma_m = 1.3$

## C.1.4. Diagonal connections

The ULS and SLS normal forces in the diagonal connections, from the RFEM base model, are listed in table C.4.

**Table C.4:** Normal forces in the diagonal connections.

| Connection | Design force (ULS) | | Force in SLS | | Ratio SLS/ULS | |
|---|---|---|---|---|---|---|
| | compr. | tension | compr. | tension | compr. | tension |
| CR1-d | 4845 | 4580 | 2946 | 2734 | 61% | 60% |
| M1-d1 | 4665 | 4747 | 2822 | 2847 | 60% | 60% |
| M2-d2 | 3966 | 3661 | 2386 | 2183 | 60% | 60% |
| CL2-d1 | 3802 | 3815 | 2270 | 2284 | 60% | 60% |
| CL2-d2 | 3948 | 3076 | 2426 | 1728 | 62% | 56% |
| M2-d1 | 3772 | 3136 | 2317 | 1813 | 61% | 58% |
| M2-d2 | 2844 | 2956 | 1688 | 1780 | 59% | 60% |
| CR3-d1 | 2714 | 3049 | 1610 | 1852 | 59% | 61% |
| CR3-d2 | 3026 | 2108 | 1893 | 1131 | 63% | 54% |
| M3-d1 | 2645 | 2152 | 1624 | 1226 | 61% | 57% |
| M3-d2 | 1953 | 1745 | 1176 | 1026 | 60% | 59% |
| CL4-d1 | 1456 | 2282 | 746 | 1438 | 51% | 63% |
| CL4-d2 | 1542 | 372 | 1005 | 11 | 65% | 4% |
| M4-d1 | 1214 | 520 | 763 | 196 | 63% | 37% |
| M4-d2 | 203 | 816 | 24 | 521 | 12% | 64% |
| CR5-d | 0 | 1066 | 0 | 715 | - | 67% |

All forces are expressed in kN.

**Table C.5:** Characteristic- and design capacities of the diagonal connections.

| Connection | Characteristic capacity | | | | | Design capacity | | UC EYM | UC BS | Ratio SLS/charac. capacity | | |
| | YM $(n_{ef}=n)$ | YM $(n_{ef})$ | EYM $(n_{ef}=n)$ | EYM $(n_{ef})$ | Block shear | EYM $(n_{ef})$ | Block shear | $(n_{ef})$ | | YM $(n_{ef})$ | EYM $(n_{ef})$ | Block shear |
|---|---|---|---|---|---|---|---|---|---|---|---|---|
| CR1-d | 12610 | 8965 | 13070 | 9289 | 7591 | 6431 | 5255 | 0.75 | 0.87 | 33% | 32% | 36% |
| M1-d1 | 12610 | 8965 | 13070 | 9289 | 7591 | 6431 | 5255 | 0.74 | 0.90 | 32% | 31% | 38% |
| M2-d2 | 12610 | 8965 | 13070 | 9289 | 7591 | 6431 | 5255 | 0.62 | 0.70 | 27% | 26% | 29% |
| CL2-d1 | 10220 | 7338 | 10590 | 7604 | 7949 | 5264 | 5503 | 0.72 | 0.69 | 31% | 30% | 29% |
| CL2-d2 | 10220 | 7338 | 10590 | 7604 | 7949 | 5264 | 5503 | 0.75 | 0.56 | 33% | 32% | 22% |
| M2-d1 | 10220 | 7338 | 10590 | 7604 | 7949 | 5264 | 5503 | 0.72 | 0.57 | 32% | 30% | 23% |
| M2-d2 | 10220 | 7338 | 10590 | 7604 | 7949 | 5264 | 5503 | 0.56 | 0.54 | 24% | 23% | 22% |
| CR3-d1 | 10220 | 7338 | 10590 | 7604 | 7949 | 5264 | 5503 | 0.58 | 0.55 | 25% | 24% | 23% |
| CR3-d2 | 10220 | 7338 | 10590 | 7604 | 7949 | 5264 | 5503 | 0.57 | 0.38 | 26% | 25% | 14% |
| M3-d1 | 8072 | 5867 | 8364 | 6079 | 8088 | 4209 | 5599 | 0.63 | 0.38 | 28% | 27% | 15% |
| M3-d2 | 8072 | 5867 | 8364 | 6079 | 8088 | 4209 | 5599 | 0.46 | 0.31 | 20% | 19% | 13% |
| CL4-d1 | 8072 | 5867 | 8364 | 6079 | 8088 | 4209 | 5599 | 0.54 | 0.41 | 25% | 24% | 18% |
| CL4-d2 | 8072 | 5867 | 8364 | 6079 | 8088 | 4209 | 5599 | 0.37 | 0.07 | 17% | 17% | 0% |
| M4-d1 | 8072 | 5867 | 8364 | 6079 | 8088 | 4209 | 5599 | 0.29 | 0.09 | 13% | 13% | 2% |
| M4-d2 | 8072 | 5867 | 8364 | 6079 | 8088 | 4209 | 5599 | 0.19 | 0.15 | 9% | 9% | 6% |
| CR5-d | 8072 | 5867 | 8364 | 6079 | 8088 | 4209 | 5599 | 0.25 | 0.19 | 12% | 12% | 9% |

All forces in this table are expressed in kN.

$M_y$ (for YM and EYM) is calculated using yield moment from theory with $f_{yk}$ of 755MPa.

Block shear is calculated with EC5 (2004) and the characteristic tensile strength of the member is considered, not the characteristic tensile capacity of the timber planks.

Characteristic densities are used.

## C.1.5. Member forces

The figures below show the member forces in the diagonals- and columns under serviceability loading.
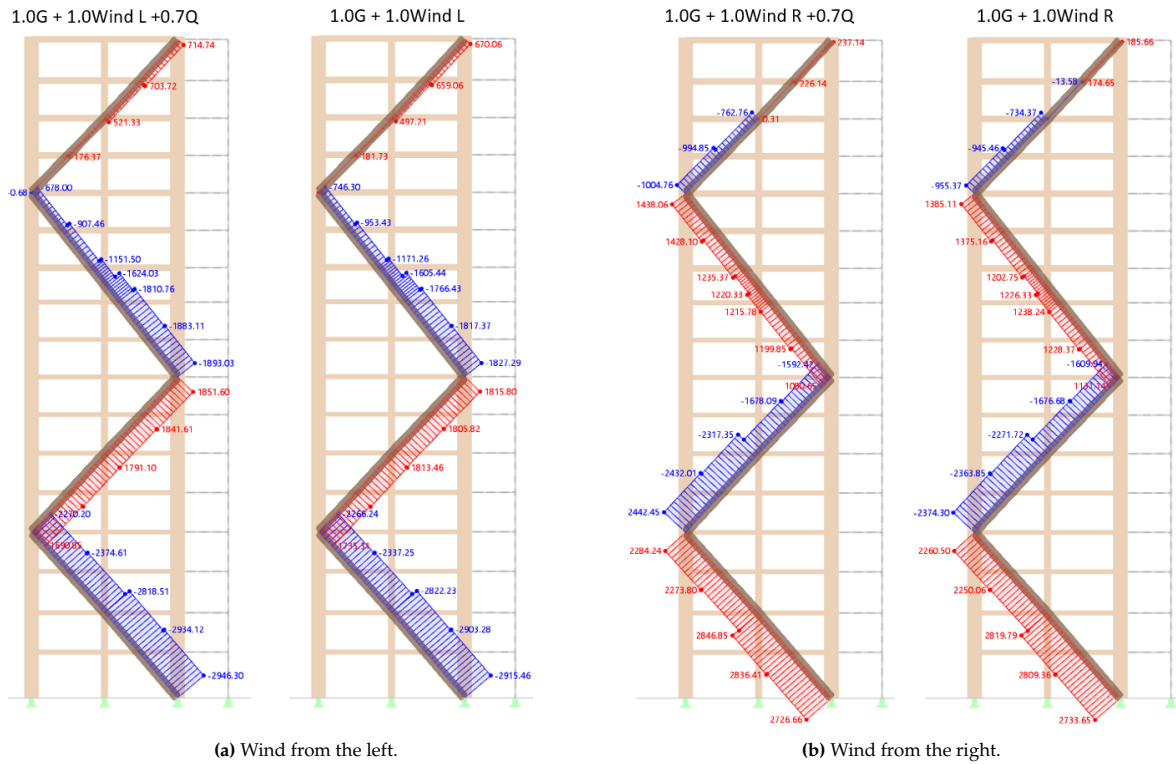


(a) Wind from the left.

(b) Wind from the right.

**Figure C.2:** Diagonal forces in SLS.



(a) Wind from the left.
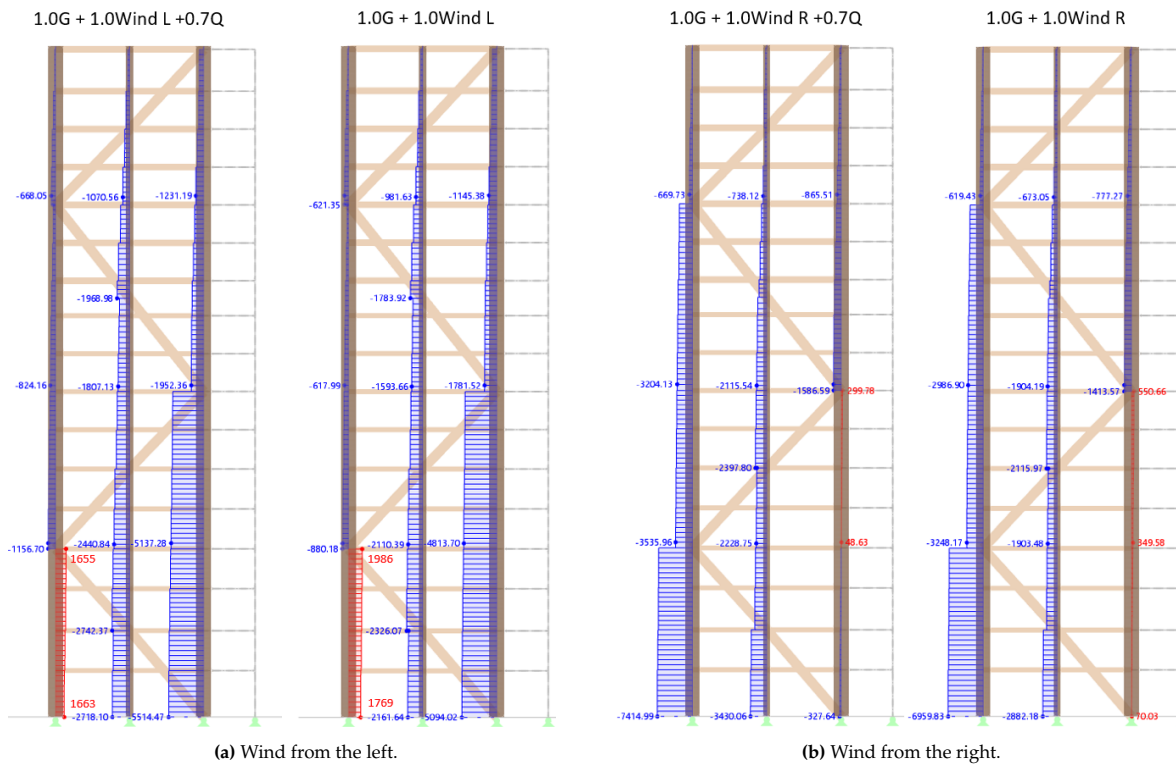
(b) Wind from the right.

**Figure C.3:** Column forces in SLS.

## C.1.6. Connection forces

The figures below show the (major) forces for the connections CL2 and CR3 under serviceability loading. These connections are chosen as an example because they have a vertical component and large loads are present.
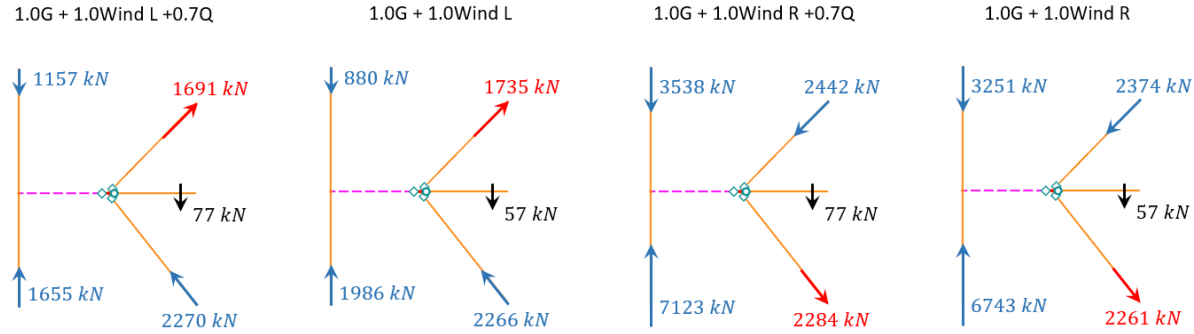


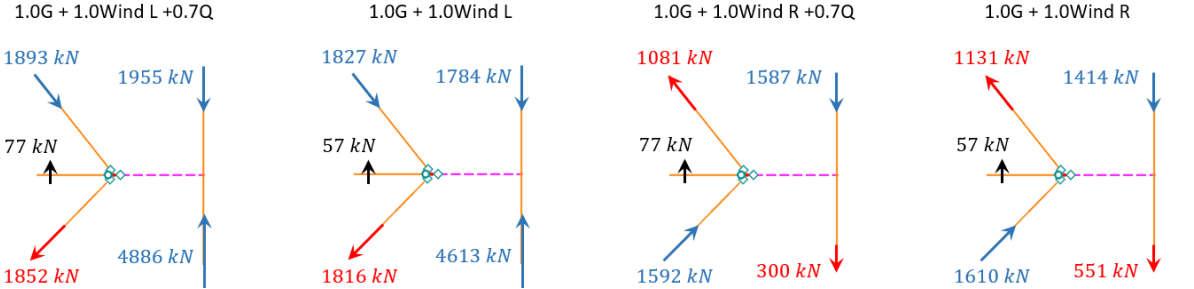**Figure C.4:** Forces in connection CL2 under serviceability loading.



**Figure C.5:** Forces in connection CR3 under serviceability loading.

# D

# Variant Study

## D.1. Maximum member forces

The maximum member forces from the RFEM models of each variant are shown in table D.1 and D.2 respectively. Table D.1 gives the forces from the models with pinned members. Table D.2 shows the forces from the models in which the elastic stiffnesses are assigned to the nodes and the E-modulus of the modelled diagonal members is altered. The forces from the models with both modelling approaches are shown because they differ slightly. This shows that the modelling approach can slightly affect the maximum member forces. Generally, the model with pinned members (approach 1) gives lower member forces in comparison to the model with approach 2.

**Table D.1:** Maximum forces [kN's] in diagonal- and corner column members from RFEM models with approach 1.

|  | SLS/ ULS | tension/ compression | Base Model | Variant | | | |
|---|---|---|---|---|---|---|---|
|  |  |  |  | **[A]** | **[B]** | **[C]** | **[D]** |
| Diagonals | SLS | (+) | 2804 | 2808 | 652 | 2383 | 2371 |
|  | SLS | (-) | 2881 | 2881 | 2376 | 2498 | 3935 |
|  | ULS | (+) | 4669 | 4674 | 1614 | 3962 | 3935 |
|  | ULS | (-) | 4736 | 4736 | 3659 | 4109 | 3738 |
| Corner Column | SLS | (+) | 1967 | 1923 | 855 | 1812 | 1026 |
|  | SLS | (-) | 7396 | 7438 | 6657 | 7663 | 5535 |
|  | ULS | (+) | 5012 | 4971 | 3330 | 4932 | 3138 |
|  | ULS | (-) | 10404 | 11461 | 10127 | 11799 | 8442 |

**Table D.2:** Maximum forces [kN's] in diagonal- and corner column members from RFEM models with (elastic) connection stiffnesses and adjusted E-modulus for diagonal elements (approach 2).

|  | SLS/ ULS | tension/ compression | Base Model | Variant | | | |
|---|---|---|---|---|---|---|---|
|  |  |  |  | **[A]** | **[B]** | **[C]** | **[D]** |
| Diagonals | SLS | (+) | 2847 | 2845 | 901 | 2398 | 2367 |
|  | SLS | (-) | 2946 | 2941 | 2127 | 2554 | 2329 |
|  | ULS | (+) | 4747 | 4739 | 1815 | 3994 | 3968 |
|  | ULS | (-) | 4845 | 4833 | 3335 | 4200 | 3861 |
| Corner Column | SLS | (+) | 1990 | 1939 | 793 | 1870 | 1079 |
|  | SLS | (-) | 7419 | 7457 | 6786 | 7688 | 5588 |
|  | ULS | (+) | 5016 | 4967 | 3277 | 4991 | 3199 |
|  | ULS | (-) | 11472 | 11515 | 10320 | 11866 | 8556 |